REGULATION OF A MURALYTIC RESUSCITATION-PROMOTING FACTOR IN *STREPTOMYCES COELICOLOR*

By RENÉE J. ST-ONGE, B.Sc., M.Sc.

A Thesis Submitted to the School of Graduate Studies in Partial Fulfillment of the Requirements for the Degree Doctor of Philosophy

McMaster University DOCTOR OF PHILOSOPHY (2016)
Hamilton, Ontario (Biology)

TITLE: Regulation of a muralytic resuscitation-promoting factor in *Streptomyces coelicolor*

AUTHOR: Renée J. St-Onge, B.Sc. (Université de Moncton), M.Sc. (Université de Moncton)

SUPERVISOR: Professor Marie A. Elliot

NUMBER OF PAGES: xviii, 176

ABSTRACT

To survive inhospitable conditions, bacteria can form fortified stress-resistant cells that are unable to grow and have little to no detectable metabolic activity. Upon detecting improved environmental conditions, these cells can reactivate metabolism and resume growth. A common aspect of establishing and exiting dormancy involves the extensive remodeling of the bacterial cell wall. In the actinobacteria, the 'resuscitation-promoting factors' (Rpfs) orchestrate the exit from dormancy through their muralytic activities.

The expression and activity of muralytic enzymes are tightly regulated. Excessive activity could weaken the cell wall, leading to lysis, while insufficient activity, in the case of the Rpfs, could compromise resuscitation from a dormant state. *rpf* genes are regulated at the level of transcription initiation; however, these genes are likely also regulated post-transcriptionally and post-translationally. For example, in *Streptomyces coelicolor*, *rpfA* is associated with several regulatory RNAs: a riboswitch motif is located within the 5′ untranslated region, while a small RNA-encoding gene is located immediately downstream of the *rpfA* stop codon.

In this work, we probed multi-level *rpfA* regulation in *S. coelicolor*, placing a particular emphasis on RNA-based control mechanisms acting post-transcriptionally. We found that *rpfA* was regulated at many levels: transcription initiation, transcript elongation and protein stability. We also discovered that *rpfA* served as a regulatory hub, receiving input from three second messengers with known functions in dormancy and/or resuscitation. During the course of this work, we also uncovered a novel riboswitch regulatory mechanism and identified previously uncharacterized activity determinants for this riboswitch class. Finally, we showed that the downstream-encoded small RNA impacted the expression of genes involved in microaerobic metabolism and, through its predicted regulation of *rpfA* expression, may coordinate cell wall remodeling and dormancy/resuscitation with the hypoxic response. This work dramatically expands our understanding of *rpf* gene regulation and actinobacterial resuscitation.

ACKNOWLEDGEMENTS

I would like to thank first and foremost my thesis supervisor, Dr. Marie Elliot (McMaster University, Hamilton, CAN), for her mentorship over the past five years. This work would not have been possible without her tireless dedication to her students' success. I would also like to thank my thesis committee members, Dr. Robin Cameron (McMaster University), Dr. Justin Nodwell (University of Toronto, Toronto, CAN) and Dr. Yingfu Li (McMaster University), for their advice and constructive criticism of my work. My gratitude also goes to past and present members of the Elliot Lab for their scientific insight and support, and to the administrative and technical support staff of McMaster University's Department of Biology.

TABLE OF CONTENTS

LIST OF TABLES

LIST OF FIGURES

LIST OF ABBREVIATIONS AND SYMBOLS

A

A	Absorbance *or* adenine
a.l.u.	Arbitrary luminescence unit
AMP	Adenosine monophosphate
Apra	Apramycin
ATCC	American Type Culture Collection
ATP	Adenosine triphosphate
ATPase	Adenosine triphosphatase
a.u.	Arbitrary unit

B

BAM	Binary alignment/map
BCM	Bicyclomycin
BLAST	Basic local alignment search tool
bp	Base-pair

C

C	Complemented mutant *or* cytosine
cAMP	3′,5′-Cyclic adenosine monophosphate
CDA	Cyclic diadenylate monophosphate
CDG	Cyclic diguanylate monophosphate
c-di-AMP	Cyclic diadenylate monophosphate
c-di-GMP	Cyclic diguanylate monophosphate
cDNA	Complementary deoxyribonucleic acid
CDS	Coding sequence
ChIP	Chromatin immunoprecipitation
cm	Centimeter
Comp.	Compensatory
Crp	3′,5′-Cyclic adenosine monophosphate receptor protein
C_T	Threshold cycle
CTP	Cytidine triphosphate

D

DAC	Diadenylate cyclase
DART-PCR	Data analysis for real-time polymerase chain reaction
Dist.	Distal
D,L-α-ABA	D,L-α-amino-*N*-butyric acid
DMSO	Dimethylsulfoxide
DNA	Deoxyribonucleic acid
DNase	Deoxyribonuclease

dNTP	Deoxynucleoside triphosphate
Down	Downstream
DUF	Domain of unknown function

E

EDC	1-ethyl-3-(3-dimethylaminopropyl)carbodiimide
EDTA	Ethylenediaminetetraacetic acid
EMBO	European Molecular Biology Organization
Endopep.	Endopeptidase
Ex	Exconjugant
Exp.	Exponential-phase

G

G	Guanine
g	Force of gravity *or* gram
gDNA	Genomic deoxyribonucleic acid
Gly	Glycine
GMP	Guanosine monophosphate
GTP	Guanosine triphosphate

H

h	Hour
H+E	Heat- and ethylenediaminetetraacetic acid-treated

I

ILP	In-line probing
IVT	*In vitro* transcribed

K

Kan	Kanamycin
kcpm	Kilo counts per minute

L

L	Ladder
L-Asn	L-asparagine
LB	Luria Bertani
LC	Loading control
LC-MS/MS	Liquid chromatography-coupled tandem mass spectrometry
LT	Lytic transglycosylase

M

M	Molar
mg	Milligram
min	Minute

mL	Milliliter
MM	Minimal medium
mM	Millimolar
mm	Millimeter
mRNA	Messenger ribonucleic acid
MS	Mannitol-soya flour
Mtb	*Mycobacterium tuberculosis*
MW	Molecular weight
MYM	Maltose-yeast extract-malt extract

N

N	Any nucleotide
n	Sample size
NA	Nutrient agar
N/A	Not applicable
NADH	Nicotinamide adenine dinucleotide
NEB	New England Biolabs
ng	Nanogram
nM	Nanomolar
NR	No reaction/untreated
NSERC	Natural Sciences and Engineering Research Council of Canada
nt	Nucleotide
NTP	Nucleoside triphosphate

O

OD	Optical density
O/E	Overexpression

P

P	Calculated probability
PCR	Polymerase chain reaction
pmol	Picomole
ppGpp	Guanosine 5′-diphosphate-3′-diphosphate
Prox.	Proximal
psi	Pound per square inch
PVDF	Polyvinylidene fluoride

Q

Q	False discovery rate-adjusted probability value
qPCR	Real-time polymerase chain reaction

R

R	Purine (adenine or guanine)
R_0	Starting fluorescence

R^2	Coefficient of determination
RBS	Ribosome binding site
RNA	Ribonucleic acid
RNase	Ribonuclease
Rpf *or* RPF	Resuscitation-promoting factor
rRNA	Ribosomal ribonucleic acid
RT	Reverse transcription

S

Sco	*Streptomyces coelicolor*
SDS	Sodium dodecyl sulfate
sec	Second
SOB	Super optimal broth
SOE	Splicing by overlap extension
sRNA	Small ribonucleic acid
SSC	Saline-sodium citrate
ssDNA	Single-stranded deoxyribonucleic acid
Stat.	Stationary-phase

T

T	Thymine
TBE	Tris-borate-ethylenediaminetetraacetic acid
TCA	Tricarboxylic acid
TES	2-[Tris(hydroxymethyl)-methylamino]-ethanesulfonic acid
TSB	Tryptone soya broth

U

U	Unit *or* uracil
Unt.	Untreated
Ups	Upstream
UTP	Uridine triphosphate
UTR	Untranslated region
UV	Ultraviolet

V

V	Volt

W

W	Watt
WT	Wild-type

Y

Y	Pyrimidine (cytosine or thymine)
YEME	Yeast extract-malt extract

YT	Yeast extract-tryptone

Symbols

α	Alpha
ß	Beta
γ	Gamma
Δ	Delta *or* mutant
λ	Lambda
µCi	Microcurie
µg	Microgram
µL	Microliter
µM	Micromolar
µm	Micrometer
σ	Sigma
ϕ	Phi
$\overline{x}$	Mean
°C	Degree Celsius
$\%_{v/v}$	Milliliters per 100 milliliters
$\%_{w/v}$	Grams per 100 milliliters

PREFACE

The present ‘sandwich’ thesis was written following the guidelines provided by the McMaster University School of Graduate Studies. Each chapter is a reproduction of a manuscript previously published in a peer-reviewed scientific journal, a manuscript in preparation, or unpublished work. Published manuscripts were modified to conform to the university guidelines. All titles and subtitles were numbered as in the *General Introduction* and *General Discussion* chapters. Figures and tables were re-numbered to ensure continuity throughout the thesis. All references were placed at the end of the thesis, along with those of the *General Introduction* and *General Discussion*.

CHAPTER 1

GENERAL INTRODUCTION

1.1 *STREPTOMYCES* BACTERIA

Streptomycetes are high G+C Gram-positive actinobacteria inhabiting diverse niches. These ubiquitous soil- and ocean-dwelling microbes are most prized for their ability to produce a wealth of bioactive secondary metabolites with important applications in both agriculture and medicine, including antibiotics and anticancer drugs (Marinelli, 2009). In addition to their great commercial value, streptomycetes play a vital role in nutrient cycling in soil ecosystems as they degrade numerous animal-, plant- and insect-derived recalcitrant biopolymers (*e.g.*, cellulose and chitin) (Loria *et al.*, 2006).

In contrast to many other bacteria, streptomycetes have a relatively complex life cycle (Fig. 1.1). It commences with the germination of a dormant spore, a process likely triggered by abundant nutrients and otherwise growth-conducive conditions. The budding germ tubes grow outward into the substrate by tip extension and branching, leading to the formation of a mesh-like filamentous mycelium, termed the vegetative (or substrate) mycelium. Once the nutrient source has been exhausted or upon detecting an as yet unknown environmental cue, multigenomic aerial hyphae emerge from the vegetative mycelium, extending into the air where they undergo a single round of coordinated septation. The aerial hyphae are thus divided into a series of pre-spore compartments that mature into unigenomic spores (Flärdh and Buttner, 2009; Elliot and Flärdh, 2012).

1.2 *STREPTOMYCES* SPORES AND BACTERIAL DORMANCY

1.2.1 *Streptomyces* spores are dormant cells.

Streptomyces spores have little to no observable metabolic activity. In wet spores, modest activity (*e.g.*, O_2 consumption, oxidation of endogenous carbon sources, CO_2 release, ATP production, nucleic acid and protein synthesis) is

apparent, though germination is not initiated (Hirsch and Ensign, 1978; Eaton and Ensign, 1980; McBride and Ensign, 1987b; McBride and Ensign, 1987a). Dry spores, however, are truly cryptobiotic, *i.e.*, they possess no detectable metabolism (Hirsch and Ensign, 1978). Endogenous carbon sources are not oxidized to CO_2, and ATP levels are low (Hirsch and Ensign, 1978).

Surviving inhospitable environments through the attenuation of metabolism is not unique to the streptomycetes. Many microorganisms respond to adverse growing conditions – typified by nutrient shortages, temperature extremes, drought and/or chemical insults – by reducing their metabolic activity and ceasing to multiply. They remain in such a state of quiescence, or 'dormancy', until they encounter more favorable growing conditions (Kaprelyants *et al.*, 1993; Kell and Young, 2000; Dworkin and Shah, 2010; Rittershaus *et al.*, 2013). When the actinobacteria, including *Micrococcus luteus* (Kaprelyants and Kell, 1993; Mukamolova *et al.*, 1998a)*, Mycobacterium smegmatis* (Shleeva *et al.*, 2004; Anuchin *et al.*, 2009), *Mycobacterium tuberculosis* (Shleeva *et al.*, 2002; Shleeva *et al.*, 2011; Salina *et al.*, 2014) and *Rhodococcus rhodochrous* (Shleeva *et al.*, 2002), are grown under suboptimal conditions, they enter a state of dormancy during extended stationary phase. The transition to dormancy is characterized by a dramatic change in cellular morphology; cells become smaller, and bacteria that are otherwise rod-shaped during active growth become ovoid or coccoid in shape (Kaprelyants and Kell, 1993; Shleeva *et al.*, 2002; Shleeva *et al.*, 2004; Anuchin *et al.*, 2009; Shleeva *et al.*, 2011; Puspita *et al.*, 2013; Salina *et al.*, 2014). Dormant cells do not actively replicate, and so only a fraction of the cell population is culturable, *i.e.*, they can form colonies on a solid medium (Kaprelyants and Kell, 1993; Mukamolova *et al.*, 1998a; Shleeva *et al.*, 2002; Shleeva *et al.*, 2004; Anuchin *et al.*, 2009; Shleeva *et al.*, 2011; Puspita *et al.*, 2013; Salina *et al.*, 2014). As is the case with *Streptomyces* spores, dormant actinobacteria display little to no detectable metabolic activity (their membranes are weakly energized, they do not actively respire, and ATP, RNA and protein levels are low) (Kaprelyants and Kell, 1993; Mukamolova *et al.*, 1995; Shleeva *et al.*, 2002; Shleeva *et al.*, 2004; Anuchin *et al.*, 2009; Shleeva *et al.*, 2011; Salina *et al.*, 2014). Dormant cells are by no means dead, as their permeable membranes are undamaged, and they can reactivate their metabolism and resume growth under appropriate conditions (Kaprelyants and Kell, 1993; Mukamolova *et al.*, 1998a; Shleeva *et al.*, 2002; Shleeva *et al.*, 2004; Anuchin *et al.*, 2009; Shleeva *et al.*, 2011; Puspita *et al.*, 2013; Salina *et al.*, 2014) (see also section 1.4).

1.2.2 *Streptomyces* spores are resistant to abiotic stresses.

Like dormant mycobacteria (Anuchin *et al.*, 2009; Shleeva *et al.*, 2011; Salina *et al.*, 2014), *Streptomyces* spores are more stress-resistant than actively growing vegetative mycelia, a feature befitting dormant cells meant to survive severe environmental conditions. In contrast to actively growing cells, *Streptomyces* spores are resistant to both heat (Hardisson *et al.*, 1978; Eaton and Ensign, 1980; Salas *et al.*, 1983) and desiccation (Martín *et al.*, 1986; Elliot and Flärdh, 2012). This resistance is owed in part to trehalose (Martín *et al.*, 1986; McBride and Ensign, 1987b), a non-reducing disaccharide comprising two glucose units that is abundant in dormant spores (Hey-Ferguson *et al.*, 1973; Martín *et al.*, 1986; McBride and Ensign, 1987a; McBride and Ensign, 1987b; McBride and Ensign, 1990). Trehalose also increases the refractivity and optical density of spores (McBride and Ensign, 1987b), thereby providing their characteristic phase-bright appearance under a phase-contrast microscope (Fig. 1.2) and their relatively high optical density in liquids (Hirsch and Ensign, 1976a; Hardisson *et al.*, 1978).

1.2.3 Extensive cell wall remodeling occurs during spore maturation.

Cell wall remodeling during spore development and maturation also contributes to the stress-resistant properties of dormant spores. In preparation for entering dormancy, streptomycetes double their cell wall thickness (Glauert and Hopwood, 1961; Bradley and Ritzi, 1968). Alteration of the cell wall may explain the resistance of spores to lysozyme, a cell wall hydrolase (Grund and Ensign, 1985). Cell wall remodeling at the onset of dormancy is not unique to the streptomycetes, but rather is a process shared by many dormancy-adopting bacteria, including *Bacillus*, *Micrococcus* and *Mycobacterium* (Mukamolova *et al.*, 1995; Cunningham and Spreadbury, 1998; Atrih and Foster, 1999; Lavollay *et al.*, 2008; Anuchin *et al.*, 2009; Shleeva *et al.*, 2011; Puspita *et al*., 2013).

1.3 GERMINATION OF *STREPTOMYCES* SPORES

Microbes that make use of dormancy to survive inhospitable environments must be able to resume active growth once growth conditions improve. In the streptomycetes, this ‘resuscitation’ corresponds to a discrete stage of their life

cycle, namely spore germination. Spore germination is divided into three steps: darkening, swelling and germ tube emergence.

1.3.1 Phase I: Spore darkening

1.3.1.1 Germination initiation is marked by an increase in endogenous metabolism.

The first stage of germination is referred to as 'darkening'. Spore darkening is characterized by a change in spore refractivity. During this stage of germination, spores, which are phase-bright when dormant, become progressively phase-dark (Fig. 1.2) (Hirsch and Ensign, 1976a; Hardisson *et al.*, 1978). This transition from phase-bright to phase-dark is accompanied by a decrease in optical density (Hirsch and Ensign, 1976a; Hardisson *et al.*, 1978).

During this phase transition, and prior to any obvious change in cellular morphology, endogenous metabolism, which was previously undetected in dormant spores, is re-established (Hirsch and Ensign, 1978). O_2 consumption (Hardisson *et al.*, 1978) and CO_2 production (Eaton and Ensign, 1980; McBride and Ensign, 1987a) are now detectable, cytochrome oxidase and catalase activities increase (Hardisson *et al.*, 1978), and intracellular ATP levels rise dramatically (Grund and Ensign, 1985). *De novo* RNA synthesis begins (Grund and Ensign, 1978; Hardisson *et al.*, 1978), and carbon-based compounds are released into the medium (Grund and Ensign, 1978; Eaton and Ensign, 1980; Grund and Ensign, 1985; McBride and Ensign, 1987a). Many of these metabolic activities are thought to involve components already present in the dormant spores, as darkening can continue unhindered in the absence of DNA replication, transcription and translation (Hardisson *et al.*, 1978). Darkening does however require active respiration (Hardisson *et al.*, 1978) and abundant ATP (Grund and Ensign, 1985), likely needed to fuel the various anabolic processes taking place in the germinating spore.

1.3.1.2 Trehalose is rapidly mobilized during spore darkening.

The change in spore refractivity and the decrease in optical density noted during spore darkening are likely owed to the rapid depletion of trehalose stores. Trehalose is rapidly hydrolyzed to glucose by the enzyme trehalase, resulting in plummeting levels of the disaccharide during germination (Hey-Ferguson *et al.*, 1973; Martín *et al.*, 1986; McBride and Ensign, 1987a). Consistent with the

decrease in trehalose levels, germinating spores are less heat- and desiccation-resistant than their dormant counterparts (Hardisson *et al.*, 1978; Eaton and Ensign, 1980; Salas *et al.*, 1983; Martín *et al.*, 1986).

The products of trehalose hydrolysis are then either completely oxidized to CO_2 or used as building blocks for the synthesis of macromolecules and secreted compounds (McBride and Ensign, 1987a). Trehalose breakdown is thought to be extremely quick, as glucose is not readily detectable in germinating spores (Hey-Ferguson *et al.*, 1973), and thus it is assumed that metabolism at this stage is fuelled primarily by the oxidation of trehalose, along with other endogenous carbon sources. Exogenous substrates are not extensively metabolized until germination nears completion (Hirsch and Ensign, 1978).

1.3.1.3 Carbon dioxide is used to replenish the tricarboxylic acid cycle by anaplerosis.

Although the precursors to macromolecular synthesis are provided in part by trehalose breakdown, building blocks are also generated by anaplerosis, a process by which the cell replaces tricarboxylic acid (TCA) cycle intermediates that have otherwise been depleted for biosynthetic purposes. In germinating spores, this process relies heavily on the availability of exogenous CO_2.

CO_2, provided by the ambient air, is strictly required for the initiation of spore germination. In its absence, dormant *Streptomyces* spores fail to darken and remain phase-bright (Hirsch and Ensign, 1976a; Grund and Ensign, 1978). Spores begin to internalize atmospheric CO_2 during the early stages of germination (Grund and Ensign, 1978), and they immediately incorporate its carbon into TCA cycle intermediates and derived amino acids, likely via carboxylation of a three-carbon intermediate derived from a storage polymer (Grund and Ensign, 1978). CO_2-derived carbon is eventually incorporated into macromolecules, including RNA and proteins (Grund and Ensign, 1978).

Consistent with this proposal, it is possible to circumvent the need for exogenous CO_2 by supplying the growth medium with a TCA cycle intermediate (Grund and Ensign, 1978). Metabolic TCA cycle inhibitors can also hinder *Streptomyces* spore germination (Grund and Ensign, 1978).

1.3.1.4 Germicidins delay the initiation of spore germination by inhibiting ATPases.

Self-targeting inhibitors called 'germicidins' regulate, in part, the initiation of spore germination. Germicidins are low-molecular-weight compounds secreted by germinating spores and stationary-phase mycelia (Hirsch and Ensign, 1978; Grund and Ensign, 1985; Petersen *et al.*, 1993; Aoki *et al.*, 2011). They inhibit spore germination and vegetative growth (Hirsch and Ensign, 1978; Grund and Ensign, 1985; Petersen *et al.*, 1993; Aoki *et al.*, 2011); however, their activity is bacteriostatic as spores germinate upon removing the inhibitor (Grund and Ensign, 1985; Aoki *et al.*, 2011). Though their biological function remains obscure, germicidins are thought to reduce spurious germination of neighboring spores when conditions cannot support active growth (Hirsch and Ensign, 1978; Grund and Ensign, 1985; Aoki *et al.*, 2011).

Germicidins block the germination of *Streptomyces* spores by inhibiting the activity of membrane-bound Ca^{2+}-activated ATPases (Grund and Ensign, 1985), thereby reducing respiration (Hirsch and Ensign, 1978; Grund and Ensign, 1982; Grund and Ensign, 1985) and decreasing intracellular ATP levels (Grund and Ensign, 1985). As ATP is strictly required for spore darkening (Grund and Ensign, 1985), germicidin-dependent dampening of ATPase activity may explain its inhibitory effect.

In order for germination to proceed, germicidins must first be cleared. Though regulation of germicidin expression and activity remains unclear, Petersen *et al.* (1993) have demonstrated that exogenous Ca^{2+} reduces the potency of the germination inhibitor. Activating dormant spores, using either heat or detergent, can also alleviate germicidin-dependent inhibition of germination and respiration (Hirsch and Ensign, 1978; Grund and Ensign, 1982; Grund and Ensign, 1985).

1.3.1.5 Ca^{2+} triggers and sustains spore germination.

Exogenous Ca^{2+} is strictly required to both initiate and complete the darkening process (Hirsch and Ensign, 1976b; Hardisson *et al.*, 1978; Eaton and Ensign, 1980). Ca^{2+} likely promotes germination initiation by stimulating the production of much-needed ATP, by directly activating Ca^{2+}-dependent ATPases (Grund and Ensign, 1985) and indirectly by antagonizing the ATPase-inhibiting germicidins (Petersen *et al.*, 1993).

1.3.2 Phase II: Spore swelling

The second stage of germination, spore swelling, is characterized by an increase in spore volume (Fig. 1.2) (Hirsch and Ensign, 1976a; Sharples and Williams, 1976) and a concomitant increase in optical density (Hardisson *et al.*, 1978). Spore swelling results from spore rehydration (Hardisson *et al.*, 1978), which is thought to increase trehalase activity (McBride and Ensign, 1990) and promote continued trehalose breakdown. Swelling also marks the beginning of *de novo* protein synthesis (Hardisson *et al.*, 1978) and the resolution of the spore wall into two discrete electron-dense layers (Fig. 1.2) (Sharples and Williams, 1976; Hardisson *et al.*, 1978). The only nutritional requirement for this stage of germination is an exogenous carbon source, although this is not sufficient to drive spore germination to completion (Hardisson *et al.*, 1978).

1.3.3 Phase III: Germ tube emergence

The emergence of a germ tube marks the end of spore germination and the beginning of growth resumption (Fig. 1.2). The optical density of the culture continues to increase during germ tube emergence (Hirsch and Ensign, 1976a; Hardisson *et al.*, 1978). The cell starts to preferentially use exogenous carbon sources, in addition to internal nutrient stores, to fuel its many metabolic processes (Hirsch and Ensign, 1978). DNA replication resumes in earnest (Hardisson *et al.*, 1978). Both DNA replication and exogenous carbon and nitrogen sources are required for germ tube emergence (Hardisson *et al.*, 1978).

The inner layer of the spore wall extends outwards to form the cell wall of the germ tube (Glauert and Hopwood, 1961; Bradley and Ritzi, 1968; Sharples and Williams, 1976; Hardisson *et al.*, 1978). Most strikingly, the cell wall thins as the germ tube extends (Glauert and Hopwood, 1961). Indeed, the cell wall of germinating spores and derived vegetative hyphae is considerably thinner than that of dormant spores (Fig. 1.2) (Glauert and Hopwood, 1961; Bradley and Ritzi, 1968; Sharples and Williams, 1976; Hardisson *et al.*, 1978); this observation of cell wall thinning and remodeling during resuscitation holds for a range of bacteria adopting dormant cell types (Mukamolova *et al.*, 1995; Cunningham and Spreadbury, 1998; Atrih and Foster, 1999; Lavollay *et al.*, 2008; Anuchin *et al.*, 2009; Shleeva *et al.*, 2011; Puspita *et al.*, 2013). In the actinobacteria, the resuscitation-promoting factors (Rpfs) mediate this essential cell wall remodeling process.

1.4 RESUSCITATION-PROMOTING FACTORS

1.4.1 Rpfs modulate dormancy and resuscitation in the actinobacteria.

Streptomyces (Mukamolova *et al.*, 1998b; Haiser *et al.*, 2009; Sexton *et al.*, 2015) and other actinobacteria (Schroeckh and Martin, 2006; Puspita *et al.*, 2013), including *Corynebacterium* (Mukamolova *et al.*, 1998b; Hartmann *et al.*, 2004), *Micrococcus* (Mukamolova *et al.*, 1998b; Mukamolova *et al.*, 2002b; Telkov *et al.*, 2006), *Mycobacterium* (Mukamolova *et al.*, 1998b; Mukamolova *et al.*, 2002a; Zhu *et al.*, 2003; Shleeva *et al.*, 2004; Tufariello *et al.*, 2004; Gupta *et al.*, 2010; Shleeva *et al.*, 2013), *Rhodococcus* (Shleeva *et al.*, 2002; Schroeckh and Martin, 2006) and *Tomitella* (Puspita *et al.*, 2013), produce at least one Rpf (Fig. 1.3), where Rpfs are extracytoplasmic proteins that modulate cell dormancy and/or resuscitation. When exogenously added to the growth medium, purified Rpfs trigger resuscitation of dormant *Micrococcus*, *Mycobacterium*, *Rhodococcus* and *Tomitella* cells, and shorten the lag phase following growth re-establishment (Mukamolova *et al.*, 1998b; Mukamolova *et al.*, 1999; Biketov *et al.*, 2000; Mukamolova *et al.*, 2002a; Shleeva *et al.*, 2002; Zhu *et al.*, 2003; Shleeva *et al.*, 2004; Shleeva *et al.*, 2011; Puspita *et al.*, 2013; Shleeva *et al.*, 2013; Nikitushkin *et al.*, 2015). Similarly, in *Corynebacterium glutamicum*, deleting the Rpf-encoding genes greatly increases lag phase duration of long-stored cells (Hartmann *et al.*, 2004). Furthermore, spontaneous resuscitation under laboratory conditions is impaired in *M. tuberculosis* mutants in which at least three of the five Rpf-encoding genes are deleted (Downing *et al.*, 2005; Kana *et al.*, 2008). Work conducted in our laboratory has revealed a similar phenomenon in the streptomycetes, whereby deleting or disrupting *rpfA*, *rpfC*, *rpfD* or *rpfE* impedes germination of dormant *Streptomyces coelicolor* spores (Haiser *et al.*, 2009; Sexton *et al.*, 2015).

Though Rpfs are primarily known for their role in resuscitation, recent works suggest they may also be involved in establishing a dormant state. In *S. coelicolor*, for example, the *rpf* genes are required for proper spore maturation and separation (Haiser *et al.*, 2009; Sexton *et al.*, 2015). Certain *rpf* genes, including *rpfA,* are up-regulated during the early stages of dormancy in different actinobacteria (Muttucumaru *et al.*, 2004; Haiser *et al.*, 2009; Salina *et al.*, 2014). Furthermore, in the mycobacteria, several *rpf* genes are up-regulated in response to stresses known to promote the transition from active growth to dormancy (Gupta *et al.*, 2010).

For pathogenic *M. tuberculosis*, the causative agent of tuberculosis in humans, Rpfs are also virulence factors as they promote pathogen reactivation from latency in the host (Tufariello *et al.*, 2006; Biketov *et al.*, 2007). Although RpfA, RpfC, RpfD and RpfE are not strictly (*i.e.*, individually) necessary for disease recrudescence, RpfB is involved in *M. tuberculosis* reactivation in immune-compromised mice models (Tufariello *et al.*, 2006).

1.4.2 Rpfs are muralytic enzymes.

Rpfs are proposed to stimulate the resuscitation of dormant cells through their ability to cleave peptidoglycan (Mukamolova *et al.*, 2006; Telkov *et al.*, 2006). Peptidoglycan is a major component of the bacterial cell wall, and it comprises linear glycan strands of alternating *N*-acetylglucosamine and *N*-acetylmuramic acid residues cross-linked by peptide side chains and interpeptide bridges (Vollmer *et al.*, 2008a). This mesh-like macromolecule is involved in growth and division, maintenance of cell shape and resistance to osmotic pressure. It also functions as a scaffold for cell wall-bound proteins, teichoic acids and other molecules (Vollmer *et al.*, 2008a).

Although the number, molecular weight and domain architecture of Rpfs vary (Fig. 1.3), all Rpfs share a conserved domain, termed the RPF domain (Mukamolova *et al.*, 2002a; Zhu *et al.*, 2003; Cohen-Gonsaud *et al.*, 2004a; Hartmann *et al.*, 2004; Puspita *et al.*, 2013; Squeglia *et al.*, 2013; Sexton *et al.*, 2015). This domain confers cell wall-cleaving (muralytic) activity to Rpfs (Mukamolova *et al.*, 2006; Telkov *et al.*, 2006; Hett *et al.*, 2008; Haiser *et al.*, 2009; Hett *et al.*, 2010; Nikitushkin *et al.*, 2013; Nikitushkin *et al.*, 2015; Sexton *et al.*, 2015). Though its precise mechanism of action remained unclear for many years, several important lines of evidence (outlined below) suggested that Rpfs break the ß1,4-glycosidic bond between *N*-acetylmuramic acid and *N*-acetylglucosamine moieties of peptidoglycan. The RPF domain adopts a three-dimensional structure similar to that of lysozyme and lytic transglycosylase (LT) (Cohen-Gonsaud *et al.*, 2004b; Cohen-Gonsaud *et al.*, 2004a; Cohen-Gonsaud *et al.*, 2005; Mukamolova *et al.*, 2006; Ruggiero *et al.*, 2009), enzymes that cleave these ß1,4-glycosidic bonds in peptidoglycan, albeit using different mechanistic approaches (Vollmer *et al.*, 2008b). Amino acid residues playing key roles in lysozyme- and/or LT-mediated peptidoglycan binding and cleavage are conserved in the RPF domain (Cohen-Gonsaud *et al.*, 2004a; Cohen-Gonsaud *et al.*, 2005; Mukamolova *et al.*, 2006; Ruggiero *et al.*, 2009; Squeglia *et al.*, 2013; Mavrici *et al.*, 2014; Maione *et al.*, 2015). Rpfs also bind (Cohen-Gonsaud *et al.*,

2005; Squeglia *et al.*, 2013) and cleave (Mukamolova *et al.*, 2006; Telkov *et al.*, 2006) *N*,*N*',*N*''-triacetylchitotriose, a peptidoglycan mimetic compound. Finally, Nikitushkin *et al.* (2015) recently demonstrated unequivocally that the Rpfs function as LTs, breaking the bond between *N*-acetylmuramic acid and *N*-acetylglucosamine, and leaving a 1,6-anhydro ring on the newly exposed terminal *N*-acetylmuramic acid residue (Vollmer *et al.*, 2008b). This is in contrast to the hydrolytic lysozyme, which releases an unmodified *N*-acetylmuramic acid residue upon cleaving the glycan strand (Vollmer *et al.*, 2008b).

Full enzymatic and resuscitation activities of Rpfs rely on a conserved catalytic glutamate residue (Mukamolova *et al.*, 2006; Telkov *et al.*, 2006). Site-directed mutagenesis of this residue attenuates, but does not abolish, the muralytic activity of the *M. luteus* Rpf (Mukamolova *et al.*, 2006; Telkov *et al.*, 2006). Concomitantly, dormant cells expressing this mutant Rpf protein are compromised in their ability to resuscitate (Mukamolova *et al.*, 2006; Telkov *et al.*, 2006). The cell wall-cleaving activity and the resuscitation ability of the *M. luteus* Rpf are also greatly impaired upon mutating one or both cysteine residues predicted to form a disulfide bridge, suggesting that this covalent bond is required for maximum activity (Mukamolova *et al.*, 2006; Telkov *et al.*, 2006). Nuclear magnetic resonance and circular dichroism experiments later suggested that disulfide bond formation stabilizes the active conformation of the *M. tuberculosis* RpfC hydrophobic catalytic cleft (Maione *et al.*, 2015).

1.4.3 Muralytic activity is required for the resuscitative activities of Rpfs.

Although a positive correlation between the muralytic and resuscitative activities of Rpfs is emerging, it is not yet fully understood how cell wall lysis ultimately leads to the resuscitation of dormant cells. Several research groups hypothesized that Rpfs remodel the cell wall to relieve physical restrictions preventing outgrowth. Others proposed an alternative model: cell wall fragments released by Rpfs are sensed by the cell and trigger resuscitation via signal transduction. In *Bacillus subtilis*, specific peptidoglycan fragments (muropeptides) released from actively growing cells stimulate the germination of dormant spores (Shah *et al.*, 2008). This process depends on a membrane-bound peptidoglycan-binding serine/threonine kinase called PrkC (Shah *et al.*, 2008). PrkC activation both induces the expression of the secreted muralytic enzyme YocH, an Rpf-like protein, and stimulates the germination of *B. subtilis* spores (Shah *et al.*, 2008; Shah and Dworkin, 2010).

Evidence collected in various mycobacterial models suggests that this mechanism may also exist in the actinobacteria. Synthetic muropeptides that bind the PrkC homologue PknB, which localizes at sites of peptidoglycan remodeling, modestly stimulate the resuscitation of dormant cells (Mir *et al.*, 2011). Muropeptides are indeed released by the concerted action of RpfB and its binding partner, the peptidoglycan endopeptidase RipA, and these products go on to stimulate the resuscitation of dormant cells (Nikitushkin *et al.*, 2015).

1.4.4 Rpfs are expressed at specific growth stages.

Rpfs are expressed during specific growth stages, coinciding with their biological functions. In the micrococci and mycobacteria, where Rpfs primarily modulate resuscitation, Rpf-encoding genes are mainly transcribed during the early stages of growth. In *M. luteus*, *rpf* transcript levels increase and remain high during lag phase. They decrease during early mid-exponential phase and are below the detection limit once the culture enters stationary phase (Mukamolova *et al.*, 2002b). Changes in Rpf abundance in the culture supernatant follow a similar trend; the protein accumulates during exponential phase, and levels decrease thereafter (Mukamolova *et al.*, 2002b; Telkov *et al.*, 2006). Similarly, Rpfs are primarily expressed in actively growing cells of *Mycobacterium bovis*, *M. smegmatis* and *M. tuberculosis* (Mukamolova *et al.*, 2002a; Shleeva *et al.*, 2004; Tufariello *et al.*, 2004).

In the actinobacteria carrying more than one *rpf* gene, each individual Rpf-encoding gene can have a distinct transcription profile. For example, in *M. smegmatis*, *rpfA* expression increases dramatically during early exponential phase, whereas *rpfB* and *rpfF* transcript levels are highest during lag phase (Shleeva *et al.*, 2013). In *M. tuberculosis*, *rpfB* is most highly expressed during mid-exponential phase (its transcript levels drop considerably thereafter), whereas *rpfC* transcript levels remain elevated well into stationary phase (Tufariello *et al.*, 2004; Gupta *et al.*, 2010). In broth-grown *S. coelicolor*, *rpfA* and *rpfC* transcripts are most abundant in actively growing cells, whereas *rpfD* transcript levels peak during stationary growth (Sexton *et al.*, 2015). Changing expression levels throughout growth and unique expression profiles for each *rpf* gene suggest tight regulatory networks tailored to the individual functions of a given *rpf* gene.

1.5 REGULATION OF *RPF* GENES

The expression and activity of cell wall-lytic enzymes must be carefully controlled to ensure cell survival and growth. While insufficient enzymatic activity could compromise the ability of a dormant cell to resume growth under appropriate growth conditions, excessive activity could weaken the cell wall, leading to cell lysis and death. To maintain the integrity of the cell wall, bacteria rigorously control the expression of the genes encoding the muralytic enzymes, often by regulating transcription initiation (Vollmer *et al.*, 2008b), although other levels of regulation are almost certainly employed.

1.5.1 Transcriptional control by sigma factors

1.5.1.1 SigB activates *rpfB* expression in response to various abiotic stresses.

Specialized sigma factors are expressed in response to specific environmental stresses and direct the RNA polymerase to the appropriate promoters to initiate transcription of the genes required for the cell to cope with the newly arisen conditions (Wösten, 1998; Feklístov *et al.*, 2014). A subset of *rpf* genes is under the control of such factors. The sigma factor SigB, for example, directs *rpfB* transcription in the mycobacteria (Sharma *et al.*, 2015). *sigB* itself is under the transcriptional control of the alternative sigma factors SigE (Manganelli *et al.*, 2001; Dainese *et al.*, 2006), SigF (Dainese *et al.*, 2006) and SigH (Raman *et al.*, 2001; Kaushal *et al.*, 2002; Dainese *et al.*, 2006), which are up-regulated by, and mediate the response to, cell envelope stress (Wu *et al.*, 1997; Manganelli *et al.*, 1999; Manganelli *et al.*, 2001), nutrient starvation (DeMaio *et al.*, 1996; Michele *et al.*, 1999; Betts *et al.*, 2002; Kahramanoglou *et al.*, 2014), and heat shock and oxidative stress (Fernandes *et al.*, 1999; Manganelli *et al.*, 1999; Manganelli *et al.*, 2001; Raman *et al.*, 2001; Manganelli *et al.*, 2002), respectively. Activation of these sigma factors is therefore thought to promote *rpfB* expression.

In addition to controlling *sigB* (and indirectly *rpfB*) expression, these stress-responsive sigma factors also regulate the expression of other *rpf* genes in the mycobacteria via as yet unknown pathways. SigB reduces *rpfC* and *rpfE* transcript levels in response to oxidative stress (Fontán *et al.*, 2009), SigE stimulates *rpfC* expression during active growth (Manganelli *et al.*, 2001), and SigF differentially regulates multiple *rpf* genes during exponential growth (Geiman

et al., 2004; Williams *et al.*, 2007). The sigma factor regulators of most *rpf* genes remain largely unknown, particularly outside of the mycobacteria.

rpf gene regulation by alternative sigma factors is thought to be maintained in the streptomycetes, which encode homologues of the mycobacterial SigE (Paget *et al.*, 1999), SigF (Potúčková *et al.*, 1995) and SigH [named SigR (Paget *et al.*, 1998)] involved in similar stress responses. Consistent with this hypothesis, *rpfA* (like *sigE*) is up-regulated in *S. coelicolor* in response to antibiotic-induced cell envelope stress (Hesketh *et al.*, 2011), and strains lacking *sigF* are phenotypically similar to *rpf* mutant strains (they produce deformed thin-walled spores) (Potúčková *et al.*, 1995; Haiser *et al.*, 2009; Sexton *et al.*, 2015), suggesting potential SigF involvement in Rpf-dependent developmental processes.

1.5.1.2 SigD activates *rpfC* expression in response to nutrient depletion.

In addition to SigB, the alternative sigma factor SigD has also been associated with *rpf* transcription control, where it directs the expression of *rpfC* in the mycobacteria (Raman *et al.*, 2004). Although not direct members of the SigD regulon, *rpfA* and *rpfE* are also affected by SigD, as deleting *sigD* results in marginal increases in transcript levels (Raman *et al.*, 2004).

sigD expression itself is up-regulated in response to nutrient deprivation and the second messenger guanosine 5′-diphosphate-3′-diphosphate (ppGpp) in the corynebacteria (Brockmann-Gretza and Kalinowski, 2006) and mycobacteria (Betts *et al.*, 2002; Dahl *et al.*, 2003; Kahramanoglou *et al.*, 2014). Upon detecting nutrient-limiting conditions, bacteria synthesize this signaling molecule to coordinate a global stress response, called the ‘stringent response’, through large-scale transcriptome changes (Potrykus and Cashel, 2008; Dalebroux and Swanson, 2012). Processes required for stress resistance are prioritized, while pathways necessary for active growth and proliferation are dampened (Potrykus and Cashel, 2008; Dalebroux and Swanson, 2012).

Nutrient limitation and the stringent response promote the onset of dormancy [*e.g.*, sporulation in *Bacillus* (Ochi *et al.*, 1981) and *Streptomyces* (Chakraburtty and Bibb, 1997; Hesketh *et al.*, 2007)]. Consistent with this, they promptly inhibit the expression of certain *rpf* genes, as Rpf activity would counter the transition into dormancy. For example, when exponential-phase *M. tuberculosis* cells are transferred from a nutrient-rich to a nutrient-poor medium (*e.g.*, buffered saline solution), *rpfA* expression decreases (Dahl *et al.*, 2003;

Gupta *et al.*, 2010). Consistent with this observation, deleting the ppGpp synthetase-encoding gene *relA* results in increased *rpfA* transcript levels (Dahl *et al.*, 2003). A similar phenomenon has been observed in the streptomycetes, where the stringent response decreases *rpfA* transcript levels through an as yet unknown mechanism (Hesketh *et al.*, 2007).

1.5.2 Transcriptional control by transcriptional regulators: Crp and its effector, cyclic AMP

ppGpp is not the only second messenger to influence *rpf* gene expression in bacteria. The nucleotide second messenger cyclic AMP (cAMP) also modulates *rpf* expression at the level of transcription initiation through its interaction with the transcriptional regulator cAMP receptor protein (Crp).

1.5.2.1 Crp is a cyclic AMP-responsive DNA-binding protein.

The Crp-cAMP system has been best studied in the model enteric bacterium *Escherichia coli* (Green *et al.*, 2014). Like *E. coli*, the actinobacteria encode homologues of Crp, including GlxR (Cg0350) in *C. glutamicum* (Kim *et al.*, 2004), Crp_{Mtb} (Rv3676) in *M. tuberculosis* (Cole *et al.*, 1998) and Crp_{Sco} (SCO3571) in *S. coelicolor* (Bentley *et al.*, 2002). These homodimeric proteins (Kim *et al.*, 2004; Akif *et al.*, 2006; Akhter *et al.*, 2007; Gallagher *et al.*, 2009; Reddy *et al.*, 2009; Kumar *et al.*, 2010; Stapleton *et al.*, 2010; Townsend *et al.*, 2014) possess two important domains: (i) an N-terminal cAMP-binding domain, and (ii) a C-terminal helix-turn-helix DNA-binding domain (Derouaux *et al.*, 2004a; Kim *et al.*, 2004; Gallagher *et al.*, 2009; Reddy *et al.*, 2009; Townsend *et al.*, 2014).

The DNA-binding domains of each Crp homologue recognize similar palindromic consensus sequences: **TGTG**NNNNNNNN**CACA** in *Corynebacterium* (Kohl *et al.*, 2008; Toyoda *et al.*, 2011; Jungwirth *et al.*, 2013), **YGTGA**NNNNNN**TCACR** in *Mycobacterium* (Bai *et al.*, 2005; Rickman *et al.*, 2005; Kahramanoglou *et al.*, 2014) and **GTG**NNNNNNGN**CAC** in *Streptomyces* (Gao *et al.*, 2012). Sequence recognition is critical for DNA binding (Bai *et al.*, 2005; Rickman *et al.*, 2005; Akhter *et al.*, 2007; Kohl *et al.*, 2008; Stapleton *et al.*, 2010; Toyoda *et al.*, 2011; Aung *et al.*, 2014).

The second messenger cAMP modulates the DNA-binding activity of Crp homologues. Crystallographic analysis of GlxR (Townsend *et al.*, 2014) and Crp_{Mtb} (Reddy *et al.*, 2009; Kumar *et al.*, 2010) revealed allosteric modifications of

the protein upon cAMP binding, resulting in a rearrangement of the DNA-binding domain into a conformation more conducive to protein-DNA interactions. Though cAMP binding has been demonstrated conclusively for several Crp homologues (Derouaux *et al.*, 2004b; Bai *et al.*, 2005; Akhter *et al.*, 2007; Reddy *et al.*, 2009; Stapleton *et al.*, 2010; Townsend *et al.*, 2014), its impact on the DNA-binding activity of Crp is species-specific. In *C. glutamicum*, GlxR binding to Crp recognition sites is primarily cAMP-dependent (Kim *et al.*, 2004; Letek *et al.*, 2006; Jungwirth *et al.*, 2008; Kohl *et al.*, 2008; Toyoda *et al.*, 2011; Jungwirth *et al.*, 2013), whereas it is largely cAMP-independent in the mycobacteria, though cAMP does increase affinity for DNA (Bai *et al.*, 2005; Rickman *et al.*, 2005; Akhter *et al.*, 2007; Reddy *et al.*, 2009; Stapleton *et al.*, 2010; Aung *et al.*, 2014). cAMP also affects the DNA-binding activity of Crp homologues differently according to the gene. For example, although DNA binding by GlxR typically requires cAMP (Kim *et al.*, 2004; Letek *et al.*, 2006; Jungwirth *et al.*, 2008; Kohl *et al.*, 2008; Toyoda *et al.*, 2011; Jungwirth *et al.*, 2013), binding to some sites, like those associated with the cell wall remodeling gene *cgR_1596* and the stress response gene *mscL*, is cAMP-independent, though cAMP does enhance GlxR's affinity for DNA (Kohl *et al.*, 2008; Toyoda *et al.*, 2011).

As is the case in *C. glutamicum* and *M. tuberculosis*, the *S. coelicolor* Crp_{Sco} interacts with Crp binding sites associated with genes involved in a broad range of cellular processes, including antibiotic biosynthesis (Derouaux *et al.*, 2004a; Gao *et al.*, 2012). Many research groups have sought to ascertain whether Crp_{Sco} requires cAMP in order to bind DNA; however, electrophoretic mobility shift assays conducted with purified recombinant or native Crp_{Sco}, in the presence and absence of cAMP, consistently failed owing to the particularly low pI of the protein (Derouaux *et al.*, 2004b; Gao *et al.*, 2012), and so it remains unclear whether cAMP is essential for DNA-binding in the streptomycetes. It should be noted that both Crp_{Sco} and cAMP are involved in similar developmental processes (Süsstrunk *et al.*, 1998; Derouaux *et al.*, 2004a), suggesting Crp_{Sco} and cAMP work together to regulate *Streptomyces* growth and development.

1.5.2.2 Crp regulates resuscitation in the actinobacteria.

Crp homologues and cAMP are intimately involved in promoting the resuscitation of dormant actinobacteria. This is exemplified in *S. coelicolor*, where both Crp_{Sco} and cAMP are required for spore germination: most spores are unable to germinate following *crp* deletion (Derouaux *et al.*, 2004a) or *cya*

disruption, where *cya* encodes the adenylate cyclase responsible for cAMP synthesis (Süsstrunk *et al.*, 1998).

cAMP also triggers the resuscitation of dormant mycobacteria in response to exogenous unsaturated fatty acids, such as oleic acid. Indeed, chemical inhibition of adenylate cyclases prevents oleic acid-mediated resuscitation of dormant *M. smegmatis* (Shleeva *et al.*, 2013). Furthermore, deleting the gene encoding the fatty acid-activated adenylate cyclase renders dormant cells insensitive to fatty acids; however, supplying exogenous cAMP to the growth medium restores the fatty acid-dependent resuscitation phenotype to adenylate cyclase-deficient strains (Shleeva *et al.*, 2013).

Further investigation revealed that cAMP-dependent resuscitation of *M. smegmatis* requires one or more Rpf proteins. *rpfA* expression is dramatically up-regulated in response to oleic acid, and inhibiting Rpf activity through supplementation of the growth medium with the chemical inhibitor 4-benzoyl-2-nitrophenylthiocyanate hampers cAMP-mediated resuscitation (Shleeva *et al.*, 2013).

cAMP likely stimulates Rpf-dependent resuscitation through its interaction with Crp. In *M. tuberculosis*, Crp_{Mtb} activates *rpfA* transcription upon binding the *rpfA* promoter region (Rickman *et al*., 2005; Kahramanoglou *et al*., 2014). Crp_{Mtb} also stimulates *rpfD* expression (Kahramanoglou *et al*., 2014), and though evidence for binding of the regulatory region is lacking (Kahramanoglou *et al.*, 2014), an *in silico* investigation revealed a Crp binding site associated with *rpfD* (Spreadbury *et al.*, 2005). Similarly, in *C. glutamicum*, GlxR binds sites upstream of both *rpf* genes (Jungwirth *et al.*, 2008; Kohl *et al.*, 2008; Toyoda *et al.*, 2011; Jungwirth *et al.*, 2013) and activates *rpf2* expression (its effect on *rpf1* expression has not been investigated) (Jungwirth *et al.*, 2008). Furthermore, GlxR is predicted to directly repress the expression of an *rpf2* transcriptional repressor (Jungwirth *et al.*, 2008).

Crp-mediated regulation of *rpf* genes is predicted to be maintained in the streptomycetes. Crp_{Sco}, cAMP and the Rpfs all contribute to spore germination and are all expressed during germination and the ensuing exponential phase or vegetative growth (Gersch *et al.*, 1979; Süsstrunk *et al.*, 1998; Derouaux *et al.*, 2004a; Haiser *et al.*, 2009; Gao *et al.*, 2012; Sexton *et al.*, 2015). This raises the tantalizing possibility that Crp_{Sco}-cAMP may function immediately upstream of the Rpfs in the resuscitation process.

1.5.2.3 Other transcriptional regulators modulate *rpf* gene expression.

Beyond Crp, other transcriptional regulators control *rpf* gene expression. In *C. glutamicum*, the LuxR-like transcriptional regulator RamA directly activates *rpf2* transcription, whereas the HTH_3 family transcriptional regulator RamB directly represses *rpf2* expression (Jungwirth *et al.*, 2008). Homologues of *ramA* (Cramer *et al.*, 2006) and *ramB* (Gerstmeir *et al.*, 2004; Krawczyk *et al.*, 2009) are present in the genomes of other actinobacteria, including the streptomycetes, and RamB recognition sites are associated with *rpfB* in *M. tuberculosis* (Krawczyk *et al.*, 2009). However, their function in the latter organisms has not been investigated.

The transcriptional regulator MtrA controls *rpfB* expression, at least in the mycobacteria. MtrA, which contributes to the regulation of cell wall metabolism, binds a site spanning the length of the *rpfB* promoter, thereby repressing its expression (Sharma *et al.*, 2015). Though there is no evidence suggesting MtrA regulates *rpfB* homologues in other organisms, MtrA-dependent regulation may be maintained as *mtrA* is highly conserved in the actinobacteria, including *Corynebacterium* and *Streptomyces* (Hoskisson and Hutchings, 2006).

1.5.3 Post-transcriptional and translational regulation by small RNAs

Although gene control by sigma factors (see section 1.5.1) and transcriptional regulators (see section 1.5.2) has been relatively well studied, *rpf* gene regulation by regulatory RNAs, such as small RNAs (sRNAs) (below) and riboswitches (see section 1.5.4), has not been investigated. Interestingly, bioinformatic analyses of certain *rpf* genes suggest regulatory RNAs are promising candidate regulators of these muralytic enzymes.

sRNAs are regulatory elements that modulate the expression of their target gene(s) through a variety of mechanisms (Fig. 1.4). Translational control is exerted through base-pairing between an sRNA and its mRNA target, with the result being (i) the liberation of a ribosome binding site (RBS) and promotion of translation, as is the case for DsrA (Sledjeski *et al.*, 1996; Majdalani *et al.*, 1998), or (ii) the occlusion of the RBS and inhibition of translation initiation, as seen for OxyS (Altuvia *et al.*, 1997; Altuvia *et al.*, 1998). Alternatively, some RNases target mRNA transcripts bound to an sRNA, leading to transcript degradation [*e.g.*, IsrR (Dühring *et al.*, 2006; Legewie *et al.*, 2008)] or increased stability following processing [*e.g.*, GadY (Opdyke *et al.*, 2004; Tramonti *et al.*, 2008; Opdyke *et al.*,

2011)]. Other sRNAs, such as 6S RNA, alter gene expression by binding regulatory proteins. In the case of 6S RNA, it adopts a secondary structure similar to an open promoter complex, thus competing with promoter DNA for binding by RNA polymerase holoenzymes carrying the housekeeping sigma factor σ^{70}. Titration of the enzyme during stationary phase thereby decreases transcription from certain σ^{70}-dependent promoters (Wassarman and Storz, 2000; Trotochaud and Wassarman, 2004; Trotochaud and Wassarman, 2005; Wassarman and Saecker, 2006).

In *S. coelicolor*, many sRNAs have been identified through computational genome-wide analyses (Pánek *et al.*, 2008; Swiercz *et al.*, 2008), direct cloning of short RNAs (Swiercz *et al.*, 2008) and deep-sequencing (Vockenhuber *et al.*, 2011; Moody *et al.*, 2013). Among these sRNAs is Scr3097, an 80-nt transcript encoded by a small convergently transcribed gene located 10 bp downstream of the *rpfA* stop codon (Moody *et al.*, 2013). Given its close proximity to the *rpfA* 3′ end, Scr3097 may impact *rpfA* expression.

1.5.4 Post-transcriptional and translational regulation by riboswitches

1.5.4.1 Riboswitches are *cis*-encoded regulatory RNAs.

Unlike sRNAs, which act on their targets in *trans*, riboswitches are *cis*-acting regulatory sequences residing mainly within the 5′ untranslated region (UTR) of their mRNA target. Like protein regulators, riboswitches sense conditions in the cell by interacting directly with specific metabolites and ions, and following conformational changes, they adjust the expression of their target gene(s) accordingly (Serganov and Nudler, 2013).

1.5.4.2 Riboswitches regulate gene expression in response to specific metabolites or ions.

Riboswitches regulate many processes in bacteria, including ion homeostasis (Cromie *et al.*, 2006; Dann *et al.*, 2007; Baker *et al.*, 2012; Hollands *et al.*, 2012; Shi *et al.*, 2014; Dambach *et al.*, 2015; Furukawa *et al.*, 2015; Price *et al.*, 2015), vitamin metabolism (Mironov *et al.*, 2002; Nahvi *et al.*, 2002; Winkler *et al.*, 2002a; Winkler *et al.*, 2002b), purine metabolism (Mandal *et al.*, 2003; Mandal and Breaker, 2004), nucleoside metabolism (Roth *et al.*, 2007), amino acid metabolism (Epshtein *et al.*, 2003; Grundy *et al.*, 2003; McDaniel *et al.*, 2003; Sudarsan *et al.*, 2003; Winkler *et al.*, 2003; Mandal *et al.*, 2004) and cell

wall metabolism (Winkler *et al.*, 2004; Collins *et al.*, 2007). Many characterized riboswitches are controlled by feedback mechanisms, responding to the products of the pathways they regulate. For example, the *rfn*-, *thi*- and B_{12}-box riboswitches, associated with genes involved in the biosynthesis and transport of vitamins and their derivatives, respond to flavin mononucleotide (Mironov *et al.*, 2002; Winkler *et al.*, 2002b), thiamine pyrophosphate (Mironov *et al.*, 2002; Winkler *et al.*, 2002a) and 5′-deoxy-5′-adenosylcobalamin (Nahvi *et al.*, 2002), respectively. G-box riboswitches alter the expression of purine metabolism genes according to intracellular guanine concentrations (Mandal *et al.*, 2003; Mandal and Breaker, 2004). The *B. subtilis lysC* riboswitch regulates the expression of amino acid metabolism genes by monitoring lysine levels (Grundy *et al.*, 2003; Sudarsan *et al.*, 2003). S-box riboswitches, which regulate the expression of genes involved in sulfur metabolism and cysteine, methionine and *S*-adenosylmethionine biosynthesis, respond to the sulfur-containing, methionine-derived ligand *S*-adenosylmethionine (Epshtein *et al.*, 2003; McDaniel *et al.*, 2003; Winkler *et al.*, 2003). The *glmS* riboswitch, which regulates the expression of a glucosamine-6-phosphate biosynthesis gene, senses glucosamine-6-phosphate (Barrick *et al.*, 2004; Winkler *et al.*, 2004; Collins *et al.*, 2007).

1.5.4.3 Riboswitches use different mechanisms to control gene expression.

A variety of regulatory mechanisms are exploited by riboswitches (Fig. 1.5). Riboswitches can impact transcript elongation processes by modulating the formation of two mutually exclusive structures: an intrinsic terminator and an antiterminator (Fig. 1.5A). For example, when bound to their ligand, certain *B. subtilis* M-box (Dann *et al.*, 2007), G-box (Mandal *et al.*, 2003; Mandal and Breaker, 2004), L-box (Grundy *et al.*, 2003; Sudarsan *et al.*, 2003), S-box (Epshtein *et al.*, 2003; McDaniel *et al.*, 2003; Winkler *et al.*, 2003), *rfn*-box (Mironov *et al.*, 2002; Winkler *et al.*, 2002b) and *thi*-box riboswitches (Mironov *et al.*, 2002) adopt an intrinsic terminator structure, thereby attenuating transcription of their cognate gene(s). Alternatively, ligand binding by a riboswitch can promote transcriptional read-through by stabilizing an antiterminator, as is the case with cobalt- and nickel-binding *czcD* riboswitches in the Firmicutes (Furukawa *et al.*, 2015) and the fluoride-responsive *crcB* riboswitch from *Bacillus cereus* (Baker *et al.*, 2012). The manganese-sensing *yoaB* riboswitch from *Lactococcus lactis* (Price *et al.*, 2015), the glycine-sensing *gcvT* riboswitch from *B. subtilis* (Mandal

et al., 2004) and the cyclic di-GMP-responsive *ompR* riboswitch from *Clostridium difficile* (Lee *et al*., 2010) are thought to function similarly.

Riboswitches can also affect transcript elongation by recruiting the termination factor Rho. The *Salmonella enterica mgtA* riboswitch promotes Rho-dependent termination following Mg^{2+} binding by increasing the accessibility of binding sites to the termination factor (Hollands *et al.*, 2012).

In contrast, some riboswitches dampen gene expression by inhibiting mRNA translation initiation (Fig. 1.5B). For example, a *thi*-box riboswitch from *E. coli* occludes the RBS upon binding its specific metabolite, resulting in mRNA translation inhibition (Winkler *et al.*, 2002a). The B_{12}-, *rfn*- and L-box riboswitches associated with *btuB* in *E. coli* (Nou and Kadner, 2000; Nahvi *et al.*, 2002), *ypaA* in *B. subtilis* (Winkler *et al.*, 2002b) and *lysC* in *E. coli* (Caron *et al.*, 2012), respectively, are thought to function similarly. On the other hand, binding of the divalent transition metal Mn^{2+} to the *E. coli mntP* riboswitch promotes translation initiation of the transcript by stabilizing a ribosome-accessible alternative structure (Dambach *et al.*, 2015).

Riboswitches can control gene expression by altering the stability of their associated mRNA transcript (Fig. 1.5C). For example, the *B. subtilis glmS* riboswitch down-regulates the expression of its cognate gene by working as a metabolite-responsive ribozyme (Winkler *et al.*, 2004; Collins *et al.*, 2007). Upon binding glucosamine-6-phosphate, it catalyzes mRNA cleavage at a site upstream of the RBS (Barrick *et al.*, 2004; Winkler *et al.*, 2004). The break generates a 5′-hydroxylated downstream product that is subsequently degraded by the 5′→3′ exoribonuclease RNase J1, ultimately reducing *glmS* mRNA abundance (Collins *et al.*, 2007). In contrast, the *E. coli lysC* riboswitch affects *lysC* expression by recruiting the RNA degradosome in response to lysine (Caron *et al.*, 2012). Lysine binding alters the conformation of the riboswitch aptamer, exposing two RNase E cleavage sites, leading to the rapid degradation of *lysC* mRNA (Caron *et al.*, 2012).

Though far less documented, some riboswitches can also exert their regulatory effects in *trans*. In the food-borne pathogen *Listeria monocytogenes*, the SreA riboswitch prematurely terminates the expression of its downstream genes in response to *S*-adenosylmethionine, and the resulting truncated transcript functions as an sRNA that represses the expression of a virulence factor upon binding its complementary sequence within the 5′ UTR of the encoding mRNA (Loh *et al.*, 2009). In *Enterococcus faecalis*, an adenosylcobalamin-responsive riboswitch attenuates the expression of EutX, an

sRNA that inhibits ethanolamine utilization genes by titrating the antiterminator protein EutV (DebRoy *et al.*, 2014).

1.5.4.4 The *ydaO* riboswitch is a cyclic di-AMP-responsive regulatory RNA.

In 2004, a putative riboswitch motif, named *ydaO* after its cognate gene in *B. subtilis*, was identified through computational analyses of conserved intergenic sequences with riboswitch-like characteristics (Barrick *et al.*, 2004). The *ydaO* riboswitch element is widespread, particularly among Gram-positive bacteria (Barrick *et al.*, 2004; Block *et al.*, 2010; Nelson *et al.*, 2013). Although the *ydaO* motif is strictly connected to transport genes in *B. subtilis*, it is almost exclusively associated with cell wall remodeling genes in the actinobacteria (Barrick *et al.*, 2004; Block *et al.*, 2010; Nelson *et al.*, 2013).

In the bacilli, the *ydaO* riboswitch functions as an 'OFF' switch, prematurely terminating transcription of its associated genes (Nelson *et al.*, 2013). Originally thought to respond to ATP (Watson and Fedor, 2012), recent work by Nelson *et al.* (2013) demonstrated unequivocally that the *ydaO* riboswitch responds to the second messenger cyclic di-AMP.

Cyclic di-AMP, a ubiquitous bacterial second messenger, is predicted to modulate the expression of certain *rpf* genes in the actinobacteria, as a *ydaO*-like riboswitch motif is associated with *rpfA* homologues in the corynebacteria, mycobacteria and streptomycetes (Haiser *et al.*, 2009; Block *et al.*, 2010; Nelson *et al.*, 2013). In *B. subtilis*, cyclic di-AMP regulates a wide variety of processes, including peptidoglycan homeostasis (Luo and Helmann, 2012; Mehne *et al.*, 2013) and sporulation (Oppenheimer-Shaanan *et al.*, 2011). Production is achieved by any one of three diadenylate cyclases (Witte *et al.*, 2008; Mehne *et al.*, 2013), of which DisA is best characterized. This enzyme forms a homo-octomer, with each subunit comprising three distinct domains: (i) a DAC (**di**a**c**denylate **c**yclase) domain, which converts ATP to cyclic di-AMP, (ii) a 'helical spine', and (iii) a DNA-binding domain (Witte *et al.*, 2008). *disA* homologues have been identified in both sporulating (*e.g.*, *Clostridium*, *Streptomyces*) and non-sporulating (*e.g.*, *Mycobacterium*) bacteria (Bejerano-Sagie *et al.*, 2006; Bai *et al.*, 2012).

DisA has been best studied in *B. subtilis*, where it evaluates general chromosome integrity and enables cells to proceed with sporulation only if the DNA is deemed to be of suitable quality. At the onset of sporulation, DisA accumulates in the cell and forms a single, mobile focus, scanning the

chromosome for damage (Bejerano-Sagie *et al.*, 2006). It produces cyclic di-AMP, which triggers sporulation (Witte *et al.*, 2008; Oppenheimer-Shaanan *et al.*, 2011). However, upon detecting damaged DNA (particularly branched DNA), the DisA focus halts its movement, binds the damaged DNA, and ceases to synthesize cyclic di-AMP (Bejerano-Sagie *et al.*, 2006; Witte *et al.*, 2008). As a result, intracellular pools of cyclic di-AMP decrease, expression of early sporulation genes is inhibited, and sporulation is delayed (Bejerano-Sagie *et al.*, 2006; Oppenheimer-Shaanan *et al.*, 2011).

Decreasing cyclic di-AMP concentrations are also owed, in part, to the cyclic dinucleotide phosphodiesterase YybT, a transmembrane protein expressed at the onset of sporulation (Oppenheimer-Shaanan *et al.*, 2011). Interestingly, ppGpp competitively inhibits YybT activity *in vitro* (Rao *et al.*, 2010), suggesting that the stringent response stimulates increases in cyclic di-AMP pools, and thus promotes sporulation in the absence of DNA damage. There are no obvious phosphodiesterase-encoding genes in *Streptomyces* genomes.

1.5.5 Post-translational regulation through protein modification, protein-protein interactions and proteolysis

While transcriptional and translational control of protein expression represent major regulatory strategies employed in bacterial cells, post-translational modification of proteins provides yet another level of control. In *C. glutamicum*, a membrane-bound protein-*O*-mannosyltransferase, Pmt, is involved in glycosylating Rpf2 (Mahne *et al*., 2006), which *in vivo* is covalently bound to mannose and galactose (Hartmann *et al.*, 2004). The impact of these post-translational modifications on enzyme activity has yet to be investigated, and whether or not Rpfs in other actinobacteria are similarly glycosylated remains to be seen, but it is worth noting that *pmt* is conserved in this bacterial group (Mahne *et al.*, 2006).

Protein-protein interactions can also effectively regulate enzyme activity. In the mycobacteria, some Rpfs possess secreted binding partners (Hett *et al.*, 2007) that are thought to modulate both their muralytic and resuscitative activities. Purified RpfB, for example, has minimal muralytic activity alone, and though it promotes resuscitation of dormant mycobacteria, it does so poorly (Hett *et al.*, 2008; Hett *et al.*, 2010; Nikitushkin *et al.*, 2015). But, when paired with the essential peptidoglycan endopeptidase RipA, efficient and synergistic cell wall digestion occurs, and resuscitation activity is greatly enhanced (Hett *et al.*, 2008; Hett *et al.*, 2010; Nikitushkin *et al.*, 2015). This interaction is subject to

competition from the peptidoglycan transpeptidase PBP1, which also associates with RipA and inhibits the synergistic association between RipA and RpfB (Hett *et al.*, 2010). Interestingly, the transcriptional regulator MtrA directly activates *ripA* expression (Plocinska *et al.*, 2012), while it inhibits *rpfB* transcription (Sharma *et al.*, 2015).

Although *S. coelicolor* lacks the protein partner RipA (Sexton *et al.*, 2015), the activity of its Rpfs is also regulated through protein-protein interactions. For example, in RpfB, the DUF348 domains promote protein dimerization, which serves to decrease the peptidoglycan cleavage activity of this enzyme (Sexton *et al.*, 2015).

Given that secreted Rpfs are eliminated from the culture medium at the onset of stationary phase (Mukamolova *et al.*, 2002b; Shleeva *et al.*, 2004; Telkov *et al.*, 2006), it is also likely that these factors are subject to proteolytic degradation. Degradation of proteins during stationary phase is common in bacteria, and is thought to provide a rich source of amino acids during starvation, for use in the synthesis of resistance proteins (Rittershaus *et al.*, 2013).

1.6 AIMS AND OUTLINE OF THESIS

In the actinobacteria, *rpf* gene expression must be tightly controlled to ensure sufficient expression to promote resuscitation and dormancy, while at the same time limiting enzymatic activity to prevent cell lysis. To date, most work has focused on transcriptional regulation by sigma factors (see section 1.5.1) and transcriptional activators and repressors (see section 1.5.2). Given the need for strict control over the expression and activity of muralytic enzymes, *rpf* gene expression is likely subject to additional levels of fine-tuning following transcription initiation through the activity of non-coding RNAs, RNA-binding proteins and/or protease-mediated protein turnover.

In the model bacterium *S. coelicolor*, *rpfA* is thought to be subject to multiple levels of regulation to ensure proper sporulation and spore germination. Previous work conducted by several research groups hints at the possibility that *rpfA* is subject to transcriptional control by the protein regulator Crp_{Sco} (see section 1.5.2.2). The recent discovery of a cyclic di-AMP-responsive riboswitch motif upstream of *rpfA* (see section 1.5.4.4) and of an sRNA-encoding gene located immediately downstream of *rpfA* (see section 1.5.3) suggests post-transcriptional control. Motivated by these observations, we set out to characterize the various networks regulating *rpfA* expression in *S. coelicolor*.

Chapter 2 describes our investigation into *rpfA* regulation. We uncovered multi-level regulation of *rpfA* expression by three distinct nucleotide second messengers with known functions in dormancy and/or resuscitation. The transcriptional regulator Crp_{Sco} activated *rpfA* transcription initiation during active growth. The riboswitch element associated with *rpfA* decreased *rpfA* transcript abundance in response to cyclic di-AMP. During the transition into stationary phase, a secreted metalloprotease rapidly degraded existing RpfA proteins in the culture medium in response to the nutrient starvation signal ppGpp. These findings were recently published in *Molecular Microbiology.*

Though we had determined that the riboswitch motif negatively impacted *rpfA* transcript abundance in cells, we had not to this point uncovered the mechanism by which this non-coding RNA exerted its effect. Chapter 3 presents our work on the riboswitch's mode of action. Using a combination of computational and experimental approaches, we discovered that the *rpfA* riboswitch, despite lacking an obvious expression platform, inhibited gene expression by modulating transcription processivity in response to cyclic di-AMP. We also identified novel activity determinants within the riboswitch element required for ligand-dependent attenuation. These findings represent unpublished work.

Our recent discovery of an sRNA-encoding gene, *SCR3097*, located immediately downstream of *rpfA* (Moody *et al.*, 2013) suggested possible sRNA-dependent regulation of *rpfA* and other genes. Chapter 4 presents our work to date investigating Scr3097-dependent gene regulation in *S. coelicolor*. Our findings suggested a role for Scr3097 in both cell wall metabolism and microaerobic energy metabolism. We discuss future directions for this project. Our findings have not been published.

1.7 FIGURES

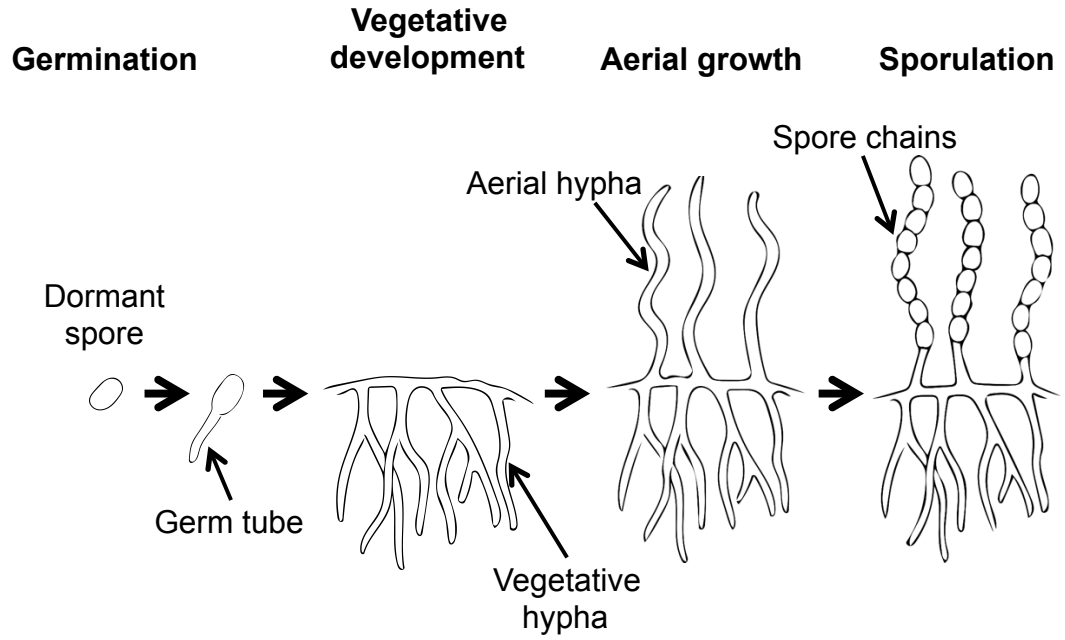

Fig. 1.1. The *Streptomyces* life cycle. *Streptomyces* spores germinate when abundant nutrients become available. The sprouting germ tubes grow into the substrate by tip extension and branching, giving rise to a filamentous, vegetative mycelium. Aerial hyphae emerge from the substrate mycelium into the air and subdivide into pre-spore compartments, which mature into reproductive, dormant spores. Image credit: David Crisante.

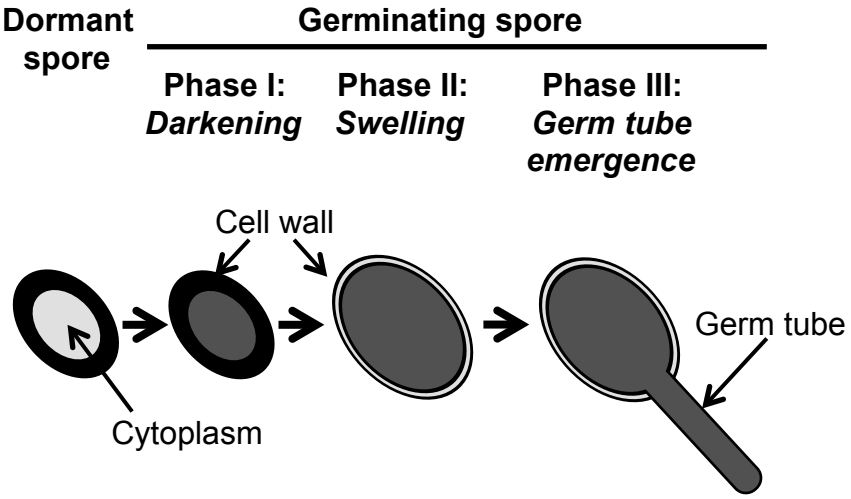

Fig. 1.2. *Streptomyces* spore germination. Spore germination is divided into three separate stages. The first step, called 'darkening', is characterized by a change in spore refractivity: spores, which are phase-bright when dormant, become progressively phase-dark. The second step, 'spore swelling', is typified by an increase in spore volume and a change in spore wall architecture. During the third and last step of germination, thin-walled germ tubes emerge from the spore, and vegetative growth begins.

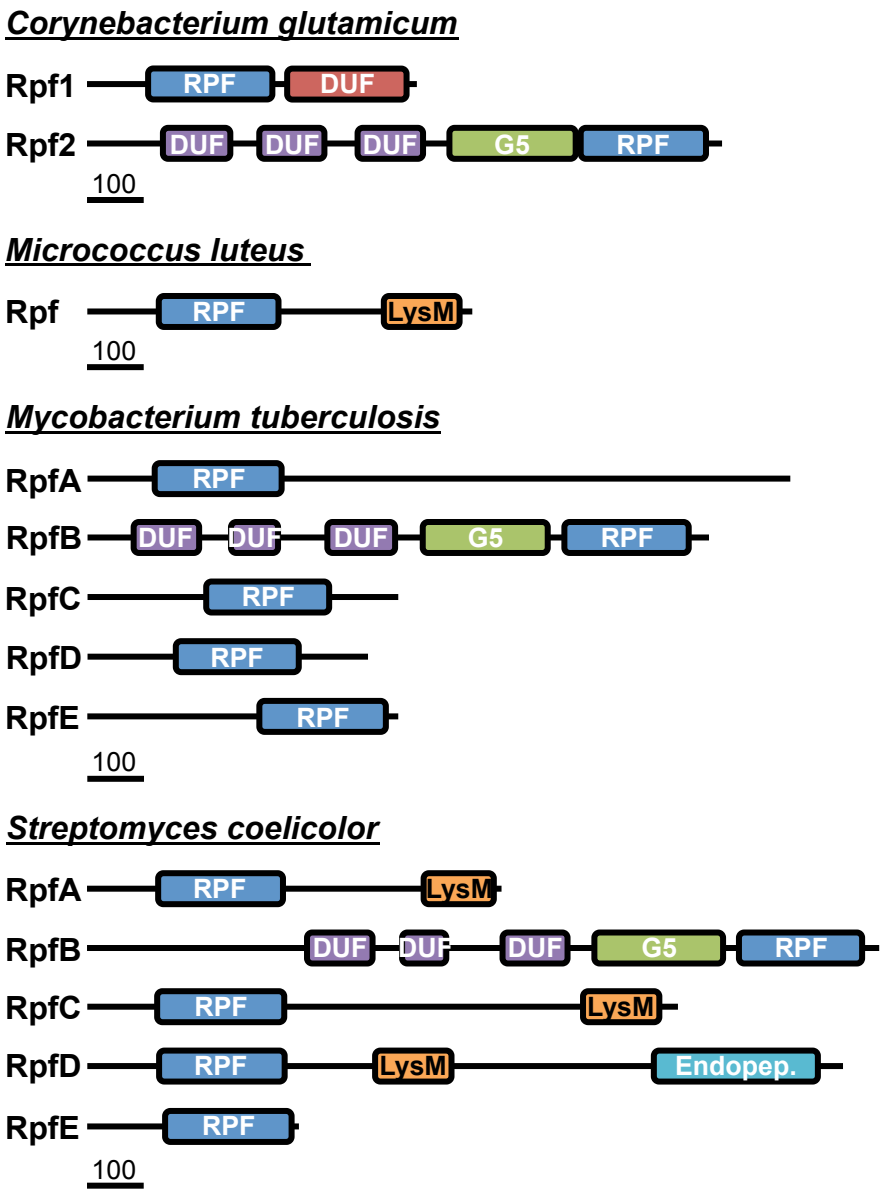

Fig. 1.3. Domain architecture of Rpf proteins. Although all Rpf proteins share the conserved transglycosylase domain (RPF), their domain architecture varies. Some Rpfs possess an *N*-acetylglucosamine-binding domain, such as the LysM domain (Buist *et al.*, 2008) or the G5 domain (Bateman *et al.*, 2005), which is thought to bind peptidoglycan. RpfB homologues also carry a domain of unknown function (DUF), DUF348 (purple), which was recently shown to promote protein dimerization (Sexton *et al.*, 2015). The *S. coelicolor* RpfD also possesses a C-terminal endopeptidase domain (Endopep.). DUF (red), DUF3235. Bar, 100 amino acid residues.

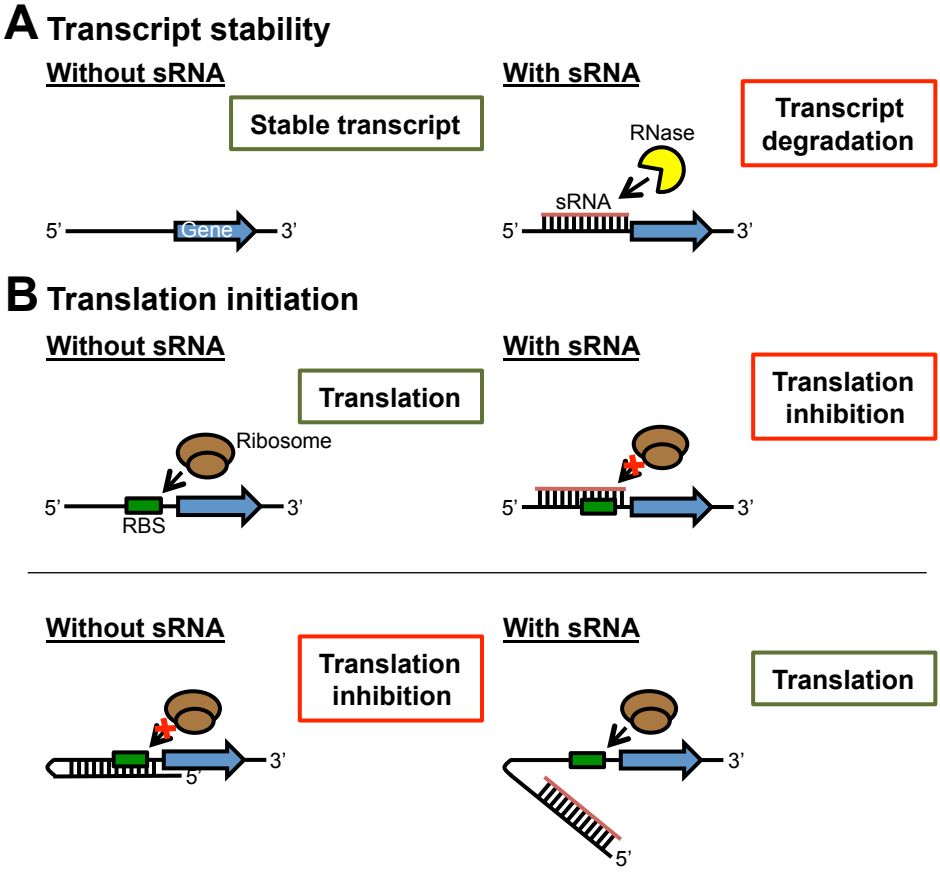

Fig. 1.4. sRNA-dependent regulation of gene expression. (A) Binding of the small RNA (sRNA) to its mRNA target recruits an RNase. (B) Upon binding the ribosome binding site (RBS) of its mRNA target, the sRNA occludes the RBS and inhibits translation of the transcript. Alternatively, by base-pairing with its mRNA target, the sRNA relieves an RBS-sequestering secondary structure, exposing the RBS for binding with the ribosome.

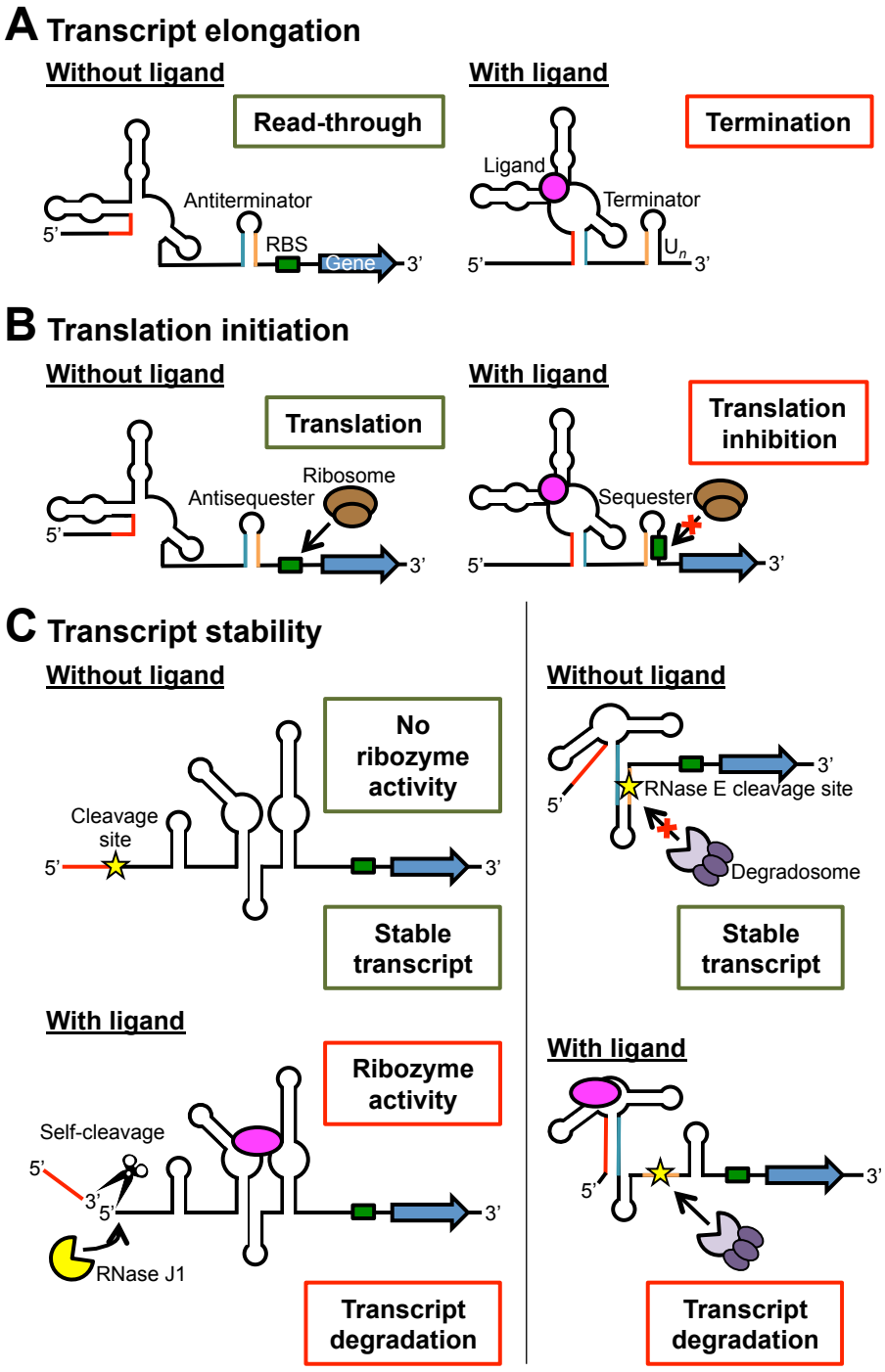

Fig. 1.5. Riboswitch-dependent regulation of gene expression. Upon binding a specific ligand, the riboswitch undergoes a conformational change, resulting in the stabilization of an alternative structure, such as an intrinsic terminator (A) or a ribosome binding site (RBS)-sequestering structure (B), which prematurely terminates transcription or inhibits translation initiation, respectively. Alternatively, structural changes promote self-cleavage (ribozyme activity) or recruit an RNase, thereby decreasing transcript stability (C).

CHAPTER 2

NUCLEOTIDE SECOND MESSENGER-MEDIATED REGULATION OF A MURALYTIC ENZYME IN *STREPTOMYCES*

Renée J. St-Onge, Henry J. Haiser, Mary R. Yousef, Emma Sherwood, Natalia Tschowri, Mahmoud Al-Bassam, Marie A. Elliot

The contents of this chapter were previously published in *Molecular Microbiology* in May 2015 (reference below). The manuscript and all associated figures and tables are used in this thesis with permission from the publisher, John Wiley and Sons.

St-Onge, R.J., Haiser, H.J., Yousef, M.R., Sherwood, E., Tschowri, N., Al-Bassam, M., and Elliot, M.A. (2015) Nucleotide second messenger-mediated regulation of a muralytic enzyme in *Streptomyces*. *Mol Microbiol* **96:** 779-795.

With few exceptions (listed below), I conducted all the experiments and performed all the data processing and analyses. I wrote the manuscript and prepared all the figures and tables. Henry J. Haiser constructed *S. coelicolor* strains E104a/pIJ82, E104a/pMC228, E104a/pMC229 and E104a/pMC230, and he monitored secreted RpfA protein levels in cultures of *S. coelicolor* strain E104a/pMC228*.* Mary R. Yousef determined the cellular localization of RpfA in liquid- and plate-grown *S. coelicolor* strain E104a/pMC228, and she conducted the initial in-line probing assays to characterize the secondary structure of the *rpfA* riboswitch in the absence of a ligand. Emma Sherwood constructed *S. coelicolor* strains M145/pIJ10257 and M145/pIJ10257-*crp*, and performed chromatin immunoprecipitation of Crp_{Sco}-bound DNA from *S. coelicolor* strains Δ*crp*/pIJ6902 and Δ*crp*/pIJ6902*crp.* Natalia Tschowri and Mahmoud Al-Bassam constructed the Δ*disA* mutant strain of *S. venezuelae* and quantified cyclic di-AMP levels in broth-grown wild-type and Δ*disA* mutant *S. venezuelae*. Each author contributed to designing the experiments, interpreting the data and editing the manuscript.

2.1 SUMMARY

Peptidoglycan degradative enzymes have important roles at many stages during the bacterial life cycle, and it is critical that these enzymes be stringently regulated to avoid compromising the integrity of the cell wall. How this regulation is exerted is of considerable interest: promoter-based control and protein-protein interactions are known to be employed; however, other regulatory mechanisms are almost certainly involved. In the actinobacteria, a class of muralytic enzymes – the 'resuscitation-promoting factors' (Rpfs) – orchestrates the resuscitation of dormant cells. In this study, we have taken a holistic approach to exploring the mechanisms governing RpfA function using the model bacterium *Streptomyces coelicolor*, and have uncovered unprecedented multi-level regulation that is coordinated by three second messengers. Our studies show that RpfA is subject to transcriptional control by the cyclic AMP receptor protein, riboswitch-mediated transcription attenuation in response to cyclic di-AMP, and growth stage-dependent proteolysis in response to ppGpp accumulation. Furthermore, our results suggest that these control mechanisms are likely applicable to cell wall lytic enzymes in other bacteria.

2.2 ABBREVIATED SUMMARY

Streptomyces bacteria have an unusual life cycle, which culminates in the development of dormant spores. Spore germination and outgrowth require the activity of dedicated cell wall-degrading enzymes, the regulation of which is poorly understood. Here, we have uncovered an intricate, multi-level regulatory network orchestrated by three different signaling molecules.

2.3 INTRODUCTION

To survive inhospitable environments, bacteria can adopt dormant states, reducing their metabolic activity and ceasing to divide, only resuming growth when exposed to favorable conditions. Dormancy can take many forms, encompassing everything from endo- and exo-spore formation by the soil-dwelling *Bacillus* and *Streptomyces*, respectively, to the low or non-replicative states of *Micrococcus* and *Mycobacterium* (Dworkin and Shah, 2010; Rittershaus *et al.*, 2013). Though dormancy triggers vary, starvation is frequently a

contributing factor. Nutrient limitation in bacteria typically leads to the initiation of a global stress response mediated by the second messenger guanosine 5′-diphosphate-3′-diphosphate, or ppGpp. This 'stringent response' activates pathways required for stress resistance (Potrykus and Cashel, 2008; Dalebroux and Swanson, 2012), including sporulation in *Bacillus* and *Streptomyces* (Ochi *et al.*, 1981; Chakraburtty and Bibb, 1997; Hesketh *et al.*, 2007).

The adoption of a 'dormant' state is typically accompanied by extensive remodeling of the cell wall (Bradley and Ritzi, 1968; Cunningham and Spreadbury, 1998; Atrih and Foster, 1999; Lavollay *et al.*, 2008). The physical restrictions imposed on the dormant cell by this modified wall must be relieved when the cell resumes active growth, and this is achieved in part by the action of cell wall lytic enzymes. In actinobacteria, including *Micrococcus*, *Mycobacterium* and *Streptomyces,* cell wall remodeling-dependent resuscitation is attributed in part to a family of extracytoplasmic proteins known as the resuscitation-promoting factors (Rpfs) (Mukamolova *et al.*, 1998b; Mukamolova *et al.*, 2002a; Zhu *et al.*, 2003; Downing *et al.*, 2005; Keep *et al.*, 2006; Mukamolova *et al.*, 2006; Telkov *et al.*, 2006; Kana *et al.*, 2008; Haiser *et al.*, 2009). Rpfs are lysozyme-like enzymes that target the sugar backbone of peptidoglycan (Cohen-Gonsaud *et al.*, 2004a; Cohen-Gonsaud *et al.*, 2005; Mukamolova *et al.*, 2006; Telkov *et al.*, 2006; Hett *et al.*, 2008; Haiser *et al.*, 2009; Ruggiero *et al.*, 2009), a major component of the bacterial cell wall. As their name suggests, the Rpfs play an important role in the resuscitation of dormant cells. In *Streptomyces*, this corresponds to spore germination, the first step in its life cycle. On solid medium, germination is followed by the growth of filamentous, vegetative hyphae, and later, the production of a second cell type (aerial hyphae) that ultimately differentiates into long chains of reproductive spores (Flärdh and Buttner, 2009). In contrast, during liquid culture growth, most streptomycetes grow vegetatively, and as nutrients become limiting they enter stationary phase instead of differentiating into spores.

Streptomyces coelicolor encodes five Rpfs amongst a whole host of other cell wall lytic enzymes that likely function at different stages of development (Haiser *et al.*, 2009). As for all cell wall lytic proteins, the expression and activity of these enzymes must be rigorously controlled, so as to prevent cell lysis. To date, our understanding of cell wall lytic enzyme governance has largely centered on transcriptional control and regulation through protein-protein interactions (Vollmer *et al.*, 2008b). In the case of the Rpfs, their muralytic activity may be modulated (at least in *Mycobacterium*) through interaction with other extracytoplasmic cell wall lytic enzymes (Hett *et al.*, 2007; Hett *et al.*, 2008). In *Corynebacterium* (Jungwirth *et al.*, 2008) and *Mycobacterium* (Rickman *et al.*,

2005), a subset of *rpf* genes is also targeted for transcriptional activation by the cyclic AMP (cAMP) receptor protein (Crp), a cAMP-binding transcription factor that regulates many fundamental biological processes in bacteria, including the switch between quiescence and active growth (Green *et al.*, 2014) .

It is conceivable that other as yet unexplored levels of regulation exist for these enzymes and their corresponding genes, with an intriguing candidate being riboswitch-mediated control. Riboswitches are *cis*-acting RNAs residing primarily within the 5′ untranslated region (UTR) of their mRNA targets (Serganov and Nudler, 2013). These regulatory elements have two domains: an upstream sensor that binds a specific cellular metabolite, and a downstream expression platform that dictates the regulatory response. Following ligand binding by the sensor domain, the expression platform of the riboswitch undergoes a conformational change, stabilizing an alternative structure that promotes or hinders the expression of the downstream encoded gene (Serganov and Nudler, 2013). Riboswitch activity most commonly impacts transcript elongation and translation initiation, but it has also been shown to affect transcript processing and stability (Serganov and Nudler, 2013).

In the corynebacteria, mycobacteria and streptomycetes, *rpfA* is associated with a long 5′ UTR that shares sequence and structural similarities with the sensor domain of the *Bacillus subtilis ydaO* riboswitch (Haiser *et al.*, 2009; Block *et al.*, 2010; Nelson *et al.*, 2013), though it appears to lack an obvious expression platform. To date, this riboswitch has been characterized exclusively in *B. subtilis*, where it prematurely terminates transcription in response to high levels of cyclic di-AMP (c-di-AMP) (Nelson *et al.*, 2013). Riboswitch-dependent regulation of cell wall lytic enzyme-encoding genes has not been investigated to date.

Given its central function in exiting dormancy [by promoting spore germination (Haiser *et al.*, 2009)] as well as its need for exquisitely tight regulation, we set out to explore *rpfA* regulation in *S. coelicolor*. We determined that RpfA levels are controlled at multiple levels, including transcription initiation, post-transcription and post-translation. These investigations revealed that the *rpfA* locus functions as a regulatory hub, integrating signals from at least three second messengers to modulate cell wall metabolism, dormancy and resuscitation.

2.4 RESULTS

2.4.1 RpfA proteins are abundant in early exponential-phase cultures.

As a first step to understanding *rpfA* regulation, we monitored RpfA production throughout growth. To facilitate detection via immunoblotting, RpfA was expressed from its native promoter as a C-terminal FLAG-tagged fusion protein. RpfA-FLAG was determined to be functional, as it complemented the heat-shock sensitivity phenotype of the Δ*rpfA* mutant (Fig. 2.1). When *S. coelicolor* was grown in a rich liquid medium, RpfA-FLAG was abundant in the culture supernatant during exponential growth and was undetectable in stationary-phase cultures (Fig. 2.2); we were never able to detect RpfA-FLAG in crude cell extracts prepared from either liquid- or plate-grown cultures (Fig. 2.3 and data not shown).

2.4.2 Crp binds the *rpfA* promoter region and activates transcription initiation.

In the streptomycetes, RpfA is involved in resuscitation from dormancy, and specifically spore germination, where loss of *rpfA* delays germination initiation (Haiser *et al.*, 2009). Germination defects have also been noted for strains lacking either the global transcriptional regulator Crp (Derouaux *et al.*, 2004a) or its effector cAMP (Süsstrunk *et al.*, 1998). Interestingly, both *rpfA* promoter activity (Sexton *et al.*, 2015) and extracellular cAMP levels (Süsstrunk *et al.*, 1998) are highest during spore germination. Furthermore, *rpfA* transcript (Sexton *et al.*, 2015) and RpfA protein (Fig. 2.2) profiles mirror those of *crp* transcripts and extracellular cAMP accumulation (Gao *et al.*, 2012), with all peaking during exponential growth. Given the shared phenotypes and similar expression profiles, we set out to investigate the possibility that Crp activated *rpfA* transcription. We first leveraged transcriptomic data obtained in a previous study (Gao *et al.*, 2012) and looked for changes in *rpfA* transcript abundance following *crp* induction in a Δ*crp* mutant. We found *rpfA* expression was dramatically up-regulated (28-fold) within 60 min of *crp* induction (Fig. 2.4A). To confirm these findings, we quantified *rpfA* transcripts in exponential-phase wild-type and *crp*-overexpressing strains using reverse transcription (RT)-coupled real-time PCR (qPCR), and found *rpfA* transcript levels were ~2-fold greater when overexpressing *crp* in a wild-type background (Fig. 2.4B). *rpfA* up-regulation was lower upon overexpressing Crp in the wild-type (Fig. 2.4B) than when inducing *crp* expression in the Δ*crp* mutant

(Fig. 2.4A); this discrepancy was likely due to background Crp production in the wild-type but not the Δ*crp* mutant. Interestingly, expression of another Rpf-encoding gene (*rpfC*) was not altered (Fig. 2.4A and 2.4B), suggesting that the Crp effect was specific to *rpfA*.

To determine whether this was a direct or an indirect response to Crp, we conducted chromatin immunoprecipitation (ChIP) assays using an anti-Crp antibody, and used qPCR to test for enrichment of *rpfA* promoter DNA. We observed enrichment of *rpfA* promoter sequences (Fig. 2.4C) at levels similar to those seen previously for known Crp targets (Gao *et al.*, 2012), suggesting that Crp specifically associated with the *rpfA* promoter, up-regulating its expression. Consistent with these findings, we identified a sequence (**TGAGA**gataggg**TCTCA**) ~300 nt upstream of the *rpfA* translation start site (68 nt upstream of the *rpfA* transcriptional start site) that is similar to the Crp consensus binding sequences identified in *Corynebacterium glutamicum* (Toyoda *et al.*, 2011), *Mycobacterium tuberculosis* (Kahramanoglou *et al.*, 2014) and *S. coelicolor* (Gao *et al.*, 2012). A Crp (Rv3676)-binding site was also identified upstream of *rpfA* in *M. tuberculosis* (Rickman *et al.*, 2005). Taken together, Crp likely triggers RpfA-dependent spore germination upon interacting with its effector cAMP.

2.4.3 The *rpfA* 5′ UTR harbors a *ydaO*-like riboswitch motif.

The growth phase-dependent changes in RpfA-FLAG levels were unlikely to be mediated solely by promoter control, as *rpfA* expression from a strong, constitutive promoter did not dramatically alter the protein expression profile (see below). Given that previous experimental analyses had revealed a long 5′ UTR for *rpfA* (Haiser *et al.*, 2009) predicted to contain a *B. subtilis ydaO*-like riboswitch (Block *et al.*, 2010; Nelson *et al.*, 2013), we set out to explore the regulatory potential of the *rpfA* 5′ UTR. We first determined the structure of this region using in-line probing experiments (Fig. 2.5), coupled with previously published bioinformatic analyses of hundreds of *ydaO* riboswitch family members, and we compared this with the available structural data for the *B. subtilis ydaO* riboswitch (Barrick *et al.*, 2004; Block *et al.*, 2010).

In comparing the resulting secondary structure (Fig. 2.6A) to the *B. subtilis ydaO* riboswitch (Fig. 2.7), several interesting features were noted. First, the *rpfA* 5′ UTR lacked an obvious pseudoknot, which in the *B. subtilis ydaO* riboswitch forms between the P7 loop and the 3′ end of the sensor domain, immediately downstream of the distal P1 stem (Fig. 2.7) (Barrick *et al.*, 2004; Block *et al.*, 2010; Watson and Fedor, 2012; Nelson *et al.*, 2013). In *B. subtilis*, pseudoknot

formation is required for maximal ligand binding efficiency *in vitro* (Nelson *et al.*, 2013), suggesting that there may be differences in ligand interaction in the streptomycetes. The *rpfA* 5′ UTR also lacked a canonical intrinsic terminator, a staple of riboswitches modulating transcript elongation, like that found immediately downstream of the sensor domain of the *B. subtilis ydaO* element (Block *et al.*, 2010; Nelson *et al.*, 2013). Terminator formation is crucial to *ydaO* riboswitch activity, as disrupting stem formation results in constitutive anti-termination (*i.e.*, read-through) (Nelson *et al.*, 2013). The absence of an obvious terminator suggested that if the *rpfA* 5′ UTR was indeed a riboswitch, it may function via a mechanism other than transcription attenuation.

2.4.4 The *rpfA* 5′ UTR controls RpfA protein abundance during the early stages of growth.

Because the *rpfA* 5′ UTR lacked an obvious intrinsic terminator, we reasoned that any riboswitch/regulatory effects might be exerted translationally. To determine whether the 5′ UTR affected RpfA protein levels, we compared RpfA-FLAG abundance in strains engineered to constitutively transcribe *rpfA-flag* with or without its 5′ UTR. We monitored RpfA-FLAG protein levels in exponential- and stationary-phase cultures, and found that removing the 5′ UTR sequence from the *rpfA* transcriptional unit led to dramatically increased levels of RpfA-FLAG during early growth (Fig. 2.6B), as would be expected if this sequence had riboswitch activity. Unexpectedly, RpfA-FLAG proteins were undetectable in stationary-phase cultures even when expressed from a constitutive promoter (P_{ermE*}) in the absence of any upstream sequence (Fig. 2.6B), suggesting some other regulatory mechanism must be exerted at this time.

While our early growth-stage results were consistent with translational control, they were also consistent with riboswitch-mediated transcription attenuation. To differentiate between these possibilities, we conducted a thorough transcriptional analysis, quantifying *rpfA* transcripts in strains both having and lacking the 5′ UTR using RT-qPCR. We found that despite there being no obvious terminator downstream of the putative sensor domain, removing the 5′ UTR sequence from the *rpfA* transcriptional unit increased transcript levels ~45-fold during early exponential growth, and these remained stable and high thereafter (Fig. 2.6C), suggesting a potential role in transcript elongation. We confirmed these results using a transcriptional luciferase reporter assay, in which wild-type *S. coelicolor* cells carrying a P_{ermE*}-driven *luxCDABE* operon, fused with or without the *rpfA* 5′ UTR, were grown in liquid medium. Our

results revealed the 5′ UTR decreased luciferase reporter activity over 90%, compared with the strain lacking the 5′ UTR (Fig. 2.6D), consistent with riboswitch activity.

We next set out to determine the fraction of transcription initiation events that culminated in complete read-through of the transcriptional unit. Using RT-qPCR, we quantified total initiated transcripts using primers targeting the *rpfA* 5′ UTR (encompassing both read-through and attenuated transcripts), and compared these levels with read-through transcripts using primers targeting the *rpfA* coding region. Read-through transcripts were abundant in actively growing cells and comparatively scarce in stationary-phase cells (Fig. 2.6E), consistent with protein abundance profiles. However, when these levels were compared with those of initiated transcripts, we found that only a very small proportion of initiated transcripts ultimately extended into the *rpfA* coding region, indicating that *rpfA* transcription was attenuated at all times examined (Fig. 2.6E). These findings were corroborated by deep-sequencing of the entire *S. coelicolor* M145 transcriptome (Moody *et al.*, 2013), where we observed a greater number of reads mapping to the *rpfA* 5′ UTR than to the coding region (Fig. 2.8). Taken together, our results suggested that the putative *rpfA* riboswitch attenuated transcription of its downstream-encoded gene throughout growth.

The lack of a canonical intrinsic terminator associated with the *rpfA* upstream sequence led us to postulate that Rho may play a role in transcription attenuation, as several riboswitches recruit Rho to attenuate the expression of their cognate genes (Hollands *et al.*, 2012). To test this hypothesis, we examined the effects of bicyclomycin, a Rho inhibitor, on transcription attenuation/riboswitch activity using our luciferase reporter system. While we do not have a positive control for Rho activity, we confirmed that bicyclomycin addition to the growth medium conferred the same phenotype as a *rho* deletion mutation in *Streptomyces venezuelae* (bicyclomycin and *rho* deletion both inhibit aerial development and sporulation) (Fig. 2.9), suggesting that it is indeed active against *Streptomyces* species. We did not observe any significant difference in luciferase activity in bicyclomycin-treated versus untreated cells (Fig. 2.9), suggesting that Rho was not required for transcription attenuation. In a further attempt to identify putative terminator sequences, we deleted contiguous regions of the 5′ UTR, including the P2, P4, P6 and P5-7 stems. In each case, we did not see any dramatic change in attenuation (Fig. 2.10). Collectively, this suggested any terminator within this region must be unusual in nature.

These deletion experiments led us to question the ligand-binding capabilities of this regulatory sequence, given the lack of effect seen after

deleting stems P6 and P5-7, which in *B. subtilis* contribute to c-di-AMP binding (Nelson *et al.*, 2013). We set about extending our deletional analyses, focusing on a key c-di-AMP binding determinant in the *ydaO* riboswitch: the single-stranded region joining stems P3 and P5, which when mutated leads to a complete abrogation of c-di-AMP binding, unlike the reduced binding seen for P6 and P7-associated pseudoknot mutations (Nelson *et al.*, 2013). When we removed this single-stranded sequence, transcription attenuation was significantly reduced (Fig. 2.10), suggesting that like in *B. subtilis*, this region may be important for riboswitch function.

2.4.5 The *rpfA* riboswitch responds to c-di-AMP.

Given the structural differences between the *B. subtilis* system and that of *rpfA*, and the results of our mutagenic experiments, we set out to examine the effect of c-di-AMP on *rpfA* transcript levels *in vivo*. c-di-AMP is produced by the diadenylate cyclase DisA (Witte *et al.*, 2008), and while our attempts to delete *disA* in *S. coelicolor* were unsuccessful, we were able to construct a *disA* mutant in *S. venezuelae*, and confirmed that this strain did not produce c-di-AMP using liquid chromatography-coupled tandem mass spectrometry (LC-MS/MS) (Fig. 2.11). Because the 5′ UTRs of *rpfA* in *S. coelicolor* and *S. venezuelae* share extensive sequence and structural similarities (Fig. 2.7), with differences limited largely to known regions of sequence and structural variability (*e.g.*, P4/P4a, P6) (Block *et al.*, 2010; Nelson *et al.*, 2013), and exhibit similar transcription attenuation properties (Fig. 2.8), these elements were expected to respond to c-di-AMP in the same way. We compared *rpfA* (coding sequence) transcript levels in wild-type *S. venezuelae* and *disA* mutant strains, and consistent with what has been seen for *B. subtilis* (Nelson *et al.*, 2013), we found full-length *rpfA* transcript levels increased nearly 5-fold upon deleting *disA.* In contrast, total *rpfA* (5′ UTR) transcript levels were unaffected by the deletion (Fig. 2.12A). We complemented these *in vivo* analyses with *in vitro* assays. Using in-line probing, we found that the *rpfA* 5′ UTR sequence effectively bound c-di-AMP, but not the closely related second messenger cyclic di-GMP (c-di-GMP), and that this binding led to a change in structure (Fig. 2.12B). Collectively, these results suggested that the sequence upstream of *rpfA* was, like its *B. subtilis* counterpart, a riboswitch that specifically bound c-di-AMP, leading to transcription attenuation.

2.4.6 The stringent response decreases RpfA abundance during stationary growth.

While control by the *rpfA* riboswitch could readily explain the overall reduced levels of RpfA through decreased transcriptional read-through, it failed to explain the absence of RpfA proteins once the culture transitioned into stationary phase (Fig. 2.2 and 2.6B). Therefore, we reasoned that additional mechanisms must exist to control protein abundance at this time. In *S. coelicolor*, the onset of stationary phase coincides with the rapid accumulation of the second messenger ppGpp (Strauch *et al.*, 1991). Given the inverse correlation between ppGpp and RpfA levels, we hypothesized that the stringent response may influence RpfA levels. The stringent response typically alters gene expression at the level of transcription initiation (Potrykus and Cashel, 2008; Dalebroux and Swanson, 2012), and so we first tested *rpfA* promoter activity in wild-type and Δ*relA* mutant strains using our luciferase reporter assay, where *relA* encodes the ppGpp synthetase. Deleting *relA* had no impact on *rpfA* promoter activity (Fig. 2.13A). Similarly, we observed the riboswitch-mediated response to be *relA*-independent (Fig. 2.14).

To further probe this phenomenon, we took advantage of our *rpfA* construct in which the native *rpfA* promoter had been replaced by a constitutive one, and the *rpfA* riboswitch had been removed, thereby ensuring continuous, high-level protein production (Fig. 2.6B). We introduced this construct into wild-type and Δ*relA* mutant strains. In the wild-type strain, RpfA-FLAG proteins were detected strictly in exponentially growing cultures, whereas these enzymes were detected throughout growth in a Δ*relA* mutant (Fig. 2.13B). This implied that the stringent response did indeed contribute to reducing RpfA levels during stationary phase.

As the stringent response can alter protease expression (Hata *et al.*, 2001; Dahl *et al.*, 2003; Hesketh *et al.*, 2007), we hypothesized that ppGpp – and the stringent response – affected RpfA post-translationally by altering its stability. To investigate this possibility, we monitored exponentially growing cells for RpfA-FLAG production and levels, following washing and inoculation into fresh or conditioned medium [cell-free supernatant of stationary-phase cultures devoid of RpfA-FLAG (Fig. 2.13)]. Following cell re-suspension in fresh broth, RpfA-FLAG was readily detected for several hours; however, when these cells were transferred into conditioned medium, RpfA-FLAG was undetectable within an hour (Fig. 2.13). Notably, loss of RpfA-FLAG occurred irrespective of riboswitch presence/absence (Fig. 2.13C).

We further probed this intriguing observation by mixing RpfA-FLAG-containing supernatant with stationary-phase culture supernatant (*i.e.*, a cell-free assay). We found RpfA-FLAG proteins could not be detected following incubation with this conditioned medium (Fig. 2.13D), suggesting a proteolytic factor was secreted during stationary phase, clearing the medium of RpfA proteins. This was supported by our observation that re-suspending washed, exponentially growing cells in conditioned medium that had been previously boiled for 15 min (such that any protease would be inactivated) led to RpfA-FLAG detection (Fig. 2.13D and 2.13E).

We extended these experiments to include the use of conditioned medium to which specific protease inhibitors had been added [a serine/cysteine protease inhibitor cocktail or a metalloprotease inhibitor (EDTA)]. We found the protease inhibitor cocktail failed to prevent RpfA-FLAG clearing in the conditioned medium (Fig. 2.13D), but treating the conditioned medium with EDTA led to RpfA-FLAG accumulation (Fig. 2.13E), suggesting that RpfA degradation was mediated, at least in part, by a secreted metalloprotease.

To test whether RpfA proteolysis was directed by the stringent response, we repeated our cell-free assays using conditioned medium prepared from wild-type and Δ*relA* mutant stationary-phase cultures. Consistent with our previous observations, we found that, unlike wild-type conditioned medium, conditioned medium prepared from the mutant culture was unable to degrade RpfA-FLAG proteins (Fig. 2.13F), suggesting that ppGpp signaling is required for the expression and/or the activation of the RpfA-targeting metalloprotease.

2.4.7 RpfA is required for normal spore germination.

Our results suggested that RpfA expression was rigorously controlled at multiple levels, and we wanted to determine the biological effect of *rpfA* mis-regulation. Given the multiple regulatory inputs affecting RpfA accumulation, and the potential pleiotropic effects associated with disrupting the different regulatory pathways, we focused our attention on the effect of regulatory changes that were specific to RpfA. We compared the behavior of a strain that both expressed *rpfA* from a constitutive promoter and lacked the riboswitch motif – thus effectively overexpressing RpfA (Fig. 2.6B) – to a riboswitch motif-containing strain that exhibited wild-type-like expression and accumulation of RpfA.

We first tested the effect of RpfA overexpression on spore germination. We knew strains lacking RpfA were delayed in germination (Haiser *et al.*, 2009), and we expected that overexpressing RpfA may accelerate germination and

outgrowth. Unexpectedly, increased RpfA production delayed the initial stages of spore germination (Fig. 2.15A), similar to the effect seen previously for an *rpfA* deletion mutant (Haiser *et al.*, 2009), suggesting that specific RpfA levels may be required for function.

We followed the behavior of this strain during subsequent growth on agar medium, and conducted a variety of phenotypic tests (*e.g.*, spore length, spore wall thickness, heat-shock resistance and cell envelope stress resistance), and found the RpfA-overexpression phenotype was virtually indistinguishable from that of the parent strain in all cases (Fig. 2.16).

We wondered whether *S. coelicolor* might respond to changes in RpfA levels by altering the expression of other *rpf* genes, as has been seen in other actinobacterial systems (Downing *et al.*, 2004). To examine this, we assessed *rpfC* and *rpfD* transcript levels in the *rpfA* mis-regulated strain. RpfA overexpression had little impact on *rpfC* transcript levels, but led to greatly increased *rpfD* transcript levels during stationary phase (Fig. 2.15B); transcripts of the other *rpf* genes (*rpfB* and *rpfE*) are not detectable under the culture conditions used (Sexton *et al.*, 2015).

2.5 DISCUSSION

Dormancy provides bacteria with an effective strategy to survive sub-optimal growth conditions, and emerging from dormancy and resuming growth require the ability to sense appropriate growth conditions and reactivate cellular metabolism. Cell wall lytic enzymes play a critical role in resuscitation, and necessarily are subject to strict regulation to prevent premature exit from dormancy and uncontrolled cell wall cleavage. The peptidoglycan fragments resulting from cell wall lytic enzyme activity can also serve as signaling molecules for other microorganisms [*e.g.*, stimulating spore germination in *B. subtilis* (Shah *et al.*, 2008), resuscitation of dormant *M. tuberculosis* (Mir *et al.*, 2011) or filamentous growth in fungi (Xu *et al.*, 2008)], and as such, there may well be selective pressure to limit the broad release of such molecules into the environment. Here, we dramatically expand the regulatory elements known to control cell wall lytic enzymes and reveal a complex regulatory interplay mediated by multiple second messengers (Fig. 2.17).

Our results revealed a role for Crp, the cAMP receptor protein in *S. coelicolor* (Derouaux *et al.*, 2004b), in the transcriptional activation of *rpfA* expression. This is consistent with previous observations for *Mycobacterium* and

Streptomyces, where Crp, cAMP and the Rpfs all contribute to the resuscitation from dormancy (Süsstrunk *et al.*, 1998; Mukamolova *et al.*, 2002a; Zhu *et al.*, 2003; Derouaux *et al.*, 2004a; Downing *et al.*, 2005; Kana *et al.*, 2008; Haiser *et al.*, 2009; Shleeva *et al.*, 2013; Sexton *et al.*, 2015). In mycobacteria, unsaturated fatty acids trigger an Rpf-dependent release from dormancy by promoting cAMP synthesis (Shleeva *et al.*, 2013), and concomitantly, Crp (Rv3676) activates *rpfA* expression in *M. tuberculosis* (Rickman *et al.*, 2005). Notably, the cAMP-dormancy connection extends beyond the actinobacteria to include fungi, where cAMP is involved in triggering spore germination, amongst other functions (Lee *et al.*, 2003).

Interestingly, *B. subtilis*, a bacterium renowned for its ability to form dormant endospores, does not normally make cAMP (Saier, 1996), although it does produce the related second messenger c-di-AMP (Oppenheimer-Shaanan *et al.*, 2011; Mehne *et al.*, 2013). In *B. subtilis*, c-di-AMP regulates a wide variety of processes, including peptidoglycan homeostasis (Luo and Helmann, 2012; Mehne *et al.*, 2013) and sporulation (Bejerano-Sagie *et al.*, 2006; Oppenheimer-Shaanan *et al.*, 2011), but how this regulation is mediated has not yet been elucidated. Though the role of c-di-AMP in the streptomycetes has not been clearly shown, it obviously has a central function in peptidoglycan metabolism and spore germination, given its riboswitch-dependent control of *rpfA* expression. In *B. subtilis*, c-di-AMP-sensing riboswitches modulate the expression of two transport systems, one specific for amino acids and a second for potassium (Barrick *et al.*, 2004; Block *et al.*, 2010; Nelson *et al.*, 2013), and while their function has not been experimentally explored, both genes are upregulated within minutes of spore germination (Keijser *et al.*, 2007), suggesting they may have an important role during resuscitation. We note that while our data are consistent with riboswitch-mediated transcription attenuation, we cannot exclude the possibility that this upstream sequence recruits a ribonuclease upon binding c-di-AMP, whose activity leads to the destabilization of the downstream *rpfA* coding sequence, like that seen for the *lysC* riboswitch in *Escherichia coli* (Caron *et al.*, 2012).

Thus far, our understanding of non-coding RNAs – and particularly small RNAs – in controlling cell wall-related functions has been largely limited to their regulation of outer membrane protein expression in Gram-negative bacteria (Vogel and Papenfort, 2006). To our knowledge, RNA-based control has not been previously associated with peptidoglycan cleavage, although it has been linked to peptidoglycan synthesis: lysine- (Grundy *et al.*, 2003; Sudarsan *et al.*, 2003) and glycine-responsive (Mandal *et al.*, 2004) riboswitches as well as a

glucosamine-6-phosphate-dependent ribozyme (Barrick *et al.*, 2004; Winkler *et al.*, 2004) all modulate the abundance of peptidoglycan precursors (diaminopimelate, glycine, *N*-acetylglucosamine) in *B. subtilis*. Bioinformatic analyses have revealed *rpfA*/*ydaO*-like riboswitches upstream of genes associated with peptidoglycan turnover in a wide range of bacteria (Barrick *et al.*, 2004; Block *et al.*, 2010; Nelson *et al.*, 2013), suggesting that riboswitch-mediated control of cell wall metabolism is pervasive.

While the opposing regulatory effects of Crp-mediated activation and c-di-AMP-responsive down-regulation of *rpfA* ensure it is only expressed when needed, these regulators do not provide a means of removing the protein when its function is no longer necessary. Our work suggests that RpfA degradation is promoted by ppGpp activity. Bacteria synthesize ppGpp in response to nutrient limitation (Potrykus and Cashel, 2008; Dalebroux and Swanson, 2012), and this can trigger entry into dormancy (Ochi *et al.*, 1981; Chakraburtty and Bibb, 1997; Hesketh *et al.*, 2007). We confirmed that ppGpp regulation here was not at a transcriptional or post-transcriptional level, and that the stringent response did not impact *rpfA* riboswitch activity. In *B. subtilis*, ppGpp also inhibits c-di-AMP phosphodiesterase activity (Rao *et al.*, 2010), thereby promoting c-di-AMP accumulation. There is no obvious DHH/DHHA1 domain-containing phosphodiesterase in the *S. coelicolor* genome, and consistent with this observation, cross-talk between ppGpp and c-di-AMP was not noted here.

Our results suggest that during stationary phase, the stringent response stimulates the expression or activation of at least one extracellular metalloprotease that targets RpfA for degradation. Expression and secretion of extracellular proteases in response to nutrient starvation is not unprecedented: in *B. subtilis*, expression of the extracellular protease AprE is stimulated by the stringent response (Hata *et al.*, 2001), and in *Streptomyces clavuligerus*, a 42-kDa metalloprotease is secreted into the medium in response to nutrient starvation (Bascarán *et al.*, 1990). A candidate for the RpfA-targeting protease is the extracellular metalloprotease SmpA (SCO2529), which is involved in establishing dormancy (Kim *et al.*, 2013). Coinciding with RpfA degradation, *smpA* expression is also regulated by ppGpp (Hesketh *et al.*, 2007) and increases during stationary phase (Huang *et al.*, 2001).

The multiple levels of regulation observed here for *rpfA*/RpfA would allow for the integration of regulatory inputs from a variety of systems, enabling exquisitely tunable expression and activity. They would further ensure that loss of any one regulatory input would not lead to uncontrolled cell wall cleavage. There are upwards of 60 cell wall lytic enzymes encoded by *S. coelicolor* (Haiser *et al.*,

2009), and it seems reasonable to expect some degree of regulatory and functional overlap, given the anticipated importance of these enzymes in the growth, development and overall fitness of this bacterium. Supporting this assertion is the fact that there are at least three additional cell wall lytic enzyme-encoding genes controlled by *rpfA*-like riboswitches in *S. coelicolor* (Haiser *et al.*, 2009), suggesting that they too would respond to c-di-AMP. At least one of these (*swlC*) is also Crp-dependent (Gao *et al.*, 2012), and the gene product of another (SwlA) contributes to spore germination (Haiser *et al.*, 2009). There are four additional *rpf* genes encoded by *S. coelicolor* (Haiser *et al.*, 2009), and while our data suggest that they too contribute to spore germination (Sexton *et al.*, 2015), they do not appear to be controlled in the same way as *rpfA*. There must be some regulatory connectivity, however, given the altered *rpfC* and *rpfD* expression when RpfA is overexpressed. While we are still in the early stages of understanding how these different enzymes collectively contribute to *Streptomyces* growth and development, we anticipate that the regulatory systems coordinating their activities may well be broadly applicable to other bacteria.

2.6 EXPERIMENTAL PROCEDURES

2.6.1 Growth conditions

S. coelicolor strains (Table 2.1) were grown at 30°C on nutrient agar (Difco), MS agar or MM agar (Kieser *et al.*, 2000), or in tryptone soya broth (Oxoid):YEME (Kieser *et al.*, 2000) (50:50) (denoted as rich medium in the figure legends) or R5 broth (Kieser *et al.*, 2000). *S. venezuelae* strains (Table 2.1) were grown in MYM liquid medium (Stuttard, 1982). *E. coli* strains (Table 2.1) were grown at 30°C (BW25113 derivatives) or 37°C (DH5α and ET12567 derivatives) in LB and SOB (without Mg^{2+} salts) (Sambrook and Russell, 2001) and on LB agar (LB with 1.5%$_{w/v}$ agar) and nutrient agar. When appropriate, media were supplemented with the following antibiotics: 100 μg mL^{-1} ampicillin, 50 μg mL^{-1} apramycin, 25 μg mL^{-1} chloramphenicol, 50 μg mL^{-1} hygromycin B, 50 μg mL^{-1} kanamycin, 25 μg mL^{-1} naladixic acid and 50 μg mL^{-1} thiostrepton. Bicyclomycin (90 μg mL^{-1}, in water) was added to growth media during attenuation assays.

For conditioned medium assays, exponential-phase cells were recovered from 12- to 15-h-old cultures by centrifugation, washed twice with sucrose (300 mM), and resuspended in fresh medium or cell-free supernatant recovered from a 46- to 48-h-old stationary-phase culture of *S. coelicolor* strain E104a/pMC229

(Table 2.1) (conditioned medium). For cell-free assays, RpfA-rich supernatant recovered from a 12- to 13-h-old exponential-phase culture of E104a/pMC229 was mixed with an equal volume of fresh medium or supernatant from a 47- to 48-h-old stationary-phase *S. coelicolor* culture. When appropriate, conditioned medium was boiled for 15 min, treated with protease inhibitor cocktail (EDTA-free cOmplete Mini, Roche) or treated with EDTA (20 mM; pH 8.0).

2.6.2 RpfA-FLAG construction

Expression from the native promoter. GenScript (Piscataway, USA) synthesized a 624-bp DNA sequence comprising 159 bp of DNA upstream of the *rpfA* transcriptional start site, the first and last 12 bp of the *rpfA* 5′ UTR, the first 10 bp and the last 56 bp of the *rpfA* coding region, and 264 bp of DNA downstream of the *rpfA* stop codon. A sequence encoding a Gly_3 flexible linker fused to 3 × FLAG (DYKDHDGDYKDHDIDYKDDDDK), flanked on either side by *Xho*I sites, was inserted immediately upstream of the *rpfA* stop codon. To facilitate cloning of the 5′ UTR into the synthesized sequence, the following mutations were introduced (numbering relative to the transcriptional start site): C11G (creates a *Nco*I site) and A235C+C236A+C237T (creates a *Nde*I site). The entire synthesized sequence was flanked with *Kpn*I-*Bgl*II (5′ end) and *Bgl*II-*Hin*dIII (3′ end) restriction sites. Upon receiving the construct, the sequence was excised from the vector (pUC57; Table 2.1) as a *Kpn*I/*Hin*dIII restriction fragment and cloned into the corresponding sites of pBluescriptII KS- (Table 2.1).

The *rpfA* coding region was then introduced into the synthesized sequence by exploiting the newly created *Nde*I site and the naturally occurring *Sal*I site near the 3′ end of the coding region. Briefly, the complete *rpfA* coding region, with 264 bp of downstream sequence, was PCR-amplified from *S. coelicolor* chromosomal DNA using iProof High-Fidelity DNA polymerase (Bio-Rad) with primers 3097START (which carries a 5′-end *Nde*I site) and 9798D (Table 2.2). The 1,020-bp product was digested with *Nde*I and *Sal*I, and the 686-bp restriction fragment was cloned into the corresponding sites of the synthesized sequence, generating plasmid pMC220 (Table 2.1).

To create the riboswitch-containing construct, the *rpfA* 5′ UTR (+7 to +234) was PCR-amplified as above using primers rpfAUTR5′ and rpfAUTR3′ (Table 2.2) engineered to contain *Nco*I and *Nde*I sites. The 252-bp product was digested with *Nco*I and *Nde*I and cloned into the corresponding sites of pMC220, generating plasmid pMC221 (Table 2.1). The fragment was excised from the

vector using *Bgl*II and cloned into the *Bam*HI site of the integrative vector pIJ82 (Table 2.1), generating pMC228 (Table 2.1).

Expression from a constitutive promoter. The *rpfA-flag* fusion gene, with or without the 5′ UTR, was PCR-amplified as above using plasmids pMC221 and pMC220 as template and primer pairs UTR5′/9798D and noUTR_ermE/9798D (Table 2.2), respectively. Products were phosphorylated and cloned into the *Eco*RV site of pMC500 (Table 2.1), downstream of P_{ermE*}. The *rpfA-flag* gene fused to P_{ermE*} was excised from the vector as a *Bgl*II restriction fragment, blunt-ended using Klenow Fragment, and cloned into the *Eco*RV site of the integrative vector pRT801 (Table 2.1), generating plasmids pMC230 and pMC229 (Table 2.1).

2.6.3 Overexpression and reporter plasmid construction

The *crp* coding sequence (with 37 bp of downstream sequence) was PCR-amplified using Phusion High-Fidelity DNA polymerase (NEB) and primers NdeICrpF and HindIIICrpR (Tables 2.2 and 2.3). P_{ermE*} with the *rpfA* 5′ UTR was PCR-amplified as above, using primers ermEF and rpfAR2-K (Tables 2.2 and 2.3) and pMC230 as template. All primers were engineered with 5′-end restriction sites appropriate for subsequent cloning experiments.

Select secondary structures were deleted from the *rpfA* riboswitch motif using splicing by overlap extension (SOE)-PCR (Horton, 1995). For cloning purposes, *Bgl*II and *Kpn*I restriction sites were engineered into the 5′ end of external primers ermEF and rpfAR2-K, which target the 5′ terminus of P_{ermE*} and nucleotides 44-63 of the *rpfA* coding region, respectively, and delimit the ends of all SOE-PCR products. A 17-nt extension was added to the 5′ end of each forward internal primer (used with rpfAR2-K to amplify the downstream half of the SOE-PCR product) (Table 2.2). This extension was entirely complementary to the reverse internal primer (used with ermEF to amplify the upstream half of the product) (Table 2.2), and allowed for hybridization of the upstream and downstream fragments during SOE-PCR. These upstream and downstream fragments were generated as described above using pMC230 as template. SOE-PCR reactions were carried out as above, using primers ermEF/rpfAR2-K and approximately equal amounts of purified upstream and downstream fragments as template. All primer pairs used, optimized amplification conditions and product sizes are summarized in Table 2.3.

PCR and SOE-PCR products were purified, digested with the appropriate restriction enzymes, and ligated to dephosphorylated, *Nde*I- and *Hin*dIII-digested pIJ10257 (*crp*) or *Bam*HI- and *Kpn*I-digested pFLUX (all other) (Table 2.1).

2.6.4 Cloning

All constructed plasmids were replicated in *E. coli* strain DH5α (Table 2.1) and extracted following standard protocols (Sambrook and Russell, 2001). Inserts were sequenced by MOBIX, McMaster University's DNA sequencing facility. Integrative plasmids were electroporated into the conjugation-proficient, methylation-deficient host *E. coli* strain ET12567/pUZ8002 (Table 2.1) and introduced into *S. coelicolor* via conjugation (Gust *et al.*, 2003).

2.6.5 Chromatin immunoprecipitation (ChIP)

crp expression was induced in exponentially growing *S. coelicolor* strains Δ*crp*/pIJ6902 (negative control) and Δ*crp*/pIJ6902*crp* (Table 2.1). Cultures were cross-linked, and Crp-associated DNA was immunoprecipitated prior to induction, and at 15 and 45 min following induction using anti-Crp antibodies. Growth conditions, antibody purification and ChIP were carried out as described previously (Gao *et al.*, 2012).

2.6.6 RNA isolation

Cells were recovered from culture aliquots by centrifugation and stored at -80°C for no more than 20 days prior to RNA isolation. Total RNA was extracted from frozen cell pellets using a bead-beating protocol, and co-extracted DNA was completely digested using TURBO DNase (Ambion), as described previously (Moody *et al.*, 2013). Total RNA was quantified using a ND-1000 spectrophotometer (NanoDrop Technologies), while RNA quality and integrity were assessed using A_{260}/A_{280} and A_{260}/A_{230} ratios, alongside agarose gel electrophoresis.

2.6.7 qPCR and RT-qPCR

Primers (Table 2.2) were designed with Primer-BLAST (www.ncbi.nlm.nih.gov/tools/primer-blast/) using sequences retrieved from StrepDB (http://strepdb.streptomyces.org.uk/). Desalted primers were purchased

from Integrated DNA Technologies. Primer pair specificity was assessed by searching the *Streptomyces* genome for potential mis-priming sites and confirmed by PCR.

Transcripts were reverse transcribed using SuperScript III reverse transcriptase (Invitrogen). Each reverse transcription reaction consisted of 500 µM each dNTP, 100 nM reverse primer (Table 2.2), 100 ng μL^{-1} DNase-treated total RNA, 1 × First-Strand Buffer, 5 mM dithiothreitol, 2 U μL^{-1} RNaseOUT and 10 U μL^{-1} SuperScript III reverse transcriptase. The first three ingredients were mixed and heated at 95°C for 5 min and rapid-cooled on ice prior to adding the remaining components. Reverse transcription was conducted at 55°C for 1 h, and the enzymes were heat-inactivated at 70°C for 15 min. 'No RT' negative controls were prepared as described above, but without RNaseOUT or reverse transcriptase. Reverse transcribed RNA samples were used immediately or stored at -20°C for a maximum of 5 days prior to processing.

cDNA was quantified using qPCR. Briefly, 20-µL singleplex reactions, consisting of 1 × PerfeCTa SYBR Green SuperMix (Quanta Biosciences) or 1 × All-in-One qPCR Mix (GeneCopoeia), 200-300 nM each primer (Table 2.2) and 8 ng μL^{-1} reverse transcribed RNA, were prepared in triplicate in clear 96-well PCR plates. An equal volume of nuclease-free water replaced the cDNA sample in the 'no template' negative controls included in each run. cDNA was PCR-amplified in a CFX96 Touch Real-Time PCR Detection System (Bio-Rad) using the cycling conditions recommended by the manufacturer, and optimized annealing temperatures (Table 2.4). Fluorescence was measured at each extension step. Each PCR run ended with a melt curve analysis (65-95°C, with 5-sec plate reads every 0.5°C increment). Baseline-corrected fluorescence data were exported from the CFX Manager software v2.1 (Bio-Rad). Transcript levels were calculated using DART-PCR (Peirson *et al.*, 2003) and normalized to total RNA mass.

For assays comparing levels of total and full-length *rpfA* transcripts, an absolute quantification strategy was used. Using the CFX Manager software v2.1, the C_T value of each sample was compared to a 5- or 6-point double-stranded DNA standard curve (C_T versus log copy number; $R^2 > 0.99$) prepared in triplicate as described above. *Bam*HI-digested pMC230, which served as standard, was quantified using a ND-1000 spectrophotometer and serially diluted in water to provide 10^4-10^9 target copies per reaction.

For ChIP-qPCR experiments, 20-µL singleplex qPCR reactions were prepared as described above, using 1 × All-in-One qPCR Mix and 2.5 µL DNA (1:10). DNA levels were calculated using DART-PCR and normalized as follows: $\overline{x}_{+Crp}$ (R_0 ChIP extract/R_0 gDNA extract)/ $\overline{x}_{-Crp}$ (R_0 ChIP extract/R_0 gDNA extract).

2.6.8 Luciferase reporter assays

One hundred and fifty microliters of culture were transferred in triplicate into a white, flat-bottomed, 96-well plate (Falcon). Emitted luminescence was quantified during 1 sec using a TECAN UltraEvolution spectrometer. Luminescence signal detected from un-inoculated media was subtracted from the raw luminescence of each sample. Background-subtracted luminescence was then normalized to dry cell weight. Luciferase reporter activity expressed by the negative control strain, carrying the empty vector pFLUX, was on average 2.5 a.u mg^{-1} dry cell.

2.6.9 Protein isolation and immunoblotting

Cellular proteins. Cells were recovered from the culture by centrifugation, washed with sucrose (300 mM) and resuspended in 5 mL of protoplast buffer (0.3 M sucrose, 1.4 mM K_2SO_4, 9.8 mM $MgCl_2$, 0.58 µM $ZnCl_2$, 1.5 µM $FeCl_3$, 0.12 µM $CuCl_2$, 0.1 µM $MnCl_2$, 52 nM $Na_2B_4O_7$, 16 nM $(NH_4)_6Mo_7O_{24}$, 0.36 mM KH_2PO_4, 25 mM $CaCl_2$, 25 mM TES buffer, pH 7.2) supplemented with a protease inhibitor cocktail and 1 mg mL^{-1} egg white lysozyme (BioShop). After ~40 min at 30°C, protoplasts were recovered by centrifugation and resuspended in sample loading buffer (31 mM Tris, 13%$_{v/v}$ glycerol, 35 mM sodium dodecyl sulfate, 75 µM bromophenol blue, 50 mM dithiothreitol, pH 6.80).

Secreted proteins. Cultures were centrifuged, and total soluble proteins were isolated from the culture supernatant using a protocol adapted from Nandakumar *et al.* (2003). Briefly, soluble proteins contained within 800 µL of culture supernatant were precipitated on ice in trichloroacetic acid (20%$_{v/v}$) for 30-45 min. Precipitated proteins were recovered by centrifugation at 16,100 × g for 5 min at 4°C, washed 2-3 times with 0.5-1 mL ice-cold acetone, and dried at room temperature for 5-10 min. To neutralize any remaining acids, protein pellets were treated with 30 µL NaOH (0.2 M) for 2 min. Proteins were resuspended in sample loading buffer and stored at -20°C until electrophoresis.

After heating the extracts at ~95°C for 5 min, proteins were size-fractionated on a denaturing, discontinuous polyacrylamide gel [12%$_{w/v}$ acrylamide:bis-acrylamide (29:1) in the stacking gel] at 200 V for 1 h in pre-cooled electrode buffer (Laemmli, 1970) using a Mini-PROTEAN Tetra Cell (Bio-Rad). To estimate protein molecular mass, 5 µL of BLUeye Prestained Protein Ladder (GeneDireX) were loaded onto each gel. Proteins were then blotted onto a 0.45-µm PVDF-Plus membrane (GE Waters & Process Technologies) or Amersham Hybond

PVDF membrane (GE Healthcare) at 15 V for 60-70 min in Bjerrum and Schaefer-Nielsen buffer (Bjerrum and Schafer-Nielsen, 1986) using a Trans-Blot SD Semi-Dry Electrophoretic Transfer Cell (Bio-Rad). Membrane blocking, primary and secondary incubations, and chemiluminescent detection were conducted using the Amersham ECL Western Blotting Detection Reagents and Analysis System (GE Healthcare). Wash buffer comprised 25 mM Tris, 0.14 M NaCl, 2.7 mM KCl and 0.1%$_{v/v}$ Tween-20 (pH 7.60). Primary and secondary incubations were carried out using a rabbit anti-FLAG antibody (1:1,500) (Cell Signaling Technology and Sigma) and horseradish peroxidase-conjugated goat anti-rabbit IgG (H&L) (1:3,000) (Cell Signaling Technology), respectively.

2.6.10 *In vitro* transcription, RNA purification and 5′-end labeling

Template DNA for *in vitro* transcription was PCR-amplified from *S. coelicolor* chromosomal DNA (structural analysis) or pMC222 (Table 2.1) (ligand binding assays) using Phusion High-Fidelity DNA polymerase with primers IVTrpfAUTR5′ (containing the phage T7 promoter sequence) and IVTrpfAUTR3′ (targeting nucleotides 14-39 of the coding region) (Table 2.2). *rpfA* 5′ UTR RNA was transcribed with the MEGAshortscript High Yield Transcription kit (Ambion), using 0-1 mM GMP and 2.5-50 nM purified template DNA.

RNA was diluted in formamide loading buffer (Sambrook and Russell, 2001) and heated at 95°C for 5 min before being size-fractionated on a denaturing polyacrylamide gel (GeneGel, 6%$_{w/v}$; BioShop). RNA was visualized by UV shadowing, and the full-length transcript was excised and eluted from the gel in crush/soak buffer (Regulski and Breaker, 2008). RNA was isopropanol-precipitated (Sambrook and Russell, 2001), re-suspended in nuclease-free water and quantified using a ND-1000 spectrophotometer.

Twenty picomoles of gel-purified, *in vitro* transcribed RNA were de-phosphorylated, 5′-end-labeled with T4 polynucleotide kinase and [γ-^{32}P]ATP (Perkin Elmer), and column-purified with NucAway Spin Columns (Ambion) using the KinaseMax kit (Ambion).

2.6.11 In-line probing of *rpfA* leader RNA

In-line probing reactions, containing 100-120 kcpm 5′ end-labeled *rpfA* leader RNA, were carried out as described by Regulski and Breaker (2008). When appropriate, reactions were supplemented with c-di-AMP or c-di-GMP (Invivogen). In parallel, RNA was also alkaline-treated (Regulski and Breaker,

2008) and, in some cases, digested with RNase T1 using the RNase T1 Biochemistry Grade kit (Ambion). Cleavage products were diluted in colorless gel-loading solution (Regulski and Breaker, 2008) and size-fractionated on a 50-cm-long denaturing polyacrylamide gel (GeneGel, 6%$_{w/v}$). The gel was dried, and RNA was visualized by autoradiography.

2.6.12 Mutant construction

disA (*SVEN_3211*) was deleted from the *S. venezuelae* ATCC 10712 (Table 2.1) chromosome using the REDIRECT PCR-targeting system for streptomycetes (Gust *et al.*, 2003). Briefly, the apramycin resistance cassette, *aac(3)IV*, was PCR-amplified from plasmid pIJ773 (Table 2.1) using cassette-specific primers Sven3211-del-F and Sven3211-del-R (Table 2.2), carrying 39-nt 5′ sequences homologous to *disA* flanking DNA. The PCR product was electroporated into the recombinogenic strain *E. coli* BW25113/pIJ790 carrying the *S. venezuelae* cosmid Sv-4-B12 (Table 2.1), where *aac(3)IV* replaced the wild-type *disA* gene via homologous recombination. Restriction mapping and PCRs confirmed successful gene replacement (data not shown). The mutagenized cosmid was electroporated into *E. coli* strain ET12567/pUZ8002 before being introduced into *S. venezuelae* strain ATCC 10712 via conjugation. Exconjugants were screened for apramycin resistance and kanamycin sensitivity, and the *disA::aac(3)IV* genotype was again confirmed by PCR using primers Sven3211-conf-F and Sven3211-conf-R (Table 2.2) (data not shown).

2.6.13 c-di-AMP extraction and quantification

c-di-AMP was extracted from cells and quantified by LC-MS/MS following the procedure of Spangler *et al.* (2010), using acetonitrile:methanol:water (40:20:20) as extraction solvent. c-di-AMP levels were normalized to total cellular proteins, isolated from cells and quantified using a bicinchoninic acid assay (Spangler *et al.*, 2010).

2.6.14 Phenotypic assays

Heat-shock assays were carried out following a protocol adapted from Haiser *et al.* (2009). Briefly, spores were diluted in 2 × YT broth (Kieser *et al.*, 2000) to a final concentration of 3-7 spores μL^{-1}. Suspensions were then heat-shocked at 57-60°C for 0, 2, 5, 10 and 30 min, immediately cooled on ice, and 50

µL of each suspension were spread in triplicate on nutrient agar. After 2 days, plates were photographed, and colonies counted using ImageJ (Abràmoff *et al.*, 2004). For each strain, spore survival was calculated by dividing the number of viable heat-shocked spores by the total number of spores, and expressed as a fold change relative to the '0 min' time-point.

To assess strain resistance to different cell wall stresses, sterile 6-mm filter paper disks containing egg white lysozyme, sodium dodecyl sulfate or vancomycin were placed on the surface of MM agar spread with *S. coelicolor* spores. After 4 days, growth inhibition zones surrounding each disk (*i.e.*, distance between the disk and the edge of the clearing) were measured.

Spore morphology was examined after inoculating spores along the base of a sterile glass coverslip inserted in MS agar at a ~45° angle and incubating for several days (until cultures were sporulating). Coverslips were then removed from the medium, mounted in glycerol ($40\%_{v/v}$) onto a microscope slide, and imaged by bright-field microscopy at 1,000 × magnification. The length of spores in chains (≥3 spores) was measured using ImageJ. Transmission electron microscopy was used to assess spore morphology after 6 days of growth on MS agar. Samples were prepared and viewed as described previously (Haiser *et al.*, 2009). Spore wall thickness was measured using ImageJ. Finally, germination assays were conducted as described by Haiser *et al.* (2009).

2.7 ACKNOWLEDGEMENTS

The authors wish to thank Volkhard Kaever (Institute of Pharmacology, Hannover Medical School, Hannover, Germany) for conducting the LC-MS/MS analyses of c-di-AMP extracts; Max Gottesman and Robert Washburn (Columbia University, New York City, USA) for providing bicyclomycin; Mervyn Bibb (John Innes Centre, Norwich, UK) for his kind gift of *S. coelicolor* strain M570; and Danielle Sexton, Matthew Moody and Stephanie Jones (McMaster University, Hamilton, Canada) for their technical assistance. This work was supported by an NSERC Discovery Grant (No. 312495), a Canadian Institutes for Health Research Grant (No. MOP-93635 and MOP-137004) and the Canada Research Chairs program (MAE). R.J.S. was supported by a Vanier Canada Graduate Scholarship, E.S. by a Post-Doctoral Research Fellowship (Department of Foreign Affairs and International Trade, Canada) and N.T. by a Long Term EMBO Fellowship.

2.8 TABLES

Table 2.1. Bacterial strains, cosmids and plasmids.

Strain	Genotype, properties and/or use	Reference
***S. coelicolor* A3(2) strains**		
M145	A3(2) SCP1$^-$ SCP2$^-$	Kieser *et al.* (2000)
Δ*crp*	M145 *SCO3571::aac(3)IV*	Gao *et al.* (2012)
E104a	M145 Δ*SCO3097* (Δ*rpfA*)	Sexton *et al.* (2015)
M570	M600 *SCO1513::hyg* (Δ*relA*)	Chakraburtty and Bibb (1997)
***S. venezuelae* strains**		
ATCC 10712	Wild-type strain	Ehrlich *et al.* (1948)
Δ*disA*	ATCC 10712 *SVEN_3211::aac(3)IV*	This study
***E.coli* strains**		
BL21(DE3)	Recombinant protein expression host; F$^-$ *ompT* *hsdS$_B$*(r_B^-, m_B^-) *gal dcm* (DE3)	Studier and Moffatt (1986)
BW25113	Cosmid mutagenesis host; *lacI*^{q} *rrnB*$_{T14}$ Δ*lacZ*$_{WJ16}$ *hsdR514* Δ*araBAD*$_{AH33}$ Δ*rhaBAD*$_{LD78}$	Datsenko and Wanner (2000)
DH5α	Plasmid construction strain; F$^-$ ϕ80*lacZ*ΔM15 Δ(*lacZYA-argF*)*U169 recA1 endA1 hsdR17*(r_K^-, m_K^+) *phoA supE44* λ$^-$ *thi-1 gyrA96 relA1*	Bethesda Research Laboratories
ET12567	Methylation-deficient strain; F$^-$ *dam13::*Tn*9 dcm6 hsdM hsdR recF143 zjj201::*Tn*10 galK2 galT22 ara14 lacY1 xyl5 leuB6 thi1 tonA31 rpsL136 hisG4 tsx78 mtli glnV44*	MacNeil *et al.* (1992)
***Streptomyces* cosmids**		
Sv-4-B12	*S. venezuelae* cosmid carrying *SVEN_3211* (*disA*)	Gift from M. Bibb and M. Buttner
Plasmids		
pBluescriptII KS-	Cloning vector; *ori* (pUC) *lacZ'* P_{lac} P_{T3} P_{T7} *bla*	Alting-Mees and Short (1989)
pMC220	*rpfA-flag* under the transcriptional control of P_{rpfA} in pBluescriptII KS- (no 5′ UTR)	This study
pMC221	*rpfA-flag*, fused to the 3′ end of the *rpfA* 5′ UTR, under the transcriptional control of P_{rpfA} in pBluescriptII KS-	This study
pET15b*crp*	*SCO3571* (*crp*) under the transcriptional control of P_{T7} in pET-15b (Novagen); *ori* (pBR322) *lacI bla*	Gao *et al.* (2012)
pFLUX	Integrative transcriptional reporter vector; *ori* (pUC18) *oriT* (RK2) *int* ϕBT1 *attP* ϕBT1 *luxCDABE* (promoterless) *aac(3)IV*	Craney *et al.* (2007)
pFLUX-Pos	P_{ermE*} transcriptionally fused to *luxCDABE* in pFLUX	Sexton *et al.* (2015)
pMC195	P_{rpfA} transcriptionally fused to *luxCDABE* in pFLUX	Sexton *et al.* (2015)
pMC222	*rpfA* 5′ UTR-*luxCDABE* under the transcriptional control of P_{ermE*} in pFLUX	This study
pMC223	*rpfA* 5′ UTR $\Delta_{37\text{-}91}$-*luxCDABE* under the transcriptional control of P_{ermE*} in pFLUX (ΔP2)	This study

pMC224	*rpfA* 5′ UTR $\Delta_{101\text{-}144}$-*luxCDABE* under the transcriptional control of P_{ermE^*} in pFLUX (ΔP4)	This study
pMC225	*rpfA* 5′ UTR $\Delta_{151\text{-}175}$-*luxCDABE* under the transcriptional control of P_{ermE^*} in pFLUX (ΔP6)	This study
pMC226	*rpfA* 5′ UTR $\Delta_{145\text{-}198}$-*luxCDABE* under the transcriptional control of P_{ermE^*} in pFLUX (ΔP5-7)	This study
pMC227	*rpfA* 5′ UTR $\Delta_{92\text{-}214}$-*luxCDABE* under the transcriptional control of P_{ermE^*} in pFLUX (ΔP3-7)	This study
pMC231	*rpfA* 5′ UTR $\Delta_{199\text{-}208}$-*luxCDABE* under the transcriptional control of P_{ermE^*} in pFLUX (ΔLIN)	This study
pIJ82	Integrative cloning vector; *ori* (pUC18) *oriT* (RK2) *int* ϕC31 *attP* ϕC31 *hyg*	Gift from H. Kieser
pMC228	*rpfA-flag*, fused to the 3′ end of the *rpfA* 5′ UTR, under the transcriptional control of P_{rpfA} in pIJ82	This study
pIJ773	Plasmid carrying *oriT* (RK2) and *aac(3)IV* flanked by FLP recognition target sites for use in REDIRECT, *bla*	Gust *et al.* (2003)
pIJ790	λ RED recombination plasmid; *oriR101 repA101ts araC bet exo gam* P_{araBAD} *cat*	Gust *et al.* (2003)
pIJ6902	Integrative expression vector; *ori* (pUC18) *oriT* (RK2) *int* ϕC31 *attP* ϕC31 P_{tipA} *aac(3)IV tsr*	Huang *et al.* (2005)
pIJ6902*crp*	*SCO3571* (*crp*) under the transcriptional control of P_{tipA} in pIJ6902	Gao *et al.* (2012)
pIJ10257	Integrative expression vector; *ori* (pUC18) *oriT* (RK2) *int* ϕBT1 *attP* ϕBT1 P_{ermE^*} *hyg*	Hong *et al.* (2005)
pIJ10257-*crp*	*SCO3571* (*crp*) under the transcriptional control of P_{ermE^*} in pIJ10257	This study
pMC500	Cloning vector; P_{ermE^*} flanked by transcription terminators, *bla*	Duong *et al.* (2012)
pRT801	Integrative expression vector; *ori* (pUC18) *oriT* (RK2) *int* ϕBT1 *attP* ϕBT1 *aac(3)IV*	Gregory *et al.* (2003)
pMC229	*rpfA-flag* under the transcriptional control of P_{ermE^*} in pRT801 (no 5′ UTR)	This study
pMC230	*rpfA-flag*, fused to the 3′ end of the *rpfA* 5′ UTR, under the transcriptional control of P_{ermE^*} in pRT801	This study
pUC57	Cloning vector; *bla*	GenScript
pUZ8002	Non-transmissible *oriT* mobilizing plasmid; RP4 *tra neo*	Paget *et al.* (1999)

Table 2.2. List of PCR primers.

Primer	Sequence[a]	Restriction site
Mutagenesis primers		
Sven3211-del-F	GGA AAG TCC GGC GCG GGC TCC GGC AAC GAA GCG CTG ATG ATT CCG GGG ATC CGT CGA CC	
Sven3211-del-R	GGC GCG GGC TAC GGG CGT CCG GTA CGT CGA GTG CGC CTA TGT AGG CTG GAG CTG CTT C	
Cloning PCR primers		
3097START	CAG TAC CAT ATG CTG TTT TCC GGC AAG G	*Nde*I
9798D	CGG TAC GGA TCC CAC GAG CAT CTC CTT CTT C	*Bam*HI
ermEF	GCA CTA GAT CTA GCC CGA CCC GAG CAC GCG C	*Bgl*II
HindIIICrpR	ATA TAA GCT TCA GAG ATG TCC CTG CAA CC	*Hin*dIII
NdeICrpF	ATA TCA TAT GGA CGA CGT TCT GCG GCG CA	*Nde*I
noUTR_ermE	CGC TCG CCA TGG AGG GGA TC	*Nco*I
P2intF	***CGA CAG CCG CAA CGC CG***G CGG GGG ACC CAA GGT AAG T	
P2intR	CGG CGT TGC GGC TGT CGG GG	
P4intF	***AGG CAG GAG CGG GGG AC***G GTG GAG CCG AGT TCC GCG A	
P4intR	GTC CCC CGC TCC TGC CTT CG	
P5-7intF	***GAG CCG GAG CGG CTA GG***C GAC AGC TCA CCT CGC AGG C	
P5-7intR	CCT AGC CGC TCC GGC TCA AC	
P6intF	***GAG CGG CTA GGG GTG GA***G GGC AAC TCA ACC GGC CCG A	
P6intR	TCC ACC CCT AGC CGC TCC GG	
P3-7intF	***AAG CGC CGA AGG CAG GA***A GGC GTC GGT GAG GGG ATC A	
P3-7intR	TCC TGC CTT CGG CGC TTG AC	
LINintF	***CTC AAC CGG CCC GAA CC***C CTC GCA GGC GTC GGT GAG G	
LINintR	GGT TCG GGC CGG TTG AGT TG	
rpfAR2-K	GCA CTG GTA CCG ACG GCG ATG ACA CGG GTG G	*Kpn*I
rpfAUTR3′	CAG TAC CAT ATG TGA TCC CCT CAC CGA CGC	*Nde*I
rpfAUTR5′	CAG TAC CCA TGG CCA TCG CGG GCC CCG ACA GC	*Nco*I
Sven3211-conf-F	GTG GTT CAC TCA CGC CGC ATG AAC GGT TC	
Sven3211-conf-R	GGC ACG TAC CTG GTG GAG GCG AAG GTG	
UTR5′	CAG TAC CCA TGG CCA TCG CGG GCC CCG ACA GC	*Nco*I
RT and qPCR primers		
5UTRF	GAA CAG TCG TCG CGT CAA G	
5UTRR	CAC TTA CCT TGG GTC CCC C	
PrpfAF2	GGT CTC AGA AGC CGT GAT CG	
PrpfAR2	ATG ACC GTA GAC ACG CGC TC	
rpfAF[b]	GAG TCC GGC GGC AAC TGG TC	
rpfAR[b]	GCT GGG ACT TGC TCG CCT GG	
SCO0974F[b]	GTT CGT ACG GCT ACC AGG TG	
SCO0974R[b]	GTC CGC TCT TCA CGG AGA T	

SCO3098F[b]	AGT ACG GCG GTC TGG ACT A
SCO3098R[b]	CTT ATC TGC TGG GAG CGA CT
SV2900F	AAG ACG GTC AAG AAG GGT GA
SV2900R	GTT CTC GAC GAC GTC CTT GTT
SVUTRF2	GTG GGG GAC CCA AGG TAA G
SVUTRR2	CCT GTG AGG TGA GCT GTC G

***In vitro* transcription primers**

IVTrpfAUTR3′	GGA CGG ACG ACG GTG CTT GCC CTT GC
IVTrpfAUTR5′	TAA TAC GAC TCA CTA TAG GGC GCT CGC CAT CGC GGG CCC

[a] 39-nt extensions are underlined twice. Restriction sites are underlined once. Regions of the forward SOE-PCR primers complementary to the reverse SOE-PCR primers are bold and italicized. The phage T7 promoter is boxed.
[b] Primers were previously published by Sexton *et al.* (2015).

Table 2.3. PCR amplification conditions.

Construct	Fragment[a]	Primers[b]		Product length (bp)	Annealing temperature (°C)[c]
		Forward	Reverse		
Crp O/E	N/A	NdeICrpF	HindIIICrpR	729	58
P_{ermE*}-UTR[WT]	N/A	ermEF	rpfAR2-K	600	None
P_{ermE*}-UTR[ΔP2]	Ups	ermEF	P2intR	325	None
	Down	P2intF	rpfAR2-K	237	70
P_{ermE*}-UTR[ΔP4]	Ups	ermEF	P4intR	389	None
	Down	P4intF	rpfAR2-K	184	None
P_{ermE*}-UTR[ΔP6]	Ups	ermEF	P6intR	439	None
	Down	P6intF	rpfAR2-K	153	None
P_{ermE*}-UTR[ΔP5-7]	Ups	ermEF	P5-7intR	433	None
	Down	P5-7intF	rpfAR2-K	130	None
P_{ermE*}-UTR[ΔP3-7]	Ups	ermEF	P3-7intR	380	None
	Down	P3-7intF	rpfAR2-K	114	None
P_{ermE*}-UTR[ΔLIN]	Ups	ermEF	LINintR	487	None
	Down	LINintF	rpfAR2-K	120	None

[a] N/A, Products were not subsequently used for SOE-PCR. Ups, upstream fragment; Down, downstream fragment.
[b] Primer sequences are presented in Table 2.2.
[c] None, A two-step amplification protocol was used.

Table 2.4. qPCR conditions.

Gene	Primers[a]	Product location[b]	Product length (bp)	Annealing temperature (°C)	PCR amplification efficiency (mean ± SD)[c]				
					Crp O/E assays	ChIP-qPCR	± UTR assays	M145 assays	Δ*disA* assays
P_{rpfA}	PrpfAF2 PrpfAR2	-296 to -241	56	61	N/A	1.002 ± 0.056	N/A	N/A	N/A
***rpfA* CDS**	rpfAF rpfAR	+160 to +292	133	61	1.034 ± 0.032	N/A	1.045 ± 0.057	0.753	N/A
	SV2900F SV2900R	+550 to +681	132	68	N/A	N/A	N/A	N/A	0.763 ± 0.063
***rpfA* 5′ UTR**	5UTRF 5UTRR	-179 to -126	54	57	N/A	N/A	N/A	0.779	N/A
	SVUTRF2 SVUTRR2	-153 to -21	133	61	N/A	N/A	N/A	N/A	83.9 ± 0.005
rpfC	SCO3098F SCO3098R	+236 to +296	61	57	1.025 ± 0.034	N/A	1.014 ± 0.038	N/A	N/A
rpfD	SCO0974F SCO0974R	+1079 to +1168	90	60	N/A	N/A	1.076 ± 0.044	N/A	N/A

[a] Primer sequences are presented in Table 2.2.
[b] Nucleotide sites are numbered relative to the start codon.
[c] PCR amplification efficiency was calculated directly from the PCR amplification plots using DART-PCR (Peirson *et al.*, 2003) or from the linear regression slope of the standard curve.

2.9 FIGURES

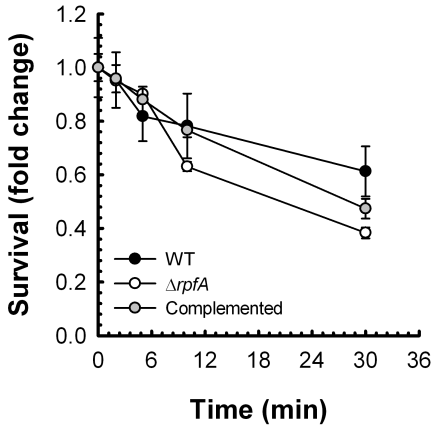

Fig. 2.1. Complementation of the Δ*rpfA* mutant heat-shock sensitivity phenotype with RpfA-FLAG. *S. coelicolor* spores were heat-shocked at ~60°C for the indicated lengths of time. Spore survival was assessed by plating and expressed as fold change relative to unheated samples (0 min). Data are presented as mean ± standard error (*n* = 3). WT, M145/pIJ82; Δ*rpfA*, E104a/pIJ82; Complemented, E104a/pMC228.

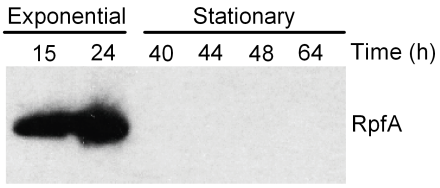

Fig. 2.2. RpfA abundance in the culture supernatant throughout growth in liquid culture. *S. coelicolor* strain Δ*rpfA* carrying an *rpfA-flag* fusion gene under the control of its own promoter (E104a/pMC228) was grown at 30°C in a liquid rich medium. At the times indicated, an aliquot of culture was harvested. Secreted, soluble proteins were extracted from the culture supernatant, and FLAG-tagged RpfA was detected by immunoblotting. Protein loading was normalized to culture volume.

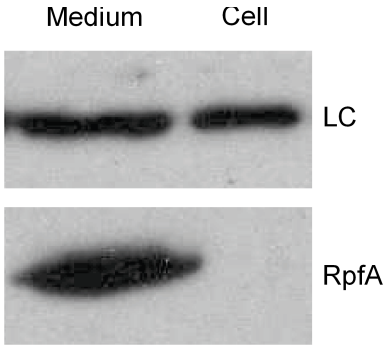

Fig. 2.3. RpfA localization. *S. coelicolor* strain Δ*rpfA* carrying an *rpfA-flag* fusion gene under the control of its own promoter (E104a/pMC228) was grown at 30°C in rich liquid medium. After 18 h, RpfA-FLAG proteins were detected in the culture supernatant (Medium) and in crude protoplast extracts (Cell) using immunoblotting. LC, loading control, non-specific binding of the anti-FLAG antibody to an unknown protein.

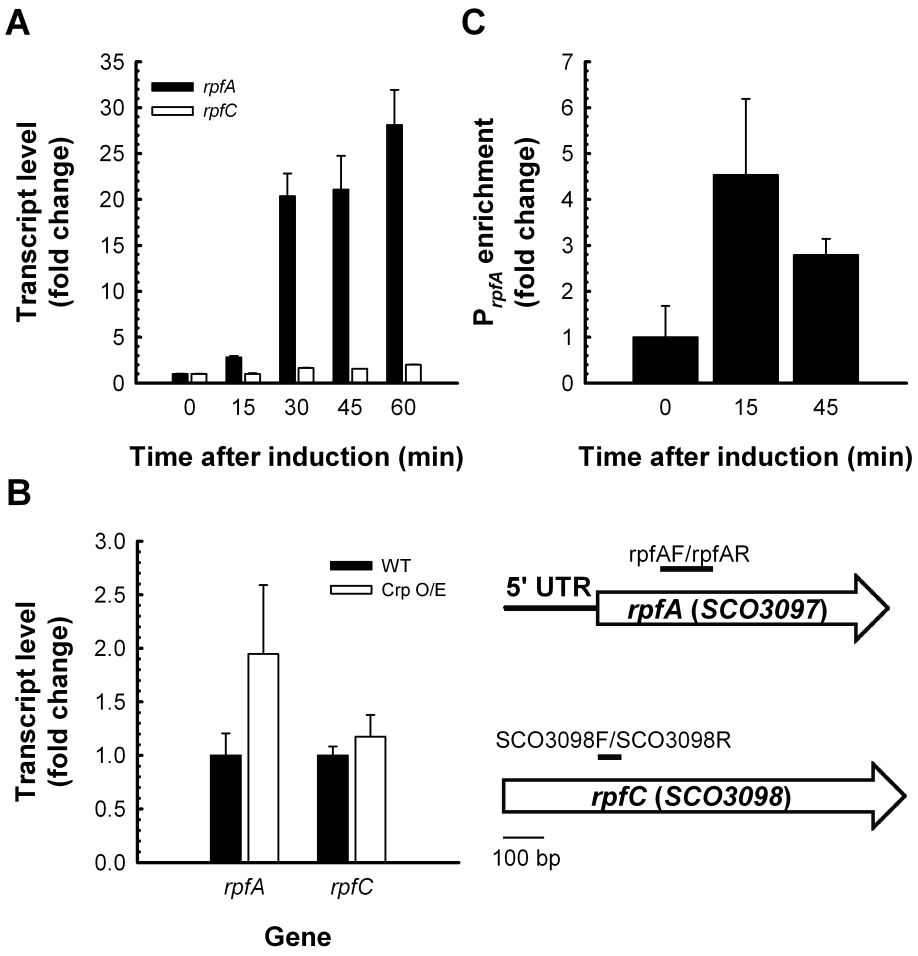

Fig. 2.4. Crp-dependent activation of *rpfA* transcription. (A) The *S. coelicolor* Δ*crp* strain (Δ*crp*/pIJ6902) and its thiostrepton-inducible derivative (Δ*crp*/pIJ6902*crp*) were grown to equal cell density in R5 broth, prior to *crp* induction. The transcriptome of each strain, both prior to and following induction, was analyzed using whole-genome microarrays (Gao *et al.*, 2012). *rpfA* and *rpfC* transcript levels in the *crp*-inducible strain were normalized to those of the empty vector strain and expressed as fold changes relative to the '0 min' time-point. Data are presented as mean ± standard error (n = 2). (B) RNA was harvested from exponentially growing *S. coelicolor* wild-type strain (WT, M145/pIJ10257) and its Crp-overexpressing derivative (Crp O/E, M145/pIJ10257-*crp*). *rpfA* and *rpfC* transcripts were quantified using RT-qPCR with primer pairs rpfAF/rpfAR and SCO3098F/SCO3098R, respectively. Transcript levels were normalized to total RNA mass and expressed as fold changes relative to expression levels in the wild-type strain. Data are presented as mean ± standard error (n = 3). Location of amplified products relative to the translation start and stop sites are indicated as bold lines above block arrows. Genes and PCR products were drawn to scale. (C) Chromatin immunoprecipitation was performed for *S. coelicolor* strains Δ*crp*/pIJ6902*crp* and Δ*crp*/pIJ6902 (empty vector strain; negative control) pre (0 min) and post (15, 45 min) *crp* induction. *rpfA* promoter DNA levels detected in affinity-purified extracts by qPCR were normalized to levels detected in genomic DNA extracts. Normalized promoter DNA levels in the *crp*-inducible strain were then expressed relative to those in the negative control strain, as described in the *Experimental Procedures.* Enrichment levels are presented as mean fold changes (relative to '0 min') ± standard error (n = 2).

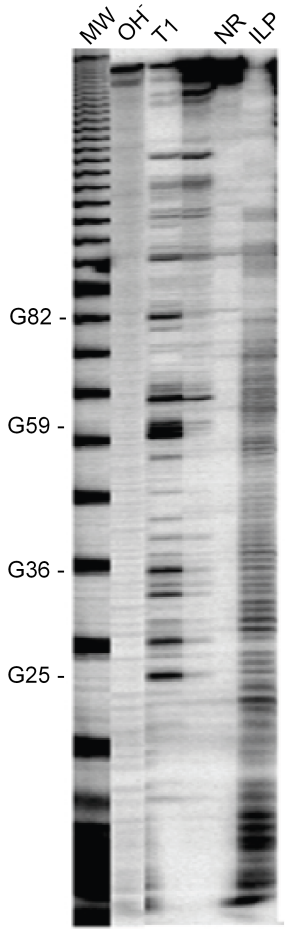

Fig. 2.5. Structural analysis of the *rpfA* 5′ UTR. In-line probing of the *S. coelicolor rpfA* leader RNA. MW, 10-bp DNA ladder (Invitrogen); OH^-, alkali-treated RNA; T1, RNA digested with RNase T1, which cleaves after G residues; NR, untreated RNA; ILP, in-line probing reaction.

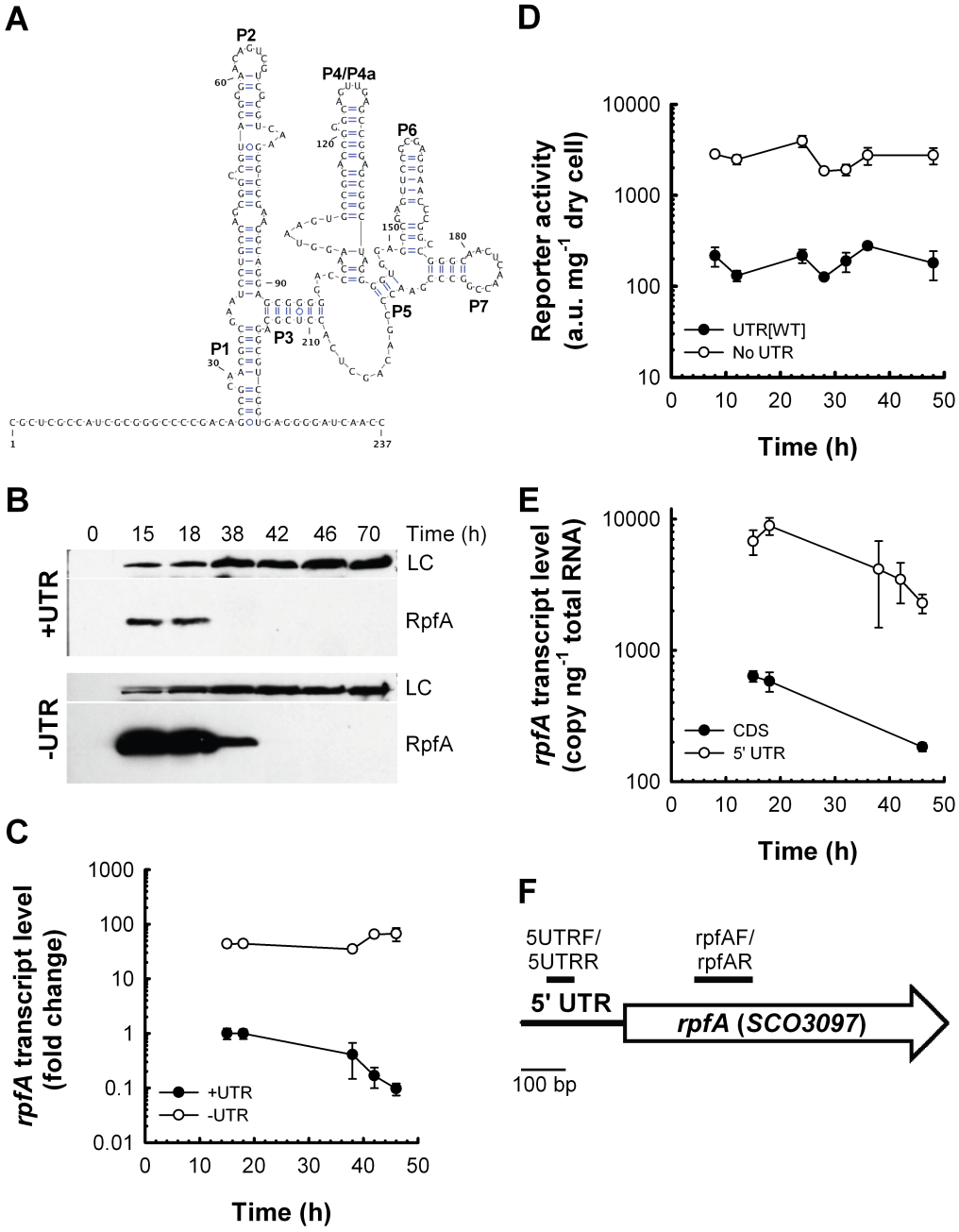

Fig. 2.6. Riboswitch-mediated regulation of *rpfA* gene expression. (A) Sequence and proposed secondary structure of the *S. coelicolor rpfA* 5′ UTR. Stem-loops are numbered P1 to P7. Structure was drawn using VARNA (Darty *et al.*, 2009). (B and C) At the times indicated, an aliquot was harvested from cultures of *S. coelicolor* constitutively transcribing *rpfA-flag* with (+UTR, E104a/pMC230) or without (-UTR, E104a/pMC229) its 5′ UTR. (B) Secreted RpfA-FLAG was detected by immunoblotting. Image is a representative of three biological replicates. LC, loading control, non-specific binding of the anti-FLAG antibody to an unknown secreted protein. (C) In parallel, RNA was extracted from cells, and *rpfA* transcripts were quantified using RT-qPCR with

primer pair rpfAF/rpfAR. Transcript levels were normalized to total RNA mass and expressed as fold changes relative to expression levels in '+UTR' at 15 h. Data are presented as mean ± standard error (*n* = 3). (D) *S. coelicolor* wild-type strains constitutively transcribing the *luxCDABE* operon with (UTR[WT], M145/pMC222) or without (No UTR, M145/pFLUX-Pos) the *rpfA* 5′ UTR, were grown in rich liquid medium. Reporter activity was quantified throughout exponential (8-24 h) and stationary growth (28-48 h). Background-subtracted luminescence was normalized to dry cell weight. Data are presented as mean ± standard error (*n* = 3). (E) RNA was extracted from liquid-grown wild-type *S. coelicolor* (M145) at the time-points indicated. *rpfA* transcripts were quantified by RT-qPCR using primers targeting either the coding region (CDS, rpfAF/rpfAR) or the 5′ UTR (5UTRF/5UTRR). Data are presented as mean ± standard error (*n* = 2-3). (F) Location of amplified PCR products relative to the transcriptional and translational start sites are indicated as bold lines above the block arrow. Gene and PCR products were drawn to scale. All associated growth curves are presented in Fig. 2.18.

B. subtilis ydaO

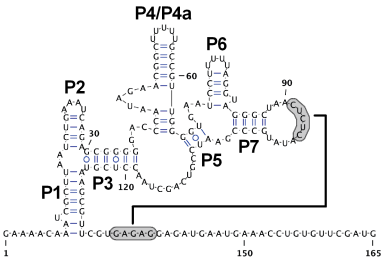

S. coelicolor rpfA

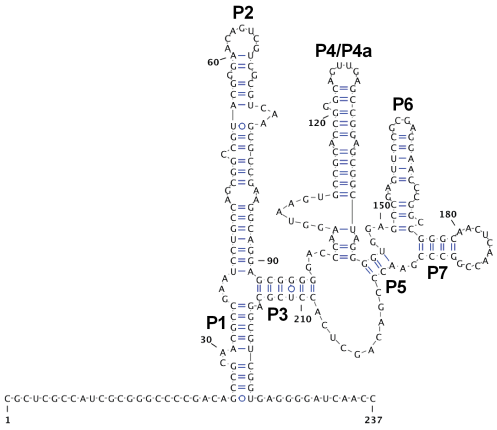

S. venezuelae rpfA

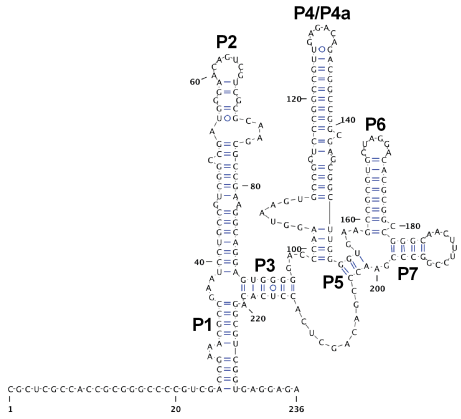

Fig. 2.7. Sequence and secondary structures of *ydaO*-like riboswitches. Stem-loops are numbered P1 to P7. Single-stranded regions forming pseudoknots are highlighted in gray. The *B. subtilis ydaO* riboswitch structure was based on Nelson *et al.* (2013). All structures were drawn using VARNA (Darty *et al.*, 2009).

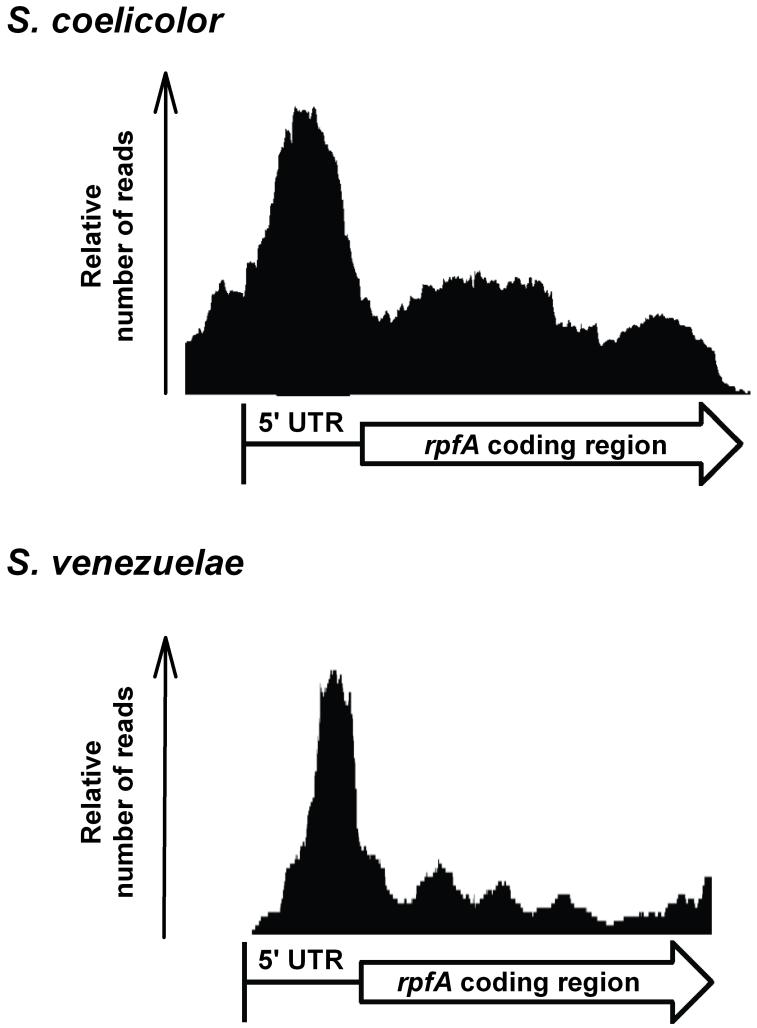

Fig. 2.8. *rpfA* transcript abundance. RNA was extracted from *S. coelicolor* wild-type strain M145 grown on MYM agar and from *S. venezuelae* wild-type strain ATCC 10712 grown in MYM broth. Transcripts were quantified using next-generation sequencing. Relative read coverage is indicated. Graphs were constructed from data collected by Moody *et al.* (2013) and E. Sherwood (unpublished results).

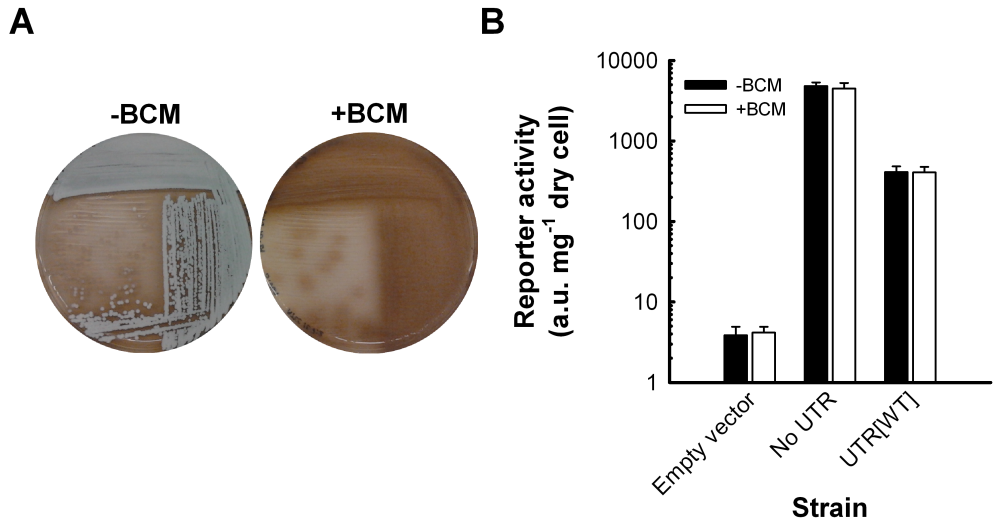

Fig. 2.9. Impact of Rho activity on *rpfA* 5′ UTR-mediated gene regulation. (A) *S. venezuelae* wild-type strain (ATCC 10712) was grown for 2 days at 30°C on MYM agar supplemented with (+BCM) or without (-BCM) 100 µg mL^{-1} bicyclomycin. (B) *S. coelicolor* wild-type strains, constitutively transcribing the *luxCDABE* operon with or without the *rpfA* 5′ UTR, were grown in a rich liquid medium. After 24 h, cultures were treated with either sterile water (-BCM) or 90 µg mL^{-1} bicyclomycin (+BCM), and luciferase reporter activity was measured. Background-subtracted luminescence was normalized to dry cell weight. Data are presented as mean ± standard error (*n* = 3). Empty vector, M145/pFLUX; No UTR, M145/pFLUX-Pos; UTR[WT], M145/pMC222.

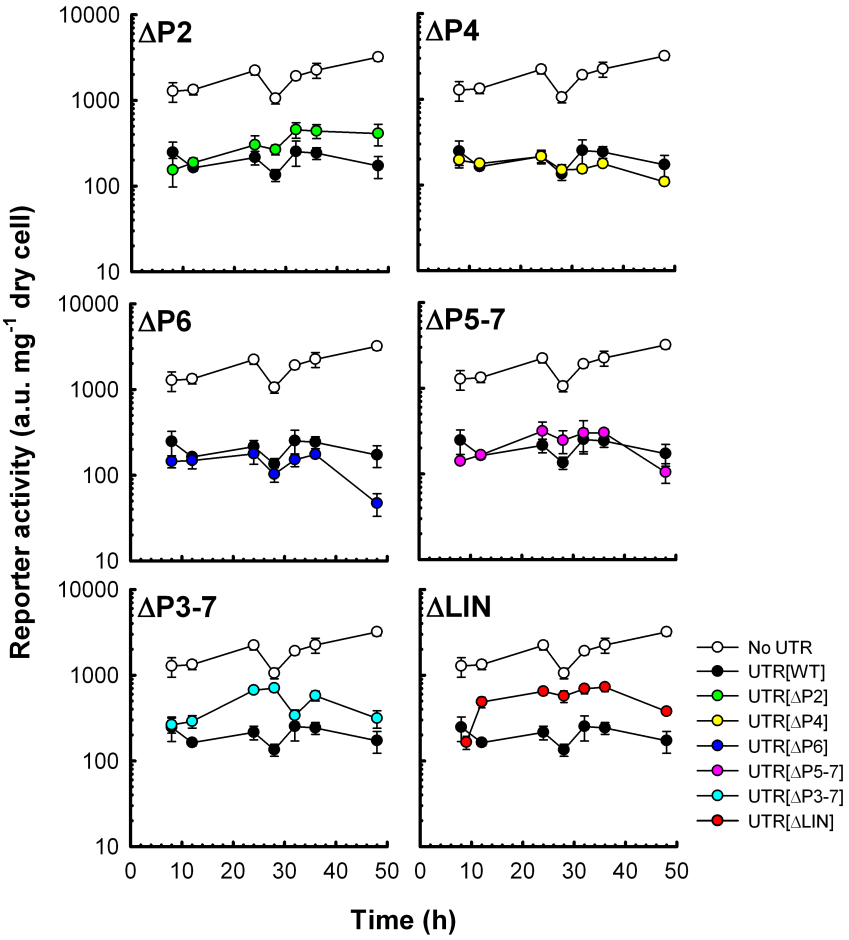

Fig. 2.10. Mutational analysis of the *rpfA* 5′ UTR. *S. coelicolor* wild-type strains, constitutively transcribing the *luxCDABE* operon with or without wild-type or mutagenized *rpfA* 5′ UTR, were grown in a rich liquid medium. Reporter activity was quantified throughout exponential (8-24 h) and stationary growth (28-48 h). Background-subtracted luminescence was normalized to dry cell weight. Data are presented as mean ± standard error (n = 4). Growth curves are presented in Fig. 2.18. Empty vector, M145/pFLUX; No UTR, M145/pFLUX-Pos; UTR[WT], M145/pMC222; UTR[ΔP2], M145/pMC223; UTR[ΔP4], M145/pMC224; UTR[ΔP6], M145/pMC225; UTR[ΔP5-7], M145/pMC226; UTR[ΔP3-7], M145/pMC227; UTR[ΔLIN], M145/pMC231.

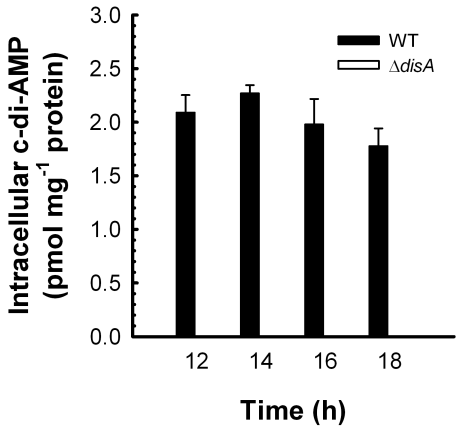

Fig. 2.11. Quantification of c-di-AMP levels in wild-type and Δ*disA* mutant strains. *S. venezuelae* wild-type (WT, ATCC 10712) and Δ*disA* mutant strains were grown in MYM broth. At the indicated times, c-di-AMP was extracted from cells and quantified by LC-MS/MS. c-di-AMP levels were normalized to total cellular proteins. Data are presented as mean ± standard error (*n* = 3).

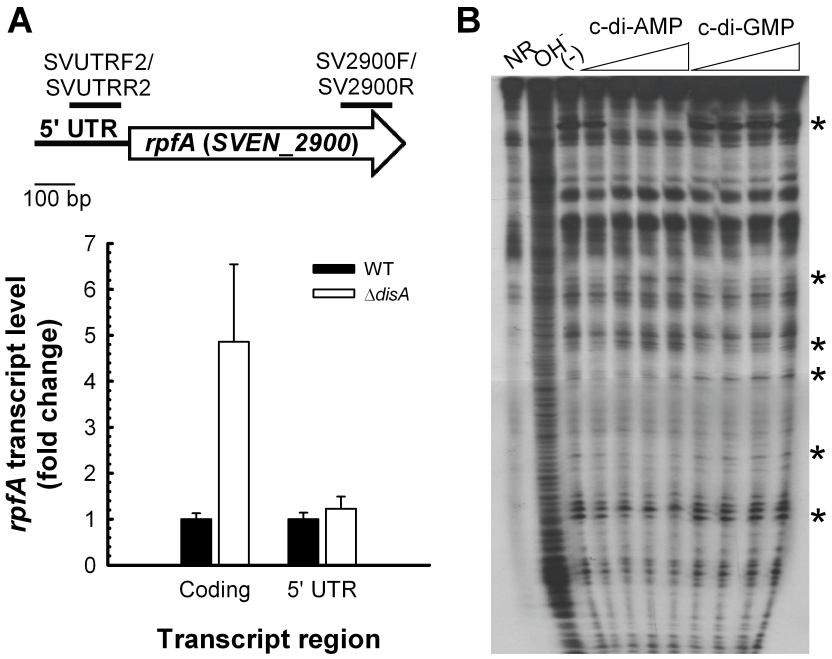

Fig. 2.12. c-di-AMP-dependent regulation of *rpfA* expression. (A) *S. venezuelae* wild-type (WT, ATCC 10712) and Δ*disA* mutant strains were grown in MYM broth. RNA was extracted from vegetative cells, and *rpfA* transcripts were quantified by RT-qPCR using primers targeting either the coding region (SV2900F/SV2900R) or the 5′ UTR (SVUTRF2/SVUTRR2). Transcript levels were normalized to total RNA mass and expressed as fold changes relative to expression levels in the wild-type strain. Data are presented as mean ± standard error (*n* = 2-3). Location of amplified PCR products relative to the transcriptional and translational start sites are indicated as bold lines above the block arrow. Gene and PCR products were drawn to scale. (B) In-line probing of the *S. coelicolor rpfA* 5′ UTR in the presence and absence of ligand (1 nM, 100 nM, 10 μM and 1 mM). Asterisks indicate select sites of altered cleavage. NR, untreated RNA; OH^-, alkali-treated RNA; (-), in-line probing reaction conducted in the absence of ligand; c-di-AMP and c-di-GMP, in-line probing reactions conducted in the presence of indicated ligand.

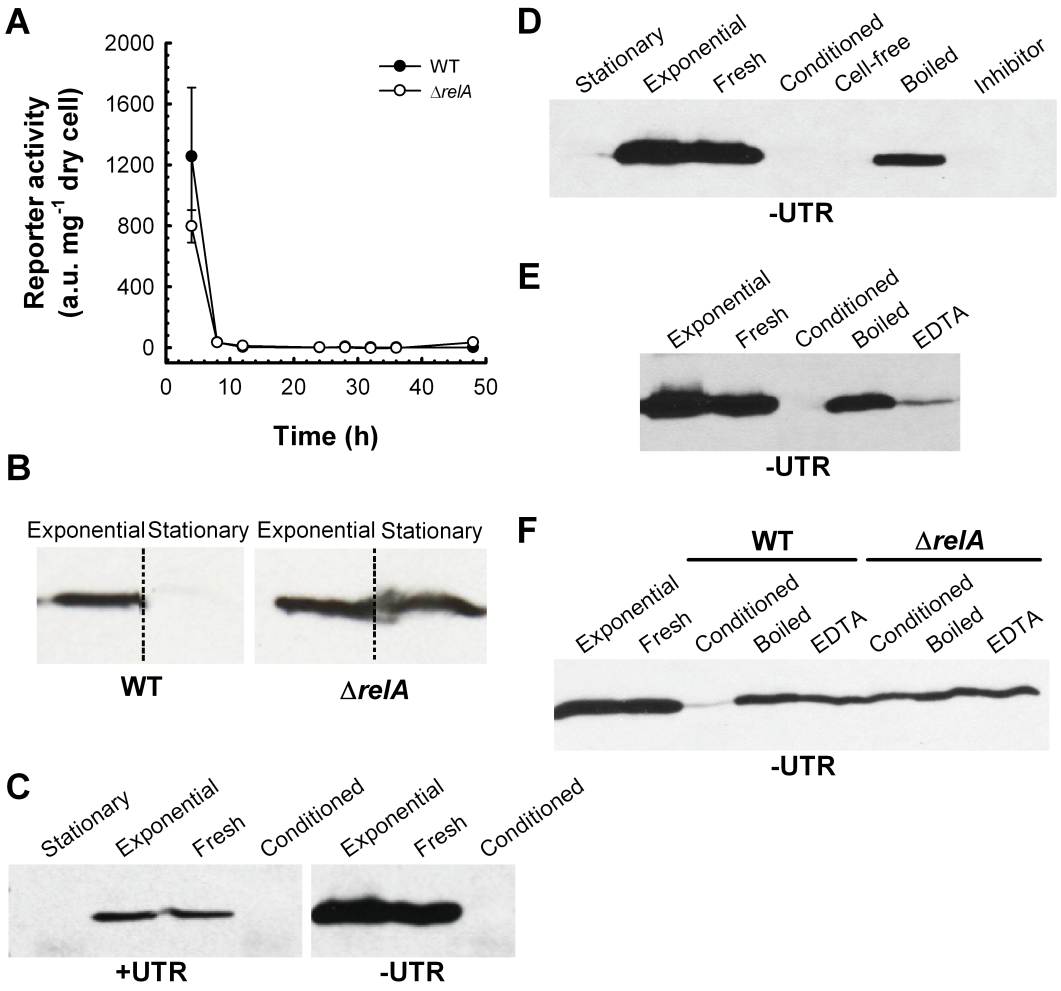

Fig. 2.13. Stringent response-mediated regulation of *rpfA* expression. (A) The *S. coelicolor* wild-type (WT, M145/pMC195) and Δ*relA* mutant (M570/pMC195), transcribing the *luxCDABE* operon from the native *rpfA* promoter, were grown at 30°C in a rich liquid medium. Luciferase reporter activity was measured throughout exponential (4-24 h) and stationary growth (28-48 h). Background-subtracted luminescence was normalized to dry cell weight. Data are presented as mean ± standard error (*n* = 2-3). Growth curves are presented in Fig. 2.18. (B) Secreted RpfA-FLAG proteins were detected in exponential- and stationary-phase cultures of *S. coelicolor* wild-type (WT, M145/pMC229) and Δ*relA* mutant (M570/pMC229) strains, constitutively transcribing *rpfA-flag* without its 5′ UTR, using immunoblotting. Growth curves are presented in Fig. 2.18. (C-E) Exponential-phase cells of *S. coelicolor* constitutively transcribing *rpfA-flag*, with (+UTR, E104a/pMC230) or without (-UTR, E104a/pMC229) the *rpfA* 5′ UTR, were recovered, washed, and resuspended in either fresh medium (Fresh), conditioned medium (cell-free supernatant recovered from a stationary-phase culture of *S. coelicolor* strain E104a/pMC229; Conditioned), boiled conditioned medium (Boiled), or conditioned medium treated with a broad-spectrum serine/cysteine protease inhibitor cocktail (Inhibitor) or EDTA (20 mM). In parallel, conditioned medium was mixed with exponential-phase supernatant in a 1:1 ratio (Cell-free). Cultures and cell-free mixtures were incubated for 1 h at 30°C. Secreted proteins were extracted from the culture supernatant of each culture/mixture, including the

stationary-phase culture used to prepare the conditioned medium (Stationary) and the exponential-phase culture from which cells were harvested (Exponential). RpfA-FLAG proteins were detected by immunoblotting. (F) RpfA-rich supernatant recovered from an exponential-phase *S. coelicolor* culture (-UTR, E104a/pMC229) was mixed with an equal volume of supernatant from stationary-phase wild-type (WT, M145) or Δ*relA* mutant (M570) cultures, left untreated, boiled or treated with EDTA (20 mM). RpfA-FLAG proteins were extracted from the mixtures after 1 h at 30°C and detected by immunoblotting. Notations are as described above. All images are representative of two to three biological replicates.

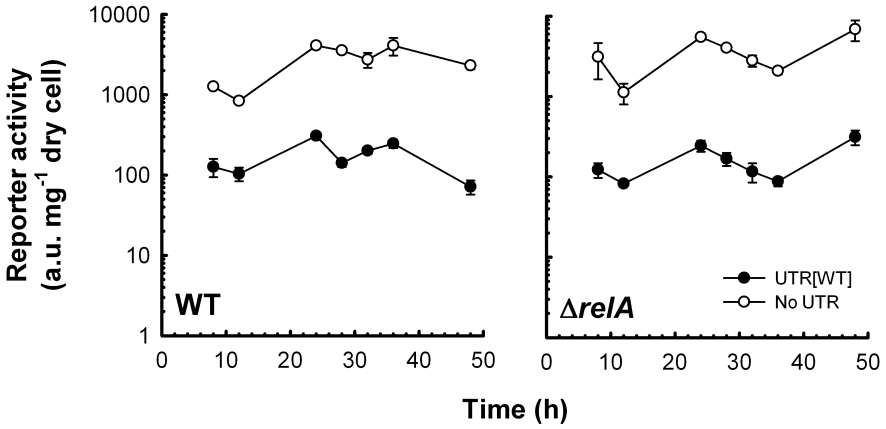

Fig. 2.14. Impact of ppGpp synthesis on *rpfA* 5′ UTR-mediated gene regulation in *S. coelicolor*. The *S. coelicolor* wild-type (M145) and Δ*relA* mutant (M570), constitutively transcribing the *luxCDABE* operon, with or without the *rpfA* 5′ UTR, were grown at 30°C in a rich liquid medium. Luciferase reporter activity was measured throughout exponential (8-24 h) and stationary growth (28-48 h). Background-subtracted luminescence was normalized to dry cell weight. Data are presented as mean ± standard error (*n* = 3). Growth curves are presented in Fig. 2.18. No UTR, pFLUX-Pos; UTR[WT], pMC222.

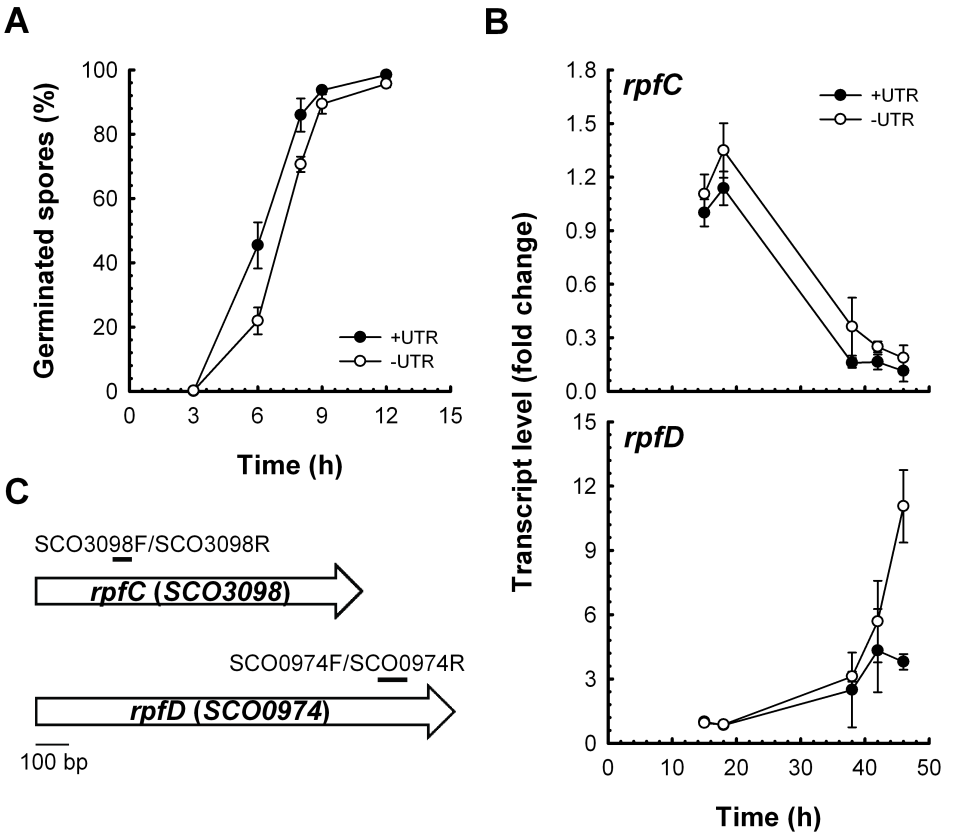

Fig. 2.15. Effect of RpfA overexpression on spore germination and *rpf* gene expression. (A) *S. coelicolor* Δ*rpfA* strains constitutively transcribing *rpfA-flag*, with (+UTR, E104a/pMC230) or without (-UTR, E104a/pMC229) the *rpfA* 5′ UTR, were grown on solid (MS) agar. At the indicated time-points post-inoculation, spores were visualized using bright-field microscopy and scored as either 'germinated' or 'non-germinated'. A minimum of 55 spores was counted per sample. The fraction of spores displaying at least one germ tube was calculated. Data are presented as mean ± standard error (n = 3). (B) Strains were grown in a rich liquid medium at 30°C. RNA was extracted from cells, and *rpfC* and *rpfD* transcripts were quantified using RT-qPCR. Transcript levels were normalized to total RNA mass and expressed as fold changes relative to expression levels in '+UTR' at 15 h. Data are presented as mean ± standard error (n = 3). Growth curves are presented in Fig. 2.18. (C) Location of amplified PCR products relative to the translational start and stop sites are indicated as bold lines above the block arrows. Genes and PCR products were drawn to scale.

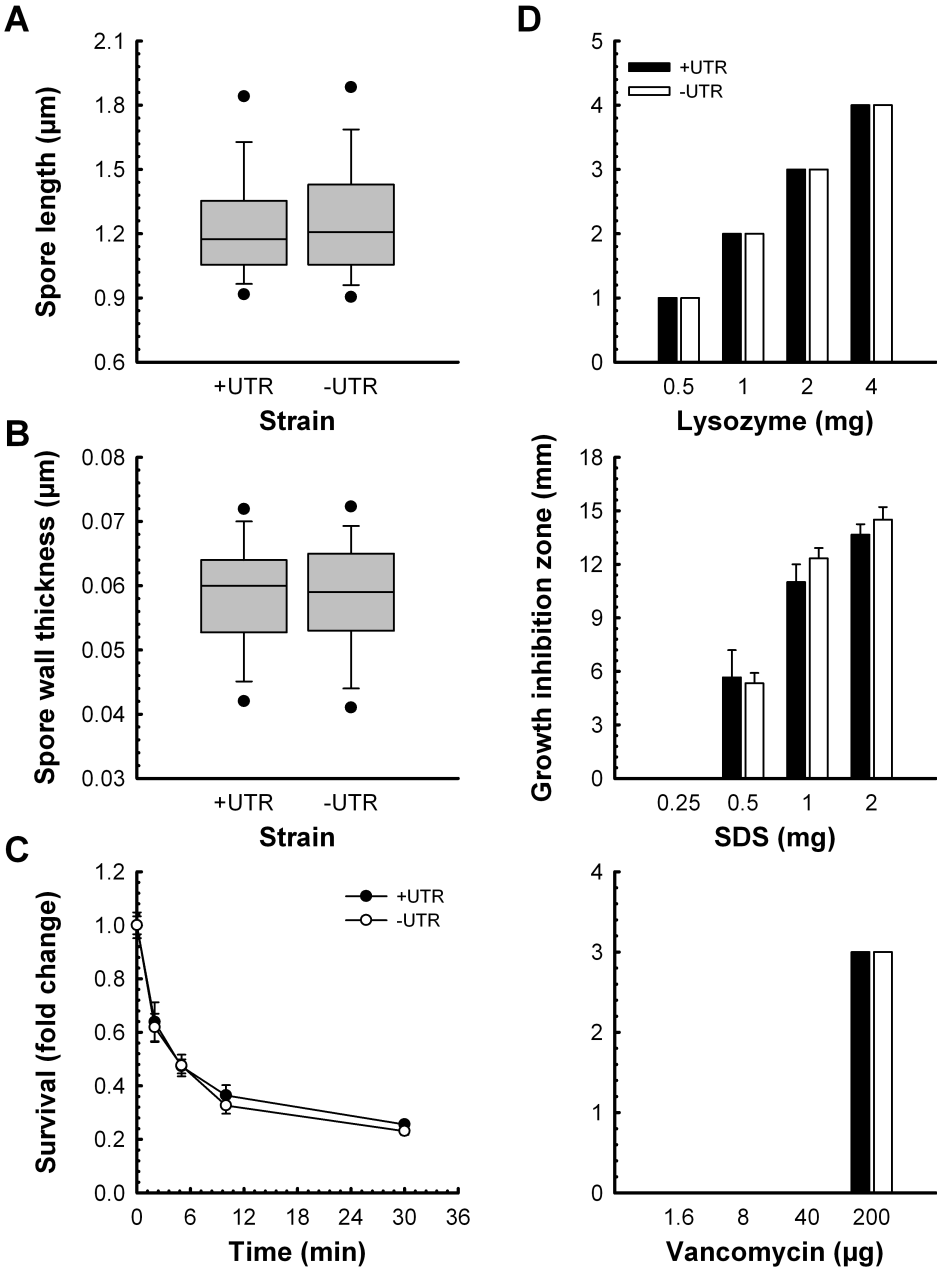

Fig. 2.16. Phenotypic impacts of RpfA overexpression. (A) *S. coelicolor* Δ*rpfA* strains, constitutively transcribing *rpfA-flag* with (*n* = 3,054) or without (*n* = 2,871) the *rpfA* 5′ UTR, were grown on MS agar. Spores were observed by bright-field microscopy, and their lengths were measured. (B) *S. coelicolor* Δ*rpfA* strains, constitutively transcribing *rpfA-flag* with (*n* = 50) or without (*n* = 56) the *rpfA* 5′ UTR, were grown on MS agar. Spores were observed by transmission electron microscopy, and their wall thickness was measured. Box plots indicate the median (center line), the 25th and 75th percentile (bottom and top of box, respectively), the 10th and 90th percentile (lower and higher whiskers, respectively), and the 5th and 95th percentile (lower and higher dots,

respectively). (C) *S. coelicolor* spores were heat-shocked at ~57°C for the indicated lengths of time. Spore survival was assessed by plating and expressed as a fold change relative to un-heated samples (0 min). Data are presented as mean ± standard deviation (*n* = 3). (D) *S. coelicolor* strains were grown on MM agar on which were placed filter paper disks containing lysozyme, sodium dodecyl sulfate (SDS) or vancomycin. After 4 days, the zones of growth inhibition surrounding each disk were measured. Data are presented as mean ± standard deviation (*n* = 3). +UTR, E104a/pMC230; -UTR, E104a/pMC229.

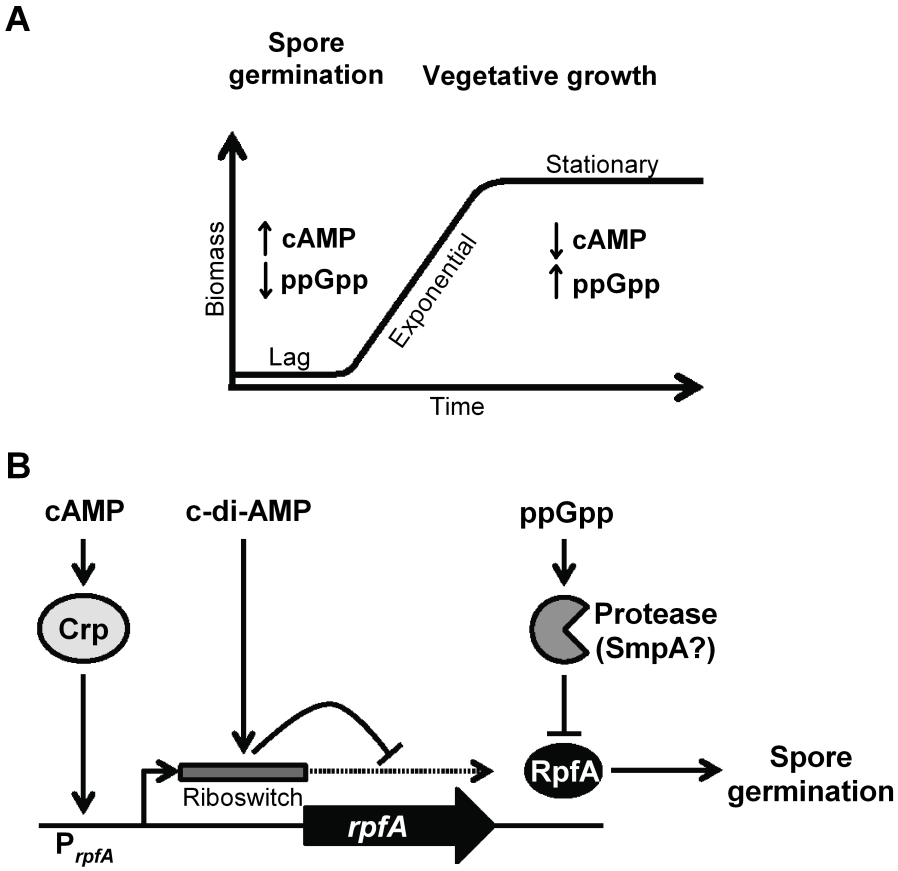

Fig. 2.17. Model depicting the multi-level regulation of *rpfA*. (A) Bacterial growth curve highlighting relative changes in second messenger levels throughout growth. (B) *rpfA* expression is regulated at the level of transcription initiation, transcript elongation and protein stability by second messengers cAMP, c-di-AMP and ppGpp, respectively. Arrows and right-angle lines denote positive and negative regulation, respectively.

Fig. 2.6B, 2.6C and 2.15B

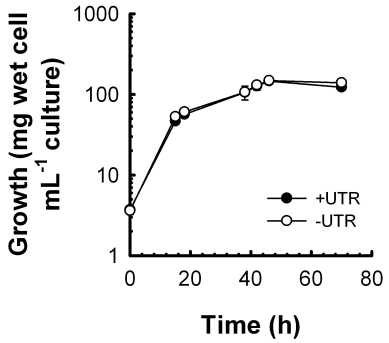

Fig. 2.6D

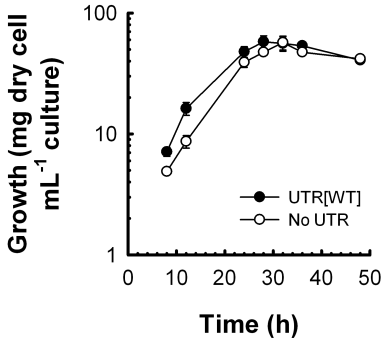

Fig. 2.6E

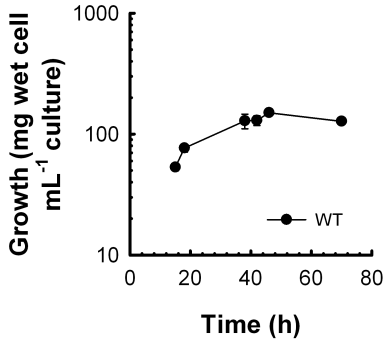

Fig. 2.13A

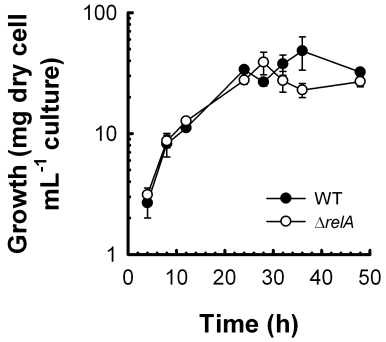

Fig. 2.13B

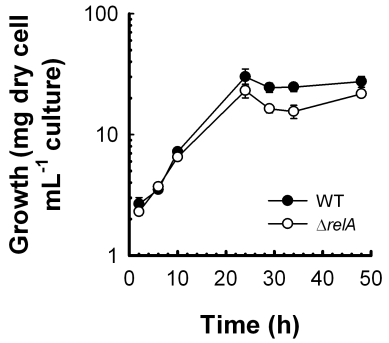

Fig. 2.10

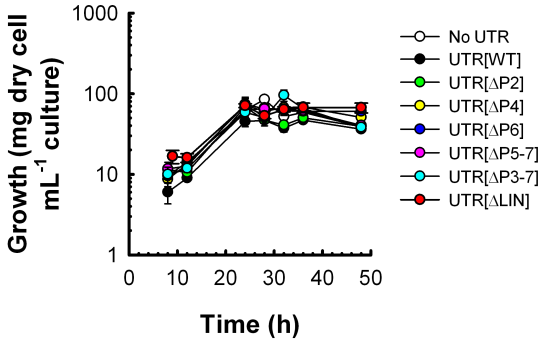

Fig. 2.14

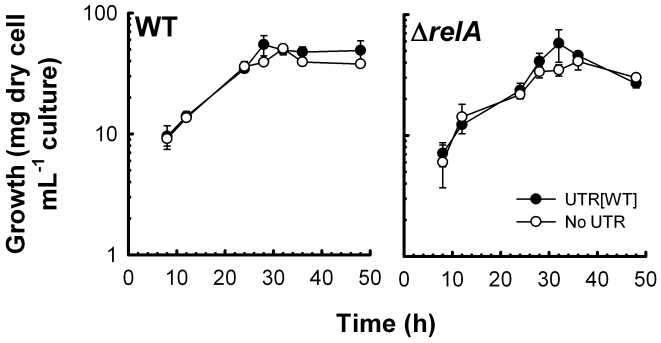

Fig. 2.18. *Streptomyces* growth. *Streptomyces* growth was monitored throughout exponential and stationary phases. Cells were periodically recovered from a culture aliquot by centrifugation. When indicated, cells were dried at 60°C. Each panel presents the growth curves associated with the indicated figure in Chapter 2. *Fig. 2.6B, 2.6C and 2.15B.* +UTR, E104a/pMC230; -UTR, E104a/pMC229. *Fig. 2.6D.* UTR[WT], M145/pMC222; No UTR, M145/pFLUX-Pos. *Fig. 2.6E*. WT, M145. *Fig. 2.13A.* WT, M145/pMC195; Δ*relA*, M570/pMC195. *Fig. 2.13B.* WT, M145/pMC229; Δ*relA*, M570/pMC229. *Fig. 2.10.* No UTR, M145/pFLUX-Pos; UTR[WT], M145/pMC222; UTR[ΔP2], M145/pMC223; UTR[ΔP4], M145/pMC224; UTR[ΔP6], M145/pMC225; UTR[ΔP5-7], M145/pMC226; UTR[ΔP3-7], M145/pMC227; UTR[ΔLIN], M145/pMC231. *Fig. 2.14.* WT, M145; Δ*relA*, M570; UTR[WT], pMC222; No UTR, pFLUX-Pos.

CHAPTER 3

A CYCLIC DI-AMP-RESPONSIVE RIBOSWITCH REGULATES TRANSCRIPTION PROCESSIVITY OF A MURALYTIC ENZYME-ENCODING GENE

Renée J. St-Onge, Volkhard Kaever, Marie A. Elliot

Chapter 3 constitutes a manuscript in preparation. I conducted all the experiments with few exceptions (listed below) and performed all the data processing and analyses. I wrote the manuscript and prepared all the figures and tables. Volkhard Kaever quantified cyclic di-AMP extracted from plate-grown *S. coelicolor* strain M145. Marie A. Elliot and I designed the experiments, interpreted the data and edited the manuscript.

3.1 ABSTRACT

Riboswitches are *cis*-acting regulatory RNAs embedded in the 5′ untranslated region of their mRNA targets. They recognize specific metabolites, and metabolite binding leads to a conformational change that modulates the expression of the downstream gene(s). In the actinobacteria, a *ydaO*-like riboswitch is associated with *rpfA*, where *rpfA* encodes a secreted muralytic enzyme involved in establishing and exiting dormancy. In the model bacterium *Streptomyces coelicolor*, the riboswitch decreases *rpfA* transcript abundance in response to the second messenger cyclic di-AMP, itself involved in cell wall metabolism and dormancy. The mechanism by which this ligand-responsive regulatory system acts, however, is entirely unknown, as there is no obvious expression platform associated with this riboswitch. To begin to understand this, we first coupled structural probing with bioinformatic analyses to determine the secondary structure of the *rpfA* riboswitch in its unbound and ligand-bound states. Using *in vitro* transcription assays, we discovered that, unlike other riboswitches characterized to date, the *rpfA* riboswitch decreased transcript abundance in response to cyclic di-AMP by inhibiting transcription processivity. Through a comprehensive mutational analysis, we determined that reduced processivity required ligand binding and involved an unusual extended stem-loop region unique to a subset of *ydaO*-like riboswitches in the actinobacteria. We further observed rapid *in vitro* degradation of *rpfA* transcripts in the presence of the second messenger, although this effect was riboswitch-independent.

3.2 INTRODUCTION

Non-coding RNAs, like riboswitches, provide an elegant means of fine-tuning gene expression after transcription has initiated. Riboswitches are *cis*-encoded regulatory RNA elements generally embedded in the 5′ untranslated region (UTR) of an mRNA. Like their protein counterparts, these regulators monitor the metabolic state of the cell through direct interaction with metabolites, and these metabolites are often the product of the pathway they regulate. Riboswitches exert their regulatory effects by switching between two mutually exclusive structures in response to ligand binding. Within the riboswitch itself, the sensor domain binds the ligand, while the downstream expression platform translates the biological signal into a regulatory response by modulating transcript

elongation, transcript stability or translation initiation (Serganov and Nudler, 2013).

In 2004, a novel riboswitch, named '*ydaO*' after its cognate gene in *Bacillus subtilis*, was discovered through computational analyses of intergenic sequences with riboswitch-like features (Barrick *et al.*, 2004). Subsequent *in silico* searches of bacterial genomes revealed that the *ydaO* element is widespread among Gram-positive bacteria, where it is associated with genes involved in cell wall remodeling, amino acid metabolism and transport, and ion transport (Barrick *et al.*, 2004; Block *et al.*, 2010; Nelson *et al.*, 2013). Because the riboswitch motif was associated with such a wide variety of seemingly unrelated genes/pathways (Barrick *et al.*, 2004; Block *et al.*, 2010; Nelson *et al.*, 2013), the ligand for this riboswitch eluded identification for nearly a decade. Ultimately, a systematic media-based ligand screening strategy revealed that the second messenger cyclic di-AMP modulates *ydaO* activity (Nelson *et al.*, 2013). Interestingly, cyclic di-AMP affects not only cell wall metabolism in a range of bacteria (Corrigan *et al.*, 2011; Luo and Helmann, 2012; Mehne *et al.*, 2013), but also sporulation in *Bacillus* (Oppenheimer-Shaanan *et al.*, 2011). Several variants of the sensor domain have now been successfully crystallized with cyclic di-AMP, revealing a pseudo two-fold symmetrical domain binding two molecules of cyclic di-AMP. Further analysis allowed the identification of key ligand-binding residues, including four A and/or U residues forming stacking interactions with the adenine moieties of cyclic di-AMP (Gao and Serganov, 2014; Jones and Ferré-D'Amaré, 2014; Ren and Patel, 2014).

In *B. subtilis*, the *ydaO* riboswitch prematurely terminates transcription of its cognate gene in response to high levels of cyclic di-AMP (Nelson *et al.*, 2013). A canonical intrinsic terminator was predicted downstream of the sensor domain (Block *et al.*, 2010; Nelson *et al.*, 2013), and mutational analyses confirmed its involvement in ligand-dependent attenuation (Nelson *et al.*, 2013). Though it is clear that terminator formation is essential for riboswitch activity (Nelson *et al.*, 2013), a mutually exclusive antiterminator, which would enable read-through in the absence of cyclic di-AMP, has not been identified, and so the means by which the riboswitch toggles between its 'ON' and 'OFF' states remains unclear.

In the actinobacteria, including *Streptomyces*, a *ydaO*-like motif is associated with *rpfA* (Haiser *et al.*, 2009; Block *et al.*, 2010; Nelson *et al.*, 2013), a gene involved in establishing and exiting dormancy. Bacteria can adopt a state of dormancy – characterized by low metabolism and an inability to replicate – to survive suboptimal growth conditions (Dworkin and Shah, 2010; Rittershaus *et al.*, 2013). Whereas some actinobacteria adopt 'cyst-like' structures during

dormancy [*e.g.*, *Mycobacterium* (Anuchin *et al.*, 2009; Shleeva *et al.*, 2011)], the streptomycetes form spores. The *Streptomyces* developmental cycle begins with the establishment of a vegetative mycelium and culminates with the raising of aerial hyphae and metamorphosis of these hyphal compartments into spores (Elliot and Flärdh, 2012). Although dormant structures can vary, all dormancy-adopting actinobacteria must remodel their cell wall at the onset of both dormancy and growth resumption (or 'resuscitation') (Glauert and Hopwood, 1961; Bradley and Ritzi, 1968; Mukamolova *et al.*, 1995; Anuchin *et al.*, 2009; Shleeva *et al.*, 2011; Puspita *et al.*, 2013).

In the actinobacteria, secreted muralytic enzymes called the resuscitation-promoting factors (Rpfs) orchestrate resuscitation through their cell wall remodeling activities (Kana and Mizrahi, 2010). Given the destructive potential of these enzymes, it is critical that their expression be tightly controlled to ensure the integrity of the cell wall throughout growth. In the streptomycetes, *rpfA* is regulated at multiple levels, including post-transcriptionally by a *ydaO*-like riboswitch (St-Onge *et al.*, 2015). We previously investigated the function of this so-called *rpfA* riboswitch in the sporulating bacterium *Streptomyces coelicolor*, and found that it negatively impacted *rpfA* transcript abundance in response to cyclic di-AMP (St-Onge *et al.*, 2015). The mechanism by which transcript levels are reduced remains unclear; unlike its counterpart in *B. subtilis* (Block *et al.*, 2010; Nelson *et al.*, 2013), the *rpfA* riboswitch lacks an intrinsic terminator, and riboswitch activity is Rho-independent (St-Onge *et al.*, 2015).

Given that the *rpfA* riboswitch lacks an obvious expression platform, we set out to determine the mechanism by which the *rpfA* riboswitch regulates gene expression in *S. coelicolor*. We found that the riboswitch utilized an unusual mechanism of control: it inhibited transcription processivity in response to cyclic di-AMP binding. We further identified novel activity determinants that distinguished the *S. coelicolor rpfA* riboswitch from the *B. subtilis* model.

3.3 RESULTS

3.3.1 *rpfA* riboswitch-dependent attenuation correlates with intracellular cyclic di-AMP levels.

As a first step towards characterizing the regulatory mechanism employed by the *rpfA* riboswitch, we monitored *rpfA* transcript abundance in plate-grown *S. coelicolor* throughout its developmental cycle. We used a transcriptional

luciferase reporter system in which reporter genes were fused to the 3′ end of the *rpfA* riboswitch, and we monitored reporter gene expression in wild-type *S. coelicolor* cells grown on a sporulation-conducive solid medium. We found that transcript levels were low throughout vegetative growth, but increased 2.7-fold during aerial development and sporulation (Fig. 3.1A).

Because the *rpfA* riboswitch binds and responds to the second messenger cyclic di-AMP (St-Onge *et al.*, 2015), we sought to connect post-transcriptional changes in *rpfA* transcript abundance with intracellular cyclic di-AMP levels. We followed ligand levels in plate-grown *S. coelicolor* using liquid chromatography-coupled tandem mass spectrometry (LC-MS/MS), and discovered that the second messenger was most abundant during vegetative growth (we were unable to monitor *rpfA* expression or cyclic di-AMP abundance during germination and early vegetative growth owing to insufficient biomass). Thereafter, cyclic di-AMP levels decreased by 53%, reaching a minimal value during sporulation (Fig. 3.1B). Our findings suggested that *rpfA* expression and cyclic di-AMP levels were inversely associated, as would be expected for an 'OFF'-acting riboswitch.

3.3.2 Cyclic di-AMP binds the *rpfA* riboswitch and alters RNA structure.

Though we had previously determined that the riboswitch negatively impacts *rpfA* transcript abundance (St-Onge *et al.*, 2015), the mechanism by which it acts remained elusive. We therefore set out to characterize the ligand-binding domain and identify the expression platform within the *rpfA* 5′ UTR. We initially took a structural probing approach, with the expectation that comparing the structure of the 5′ UTR in the presence and absence of the ligand may provide valuable insight into the mechanism underlying riboswitch control. For example, mutually exclusive terminator and antiterminator structures would indicate regulation at the level of transcript elongation. Using in-line probing, we assessed the secondary structure of the *rpfA* riboswitch in both its unbound and cyclic di-AMP-associated states (Fig. 3.2). We determined that cyclic di-AMP binding protected against scission within the P0, P1 and P3 stems, the P7 stem-loop region, the proximal P2 bulge and the single-stranded region bridging stems P3 and P5, suggesting that these regions were stabilized upon ligand binding. Reduced cleavage in the presence of cyclic di-AMP was also noted in similar regions within the *ydaO* riboswitches from *B. subtilis*, *Clostridium acetobutylicum*, *Nostoc punctiforme* and *Syntrophus aciditrophicus* (Nelson *et al.*, 2013). These regions are highly conserved at the sequence and/or structure levels (Block *et al.*,

2010; Nelson *et al.*, 2013), and several of these regions harbor cyclic di-AMP-binding residues (*e.g.*, P1, single-stranded region) (Gao and Serganov, 2014; Jones and Ferré-D'Amaré, 2014; Ren and Patel, 2014). In contrast, the P4a stem structure was consistently cleaved, irrespective of ligand status, suggesting a lack of structural rearrangement in this region. We also found that the upper P2 stem was more prone to cleavage in the presence of cyclic di-AMP, suggesting enhanced structural flexibility upon ligand binding. This was unexpected as in-line probing analyses of *ydaO* riboswitches from different species had indicated that the P2 stem-loop was not differentially cleaved (Nelson *et al.*, 2013), and co-crystallization of several *ydaO*-like riboswitch sensor domains with cyclic di-AMP suggested that this region lacked ligand binding residues (Gao and Serganov, 2014; Jones and Ferré-D'Amaré, 2014; Ren and Patel, 2014).

Whereas *ydaO*-like riboswitches studied to date have obvious expression platforms [*e.g.*, a typical intrinsic terminator in *B. subtilis* (Block *et al.*, 2010; Nelson *et al.*, 2013) and *Thermoanaerobacter tengcongensis* (Ren and Patel, 2014), a ribosome binding site-sequestering stem in *Thermoanaerobacter pseudethanolicus* (Gao and Serganov, 2014)], the *rpfA* riboswitch appeared to consist solely of the sensor domain (Fig. 3.2A). Because the *rpfA* 5′ UTR lacked structural features commonly associated with expression platforms regulating transcript elongation, we extended our search into the upstream region of the coding sequence. We noted a string of U residues within the first dozen nucleotides of the *rpfA* coding region, and reasoned that it may comprise the poly(U) tail of an intrinsic terminator. However, substituting the poly(U) sequence with an arbitrary sequence did not alleviate riboswitch-dependent attenuation and had little impact on ligand binding (Fig. 3.3).

3.3.3 Cyclic di-AMP promotes general transcript degradation.

Given the lack of an obvious intrinsic terminator associated with the *rpfA* riboswitch, and that riboswitch activity is Rho-independent (St-Onge *et al.*, 2015), we hypothesized that the riboswitch was regulating transcript stability by recruiting specific RNases to the mRNA in response to cyclic di-AMP binding. To determine if the riboswitch promoted transcript degradation upon associating with the second messenger, we conducted *in vitro* stability assays. We incubated free and ligand-bound riboswitch RNA with exponential-phase *S. coelicolor* cell-free lysate as a source of RNases, and monitored transcript degradation. We found that riboswitch-associated transcripts were degraded more rapidly when cyclic di-AMP was present than when the closely related second messenger cyclic di-

GMP was added (the riboswitch does not bind cyclic di-GMP) (Fig. 3.4 and 3.5). Boiling the cell lysate with EDTA (20 mM) abrogated RNA degradation, as would be expected if RNases in the lysate were responsible for transcript turnover (Fig. 3.4 and 3.5).

To determine whether transcript degradation was specific for the ligand-bound riboswitch, or if it represented a more general destabilization phenomenon, we repeated our assays using (i) a fragment of the human 18S rRNA that was predicted to be unresponsive to cyclic di-AMP, and (ii) a panel of riboswitch mutants, including variants able to bind cyclic di-AMP ($P2_{Prox.}$) and ones unable to bind the ligand (LIN and P3-7) (described in detail below). We reproducibly observed greater transcript degradation in the presence of cyclic di-AMP, compared to cyclic di-GMP, irrespective of the ligand-binding status of the RNA (Fig. 3.4 and 3.5). This suggested that the effect of cyclic di-AMP on *rpfA* transcript stability was riboswitch-independent, and that the second messenger served an as yet unexplored function in modulating general transcript stability.

3.3.4 Cyclic di-AMP inhibits riboswitch-dependent transcription processivity.

Given the riboswitch, in conjunction with cyclic di-AMP, was not specifically modulating *rpfA* transcript stability, we postulated that the non-coding RNA could be mediating attenuation either by inhibiting transcription processivity or by stabilizing an atypical as yet uncharacterized transcription terminator. To determine whether the riboswitch promoted premature transcription termination, we investigated the effect of cyclic di-AMP on *rpfA* riboswitch read-through using an *in vitro* transcription assay. We found that cyclic di-AMP significantly decreased the yield of full-length transcripts by 45% (Fig. 3.6). To rule out any direct effects of cyclic di-AMP on RNA polymerase activity, we transcribed, in parallel, a fragment of human 18S rRNA, and found that cyclic di-AMP did not significantly impact 18S rRNA synthesis (Fig. 3.6), suggesting that cyclic di-AMP regulated *rpfA* expression through its interaction with the riboswitch. Notably, prematurely terminated products were not detected following transcription in the presence of ligand (Fig. 3.7). This indicated that a classically defined termination event did not occur, and instead supported the notion that the riboswitch regulated transcription processivity in response to the second messenger.

3.3.5 Riboswitch-mediated transcription inhibition requires cyclic di-AMP binding and the P2 stem.

To further explore the mechanism underlying this ligand-dependent modulation of transcription processivity, we sought to identify the sequences and structures required for maximum riboswitch activity. We exploited our luciferase reporter assay, and screened a panel of deletion and substitution riboswitch mutants (Fig. 3.8) for loss of attenuation activity *in vivo*, focusing our attention on vegetative growth, when cyclic di-AMP levels were at their highest (Fig. 3.1B). To effectively differentiate loss-of-function mutants that were unable to bind cyclic di-AMP from ligand-binding mutants adopting a constitutively 'ON' state, we coupled these assays with *in vitro* ligand binding experiments.

We first deleted several conserved stem-loop structures (P2, P4, P6, P5-7) from the *rpfA* riboswitch, and found that these changes had little to no impact on riboswitch attenuation activity during vegetative growth (Fig. 3.9). These results were unexpected, as both the P4a and P6 stem structures are important for *ydaO* riboswitch-dependent attenuation. In *Bacillus*, mutating stem P4a residues impacts riboswitch activity (Block *et al.*, 2010), and destabilizing stem P6 abolishes cyclic di-AMP binding (Nelson *et al.*, 2013) and reduces expression (Block *et al.*, 2010). Furthermore, nucleotides within stems P5 and P7, as well as residues within the P5-P6 junction, of different *ydaO*-like riboswitches interact directly with the ligand (Gao and Serganov, 2014; Jones and Ferré-D'Amaré, 2014; Ren and Patel, 2014). Changes to the P7 stem sequence impede riboswitch-dependent attenuation in *B. subtilis* (Block *et al.*, 2010), and substituting an unpaired adenine residue within the P5-P6 junction (Jones and Ferré-D'Amaré, 2014) or altering the sequence of the P5 or P7 stem (with compensatory mutations maintaining structure) (Gao and Serganov, 2014) reduces or completely abolishes cyclic di-AMP binding.

Similarly, we found that substituting the proximal or distal P0 or P1 stem sequence with its complementary sequence did not relieve attenuation, while substituting the proximal P0 stem sequence, with or without compensatory mutations in the distal region, increased riboswitch-dependent attenuation (Fig. 3.9). Interestingly, several important ligand-binding residues are located within the cognate regions in *ydaO*-like riboswitch sensors from *Bacillus* and *Thermoanaerobacter* (Gao and Serganov, 2014; Jones and Ferré-D'Amaré, 2014; Ren and Patel, 2014).

In contrast, we noted a marked increase in *rpfA* expression *in vivo* (Fig. 3.10) as well as a complete loss of ligand binding *in vitro* (Fig. 3.11) upon deleting

stems P3 to P7 (P3-7). Indeed, approximately three quarters of cyclic di-AMP-binding residues are located in the equivalent regions of other characterized *ydaO*-like riboswitches (Gao and Serganov, 2014; Jones and Ferré-D'Amaré, 2014; Ren and Patel, 2014). We observed a similar loss in attenuation and ligand-binding activities upon deleting the single-stranded region bridging stems P3 and P5 (LIN) (Fig. 3.10 and 3.11), consistent with previous works showing that cyclic di-AMP binding and gene regulation by the *B. subtilis ydaO* riboswitch rely on highly conserved nucleotides within the single-stranded region (Nelson *et al.*, 2013; Jones and Ferré-D'Amaré, 2014). We also found that these mutations rendered the riboswitch unresponsive to cyclic di-AMP. Using our *in vitro* transcription system, we found that mutant riboswitch yields were similar whether the riboswitch was transcribed in the presence or absence of cyclic di-AMP (Fig. 3.6). Our results suggested that, in contrast to our RNA stability experiments, cyclic di-AMP binding was essential for ligand-dependent inhibition of transcription processivity.

The most striking loss of riboswitch activity occurred upon substituting the proximal (but not the distal) P2 stem sequence with its complementary sequence (Fig. 3.10). We confirmed these findings *in vitro* using our transcription assay, where we observed similar transcript levels for the proximal P2 stem mutant in the presence and absence of ligand (Fig. 3.6). Notably, neither the proximal nor distal P2 stem mutations compromised ligand binding: both mutant riboswitches bound cyclic di-AMP with wild-type affinity (Fig. 3.11). Given that the proximal P2 stem substitutions relieved riboswitch-dependent attenuation without affecting ligand binding, we reasoned that the P2 stem mutant was constitutively 'ON' owing to disruption of the expression platform, *i.e.*, the P2 stem mutant could bind the ligand, but had lost the ability to undergo the appropriate structural rearrangement required to inhibit processivity. Consistent with this hypothesis, the proximal P2 stem mutant lost cyclic di-AMP-dependent structural modulation within the P2 stem region (Fig. 3.11). Collectively, this suggested that the P2 stem region was an integral component of the expression platform for the *rpfA* riboswitch, where it acted to modulate transcription processivity.

3.4 DISCUSSION

In *S. coelicolor*, a cyclic di-AMP-responsive riboswitch attenuates the expression of *rpfA* (St-Onge et al., 2015), encoding a resuscitation- and dormancy-promoting secreted muralytic enzyme (Haiser *et al.*, 2009; Sexton *et*

al., 2015). The *rpfA* riboswitch is unusual in that it lacks an obvious expression platform, suggesting the *rpfA* riboswitch may exploit a novel regulatory mechanism in response to ligand binding. Our work here suggests that the riboswitch inhibits transcription processivity upon binding cyclic di-AMP.

Modulation of transcription processivity, while not documented previously for a riboswitch, is not unprecedented as a means of regulation by a non-coding RNA element. It has been best studied in the lambdoid phage HK022, where processive antitermination enables transcriptional read-through of terminators upstream of the early phage genes. In the HK022 system, processive antitermination relies entirely on *cis*-acting RNA elements, called *put* (for **p**olymerase **ut**ilization), and does not require any accessory proteins (King *et al.*, 1996). Transcription of the *put* site generates a simple V-shaped two-stem-loop RNA (King *et al.*, 1996). Binding of this structure by the RNA polymerase ß′ subunit increases the elongation rate and reduces termination efficiency at downstream sites (King *et al.*, 1996).

Our results are consistent with an analogous mechanism of action for the *rpfA* riboswitch: *in vitro* experiments (with no added proteins apart from RNA polymerase) revealed reduced full-length transcripts in the presence of ligand (Fig. 3.6), with no evidence of prematurely terminated transcripts (Fig. 3.7), while *in vivo* investigations suggested transcriptional regulation (Fig. 3.1A), despite there being no obvious expression platform (Fig. 3.2A) or intrinsic terminator present (St-Onge *et al.*, 2015), and Rho not playing a role (St-Onge *et al.*, 2015). The presence of the second messenger may stabilize a structure that interacts with RNA polymerase, rendering the enzyme less proficient [as opposed to more proficient with the HK022 *put* system (King *et al.*, 1996)] and leading to decreased yields without any terminated product accumulating. We acknowledge that while our *in vitro* experiments suggested that additional protein factors were not required, we cannot exclude the possibility that they may contribute to regulation *in vivo*.

Of particular note is the fact that cyclic di-AMP-mediated gene attenuation relied not only on the ability to interact with the ligand, but also on a sequence within the proximal region of the P2 stem. Though dispensable for binding (Fig. 3.11), this sequence was crucial for ligand-dependent gene attenuation, both *in vitro* (Fig. 3.6) and *in vivo* (Fig. 3.10). Riboswitch activity relied solely on the proximal sequence, and not on P2 stem formation, as disrupting the P2 stem by altering the distal stem sequence had no impact on attenuation activity *in vivo* (Fig. 3.10). Our results suggested that at least a portion of the expression platform was found within the proximal P2 stem. Interestingly, the P2 stem region

of the *S. coelicolor rpfA* riboswitch underwent prominent structural rearrangements in response to cyclic di-AMP (Fig. 3.2), which may reflect conformational changes within the expression platform.

When compared with other regions, particularly within the sensor domain, the P2 stem is poorly conserved, both in sequence and in length (Block *et al.*, 2010; Nelson *et al.*, 2013). It is interesting to note that the P2 stem is particularly elongated in the *rpfA* riboswitches from streptomycetes (this study) (St-Onge *et al.*, 2015), being four to nine times longer than its equivalent in the characterized *B. subtilis*, *C. acetobutylicum*, *S. aciditrophicus*, *T. pseudethanolicus* and *T. tengcongensis ydaO*-like riboswitches (Block *et al.*, 2010; Nelson *et al.*, 2013; Gao and Serganov, 2014; Jones and Ferré-D'Amaré, 2014; Ren and Patel, 2014). It seems that these systems compensate for the lack of an extended P2 stem with a separate expression platform, located downstream of the sensor domain (Block *et al.*, 2010; Nelson *et al.*, 2013; Gao and Serganov, 2014; Ren and Patel, 2014).

The contribution of the P2 stem in ligand binding and gene regulation by *ydaO*-like riboswitches has not been explored to date. Though crystallographic analyses of cyclic di-AMP-bound *ydaO*-like sensor domains suggest that the P2 stem is not involved in ligand binding (Gao and Serganov, 2014; Jones and Ferré-D'Amaré, 2014; Ren and Patel, 2014), consistent with our observations here (Fig. 3.11), this region has not been subjected to mutational analyses, and thus it remains possible that this region contributes to regulation in these other systems as well.

In addition to regulating transcription processivity, cyclic di-AMP may also regulate *rpfA* transcript stability, albeit in a riboswitch-independent fashion. *rpfA* transcripts were more readily degraded *in vitro* by RNases in the presence of cyclic di-AMP than in the presence of its close relative cyclic di-GMP (Fig. 3.4). Because (i) ligand binding was dispensable for degradation, and (ii) unrelated transcripts were also destabilized by the second messenger (Fig. 3.4), cyclic di-AMP may impact general RNA stability in the streptomycetes, possibly via allosteric modulation of RNases. With cyclic di-AMP levels decreasing throughout differentiation (Fig. 3.1B), and *rpfA* transcript levels concomitantly rising (Haiser *et al.*, 2009; Sexton *et al.*, 2015), through both reduced riboswitch-mediated attenuation and increased transcript stability, the streptomycetes ultimately amass stores of *rpfA* mRNAs during sporulation. Consistently, many dormancy-adopting bacteria increase mRNA stability as a means of maintaining adequate levels of needed proteins during quiescence (Rittershaus *et al.*, 2013). Indeed, recent studies have shown that, in addition to its roles in stimulating resuscitation,

rpfA is required to establish dormancy. In the streptomycetes, deleting *rpfA* leads to spore defects (Haiser *et al.*, 2009; Sexton *et al.*, 2015). *rpfA* is also up-regulated at the onset of dormancy in many actinobacteria (Muttucumaru *et al.*, 2004; Haiser *et al.*, 2009). Abundant *rpfA* transcripts in spores may also enable rapid protein synthesis during spore germination, when RpfA is required for resuscitation (Haiser *et al.*, 2009; Sexton *et al.*, 2015).

Cyclic di-AMP was detected in both vegetative and differentiating cultures of *S. coelicolor* (Fig. 3.1B), suggesting that the riboswitch attenuated *rpfA* expression throughout growth, albeit to different extents. Because *rpfA* is required for proper spore germination (Haiser *et al.*, 2009; Sexton *et al.*, 2015), it is likely that cyclic di-AMP levels in germinating spores are considerably lower to allow efficient *rpfA* transcription and mRNA accumulation. Indeed, *rpfA* promoter activity peaks during spore germination and outgrowth, and both *rpfA* transcripts and RpfA proteins are abundant in early exponential phase/vegetative growth (Sexton *et al.*, 2015; St-Onge *et al.*, 2015). Though cyclic di-AMP levels were not measured at that time, owing to insufficient biomass for nucleotide extraction and quantification, others have noted an absence of the second messenger in *Streptomyces venezuelae* during the early stages of growth (N. Tschowri and M. Al-Bassam, unpublished).

3.5 EXPERIMENTAL PROCEDURES

3.5.1 Growth conditions

S. coelicolor strains (Table 3.1) were grown at 30°C on MYM agar (Stuttard, 1982) supplemented with 2 µL mL^{-1} trace element solution (Hopwood and Wright, 1978) or in tryptone soya broth (TSB) (Oxoid):YEME (Kieser *et al.*, 2000) (50:50). When appropriate, the agar plates were overlaid with sterile cellophane prior to inoculation to facilitate the recovery of *Streptomyces* biomass. *Escherichia coli* strains DH5α, ET12567/pUZ8002 and their derivatives (Table 3.1) were grown at 37°C in SOB (without Mg^{2+} salts) and LB broth (Sambrook and Russell, 2001) and on nutrient (Difco) and LB agar (LB broth with 1.5%$_{w/v}$ agar). To select for mutations and/or plasmids, media were supplemented with one or more of the following antibiotics: 50 µg mL^{-1} apramycin, 25 µg mL^{-1} chloramphenicol, 50 µg mL^{-1} kanamycin.

3.5.2 Cyclic di-AMP extraction and quantification

S. coelicolor strain M145 (Table 3.1) was grown at 30°C on MYM agar overlaid with cellophane. After 24, 48 and 72 h, cyclic di-AMP was extracted from cells using a protocol adapted from Spangler *et al.* (2010). Briefly, biomass (264 ± 42 mg) was recovered from the plate culture and homogenized in 3 mL ice-cold extraction solvent (methanol:acetonitrile:water, 40:40:20). The homogenate was incubated on ice for 15 min and then heated at ~95°C for 10 min. After cooling on ice for 5 min, the homogenate was centrifuged at 1,900 × g for 10 min at 4°C, and the supernatant was collected. The pellet was extracted twice more using 2 mL ice-cold extraction solvent, as described above but omitting the heating and subsequent cooling steps. The recovered extract was placed at -20°C for at least 24 h, and centrifuged at 1,900 × g for 10 min at 4°C. The supernatant was retrieved and evaporated to dryness using a Genevac HT-4X (SP Scientific). The resulting residue was resuspended in 200 µL water, and cyclic di-AMP contained therein was quantified by reverse-phase LC-MS/MS, as described previously (Spangler *et al.*, 2010). Levels were normalized to wet cell weight.

3.5.3 Luciferase reporter constructs

Nucleotide changes were introduced into the *rpfA* riboswitch, fused to the 3′ end of P_{ermE*}, using splicing by overlap extension (SOE)-PCR (Horton, 1995). Primers were designed following Horton (1995). The forward mutagenic primers were used with rpfAR2-K to amplify the downstream fragment of the target, whereas the reverse mutagenic primers were used with ermEF to amplify the corresponding upstream fragment (Table 3.3). A 17-nt sequence – incorporating the modifications to be introduced into the riboswitch construct – was added to the 5′ end of each forward mutagenic primer. To promote the annealing of both the upstream and downstream products, the complementary mutations were also engineered into the 5′ end of each reverse mutagenic primer. Primers were purchased from Integrated DNA Technologies. Primer sequences are presented in Table 3.2.

Upstream and downstream overlapping products were PCR-amplified from plasmid pMC230 (Table 3.1) using Phusion High-Fidelity DNA polymerase (Thermo, NEB) with 5%$_{v/v}$ dimethylsulfoxide (DMSO) and the appropriate primer pairs (Table 3.3). Optimized amplification conditions and product lengths are indicated in Table 3.3. Products were column-purified using the PureLink PCR Purification kit (Invitrogen). The upstream and downstream products were then

mixed, annealed together and extended by PCR using Phusion High-Fidelity DNA polymerase with external primers ermEF and rpfAR2-K (Table 3.3), as described above. The SOE-PCR products were gel-extracted using the MicroElute Gel Extraction kit (Omega BioTek). Products were then digested with restriction enzymes *Bgl*II and *Kpn*I, column-purified and ligated to dephosphorylated, *Bam*HI- and *Kpn*I-digested pFLUX (Table 3.1) using T4 DNA ligase (Invitrogen). Reporter constructs were then electroporated into *E. coli* strain DH5α using the protocol by Gust *et al.* (2003). Plasmids were extracted from transformants using standard protocols (Sambrook and Russell, 2001), and insert sequences were confirmed by sequencing with primer pFLUXR (Table 3.2). Reporter constructs were electroporated into the methylation-deficient *E. coli* donor strain ET12567/pUZ8002 and moved into *S. coelicolor* strain M145 by conjugation (Gust *et al.*, 2003). Successful plasmid integration was confirmed by colony PCR using *Taq* DNA polymerase (GeneDireX) with 5%$_{v/v}$ DMSO, 300 nM each primer ermEF and pFLUXR (Table 3.3) and crude cell lysate as DNA template.

Compensatory mutant riboswitches $P0_{Comp.}$ and $P1_{Comp.}$ were engineered using a similar strategy, by introducing the $P0_{Dist.}$ and $P1_{Prox.}$ mutations into plasmids pMC231 and pMC235 (Table 3.1), respectively. $P0_{Dist.}$ and $P1_{Prox.}$ upstream and downstream overlapping products were thus PCR-amplified using plasmids pMC231 and pMC235, respectively, as template instead of pMC230.

3.5.4 Reporter assays

Fifteen microliters of *S. coelicolor* spore suspension [OD_{450} = 0.150, in 2 × YT broth (Kieser *et al.*, 2000)] were spread, in triplicate, on 200 µL MYM agar in white flat-bottomed 96-well plates (Thermo). Plate cultures were incubated at 30°C, and the emitted luminescence was periodically measured for 2 sec using a TECAN UltraEvolution spectrometer. The luminescence signal emitted by the empty vector control (M145/pFLUX) (Table 3.1) was subtracted from the raw luminescence of each sample. Background-subtracted luminescence was normalized to that of the positive control strain, constitutively expressing the reporter without the *rpfA* riboswitch (M145/pFLUX-Pos) (Table 3.1).

3.5.5 *In vitro* transcription, RNA purification and 5′-end-labeling

In vitro transcription templates comprised phage T7 promoter-driven wild-type or mutant *rpfA* riboswitch fused to the first 39 bp of the *rpfA* coding region.

Templates were PCR-amplified from recombinant pFLUX plasmids (Table 3.1) using Phusion High-Fidelity DNA polymerase with 5%$_{v/v}$ DMSO and primers IVTrpfAUTR5′ and IVTrpfAUTR3′ (Tables 3.2 and 3.3). The phage T7 RNA polymerase promoter sequence was engineered into the 5′ end of the forward primer IVTrpfAUTR5′, and two G residues were inserted between the promoter and the priming sequence to increase transcription initiation efficiency. Products were subsequently column-purified. Plasmid pTRI-RNA 18S (Table 3.1) was used as template for 18S rRNA synthesis.

RNA was transcribed *in vitro* using the MEGAshortscript High Yield Transcription kit (Ambion). Briefly, a 40- or 80-µL reaction, comprising 1 × T7 Reaction Buffer, 7.5 mM each NTP, 50 nM template DNA and 4 or 8 µL T7 Enzyme Mix, was incubated at 37°C for 4 h. The template DNA was subsequently digested for 1 h at 37°C using 8 or 16 U TURBO DNase.

In vitro transcribed RNA was denatured at 95°C for 5 min in RNA gel-loading buffer (Sambrook and Russell, 2001) or Gel Loading Buffer II (Ambion) and immediately size-fractionated on a 50-cm-long continuous denaturing urea-polyacrylamide gel [6%$_{w/v}$ Gene-Gel, BioShop or SequaGel UreaGel-6, National Diagnostics) in 1 × TBE buffer (Sambrook and Russell, 2001) for 70-90 min at 60 W using the Sequi-Gen GT Nucleic Acid Electrophoresis Cell (Bio-Rad). RNA was visualized by UV shadowing, excised from the gel and extracted three times at 37°C with 350-500 µL crush/soak buffer, as described by Regulski and Breaker (2008). Gel-extracted RNA was then precipitated (Sambrook and Russell, 2001), resuspended in nuclease-free water and quantified using spectrophotometry.

Using the KinaseMax kit (Ambion), 20 pmol gel-purified RNA were subsequently dephosphorylated with calf intestine alkaline phosphatase and 5′-end-labeled with T4 polynucleotide kinase and [γ-^{32}P]ATP (Perkin Elmer). Unincorporated NTPs were removed from the reaction using NucAway Spin Columns (Ambion).

3.5.6 In-line probing

^{32}P-5′-end-labeled riboswitch RNA was re-folded by heating at 95°C for 2 min and cooling to room temperature for 10 min. Approximately 100 nM RNA was then incubated at room temperature for ~40 h in 1 × in-line reaction buffer (Regulski and Breaker, 2008). When appropriate, reactions were supplemented with 1 nM to 1 mM cyclic di-AMP or cyclic di-GMP (Invivogen). RNA cleavage products were diluted in an equal volume of 2 × colorless gel-loading solution (Regulski and Breaker, 2008) and size-fractionated on a denaturing urea-

polyacrylamide gel, as for RNA gel purification. Undigested, alkaline-treated and RNase T1-treated precursor RNAs, prepared as described by Regulski and Breaker (2008), were also size-fractionated alongside the digested RNA. The gel was dried at 80°C for 2 h using a Model 583 Gel Dryer (Bio-Rad), and RNA was visualized by autoradiography.

3.5.7 *In vitro* stability assays

Exponential-phase cells of *S. coelicolor* strain M145 (2.52 ± 0.83 g wet cells), grown at 30°C in TSB:YEME (50:50), were collected by centrifugation at 1,900 × g for 10 min. Cells were resuspended in 50 mL lysis buffer (10 mM Tris, 0.1 M NaCl, $5\%_{v/v}$ glycerol) and lysed at 30,000 psi using a Constant Cell Disruption System with a continuous-flow head (Constant Systems). Lysates were clarified by centrifugation at 15,000 × g for 10 min (4°C). When appropriate, RNases were inactivated by adding 20 mM EDTA to the lysate and heating the mixture at 95°C for 15 min.

^{32}P-5′-end-labeled riboswitch RNA was re-folded by heating at 95°C for 2 min and cooling to room temperature for 10 min. To enable binding to the ligand, ~0.1 µM labeled RNA was incubated at room temperature for 60-70 min with 751 µM cyclic di-AMP or cyclic di-GMP in 1 × in-line reaction buffer (final concentrations are indicated). RNA degradation was initiated immediately by adding 1 µL cell lysate μL^{-1} reaction or an equal volume of lysis buffer (‘0 min’ samples). The reaction was incubated at ~30°C, and aliquots were taken periodically over the course of 90 min and flash-frozen in liquid nitrogen. RNA degradation products were diluted in an equal volume of 2 × colorless gel-loading solution and size-fractionated on a denaturing urea-polyacrylamide gel, as for RNA gel purification. The gel was dried as described above and visualized using a Typhoon FLA 9500 phosphorimager (GE Healthcare). RNA was quantified by densitometry using ImageQuant TL (GE Healthcare), and transcript abundance was expressed relative to untreated RNA (‘0 min’).

3.5.8 *In vitro* transcription assays

Templates for *in vitro* transcription assays comprised phage T7 promoter-driven wild-type or mutant *rpfA* riboswitch fused to the first 63 bp of *rpfA* and 126 bp of pFLUX vector sequence. DNA templates were PCR-amplified from recombinant pFLUX derivatives (Table 3.1) using Phusion High-Fidelity DNA polymerase with $5\%_{v/v}$ DMSO and primers IVTrpfAUTR5′ and pFLUXR (Table

3.3). Products were subsequently gel-purified using the MicroElute Gel Extraction kit. For negative control reactions, plasmid pTRI-RNA 18S was used as template.

Transcription was initiated by combining the DNA template with 1 × T7 Reaction Buffer (Ambion), 0.4 μCi μL^{-1} [α-^{32}P]CTP (Perkin Elmer), 100 μM each GTP, CTP and UTP (NEB), 1 mM cyclic di-AMP (Invivogen) or an equal volume of nuclease-free water, and 0.1 μL μL^{-1} T7 Enzyme Mix (Ambion) (final concentrations are indicated). After 10 min at 37°C, 50 U mL^{-1} heparin (prevents *de novo* transcription initiation) and 100 μM ATP (NEB) were added to the reaction. Transcript elongation continued at 37°C for 30 min, after which time the reaction was stopped by adding an equal volume of 2 × colorless gel-loading solution. Transcripts were then size-fractionated on a denaturing urea-polyacrylamide gel, as for RNA gel purification. The gel was dried and visualized by phosphorimaging, as described above.

RNA was quantified by densitometry using ImageQuant TL, and transcript abundance was expressed relative to levels generated in the absence of cyclic di-AMP. To test for significant differences in RNA levels in the presence and absence of ligand, unpaired *t*-tests were conducted. Normal distribution of data and equal variance were confirmed ($P \geq 0.05$).

3.6 ACKNOWLEDGEMENTS

The authors wish to thank Dr. Emma Sherwood, David Crisante and Suzanne Boursalie (McMaster University, Hamilton, CAN) for their technical assistance, and Drs. Tina Henkin (Ohio State University, Columbus, USA), Daniel Lafontaine (Université de Sherbrooke, Sherbrooke, CAN) and Wade Winkler (University of Maryland, College Park, USA) for helpful discussion. This work was supported by an NSERC Discovery Grant (No. 04681) and an NSERC Discovery Accelerator supplement to M.A.E. R.J.S. was supported by a Vanier Canada Graduate Scholarship.

3.7 TABLES

Table 3.1. Bacterial strains and plasmids.

Strain/ plasmid	Genotype, properties and/or use	Reference
***S. coelicolor* A3(2) strains**		
M145	A3(2) SCP1$^-$ SCP2$^-$	Kieser *et al.* (2000)
***E. coli* strains**		
DH5α	Plasmid construction strain; F$^-$ ϕ80*lacZ*ΔM15 Δ(*lacZYA-argF*)*U169 recA1 endA1 hsdR17*(r_K^-, m_K^+) *phoA supE44* λ$^-$ *thi-1 gyrA96 relA1*	Bethesda Research Laboratories
ET12567	Methylation-deficient strain; F$^-$ *dam13::*Tn*9 dcm6 hsdM hsdR recF143 zjj201::*Tn*10 galK2 galT22 ara14 lacY1 xyl5 leuB6 thi1 tonA31 rpsL136 hisG4 tsx78 mtli glnV44*	MacNeil *et al.* (1992)
Plasmids		
pFLUX	Integrative transcriptional reporter vector; *ori* (pUC18) *oriT* (RK2) *int* ϕBT1 *attP* ϕBT1 *luxCDABE* (promoterless) *aac(3)IV*	Craney *et al.* (2007)
pFLUX-Pos	P_{ermE^*} transcriptionally fused to *luxCDABE* in pFLUX	Sexton *et al.* (2015)
pMC222	*rpfA* 5′ UTR-*luxCDABE* under the transcriptional control of P_{ermE^*} in pFLUX (WT)	St-Onge *et al.* (2015)
pMC231	*rpfA* 5′ UTR (G14C G15C G16C C17G C18G C19G C20G)-*luxCDABE* under the transcriptional control of P_{ermE^*} in pFLUX ($P0_{Prox.}$)[a]	This study
pMC232	*rpfA* 5′ UTR (G227C G228C G229C G230C A231T T232A C233G)-*luxCDABE* under the transcriptional control of P_{ermE^*} in pFLUX ($P0_{Dist.}$)[a]	This study
pMC233	*rpfA* 5′ UTR (G14C G15C G16C C17G C18G C19G C20G G227C G228C G229C G230C A231T T232A C233G)-*luxCDABE* under the transcriptional control of P_{ermE^*} in pFLUX ($P0_{Comp.}$)[a]	This study
pMC234	*rpfA* 5′ UTR (C27G G28C C29G A30T A31T C32G G33C C34G)-*luxCDABE* under the transcriptional control of P_{ermE^*} in pFLUX ($P1_{Prox.}$)[a]	This study
pMC235	*rpfA* 5′ UTR (G217C C218G G219C T220A C221G G222C)-*luxCDABE* under the transcriptional control of P_{ermE^*} in pFLUX ($P1_{Dist.}$)[a]	This study
pMC236	*rpfA* 5′ UTR (C27G G28C C29G A30T A31T C32G G33C C34G G217C C218G G219C T220A C221G G222C)-*luxCDABE* under the transcriptional control of P_{ermE^*} in pFLUX ($P1_{Comp.}$)[a]	This study
pMC223	*rpfA* 5′ UTR $\Delta_{37\text{-}91}$-*luxCDABE* under the transcriptional control of P_{ermE^*} in pFLUX (P2)[a]	St-Onge *et al.* (2015)
pMC237	*rpfA* 5′ UTR (A55T C56G G57C G59C A60T)-*luxCDABE* under the transcriptional control of P_{ermE^*} in pFLUX ($P2_{Prox.}$)[a]	This study
pMC238	*rpfA* 5′ UTR (T68A C69G C71G G72C T73A)-*luxCDABE* under the transcriptional control of P_{ermE^*} in pFLUX ($P2_{Dist.}$)[a]	This study

pMC224	*rpfA* 5′ UTR $\Delta_{101\text{-}144}$-*luxCDABE* under the transcriptional control of P_{ermE^*} in pFLUX (P4)[a]	St-Onge *et al.* (2015)
pMC225	*rpfA* 5′ UTR $\Delta_{151\text{-}175}$-*luxCDABE* under the transcriptional control of P_{ermE^*} in pFLUX (P6)[a]	St-Onge *et al.* (2015)
pMC226	*rpfA* 5′ UTR $\Delta_{145\text{-}198}$-*luxCDABE* under the transcriptional control of P_{ermE^*} in pFLUX (P5-7)[a]	St-Onge *et al.* (2015)
pMC227	*rpfA* 5′ UTR $\Delta_{92\text{-}214}$-*luxCDABE* under the transcriptional control of P_{ermE^*} in pFLUX (P3-7)[a]	St-Onge *et al.* (2015)
pMC231	*rpfA* 5′ UTR $\Delta_{199\text{-}208}$-*luxCDABE* under the transcriptional control of P_{ermE^*} in pFLUX (LIN)[a]	St-Onge *et al.* (2015)
pMC239	*rpfA* 5′ UTR (T239G T242A T244C T245G T246A T247C)-*luxCDABE* under the transcriptional control of P_{ermE^*} in pFLUX [Poly(U)][a]	This study
pMC230	*rpfA-flag*, fused to the 3′ end of the *rpfA* 5′ UTR, under the transcriptional control of P_{ermE^*}; *ori* (pUC18) *oriT* (RK2) *int* ϕBT1 *attP* ϕBT1 *aac(3)IV*	St-Onge *et al.* (2015)
pTRI-RNA 18S	Control template; Partial human 18S rRNA gene fragment under the transcriptional control of P_{T7}; *Eco*RI- and *Bam*HI-digested plasmid	Ambion
pUZ8002	Non-transmissible *oriT* mobilizing plasmid; RP4 *tra neo*	Paget *et al.* (1999)

[a] Numbering is relative to the *rpfA* transcriptional start site, as determined by 5′ rapid amplification of cDNA ends (Haiser *et al.*, 2009).

Table 3.2. List of PCR primers.

Primer	Sequence[b]	Restriction site
Cloning PCR primers		
ermEF[a]	GCA CTA GAT CTA GCC CGA CCC GAG CAC GCG C	*Bgl*II
P1dintF	***GCG TCG GTG ACC CCT AG***A CAT ATG CTG TTT TCC GGC A	
P1dintF2	***TCA CCT CGC AGC GCA GC***G TGA GGG GAT CAC ATA TGC T	
P1dintR	***CTA GGG G***TC ACC GAC GCC TGC GAG GTG	
P1dintR2	***GCT GCG*** CTG CGA GGT GAG CTG TCG GG	
P1pintF	***TAC CCA TGG CCC CGG GG***G ACA GCC GCA ACG CCG AAT C	
P1pintF2	***CCC GAC AGC GCG TTG CG***C GAA TCC TGC CAG CGG CCG T	
P1pintR	***CCC CGG G***GC CAT GGG TAC TGA TCG AA	
P1pintR2	***CGC AAC GC***G CTG TCG GGG CCC GCC ATG G	
P2dintF	***GGG AAC AGT CGA GGG CA***C AAG CGC CGA AGG CAG GAG C	
P2dintR	***TGC CCT*** CGA CTG TTC CCG TAC GGC CG	
P2pintF	***CCA GCG GCC GTT GCG CT***A CAG TCG TCG CGT CAA GCG C	
P2pintR	***AGC GCA*** ACG GCC GCT GGC AGG ATT CG	
pFLUXR	GCC GAA GTT GAT GGA CTG GA	
rpfAR2-K[a]	GCA CTG GTA CCG ACG GCG ATG ACA CGG GTG G	*Kpn*I
UintF	***ATC ACA TAG GCA GCG AC***C CGG CAA GGG CAA GCA CCG T	
UintR	***GTC GCT GCC*** TAT GTG ATC CCC TCA CCG AC	
***In vitro* transcription primers**		
IVTrpfAUTR3′[a]	GGA CGG ACG ACG GTG CTT GCC CTT GC	
IVTrpfAUTR5′[a]	TAA TAC GAC TCA CTA TAG GGC GCT CGC CAT CGC GGG CCC	

[a] Primer sequences were previously published by St-Onge *et al.* (2015).
[b] Restriction sites are underlined. The phage T7 promoter is boxed. Primer extensions, incorporating specific mutations, are bold and italicized.

Table 3.3. PCR amplification conditions.

PCR product	Fragment[c]	Primers[d]		Product length (bp)	Annealing temperature (°C)[e]	Extension time (sec)
		Forward	Reverse			
Cloning[a]						
P_{ermE}←$P0_{Prox.}$	Ups	ermEF	P1pintR	309	59	15
P_{ermE}←$P0_{Prox.}$	Down	P1pintF	rpfAR2-K	308	N/A	15
P_{ermE}←$P0_{Dist.}$	Ups	ermEF	P1dintR	522	N/A	15
P_{ermE}←$P0_{Dist.}$	Down	P1dintF	rpfAR2-K	95	65	15
P_{ermE}←$P1_{Prox.}$	Ups	ermEF	P1pintR2	323	N/A	15
P_{ermE}←$P1_{Prox.}$	Down	P1pintF2	rpfAR2-K	294	N/A	15
P_{ermE}←$P1_{Dist.}$	Ups	ermEF	P1dintR2	511	N/A	15
P_{ermE}←$P1_{Dist.}$	Down	P1dintF2	rpfAR2-K	106	61	15
P_{ermE}←$P2_{Prox.}$	Ups	ermEF	P2pintR	349	N/A	15
P_{ermE}←$P2_{Prox.}$	Down	P2pintF	rpfAR2-K	268	N/A	15
P_{ermE}←$P2_{Dist.}$	Ups	ermEF	P2dintR	362	N/A	15
P_{ermE}←$P2_{Dist.}$	Down	P2dintF	rpfAR2-K	255	N/A	15
P_{ermE}←Poly(U)	Ups	ermEF	UintR	536	61	15
P_{ermE}←Poly(U)	Down	UintF	rpfAR2-K	81	N/A	15
SOE-PCR	N/A	ermEF	rpfAR2-K	600	62	15
Confirmation of plasmid introduction[b]						
Colony PCR	N/A	ermEF	pFLUXR	715	61	45
***In vitro* transcription templates**[a]						
In vitro transcription templates	N/A	IVTrpfAU TR5′	IVTrpfAU TR3′	173-296	N/A	15
In vitro transcription assay templates	N/A	IVTrpfAU TR5′	pFLUXR	323-446	66	15

[a] Mutant riboswitches (fused to the 3′ end of the *ermE** promoter) and *in vitro* transcription templates were PCR-amplified using Phusion High-Fidelity DNA polymerase following the manufacturer's instructions.
[b] Colony PCRs used to confirm the genotype of reporter strains were performed using *Taq* DNA polymerase with the following amplification conditions: (i) an initial 3-min denaturation step at 95°C, (ii) 35 amplification cycles consisting of a 30-sec denaturation step at 95°C, a 30-sec annealing step, and an extension step at 72°C, and (iii) a final 5-min extension step at 72°C.
[c] Ups, upstream fragment; Down, downstream fragment.
[d] Primer sequences are located in Table 3.2.
[e] N/A, a two-step PCR amplification protocol was used.

3.8 FIGURES

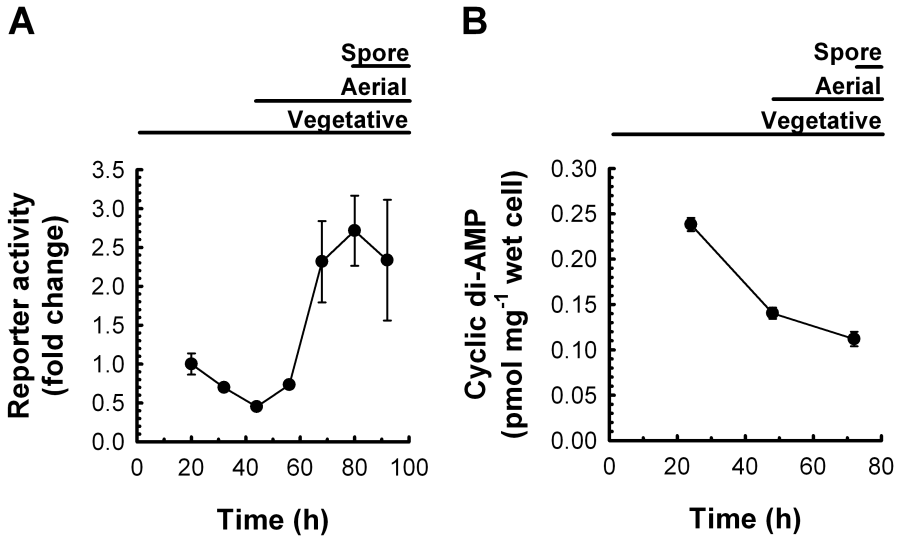

Fig. 3.1. Riboswitch attenuation activity and cyclic di-AMP abundance in *S. coelicolor* throughout development. (A) Wild-type *S. coelicolor*, constitutively expressing the *rpfA* riboswitch transcriptionally fused to the luciferase reporter gene cluster (M145/pMC222), was grown on a sporulation-conducive solid medium. Reporter activity was quantified throughout growth and development. Background-subtracted luminescence was normalized to that of the positive control strain, constitutively expressing the reporter without the *rpfA* riboswitch (M145/pFLUX-Pos). Normalized reporter activity was expressed as mean fold changes ± standard deviation (n = 3) relative to '20 h'. Figure is representative of eight independent experimental replicates. (B) Wild-type *S. coelicolor* (M145) was grown at 30°C on a sporulation-conducive solid medium. At the indicated times, cyclic di-AMP was extracted from cells and quantified by LC-MS/MS. Cyclic di-AMP levels were normalized to wet cell weight. Data are presented as mean ± standard error (n = 4).

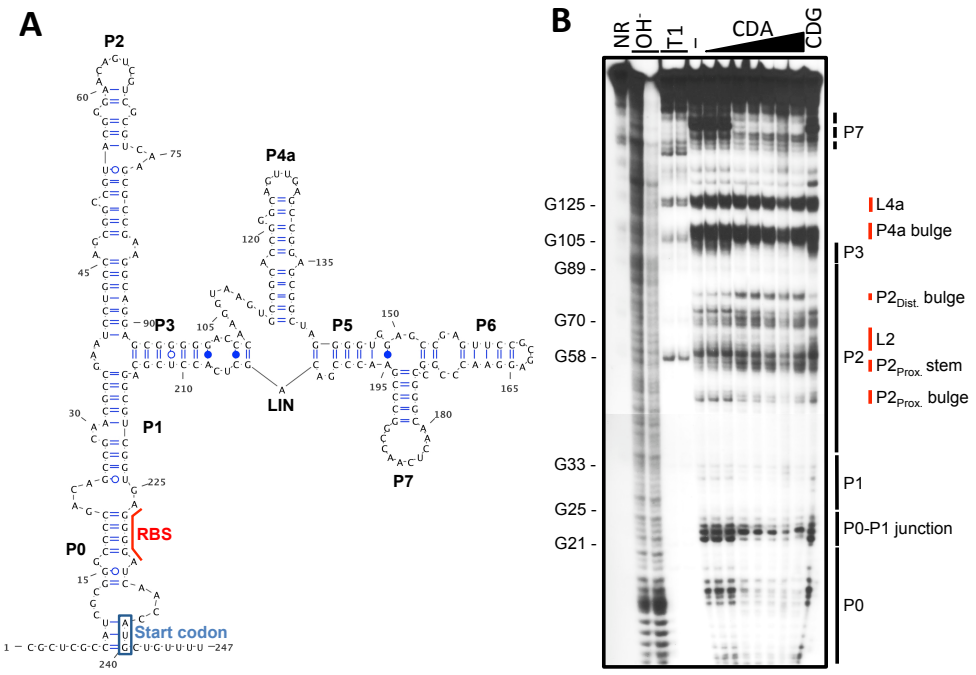

Fig. 3.2. The secondary structure model of the *rpfA* riboswitch. (A) Predicted *rpfA* riboswitch secondary structure. RBS, ribosome binding site. (B) ^{32}P-5′-end-labeled *rpfA* riboswitch RNA was incubated in the absence of ligand (-) or in the presence of either cyclic di-AMP (CDA) or cyclic di-GMP (CDG) for ~40 h at room temperature. Cleaved products were size-fractionated on a denaturing urea-polyacrylamide gel and visualized by autoradiography. Image is representative of two independent replicates. NR, untreated RNA; OH^-, alkali-treated RNA; T1, RNase T1-treated RNA.

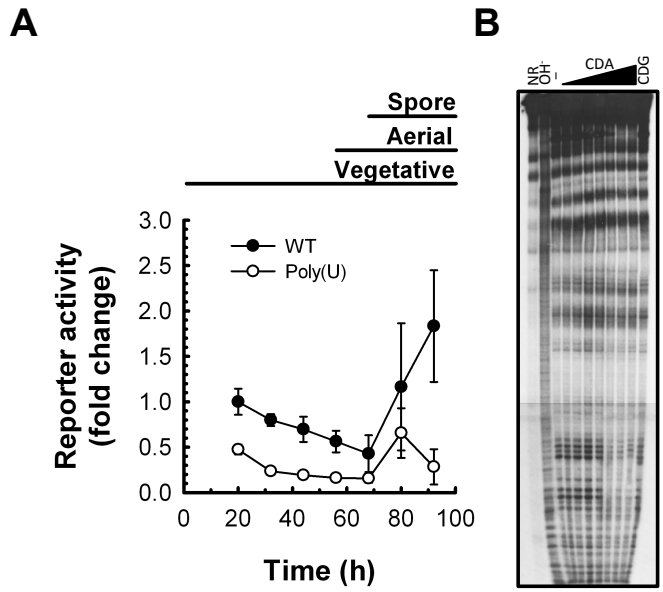

Fig. 3.3. Impact of the poly(U) sequence on riboswitch activity and cyclic di-AMP binding. (A) *S. coelicolor* wild-type strains, constitutively transcribing the luciferase reporter gene cluster fused to the 3′ end of either the wild-type *rpfA* riboswitch (M145/pMC222, WT) or a mutant derivative in which the poly(U) sequence was altered [M145/pMC239, Poly(U)], were grown on a sporulation-conducive solid medium. Reporter activity was quantified throughout growth and development. Background-subtracted luminescence of each strain was normalized to that of the positive control strain, constitutively expressing the reporter without the *rpfA* riboswitch (M145/pFLUX-Pos). Normalized reporter activity was expressed as mean fold changes ± standard deviation (n = 3) relative to that of 'WT, 20 h'. Figure is representative of two independent experimental replicates. (B) ^{32}P-5′-end-labeled poly(U) mutant *rpfA* riboswitch RNA was incubated in the absence of ligand (-) or in the presence of either cyclic di-AMP (CDA) or cyclic di-GMP (CDG) for ~40 h at room temperature. Cleaved products were size-fractionated on a denaturing urea-polyacrylamide gel and visualized by autoradiography. Image is representative of two independent replicates. NR, untreated RNA; OH^-, alkali-treated RNA.

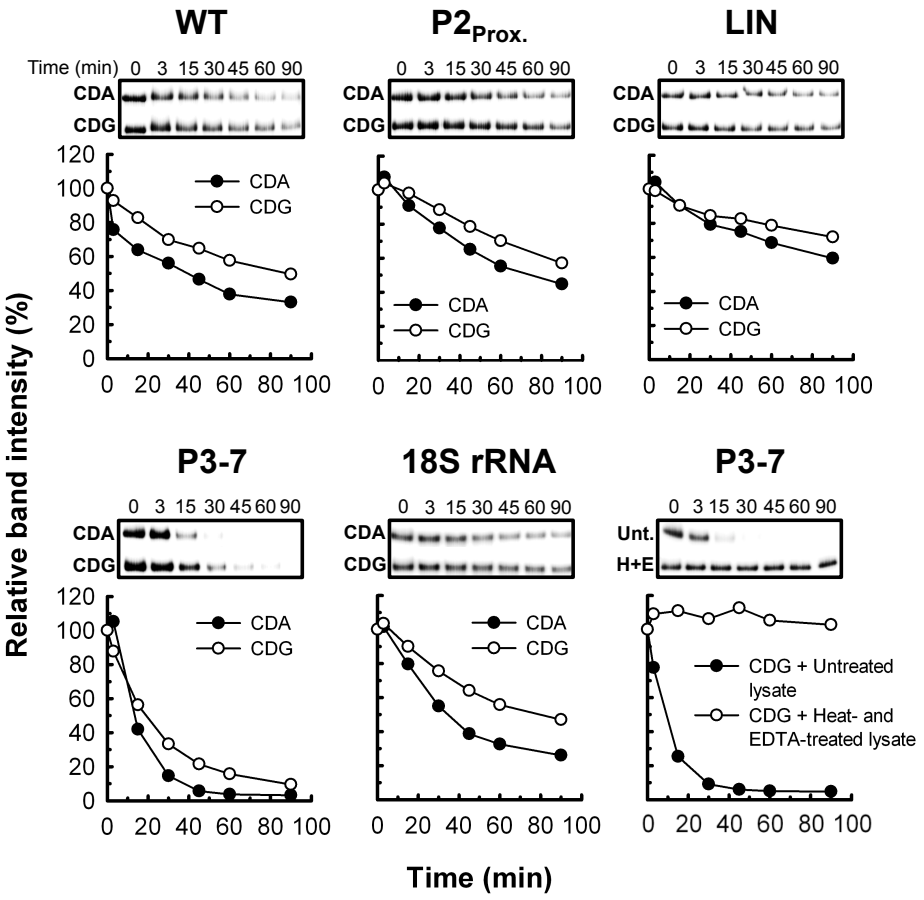

Fig. 3.4. Cyclic di-AMP impact on *rpfA* transcript stability. ^{32}P-5′-end-labeled *rpfA* riboswitch RNA and partial human 18S rRNA (negative control) were folded and incubated with cyclic di-AMP (CDA) or cyclic di-GMP (CDG) in a buffered solution. Degradation reactions were initiated by supplementing the mixtures with clarified wild-type *S. coelicolor* (M145) lysate. When appropriate, lysate was boiled with 20 mM EDTA at 95°C for 15 min (H+E). After the times indicated, an aliquot of the reaction was collected. Degradation products were size-fractionated on a denaturing urea-polyacrylamide gel, visualized by phosphorimaging, and full-length transcripts were quantified using densitometry. Transcript abundance at any given time-point was expressed relative to transcript levels at 0 min. Figure is representative of two independent experimental replicates. Full-length gel images are presented in Fig. 3.5. Unt., untreated lysate.

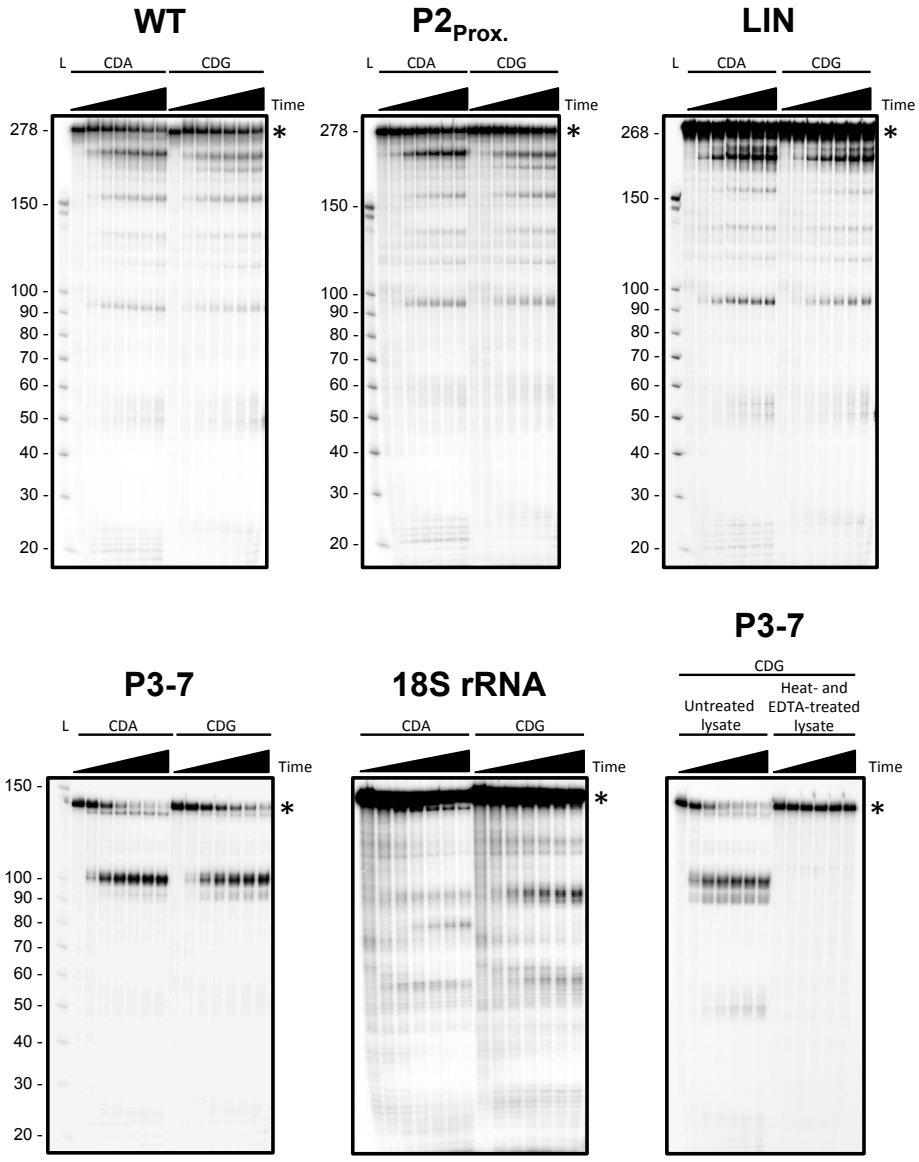

Fig. 3.5. Denaturing polyacrylamide gel electrophoresis analysis of riboswitch RNA degradation products. ^{32}P-5′-end-labeled *rpfA* riboswitch RNA and partial human 18S rRNA (negative control) were folded and incubated with cyclic di-AMP (CDA) or cyclic di-GMP (CDG) in a buffered solution. Degradation reactions were initiated by supplementing the mixtures with clarified wild-type *S. coelicolor* (M145) lysate. When appropriate, lysate was boiled with 20 mM EDTA at 95°C for 15 min. Aliquots of the reaction were collected periodically over the course of 90 min. Degradation products were size-fractionated on a denaturing urea-polyacrylamide gel and visualized by phosphorimaging. Figure is representative of two independent experimental replicates. L, Decade Marker RNA (Ambion), in nt; *, full-length transcript.

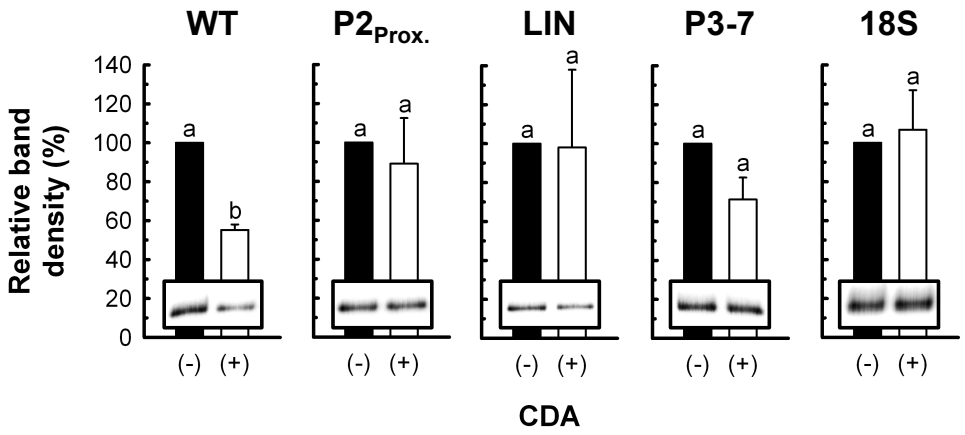

Fig. 3.6. Cyclic di-AMP impact on *rpfA* transcript elongation. *rpfA* riboswitch RNA and partial human 18S rRNA (negative control) were transcribed *in vitro* from an engineered phage T7 promoter using phage T7 RNA polymerase. Reactions were supplemented with 0 mM (-) or 1 mM (+) cyclic di-AMP (CDA). Products were intrinsically labeled with ^{32}P, size-fractionated on a denaturing urea-polyacrylamide gel and visualized by phosphorimaging. Full-length transcripts were quantified using densitometry, and abundance was expressed relative to RNA levels synthesized in the absence of cyclic di-AMP. Data are presented as mean ± standard error (n = 3). Group means annotated with different letters were significantly different (t-test; $P \leq 0.05$). Full-length gel images are presented in Fig. 3.7.

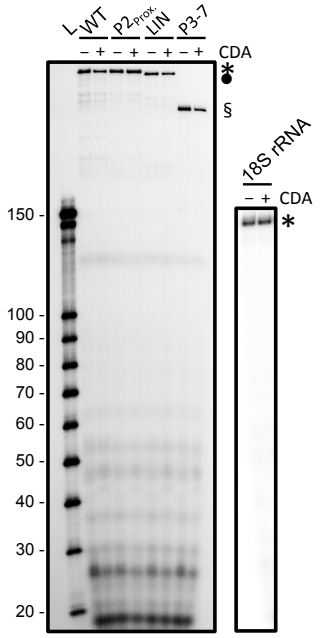

Fig. 3.7. Denaturing polyacrylamide gel electrophoresis analysis of *in vitro* transcribed riboswitch RNA. *rpfA* riboswitch RNA and partial human 18S rRNA (negative control) were transcribed *in vitro* from an engineered phage T7 promoter using phage T7 RNA polymerase. Reactions were supplemented with 0 mM (-) or 1 mM (+) cyclic di-AMP (CDA). Products were intrinsically labeled with ^{32}P, size-fractionated on a denaturing urea-polyacrylamide gel and visualized by phosphorimaging. Image is representative of three independent experimental replicates. L, Decade Marker RNA (Ambion), in nt; *, full-length WT, $P2_{Prox.}$ and 18S transcripts; • , full-length LIN transcript; § , full-length P3-7 transcript.

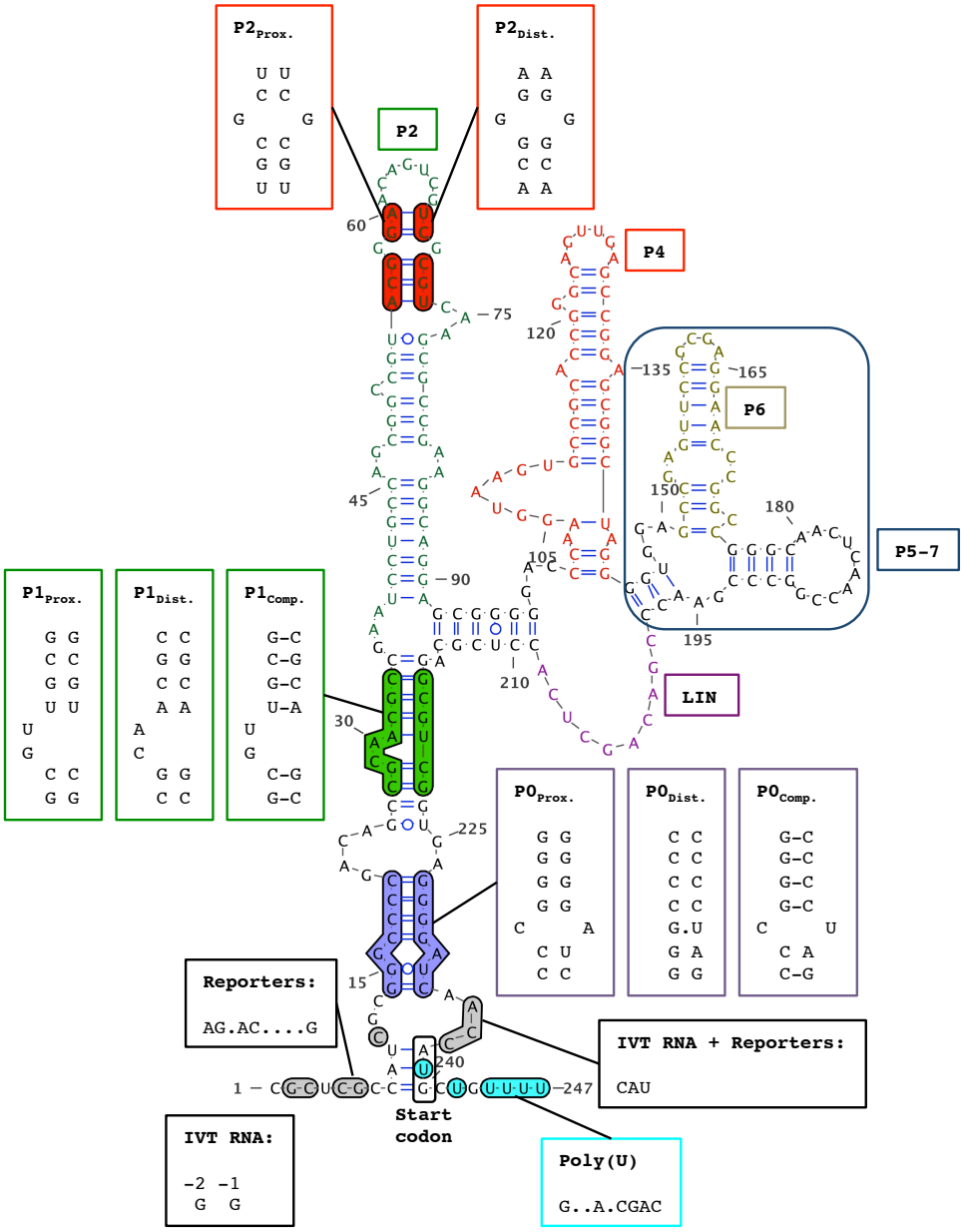

Fig. 3.8. Mutation of the *S. coelicolor rpfA* riboswitch. Regions of the *S. coelicolor rpfA* riboswitch were either deleted (colored letters) or substituted (highlighted letters). The 'P3-7' mutant, in which residues 92 to 214 were deleted, is not indicated here for clarity. Two G residues were added at the 5′ end of each *in vitro* transcribed RNA (IVT). The 5′ end of the riboswitch in each luciferase reporter construct carried additional mutations stemming from cloning. Both *in vitro* transcribed RNA and reporter constructs carried an ACC → CAU mutation at the 3′ end of the riboswitch. Structure was drawn using VARNA (Darty *et al.*, 2009).

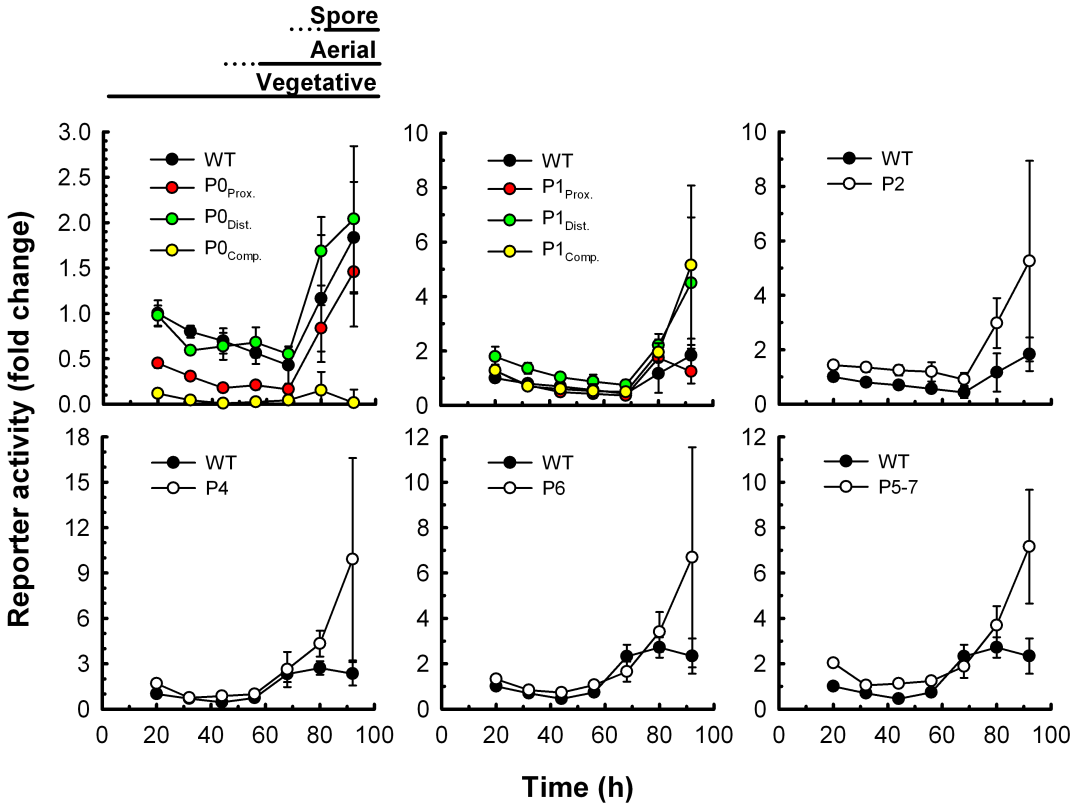

Fig. 3.9. *rpfA* riboswitch activity throughout development. *S. coelicolor* wild-type strains, constitutively expressing wild-type or mutant *rpfA* riboswitches transcriptionally fused to the luciferase reporter gene cluster, were grown on a sporulation-conducive solid medium. Reporter activity was quantified throughout growth and development. Background-subtracted luminescence of each strain was normalized to that of the positive control strain, constitutively expressing the reporter without the *rpfA* riboswitch (M145/pFLUX-Pos). Normalized reporter activity was expressed as mean fold changes ± standard deviation (*n* = 3) relative to that of 'WT, 20 h'. Figure is representative of at least six independent experimental replicates. WT, M145/pMC222; $P0_{Prox.}$, M145/pMC231; $P0_{Dist.}$, M145/pMC232; $P0_{Comp.}$, M145/pMC233; $P1_{Prox.}$, M145/pMC234; $P1_{Dist.}$, M145/pMC235; $P1_{Comp.}$, M145/pMC236; P2, M145/pMC223; P4, M145/pMC224; P6, M145/pMC225; P5-7, M145/pMC226.

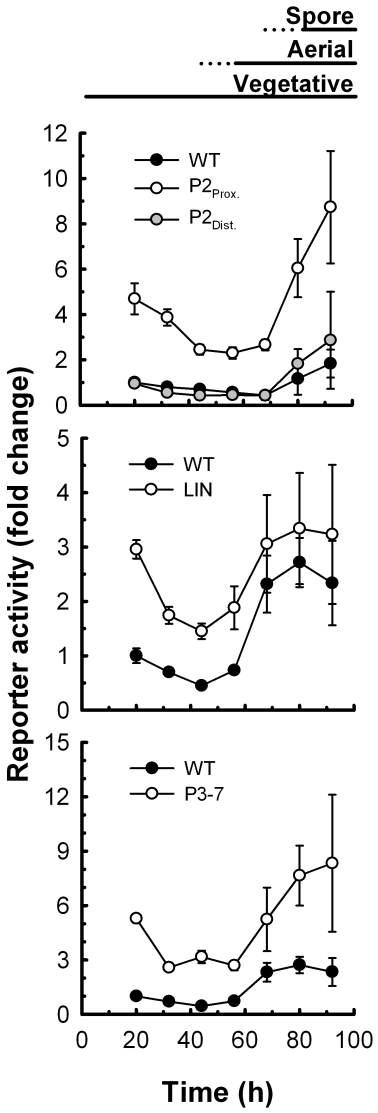

Fig. 3.10. *rpfA* riboswitch activity throughout development. *S. coelicolor* wild-type strains, constitutively expressing wild-type or mutant *rpfA* riboswitches transcriptionally fused to the luciferase reporter gene cluster, were grown on a sporulation-conducive solid medium. Reporter activity was quantified throughout growth and development. Background-subtracted luminescence of each strain was normalized to that of the positive control strain, constitutively expressing the reporter without the *rpfA* riboswitch (M145/pFLUX-Pos). Normalized reporter activity was expressed as mean fold changes ± standard deviation (n = 3) relative to that of 'WT, 20 h'. Figure is representative of at least two independent experimental replicates. WT, M145/pMC222; $P2_{Prox.}$, M145/pMC237; $P2_{Dist.}$, M145/pMC238; LIN, M145/pMC231; P3-7, M145/pMC227.

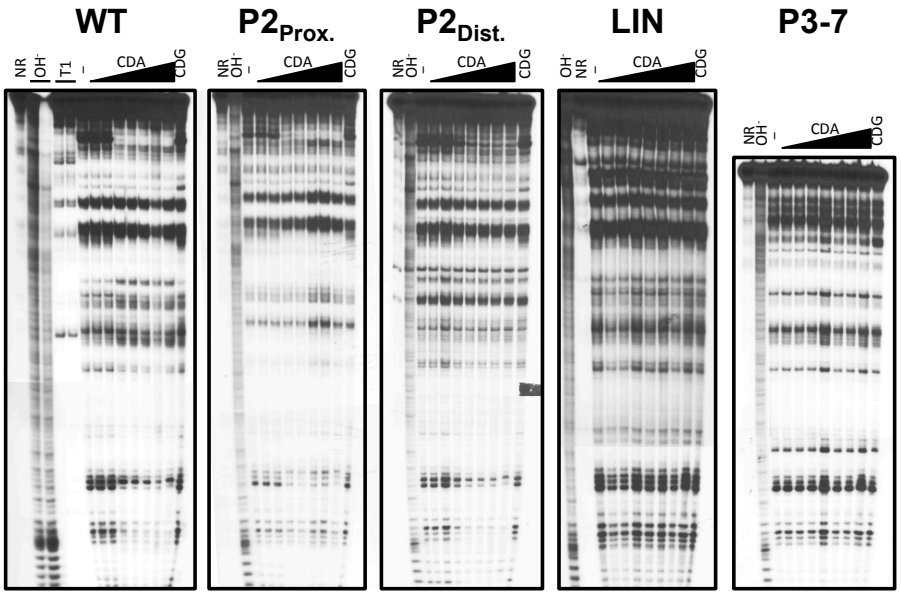

Fig. 3.11. Cyclic di-AMP binding by wild-type and mutant *rpfA* riboswitches. ^{32}P-5′-end-labeled wild-type and mutant *rpfA* riboswitch RNAs were incubated in the absence of ligand (-) or in the presence of either cyclic di-AMP (CDA) or cyclic di-GMP (CDG) for ~40 h at room temperature. Cleaved products were size-fractionated on a denaturing urea-polyacrylamide gel and visualized by autoradiography. Image is representative of two independent replicates. NR, untreated RNA; OH^-, alkali-treated RNA; T1, RNase T1-treated RNA.

CHAPTER 4

A SMALL NON-CODING RNA IS EXPRESSED OPPOSITE A MURALYTIC ENZYME-ENCODING GENE IN *STREPTOMYCES COELICOLOR*

Renée J. St-Onge, Matthew J. Moody, Marie A. Elliot

Chapter 4 comprises unpublished data. I conducted all the experiments and performed all the data processing and analyses, with the exception of the RNA-seq data processing and analyses, which were performed by Matthew J. Moody. I wrote the manuscript and prepared all the figures and tables. Marie A. Elliot and I contributed to designing the experiments, interpreting the data and editing the manuscript.

4.1 ABSTRACT

Non-coding regulatory RNAs fine-tune gene expression post-transcriptionally. Although these RNA regulators are prevalent in the clinically important *Streptomyces* bacteria, their inducing conditions, biological functions and mechanisms of action remain largely unknown. In the model *Streptomyces coelicolor*, a novel small RNA (sRNA) called Scr3097 is encoded downstream of *rpfA*, a gene whose protein product has important roles in both establishing and exiting a dormant state. In this work, we investigated Scr3097-dependent gene regulation in *S. coelicolor*. Using northern blot analyses, we found that, in liquid cultures, Scr3097 was detected exclusively in exponential-phase cells. In contrast, we observed the sRNA throughout growth and development in plate-grown cultures, with levels increasing during the transition from active growth to dormancy. Using a combination of phenotypic screens and transcriptional analyses, we found that Scr3097 was involved in microaerobic energy metabolism. The sRNA affected the expression of respiratory nitrate reductase-encoding genes, whose products are involved in electron transport under low oxygen. Scr3097 also decreased tolerance to high levels of ammonium, a product of complete nitrate reduction. Conditions promoting Scr3097 accumulation are currently unknown; however, we found that *rpfA* was required for maximum expression.

4.2 INTRODUCTION

While protein regulators, such as sigma factors, transcriptional activators and transcriptional repressors, control transcription initiation, small RNAs (sRNAs) typically fine-tune gene expression once transcription is well underway. These short non-coding transcripts are synthesized in response to specific conditions and in turn modulate the expression of target genes accordingly. sRNAs primarily impact transcript stability and translatability through their interaction with specific mRNA targets. They can also affect gene expression by titrating protein regulators away from their intended genes through target mimicry, though such protein sequestration has been observed less frequently than mRNA modulation (Waters and Storz, 2009).

sRNAs are generally classified as either *trans*-encoded sRNAs or *cis*-encoded antisense sRNAs. *Trans*-encoded sRNAs are encoded by genes located away from their targets and are only partially complementary to their

target mRNAs. In contrast, antisense sRNAs are encoded by genes located opposite their target genes. These *cis*-encoded transcripts therefore share complete complementarity with their associated mRNA (Waters and Storz, 2009).

The prevalence of sRNA-mediated gene regulation in bacteria is now widely accepted (Waters and Storz, 2009; Storz *et al.*, 2011). Most sRNAs, however, have been identified and functionally characterized in the model bacterium *Escherichia coli* (Wassarman, 2002; Gottesman, 2004; Storz *et al.*, 2004). In the clinically important streptomycetes, sRNA-based regulation is expected to be extensive given the complexity of their life cycle and the flexibility of their metabolism. Their developmental cycle begins with a dormant spore, which germinates upon sensing growth-conducive conditions, and ultimately forms a mesh-like filamentous mycelium. The mycelium continues to grow until nutrient deprivation or other environmental signals trigger the erection of aerial hyphae and subsequent sporulation. Coincident with differentiation, the streptomycetes activate an elaborate secondary metabolic network, leading to the production of bioactive molecules such as antibiotics (Flärdh and Buttner, 2009). The intricacies of this life cycle require multiple regulatory inputs and controls, in line with the observation that a significant proportion of the *Streptomyces* genome is dedicated to gene regulation (>10% of protein-encoding genes) (Bentley *et al.*, 2002).

There has been growing interest in understanding how sRNAs contribute to gene regulation in the streptomycetes. Some sRNAs have been identified in the model *Streptomyces coelicolor* through computational analyses (Pánek *et al.*, 2008; Swiercz *et al.*, 2008), direct cloning of short transcripts (Swiercz *et al.*, 2008) and transcriptomic studies using deep sequencing (Vockenhuber *et al.*, 2011; Moody *et al.*, 2013). Though the expression of many of the identified sRNAs has been experimentally validated using either northern analyses (Swiercz *et al.*, 2008; Vockenhuber *et al.*, 2011; Moody *et al.*, 2013) or reverse transcription (RT)-coupled PCR (Pánek *et al.*, 2008; Moody *et al.*, 2013), there is little known about the conditions that stimulate sRNA expression, the mRNA/protein targets of the non-coding transcripts, or the mechanisms by which these sRNAs regulate expression.

As a first step to addressing these gaps in our understanding of *Streptomyces* sRNA biology, we conducted a comprehensive study to identify sRNAs expressed by different *Streptomyces* species throughout their developmental cycle. We identified a never-before-characterized sRNA-encoding gene, *SCR3097*, downstream of *rpfA* (Moody *et al.*, 2013), encoding a secreted muralytic enzyme involved in both sporulation and spore germination (Haiser *et*

al., 2009; Sexton *et al.*, 2015). In this study, we began to explore Scr3097-dependent regulation in *S. coelicolor*.

4.3 RESULTS

4.3.1 An sRNA-encoding gene is located immediately downstream of the *rpfA* stop codon.

Work previously conducted in our laboratory led to the identification of hundreds of putative non-coding sRNAs in *S. coelicolor* (Moody *et al.*, 2013). Among these, we identified Scr3097, an 80-nt transcript encoded by a small gene located on the strand opposite *rpfA*, immediately downstream of *rpfA*, ending 10 bp after the *rpfA* stop codon (Fig. 4.1A). *In silico* secondary structure predictions suggested that Scr3097 adopts a three-way junction structure dominated by one major stem-loop (Fig. 4.1B).

To determine how widespread *SCR3097* is among bacteria, we searched the nucleotide collection of the National Center for Biotechnology Information database for orthologous genes using BLAST (Altschul *et al.*, 1990) (August 2013) and discovered that the sRNA was found in a range of streptomycetes in similar genetic contexts (Fig. 4.1A, 4.1B and 4.1C). Interestingly, in *Streptomyces venezuelae*, which seemingly lacks *SCR3097* based on our sequence homology searches, a transcription start site is located between *rpfA* and *eno* (encoding enolase) in the reverse orientation relative to both genes (Matthew Bush and Mark Buttner, personal communication), suggesting that the sRNA-encoding gene may be more widely conserved than suggested by our *in silico* homology searches.

4.3.2 Scr3097 is differentially expressed throughout growth.

As a first step to understanding the biological function(s) of Scr3097, we monitored sRNA transcript levels in broth- and plate-grown wild-type *S. coelicolor* using northern blotting. We found that in liquid cultures, Scr3097 transcripts were highly abundant in exponential-phase cells only; transcripts were not detectable once the culture transitioned into stationary phase (Fig. 4.2A). The sRNA was never detected in an *SCR3097* deletion mutant (Fig. 4.2B and 4.2C), confirming the specificity of the Scr3097-targeting probe for exponential-phase samples

(there was occasionally a non-specific smear observed in all stationary-phase samples, including the *SCR3097* mutant).

We observed a different abundance profile when *S. coelicolor* was grown on a solid medium. Although we detected Scr3097 throughout development, transcript levels were highest during morphological differentiation (aerial development and sporulation) (Fig. 4.2A).

To complement our transcript abundance data, we monitored *SCR3097* promoter activity in wild-type *S. coelicolor* grown on plates using a transcriptional luciferase reporter assay. Using our RNA-seq data (Moody *et al.*, 2013), we mapped the first nucleotide of the mature Scr3097 transcript, and fused 222 bp of upstream DNA to the luciferase reporter gene cluster (Fig. 4.3A), but were unable to detect *SCR3097* promoter activity in plate-grown cultures (Fig. 4.3B). If Scr3097 was processed from a larger transcript, its promoter may be located further upstream than expected. Alternatively, additional regulatory regions not included in our reporter construct may be required for promoter activity. With this in mind, we created a second reporter construct, in which we included 749 bp of upstream DNA (Fig. 4.3A); however, promoter activity remained undetectable (Fig. 4.3B).

To verify expression from these constructs, we complemented an *SCR3097* deletion mutant with an ectopic copy of *SCR3097*, together with 222 bp of upstream DNA, and monitored sRNA transcript abundance throughout growth in a rich liquid medium using northern blotting. We detected Scr3097 in exponential-phase cells of the complemented mutant, as we did in the wild-type strain (Fig. 4.2B), demonstrating that the promoter (at least) was indeed present in our reporter constructs. Notably, the transcript was far less abundant in the complemented strain than in the wild-type background, suggesting that either there were missing regulatory sequences in the complementation construct, or that Scr3097 expression/accumulation was sensitive to chromosome positional effects. We are currently working to differentiate between these possibilities (see below). Our results did, however, suggest that *SCR3097* promoter activity was low, but that mature transcripts were sufficiently stable to promote accumulation.

Though we were unable to monitor *SCR3097* promoter activity using reporter assays, the activity of its predicted homologue in *S. venezuelae* was successfully detected by 5′ triphosphate end capture RNA-seq (Matthew Bush and Mark Buttner, personal communication). Interestingly, in *S. venezuelae*, the sRNA-encoding gene promoter was most active during differentiation; it was not detectable during vegetative growth (Matthew Bush and Mark Buttner, personal

communication). These observations were consistent with our findings for plate-grown *S. coelicolor* cultures.

4.3.3 Scr3097 is involved in nitrogen source utilization, ammonium toxicity and lactate resistance.

To determine the biological function of Scr3097, we investigated the impact of deleting the sRNA-encoding gene on *S. coelicolor* grown under different conditions. We first studied the requirement for Scr3097 for growth in the presence of different nucleobases, sugars and amino acids. Unexpectedly, we found that wild-type *S. coelicolor* did not grow on media supplemented with L-asparagine, while the *SCR3097* mutant strain grew robustly (Fig. 4.4A). Though our findings were very reproducible with the particular amino acid preparation, we were unable to replicate our results with other batches of L-asparagine, suggesting that the component responsible for wild-type growth inhibition was a contaminant in the original preparation. In an attempt to identify the contaminant, we analyzed the composition of the active preparation by liquid chromatography-coupled mass spectrometry, but failed to identify the active component.

Given a potential connection to amino acids, we hypothesized that the sRNA may be involved in nitrogen utilization, and sought to investigate this further by leveraging commercially available phenotypic arrays, and focused on those involving different nitrogen sources. We found that deleting *SCR3097* hampered the ability of *S. coelicolor* to use xanthosine and D,L-α-amino-*N*-butyric acid as sole nitrogen sources (Fig. 4.4B).

We also investigated the impact of the sRNA on ammonium and osmotic stress resistance, and noted that the *SCR3097* deletion mutant exhibited increased resistance to ammonium (Fig. 4.4C) and decreased resistance to lactate (Fig. 4.4D) when compared with the wild-type parent.

4.3.4 Scr3097 affects transcript levels of genes involved in energy metabolism and cell wall remodeling.

To identify the genes (directly or indirectly) regulated by Scr3097, we first computationally predicted the mRNA targets using CopraRNA (Wright *et al.*, 2014) and tested these predictions by monitoring target gene expression in liquid-grown wild-type and mutant strains using RT-coupled real-time PCR (qPCR). Scr3097 was predicted to bind *SCO4239*, encoding a small membrane protein (upstream of the stop codon), and *nuoF*, encoding an NADH dehydrogenase

subunit (within the coding region) (Fig. 4.5). Consistent with our *in silico* predictions, we found that deleting *SCR3097* decreased *SCO4239* and *nuoF* transcript abundance by 56% and 36%, respectively, during exponential growth (Fig. 4.6A), suggesting that the sRNA promoted the accumulation of these transcripts.

To complement our computational analyses, we identified differentially regulated genes in liquid-grown wild-type and mutant *S. coelicolor* using RNA-seq, and confirmed our findings using RT-qPCR. Our analyses identified several genes up-regulated in the mutant, including the *nar-2* operon genes, encoding a respiratory nitrate reductase. Deleting *SCR3097* increased *nar-2* expression 2- to 3-fold during stationary phase, but had no impact on expression during exponential phase (Fig. 4.6B). *as2758*, encoding an RNA antisense to a ß-*N*-acetylglucosaminidase-encoding gene (*SCO2758*), was also up-regulated in the mutant strain. Interestingly, As2758 is partially complementary to *narG2*, the first gene of the *nar-2* operon (Fig. 4.7).

Our RNA-seq analyses led to two additional discoveries regarding Scr3097 and the adjacent gene *rpfA*. The first was that we were able to map the site of transcription termination for the *rpfA* gene, and found that it mapped precisely to *SCR3097*: the strongest stem-loop structure within Scr3097 likely represents the transcriptional terminator of *rpfA* (Fig. 4.1D). This was further supported by *in silico* predictions of intrinsic terminators. Therefore, deleting *SCR3097* would lead to a concomitant loss of the *rpfA* terminator. The second observation was that high-level antisense transcripts were being generated relative to the *rpfA* coding region, likely resulting from transcriptional read-through of the antibiotic resistance cassette used to replace *SCR3097* (the resistance gene is expressed from an independent internal promoter). These observations meant that the regulatory differences ascribed to Scr3097 could indeed be due to loss of the sRNA, and/or they could be due to *rpfA* misregulation.

4.3.5 Relative contributions of *rpfA* and *SCR3097* to the *SCR3097* deletion phenotype.

To address the complications associated with the *SCR3097* mutant construct, we set out to create a series of strains that would allow us to effectively differentiate the relative contributions of RpfA and Scr3097. We deleted the entire *rpfA-SCR3097* region and re-introduced, as appropriate, an ectopic copy of *rpfA* and/or *SCR3097* under the control of their native promoters. We are currently

repeating our phenotypic and expression analyses with these new mutant and complemented strains.

4.3.6 *rpfA* increases Scr3097 transcript abundance in exponential-phase cells.

Given the base-pairing potential between Scr3097 and the *rpfA* 3′ untranslated region (UTR), we considered the possibility that *rpfA* affected Scr3097 transcript abundance. To address this possibility, we monitored Scr3097 expression in a mutant strain in which the *rpfA* promoter, 5′ UTR and coding region were deleted (the 3′ UTR remained). Using northern blotting, we found that Scr3097 abundance decreased dramatically upon deleting *rpfA* (Fig. 4.2C), suggesting the encoded protein and/or expression of the 3′ UTR were required for Scr3097 accumulation. Because expression of transcripts antisense to *SCR3097* (from the promoter of the antibiotic resistance cassette used to replace *rpfA*) could have inadvertently impacted Scr3097 transcript abundance, we will be repeating these assays using our new mutant and complemented constructs (described in section 4.3.5).

4.4 DISCUSSION

sRNAs contribute to the control of a variety of processes, including cell wall metabolism (Waters and Storz, 2009). In this work, we have initiated investigations into the antisense sRNA Scr3097, encoded opposite a gene involved in cell wall remodeling.

We have evidence that Scr3097 regulates the expression of several genes in the cell, either directly or indirectly, and those genes whose expression was shown to be influenced by Scr3097 point to a potential role for Scr3097 in microaerobic energy metabolism. Scr3097 (modestly) inhibited the expression of a membrane-associated respiratory nitrate reductase (Fig. 4.6B), which uses nitrate as an alternative electron acceptor under low-oxygen conditions (van Keulen *et al.*, 2005). It also affected the expression of NADH dehydrogenase (Fig. 4.6A), an important component of the electron transport chain. Though *S. coelicolor* is considered an obligate aerobe, it is capable of growth under microaerobic conditions and can survive for weeks in the complete absence of oxygen (van Keulen *et al.*, 2007; Fischer *et al.*, 2010). In mycelial cells, Nar-2 is the primary nitrate reductase catalyzing the reduction of nitrate into nitrite

(Fischer *et al.*, 2010; Fischer *et al.*, 2014). Though basal levels of Nar-2 enzymes are maintained in aerobically grown mycelia, Nar-2 abundance increases dramatically in response to hypoxia (Fischer *et al.*, 2014). Nar-2-dependent nitrate reduction also relies on the nitrate:nitrite antiporter NarK2 (Fischer *et al.*, 2014).

Because nitrite is toxic, the bacterium must either export the compound to the extracellular milieu or break it down into benign products (*e.g.*, reducing nitrite to ammonium). Upon reducing nitrate, *S. coelicolor* releases nitrite into the growth medium, likely via NarK2 (Fischer *et al.*, 2010; Fischer *et al.*, 2014). This by-product of nitrate reduction does not appear to be further reduced into ammonium (Fischer *et al.*, 2010), though *S. coelicolor* does encode nitrite reductases capable of performing this reaction (van Keulen *et al.*, 2007). Interestingly, Scr3097 was also found to decrease the tolerance to high levels of ammonium (Fig. 4.4C).

Further supporting our hypothesis that Scr3097 is involved in microaerobic energy metabolism was our observation that Scr3097 contributed to lactate resistance (Fig. 4.4D). Lactate is typically generated by lactate dehydrogenase during anaerobic metabolism, with *S. coelicolor* encoding two fermentative D-lactate dehydrogenases (van Keulen *et al.*, 2005).

The extensive complementarity between the antisense sRNA and the *rpfA* 3′ UTR (Fig. 4.1D) hints at a role for Scr3097 in *rpfA* regulation. We are in the process of exploring this possibility by comparing cell wall stress resistance, germination efficiencies and spore morphologies of our Scr3097^{+} and Scr3097^{-} strains. Given that RpfA is involved in cell wall remodeling, spore germination and sporulation (Haiser *et al.*, 2009; Sexton *et al.*, 2015), these tests may reveal an obvious phenotype if Scr3097 does indeed regulate *rpfA* expression.

Given that Scr3097 has the potential to base-pair with the 3′ end of the *rpfA* transcript, we believe that it may impact *rpfA* transcript stability or termination. Though less common than 5′ UTR-associated sRNAs, 3′ UTR-binding sRNAs are not unprecedented. During stationary phase, *E. coli* expresses the antisense RNA GadY to regulate the expression of the acid-responsive transcriptional activator GadX. Upon binding the *gadX* 3′ UTR, GadY recruits the endoribonuclease RNase III to the sRNA:mRNA duplex, and subsequent processing serves to stabilize the *gadX* transcript, leading to increased abundance of acid response proteins (Opdyke *et al.*, 2004; Opdyke *et al.*, 2011). We will be addressing this possibility using our *in vitro* stability assay (presented in Chapter 3), where *rpfA* transcripts will be degraded in the presence and absence of Scr3097. Alternatively, given that Scr3097 is predicted to target the

rpfA intrinsic terminator, it is also possible that the sRNA impacts transcription termination. In *Vibrio anguillarum*, the antisense RNA RNAß promotes transcription termination within the iron uptake-biosynthesis operon upon binding the polycistronic mRNA transcript (Stork *et al.*, 2007). Using our *in vitro* transcription assay (also described in Chapter 3), we will evaluate the effect of Scr3097 on *rpfA* transcription termination.

Our preliminary results (pending confirmation by complementation) suggested that Scr3097 repressed the expression of nitrate respiration during stationary phase, at least under the aerobic conditions used here. Its predicted regulation of the transglycosylase RpfA and the ß-*N*-acetylglucosaminidase SCO2758 points to coordinated regulation of cell wall remodeling, spore germination/sporulation and microaerobic energy metabolism. Coupling of these processes was previously noted in *Mycobacterium tuberculosis*, where oxygen depletion triggers cell wall thickening (Cunningham and Spreadbury, 1998).

Though our findings cannot be unequivocally tied to Scr3097 at this stage (owing to the concurrent deletion of the *rpfA* 3′ UTR and antisense RNA expression), they nevertheless implicate the sRNA in microaerobic energy metabolism. Future studies will involve (i) assigning particular phenotypes to *SCR3097* deletion, (ii) identifying the mRNA/protein binding partners of Scr3097 using *in vivo* pull-down assays coupled with deep-sequencing and mass spectrometry, (iii) evaluating the sRNA's impact on target gene expression using northern blotting or RT-qPCR, and (iv) determining the mode of action of the sRNA.

4.5 EXPERIMENTAL PROCEDURES

4.5.1 *In silico* analyses

BLAST (Altschul *et al.*, 1990) was used to search the nucleotide collection of the National Center for Biotechnology Information database for *SCR3097* gene homologues (August 2013), and sequences were aligned using Clustal Omega (Sievers *et al.*, 2011). The secondary structures of Scr3097 and As2758 sRNAs were predicted using Mfold (Zuker, 2003). The consensus secondary structure of Scr3097 was predicted using RNAalifold (Bernhart *et al.*, 2008). Intrinsic terminators were predicted using WebGeSTer (Mitra *et al.*, 2010). mRNA targets of Scr3097 were computationally predicted using CopraRNA (Wright *et al.*, 2014).

4.5.2 Growth conditions

S. coelicolor strains (Table 4.1) were grown at 30°C in tryptone soya broth (TSB) (Oxoid):YEME (Kieser *et al.*, 2000) (50:50) and in a minimal liquid medium (27 mM mannitol, 2.4 mM $MgSO_4$, 5%$_{w/v}$ polyethylene glycol 6000, 11 µM $CaCl_2$, 4.5 µM $FeSO_4$, 6.3 µM $MnCl_2$, 4.3 µM $ZnSO_4$, 15 mM phosphate buffer, pH 6.80) supplemented with 7.6 or 500 mM $(NH_4)_2SO_4$ [modified from Kieser *et al.* (2000)]. Strains were also grown on minimal medium (MM) agar (Kieser *et al.*, 2000), nutrient agar (NA) (Difco), MYM agar (Stuttard, 1982) supplemented with 2 µL mL^{-1} trace element solution (Hopwood and Wright, 1978) and MS agar (Kieser *et al.*, 2000). When appropriate, media were supplemented with 56 µg mL^{-1} L-asparagine. *E. coli* strains (Table 4.1) were grown at 30°C (BW25113 derivatives) or 37°C (DH5α and ET12567 derivatives) in LB and SOB without added Mg^{2+} (Sambrook and Russell, 2001) and on LB agar (LB with 1.5%$_{w/v}$ agar) and NA. Plasmid, cosmid and mutation marker selections were achieved by supplementing the medium with one or more of the following antibiotics: 100 µg mL^{-1} ampicillin, 50 µg mL^{-1} apramycin, 25 µg mL^{-1} chloramphenicol, 50 µg mL^{-1} hygromycin B, 50 µg mL^{-1} kanamycin, 25 µg mL^{-1} nalidixic acid.

4.5.3 Deletion of *rpfA* and *SCR3097*

The *rpfA* gene locus (-277 to +732, numbering relative to the *rpfA* start codon) (Fig. 4.8A), the stable *SCR3097* transcription region (+748 to +821) (Fig. 4.9A) and the *rpfA-SCR3097* gene locus of *S. coelicolor* (-277 to +864) (Fig. 4.10A) were deleted and replaced with the apramycin resistance cassette *aac(3)IV* using a PCR-directed gene replacement strategy optimized for use in the streptomycetes (Gust *et al.*, 2003). Briefly, extended knockout cassettes, each comprising *aac(3)IV* bordered on either side by 39 bp of DNA flanking the region to be deleted, were PCR-amplified using Phusion High-Fidelity DNA polymerase (Thermo, NEB) with 3-5%$_{v/v}$ dimethylsulfoxide (DMSO), 500 nM each long primer (Tables 4.2 and 4.3) and 0.2-0.4 ng µL^{-1} *aac(3)IV*, excised from plasmid pIJ773 (Table 4.1) using restriction enzymes *Eco*RI and *Hin*dIII. Optimized amplification conditions and product lengths are detailed in Table 4.3. The PCR products were gel-purified using the MicroElute Gel Extraction kit (Omega BioTek) or the PureLink Quick Gel Extraction kit (Invitrogen).

Using the protocol established by Gust *et al.* (2003), the extended knockout cassettes were electroporated into the recombinogenic *E. coli* strain BW25113/pIJ790 (Table 4.1) carrying the *S. coelicolor* cosmid StE41 (Table 4.1),

in which a double cross-over event replaced the wild-type locus with *aac(3)IV* by homologous recombination. Cosmid DNA was extracted from an apramycin-resistant clone using standard methods (Sambrook and Russell, 2001). Isolated cosmid DNA was then electroporated into the methylation-deficient *E. coli* donor strain ET12567/pUZ8002 (Table 4.1) and mobilized into *S. coelicolor* strain M145 (Table 4.1) by conjugation, as described by Gust *et al.* (2003). Apramycin-resistant, kanamycin-sensitive double cross-over exconjugants were isolated (Fig. 4.8B, 4.9B and 4.10B), and their genotype was confirmed by PCR-amplifying the wild-type and mutant loci using *Taq* DNA polymerase (GeneDireX, Norgen BioTek) with 5%$_{v/v}$ DMSO, 300 nM each primer (Tables 4.2 and 4.3) and crude cell lysate as template (Fig. 4.8C, 4.9C and 4.10C).

4.5.4 Construction of complementation and reporter constructs

DNA regions used for complementing a deletion mutant (*rpfA,* -504 to +816; *SCR3097*, +457 to +1,046; the entire *rpfA-SCR3097* locus, -504 to +1,046; numbering relative to the *rpfA* start codon) or constructing reporter fusions [$P_{SCR3097}$ (short), +793 to +1,046; $P_{SCR3097}$ (long), +793 to +1,573] (Fig. 4.3A and 4.11) were PCR-amplified using Phusion High-Fidelity DNA polymerase with 5%$_{v/v}$ DMSO, 500 nM each appropriate primer (Tables 4.2 and 4.3) and 0.2-3 ng μL^{-1} cosmid StE41. Restriction sites were engineered into the 5′ end of each forward and reverse primer (Table 4.2). Primer pairs used, alongside amplification conditions and product lengths, are presented in Table 4.3. PCR products were column-purified using the PureLink PCR Purification kit (Invitrogen) and digested with restriction enzymes *Bam*HI and either *Xba*I (complementation) or *Kpn*I (reporter). Digested products were then column-purified and ligated to dephosphorylated, *Bam*HI- and *Xba*I-digested plasmid pIJ82 (Table 4.1) (complementation) or dephosphorylated, *Bam*HI- and *Kpn*I-digested plasmid pFLUX (Table 4.1) (reporter) using T4 DNA ligase (Invitrogen). Recombinant plasmids were then electroporated into *E. coli* strain DH5α (Table 4.1), extracted, and sent to MOBIX (McMaster University's DNA sequencing facility) to confirm insert sequences. Recombinant plasmids were electroporated into *E. coli* strain ET12567/pUZ8002 and mobilized into *S. coelicolor* strains E119, E120 (Table 4.1) (complementation) or M145 (reporter) by conjugation. Successful introduction of the recombinant plasmids into the host was confirmed by PCR-amplifying the region of interest using *Taq* DNA polymerase with 5%$_{v/v}$ DMSO, 300 nM each appropriate primer (Tables 4.2 and 4.3) and crude cell lysate as template (Fig. 4.11).

4.5.5 Reporter assays

Fifteen microliters of *S. coelicolor* spore suspension [OD_{450} = 0.150, in 2 × YT (Kieser *et al.*, 2000)] were spread, in triplicate, on 200 µL MYM agar in white 96-well plates (Thermo), and plate cultures were incubated at 30°C for 101 h. Emitted luminescence was measured periodically for 2 sec using a TECAN UltraEvolution spectrometer. Luminescence emitted from the negative control strain, carrying a promoterless luciferase reporter gene cluster (M145/pFLUX) (Table 4.1), was subtracted from sample luminescence values.

4.5.6 RNA isolation

S. coelicolor strains were grown at 30°C in TSB:YEME (50:50). Cells were collected from exponential- and stationary-phase cultures by centrifugation (1,900-3,000 × g for 5-10 min at 4°C) and frozen at -80°C for 1-24 days. Total RNA was extracted from cells as described by Moody *et al.* (2013), and co-extracted DNA was completely digested using TURBO DNase (Ambion). Absence of co-extracted genomic DNA was confirmed by PCR-amplifying *rpfA* or *rpoB* (encoding the RNA polymerase ß subunit) using *Taq* DNA polymerase with 5%$_{v/v}$ DMSO, 300 nM each primer (Tables 4.2 and 4.3) and 25 ng µL^{-1} total RNA as template.

Isolated RNA was quantified using a ND-1000 spectrophotometer (NanoDrop Technologies). RNA integrity was confirmed by size-fractionating 1.6-2.0 µg total RNA on a 2%$_{w/v}$ agarose gel at 70-100 V for 30-40 min in 1 × TBE buffer (Sambrook and Russell, 2001), and extract purity was verified by measuring the A_{260}/A_{280} (1.88-2.03) and A_{260}/A_{230} ratios (2.19-2.33).

Total RNA from wild-type *S. coelicolor* (M145) grown at 30°C in TSB:YEME (50:50) and on MS agar was similarly isolated during a previous study (Sexton *et al.*, 2015).

4.5.7 Northern blotting

Probes were prepared by ^{32}P-5′-end-labeling 0.1 µM ssDNA oligonucleotides with 0.5 U µL^{-1} T4 polynucleotide kinase (Fermentas, Invitrogen) using 250 nM [γ-^{32}P]ATP (Perkin Elmer). After 30 min at 37°C, unincorporated nucleotides were removed using the PureLink PCR Purification kit.

DNase-treated total RNA (8-25 µg) was heated at ~95°C for 5 min in RNA gel-loading buffer (Sambrook and Russell, 2001) and size-fractionated at 200 V

for ~40 min on a continuous 6%$_{w/v}$ denaturing urea-polyacrylamide gel (BioShop) in 1 × TBE buffer using a Mini-PROTEAN Tetra Cell (Bio-Rad). RNA was then blotted onto a Zeta-Probe nylon blotting membrane (Bio-Rad) at 15 V for 40-45 min in 0.5 × TBE buffer using a Trans-Blot SD Semi-Dry Electrophoretic Transfer Cell (Bio-Rad). RNA was cross-linked to the membrane by baking the membrane at 55°C for 2 h with EDC cross-linking solution, as described by Pall and Hamilton (2008). ^{32}P-5′-end-labeled probe complementary to the transcript of interest (0.4-1.6 pmol) was denatured at ~95°C for 5 min and then incubated with the membrane overnight at 42°C in ULTRAhyb-Oligo Hybridization Buffer (Ambion). Unbound probe was removed by washing the membrane 2-3 times for 2-5 min each at 42°C in 2 × SSC with 0.1%$_{w/v}$ sodium dodecyl sulfate (SDS) (Sambrook and Russell, 2001). When appropriate, the membrane was also washed once at 42°C for 2-3 min in 0.2 × SSC with 0.1%$_{w/v}$ SDS (Sambrook and Russell, 2001). Bound transcripts were visualized by autoradiography. Membranes were stripped of the probe by incubating the membrane for 40 min at 70°C in 0.2 × SSC with 0.1%$_{w/v}$ SDS. Successful removal of the probe was confirmed by autoradiography or phosphorimaging.

4.5.8 RNA-seq

Total RNA isolated from *S. coelicolor* wild-type (M145) and mutant (E119) mycelia grown at 30°C in TSB:YEME (50:50) was submitted to the Farncombe Metagenomics Facility for RNA-seq. Briefly, rRNA contained within the extracts was depleted using the Ribo-Zero Magnetic kit for bacteria (Epicentre). mRNA fragmentation, first and second strand cDNA synthesis, adaptor ligation and PCR-based enrichment of adaptor-ligated cDNA were performed using the NEBNext Ultra Directional RNA Library Prep kit for Illumina (NEB). cDNA sequencing was conducted using a HiSeq 1500 (Illumina). Reads were reverse complemented using the FASTX-Toolkit (http://hannonlab.cshl.edu/fastx_toolkit/) and aligned to the *S. coelicolor* A3(2) genome sequence using Bowtie2 (Langmead *et al.*, 2009) after trimming low-quality 3′ ends using PRINSEQ (Schmieder and Edwards, 2011). Quality trimmed reads were converted to BAM format, and then sorted and indexed using SAMtools (Li *et al.*, 2009) for subsequent visualization using the Integrated Genomics Viewer (Robinson *et al.*, 2011). Differentially expressed genes were then identified using Rockhopper (McClure *et al.*, 2013) with default settings and sorted by *Q* value.

4.5.9 RT-qPCR

Transcripts of interest were reverse transcribed using SuperScript III reverse transcriptase (Invitrogen) with 100 nM gene-specific reverse primer (Tables 4.2 and 4.3) and 100 ng μL^{-1} total RNA. cDNA was stored at -20°C overnight.

cDNA was then amplified by qPCR using PerfeCTa SYBR Green SuperMix (Quanta Biosciences) with 300 nM each primer (Tables 4.2 and 4.3) and 8-12.5 ng μL^{-1} reverse transcribed total RNA. 'No template' controls, in which an equal volume of nuclease-free water replaced the cDNA template, were prepared in parallel and included in each run. Reactions were conducted, in triplicate, in clear 96-well PCR plates with a CFX96 Touch Real-Time PCR Detection System (Bio-Rad). The amplification conditions recommended by the manufacturer (Quanta Biosciences) were used with an optimized annealing/extension temperature (Table 4.3). A melt curve analysis (65-95°C with 5-sec fluorescence reads every 0.5°C increase) was conducted at the end of each run.

Collected fluorescence data were baseline-corrected using the CFX Manager software (Bio-Rad). Relative transcript abundance normalized to total RNA mass was calculated using the DART-PCR workbook (Peirson *et al.*, 2003).

4.5.10 Biolog Phenotype MicroArray assays

S. coelicolor spores (9.7 µL of a spore suspension, OD_{450} = ~0.1, in inoculating fluid) were inoculated into 90.3 µL medium in clear 96-well plates containing different nitrogen sources (PM3B, Biolog) or different osmotic stressors (PM9, Biolog). Base minimal medium composition, comprising various proprietary Biolog components, was as follows: 1 × IF-0a (PM3B) or IF-10b (PM9) GN/GP Base inoculating fluid (Biolog), 25 mM glucose, 15 mM NH_4Cl (PM9 only), 5 mM $MgCl_2$, 5 mM Na_2SO_4, 50 µM $CaCl_2$, 50 µM $FeCl_2$, 50 µM $MnCl_2$, 50 µM $ZnCl_2$, 1 × Redox Dye Mix D (Biolog), 10 mM phosphate buffer, pH 7. Plate cultures were incubated at 30°C for 71 h (PM9) or 96 h (PM3B). Growth was visually inspected.

4.6 ACKNOWLEDGEMENTS

This work was supported by an NSERC Discovery Grant (No. 04681) and an NSERC Discovery Accelerator supplement to M.A.E. R.J.S. was supported by a Vanier Canada Graduate Scholarship (NSERC).

4.7 TABLES

Table 4.1. Bacterial strains, cosmids and plasmids.

Strain/ vector	Genotype, properties and/or use	Reference
***S. coelicolor* A3(2) strains**		
M145	A3(2) SCP1$^-$ SCP2$^-$	Kieser *et al.* (2000)
E118	M145 *rpfA::aac(3)IV*	This study
E119	M145 *SCR3097::aac(3)IV*	This study
E120	M145 *rpfA-SCR3097::aac(3)IV*	This study
***E. coli* strains**		
BW25113	Cosmid mutagenesis host; *lacI*^{q} *rrnB*$_{T14}$ Δ*lacZ*$_{WJ16}$ *hsdR514* Δ*araBAD*$_{AH33}$ Δ*rhaBAD*$_{LD78}$	Datsenko and Wanner (2000)
DH5α	Plasmid construction strain; F$^-$ ϕ80*lacZ*ΔM15 Δ(*lacZYA-argF*)*U169 recA1 endA1 hsdR17*(r_K^-, m_K^+) *phoA supE44* λ$^-$ *thi-1 gyrA96 relA1*	Bethesda Research Laboratories
ET12567	Methylation-deficient strain; F$^-$ *dam13::*Tn*9 dcm6 hsdM hsdR recF143 zjj201::*Tn*10 galK2 galT22 ara14 lacY1 xyl5 leuB6 thi1 tonA31 rpsL136 hisG4 tsx78 mtli glnV44*	MacNeil *et al.* (1992)
***S. coelicolor* cosmids**		
StE41	*rpfA*$^+$ *SCR3097*$^+$ *bla kan*	Redenbach *et al.* (1996)
StE41a	StE41 *rpfA::aac(3)IV*	This study
StE41b	StE41 *SCR3097::aac(3)IV*	This study
StE41c	StE41 *rpfA-SCR3097::aac(3)IV*	This study
Plasmids		
pFLUX	Integrative transcriptional reporter vector; *ori* (pUC18) *oriT* (RK2) *int* ϕBT1 *attP* ϕBT1 *luxCDABE* (promoterless) *aac(3)IV*	Craney *et al.* (2007)
pFLUX-Pos	P_{ermE*} transcriptionally fused to *luxCDABE* in pFLUX	Sexton *et al.* (2015)
pMC240	*SCR3097* promoter region (+793 to +1,046) transcriptionally fused to *luxCDABE* in pFLUX[a]	This study
pMC241	*SCR3097* promoter region (+793 to +1,573) transcriptionally fused to *luxCDABE* in pFLUX[a]	This study
pIJ82	Integrative cloning vector; *ori* (pUC18) *oriT* (RK2) *int* ϕC31 *attP* ϕC31 *hyg*	Gift from H. Kieser
pMC242	*rpfA* under the transcriptional control of P_{rpfA} (-504 to +816) in pIJ82[a]	This study
pMC243	*SCR3097* under the transcriptional control of $P_{SCR3097}$ (+457 to +1,046) in pIJ82[a]	This study
pMC244	*rpfA* and *SCR3097* under the transcriptional control of P_{rpfA} and $P_{SCR3097}$, respectively (-504 to +1,046), in pIJ82[a]	This study
pIJ773	Plasmid carrying *oriT* (RK2) and *aac(3)IV* flanked by FLP recognition target sites for use in REDIRECT, *bla*	Gust *et al.* (2003)
pIJ790	λ RED recombination plasmid; *oriR101 repA101ts araC bet exo gam* P_{araBAD} *cat*	Gust *et al.* (2003)
pUZ8002	Non-transmissible *oriT* mobilizing plasmid; RP4 *tra neo*	Paget *et al.* (1999)

[a] Numbering relative to the *rpfA* start codon.

Table 4.2. List of PCR primers.

Primer[a]	Sequence[b]	Restriction site
Mutagenesis primers		
DBLKOR	GGA CCG AGC CTA ACC GGC TCC GGG CGA TCG GCC AGC CGA TGT AGG CTG GAG CTG CTT C	
SCO3097KOF	TTT GGA TCT CGT GAG AGA TAG GTC TCA GAA GCC GTG ATC ATT CCG GGG ATC CGT CGA CC	
SCO3097REV[c]	CAC GCA CCG GGG CGG GAG TCA CGG GAC CGC CGC CGC TTA TGT AGG CTG GAG CTG CTT C	
SCR3097KOF	CCA CCC GCT GGA CAG AAC CGA GAG TAA ATT GTT TCC GAA ATT CCG GGG ATC CGT CGA CC	
SCR3097KOR	CCG GGC CAG CAG CTG CAC CTG AAG TAA GCG GCG GCG GTC TGT AGG CTG GAG CTG CTT C	
PCR primers		
3097down(2)	CCG AAC GGA ACA AAG GCG	
pFLUXR	GCC GAA GTT GAT GGA CTG GA	
PrpfAF-X	GCA CTT CTA GAC GAC AGT CTC TGG GCC ATC	*Xba*I
PSCR3097-B	GCA CTG GAT CCC CTC GGG AGT CCA GGA TTT	*Bam*HI
rpfAF[d]	GAG TCC GGC GGC AAC TGG TC	
rpfAR[d]	GCT GGG ACT TGC TCG CCT GG	
rpfAT-B	GCA CTG GAT CCC AAA GGC GGA ACA TGA AAA G	*Bam*HI
rpoBF[e]	TCG ACC ACT TCG GCA ACC GC	
rpoBR[e]	GCG CTC CAT ACG GGC GAG AC	
SCO0216F	TGG CAG GAG ACG ATC ACT TC	
SCO0216R	CCG GTA GAT GGT GTC CGA AT	
SCO0217F	CTG TTC TCC AAT CCG GAC CT	
SCO0217R	TAG GTG ACC GGC TCG TAG TA	
SCO0218F	CTG GTT CAC CGG TCA GGA A	
SCO0218R	AAG GTC TCC ACG TAG TGC TG	
SCO0219F	GTC CCC TAC ATC TGC CTG G	
SCO0219R	AGG TGG AAC AGC GGA CTG	
SCO3096R-B	GCA CTG GAT CCC CTC GGG AGT CCA GGA TTT	*Bam*HI
SCO3096R-B2	GCA CTG GAT CCG GCA CGA GCA TCT CCT TCT T	*Bam*HI
SCO3096R-B3	GCA CTG GAT CCG GAC CTT CTT GAG GGT GTG G	*Bam*HI
SCO3096R-X	GCA CTT CTA GAC CTC GGG AGT CCA GGA TTT	*Xba*I
SCO3097F-B	GCA CTG GAT CCC GCT CCA CCG AGC AGA A	*Bam*HI
SCO4239F	CTC CAC CAC CCG ACA GAC	
SCO4239R	CAG GAC GAA GGC GAG AGA G	
sco4567 in fwd[f]	GAT CGC GTA CGT CAA GGA GT	
SCO4567R	CCC TGA GGA ATG AAC TGC CA	
SCR3097F	GCA CGA GCA TCT CCT TCT TC	
SCR3097R-K	GCA CTG GTA CCG GGA CTT TTC ATG TTC CGC C	*Kpn*I
Northern probes		
SCR3097-probe	TTC ATG TTC CGC CTT TGT TCC GTT C	
5S[g]	CCC TGC AGT ACC ATC GGC GCT	

[a] All primers and probes were purchased from Integrated DNA Technologies.

[b] Sequences complementary to DNA flanking the region to be deleted are underlined once. Restriction sites are underlined twice.
[c] Primer sequence was previously published by Haiser *et al.* (2009).
[d] Primer sequences were previously published by Sexton *et al.* (2015).
[e] Primer sequences were previously published by Hindra *et al.* (2014).
[f] Primer sequence was previously published by Moody *et al.* (2013).
[g] Probe sequence was previously published by Swiercz *et al.* (2008).

Table 4.3. PCR amplification conditions.

Construct	Primers[a]		Length (bp)	Annealing temperature (°C)	Extension time (min:sec)
Extended knockout cassettes[b]					
rpfA	SCO3097KOF	SCO3097REV	1,460	50-55	0:30
SCR3097	SCR3097KOF	SCR3097KOR	1,460	50-55	0:30
rpfA-SCR3097	SCO3097KOF	DBLKOR	1,460	50-55	0:30
Cloning complementation and reporter constructs[c]					
rpfA	PrpfAF-X	rpfAT-B	1,342	65	0:20
SCR3097	SCO3096R-X	SCO3097F-B	612	65	0:15
rpfA-SCR3097	PrpfAF-X	PSCR3097-B	1,572	66	0:24
$P_{SCR3097}$ (short)	SCO3096R-B	SCR3097R-K	276	65	0:15
$P_{SCR3097}$ (long)	SCO3096R-B3	SCR3097R-K	803	66	0:17
Confirming mutant genotypes[d]					
rpfA	rpfAF	3097down(2)	667	60	0:45
rpfA::aac(3)IV	SCO3097KOF	3097down(2)	1,515	60	1:31
SCR3097	SCR3097F	SCR3097-probe	201	59	0:45
SCR3097:: aac(3)IV	SCR3097F	SCR3097KOR	1,600	59	1:36
rpfA-SCR3097	rpfAF	SCO3096R-B2	853	54	0:45
rpfA-SCR3097:: aac(3)IV	SCO3097KOF	SCO3096R-B2	1,569	53	1:34
Confirming plasmid introduction[d]					
rpfA	rpfAF	rpfAR	133	61	0:45
SCR3097	SCO3096R-X	SCO3097F-B	612	60	0:45
rpfA-SCR3097	PrpfAF-X	PSCR3097-B	1,572	53	1:34
$P_{SCR3097}$ (short)	SCO3096R-B2	pFLUXR	391	60	0:45
$P_{SCR3097}$ (long)	SCO3096R-B3	pFLUXR	918	53	0:45
Confirming absence of contaminating genomic DNA in RNA extracts[d]					
rpfA	rpfAF	rpfAR	133	61	0:45
rpoB	rpoBF	rpoBR	86	61	0:45
RT-qPCR[e]					
narG2	SCO0216F	SCO0216R	150	60	0:45
narH2	SCO0217F	SCO0217R	56	60	0:45
narJ2	SCO0218F	SCO0218R	54	60	0:45
narI2	SCO0219F	SCO0219R	137	60	0:45
nuoF	SCO4567inFWD	SCO4567R	87	61	0:45
SCO4239	SCO4239F	SCO4239R	73	61	0:45

[a] Primer sequences are located in Table 4.2.

[b] PCR amplifications of extended apramycin resistance cassettes were performed using Phusion High-Fidelity DNA polymerase. Amplification conditions were as follows: (i) an initial 3-min denaturation step at 98°C, (ii) 35 amplification cycles consisting of a 10-sec

denaturation step at 98°C, a 30-sec annealing step at 50°C for the first 10 cycles then 55°C for the remaining 25 cycles, and a 30-sec extension step at 72°C, and (iii) a final 10-min extension step at 72°C.

[c] PCR amplifications of DNA for cloning experiments were performed using Phusion High-Fidelity DNA polymerase. Amplification conditions were as suggested by the manufacturer.

[d] PCR amplifications designed to confirm strain genotype and the absence of genomic DNA were conducted using *Taq* DNA polymerase. Amplification conditions were as follows: (i) an initial 3-min denaturation step at 95°C, (ii) 35 amplification cycles consisting of a 30-sec denaturation step at 95°C, a 30-sec annealing step, and an extension step at 72°C, and (iii) a final 5-min extension step at 72°C.

[e] qPCR amplifications of cDNA were performed using PerfeCTa SYBR Green SuperMix. Amplification conditions were as suggested by the manufacturer.

4.8 FIGURES

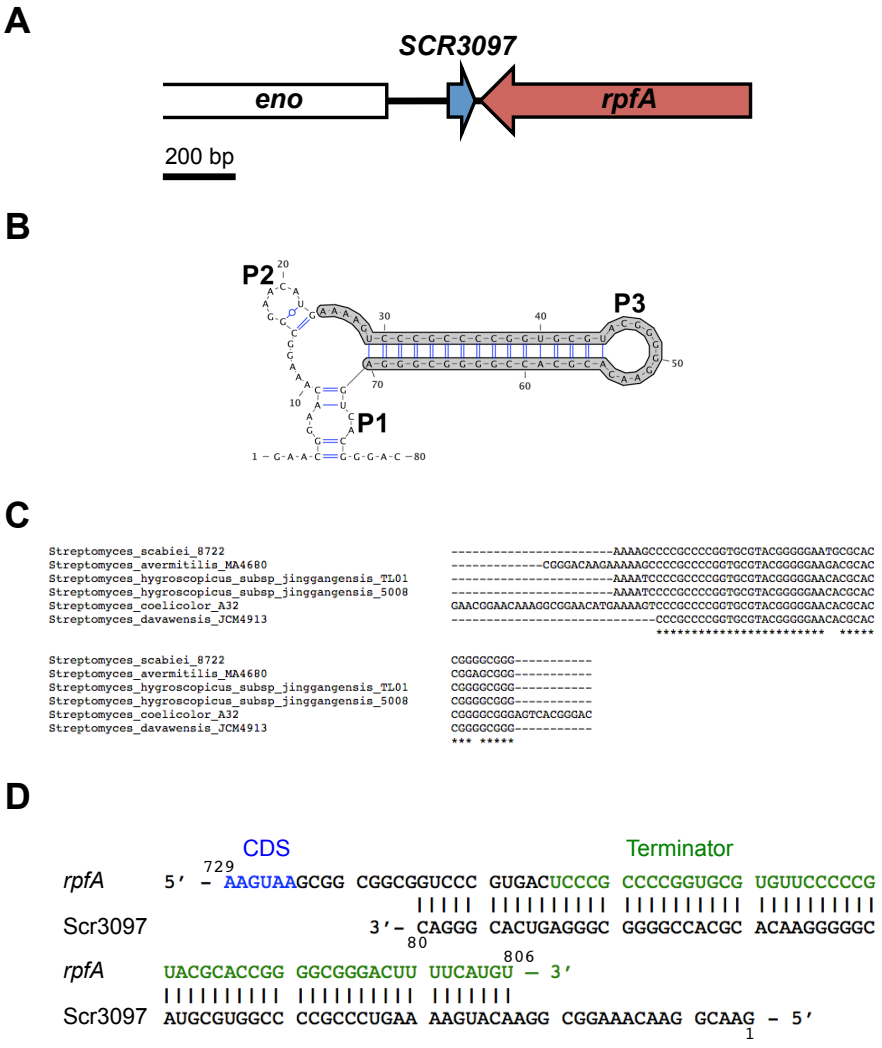

Fig. 4.1. Bioinformatic analysis of the sRNA Scr3097. (A) Genetic context of *SCR3097* in the streptomycetes. Genes were drawn to scale. (B) Predicted secondary structure of the *S. coelicolor* Scr3097. Conserved sequences and structures are highlighted in gray. The structure was drawn using VARNA (Darty *et al.*, 2009). (C) The genomes of various *Streptomyces* species were searched for sequences homologous to the *S. coelicolor SCR3097*. Homologous sequences were aligned. Asterisks indicate conserved nucleotides. (D) Predicted pairing between Scr3097 and the *rpfA* 3′ UTR. Numbering of the *rpfA* mRNA and Scr3097 is relative to the *rpfA* start codon and the first nucleotide of the mature Scr3097 transcript, respectively. CDS, *rpfA* coding sequence.

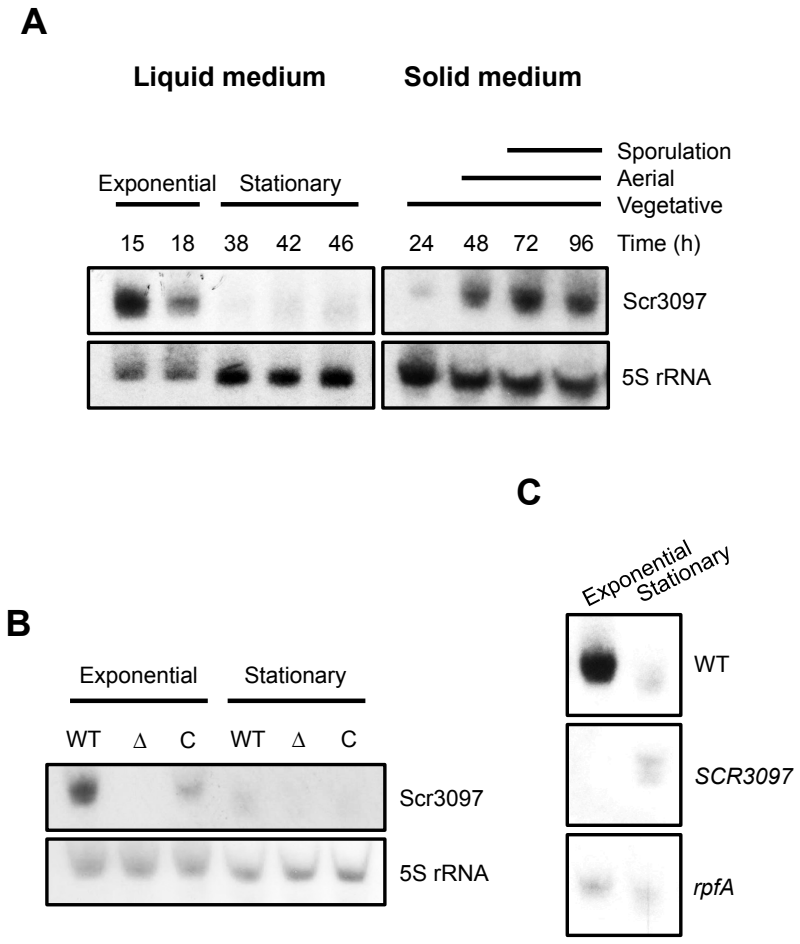

Fig. 4.2. Scr3097 abundance throughout growth and development. (A) Wild-type *S. coelicolor* (M145) was grown at 30°C in a liquid rich medium or on a sporulation-conducive solid medium (MS agar). At the times indicated, total RNA was extracted from cells, and Scr3097 and 5S rRNA (control) transcripts were detected using northing blotting. (B) *S. coelicolor* wild-type (M145/pIJ82, WT), *SCR3097* mutant (E119/pIJ82, Δ) and complemented mutant (E119/pMC243, C) strains were grown at 30°C in a liquid rich medium. Total RNA was extracted from exponential- and stationary-phase cells, and Scr3097 and 5S rRNA (control) transcripts were detected using northern blotting. (C) *S. coelicolor* wild-type (M145, WT), *SCR3097* mutant (E119, *SCR3097*) and *rpfA* mutant (E118, *rpfA*) strains were grown at 30°C in a liquid rich medium. Total RNA was extracted from exponential- and stationary-phase cells, and Scr3097 transcripts were detected using northern blotting. All images are representative of three biological replicates.

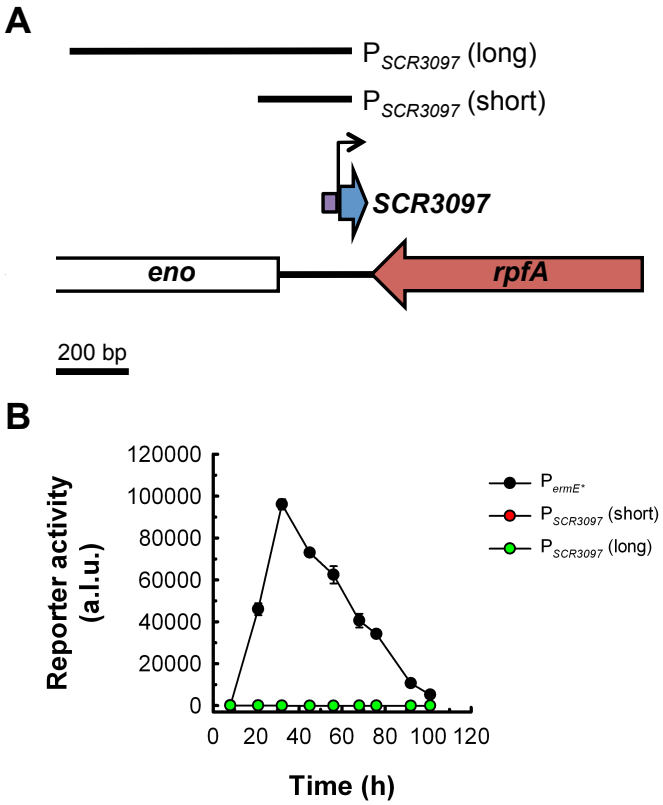

Fig. 4.3. *SCR3097* promoter activity throughout development. (A) Schematic of the *SCR3097* promoter regions cloned into the reporter vector. Genes and cloned regions were drawn to scale. (B) Wild-type *S. coelicolor* strains, expressing the luciferase reporter gene cluster from a strong promoter (P_{ermE*}) or the *SCR3097* promoter region, were grown at 30°C on a sporulation-conducive medium (MYM agar). Background-subtracted luminescence was periodically measured. Data are presented as mean ± standard error (n = 3). P_{ermE*}, M145/pFLUX-Pos; $P_{SCR3097}$ (short), M145/pMC240; $P_{SCR3097}$ (long), M145/pMC241.

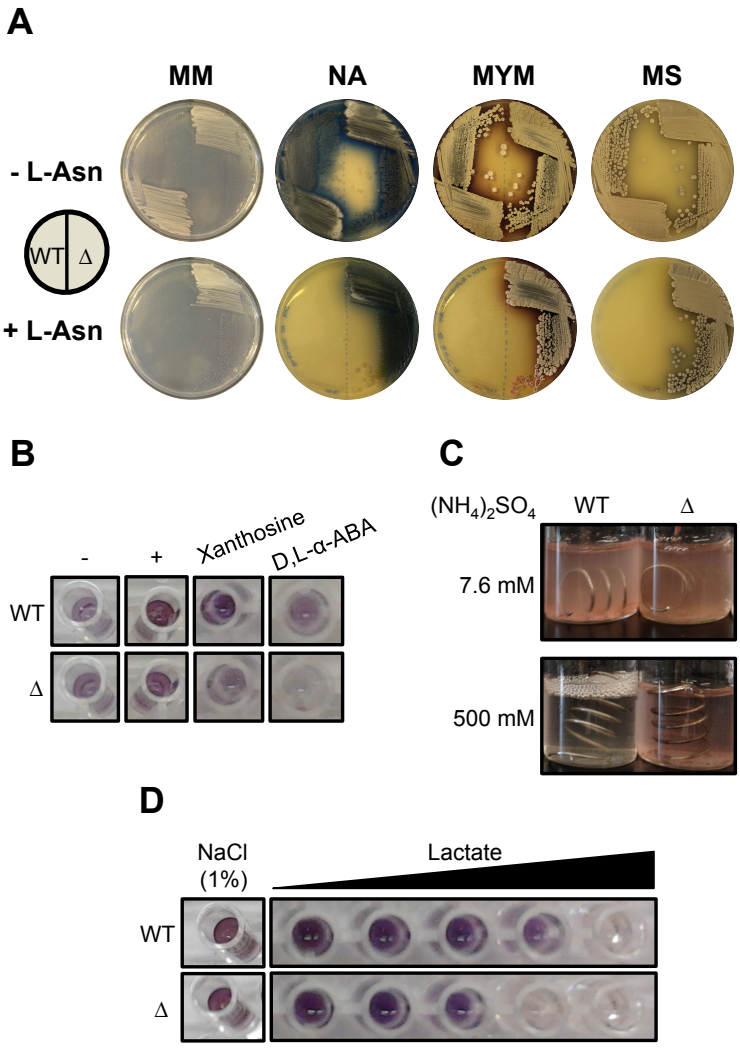

Fig. 4.4. Phenotypic effects of deleting *SCR3097*. (A) *S. coelicolor* wild-type (M145, WT) and *SCR3097* mutant (E119, Δ) strains were grown on MM, NA, MYM and MS agar supplemented with 0 (- L-Asn) or 56 µg mL^{-1} (+ L-Asn) L-asparagine. Plate cultures were incubated at 30°C for 4 days. (B) Wild-type and mutant strains were grown at 30°C for 96 h in a phosphate-buffered glucose minimal medium supplemented with xanthosine or D,L-α-amino-*N*-butyric acid (D,L-α-ABA) as sole nitrogen source. Cultures were inspected for reduced tetrazolium dye (purple pigment), indicating respiration. -, no nitrogen source; +, supplemented with L-asparagine. (C) Wild-type and mutant strains were grown at 30°C for 4 days in a phosphate-buffered mannitol minimal medium supplemented with 7.6 or 500 mM $(NH_4)_2SO_4$. (D) Wild-type and mutant strains were grown at 30°C for 71 h at 30°C in a phosphate-buffered glucose minimal medium supplemented with sodium lactate (8-12%$_{w/v}$) or NaCl (1%$_{w/v}$) (control). Cultures were inspected for reduced tetrazolium dye.

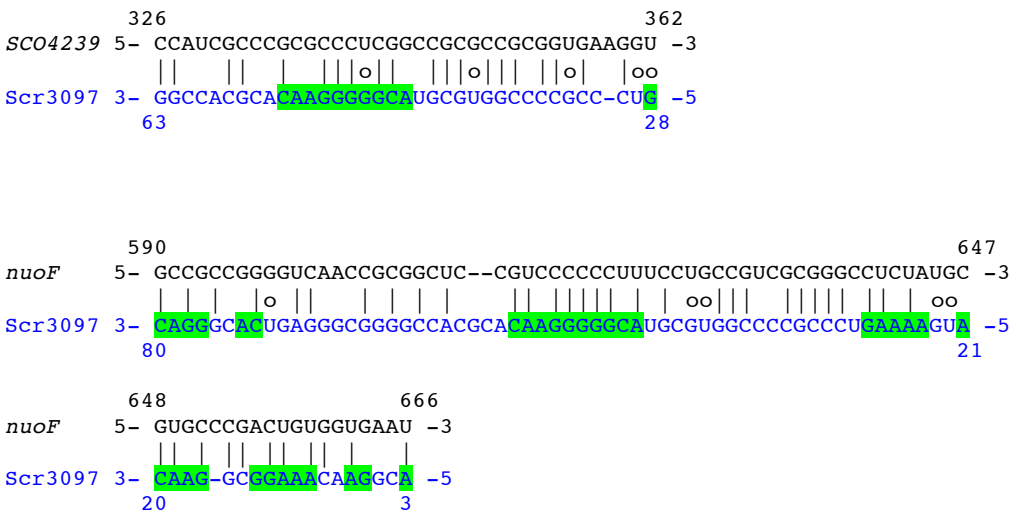

Fig. 4.5. Potential base-pairing between Scr3097 and its *in silico* predicted mRNA targets. *SCO4239* and *nuoF* mRNAs are in black, whereas Scr3097 is in blue.

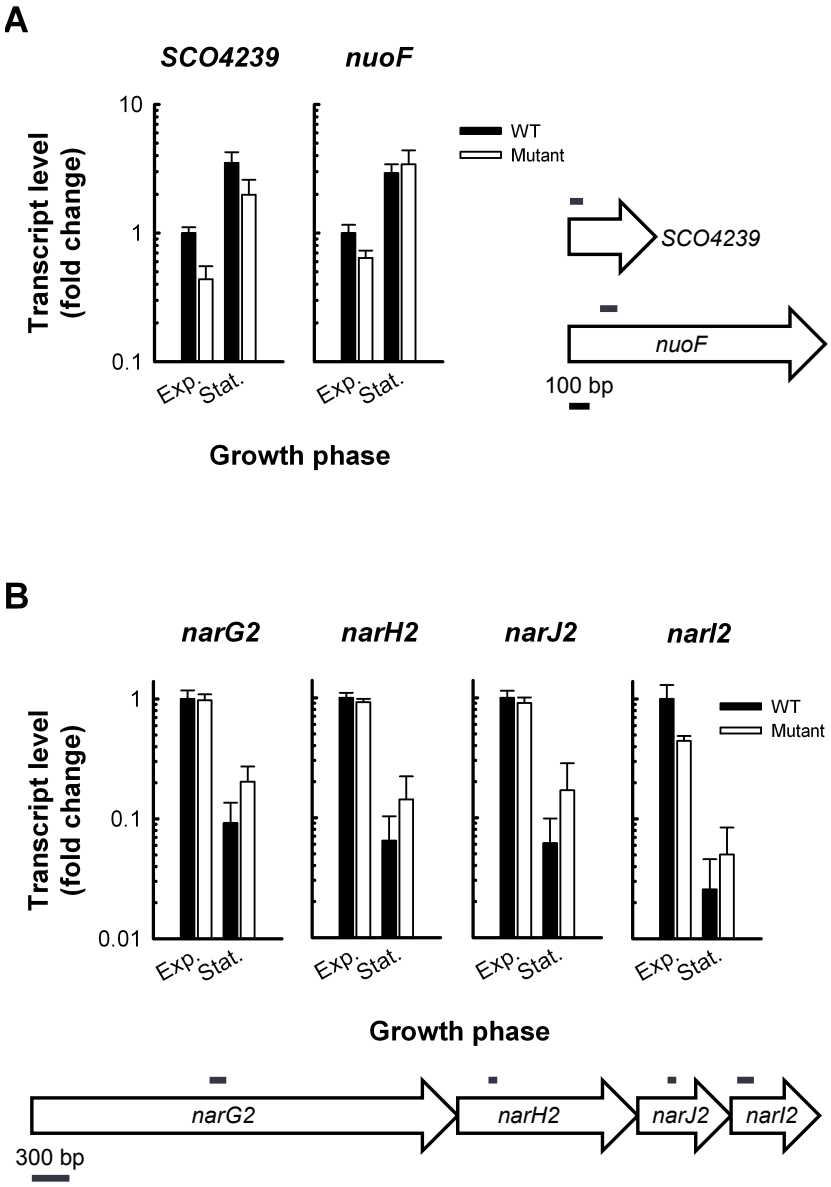

Fig. 4.6. Impact of Scr3097 on gene expression. *S. coelicolor* wild-type [(A) M145, (B) M145/pIJ82, WT] and *SCR3097* mutant [(A) E119, (B) E119/pIJ82, Mutant] strains were grown at 30°C in a rich liquid medium. Total RNA was extracted from exponential-phase (Exp.) and stationary-phase (Stat.) cells, and transcripts were quantified using RT-qPCR. Transcript levels were normalized to total RNA mass and expressed as fold changes relative to expression levels in exponential-phase wild-type cells. Data are presented as mean ± standard error (*n* = 2-3). The location of each amplified product relative to the translation start and stop sites is indicated by a bold line above block arrows. Genes and PCR products were drawn to scale.

A

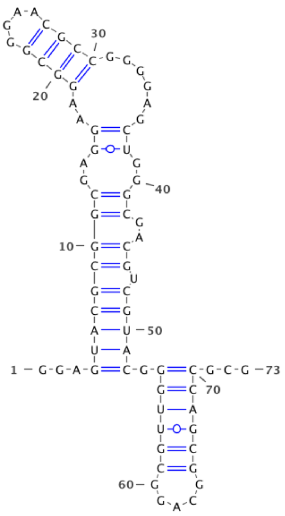

B

```
          871                                                    901
narG2 5′ – AAGGCGGUCG CCGUCAGC--CC CG-ACUACGCC GACAACGUGA – 3′
          ||||||| ||||| ||   || || || ||| | |
As2758    3′ – CGCCAGC GGCAGGCGUUGG GCAUGCUGCAG C – 5′
              72                                 42
```

Fig. 4.7. Bioinformatic analysis of the antisense RNA As2758. (A) Predicted secondary structure of the *S. coelicolor* As2758. The structure was drawn using Varna (Darty *et al.*, 2009). (B) Predicted pairing between As2758 and *narG2* mRNA. Numbering of the *narG2* mRNA and As2758 is relative to the *narG2* start codon and the first nucleotide of the mature As2758 transcript, respectively.

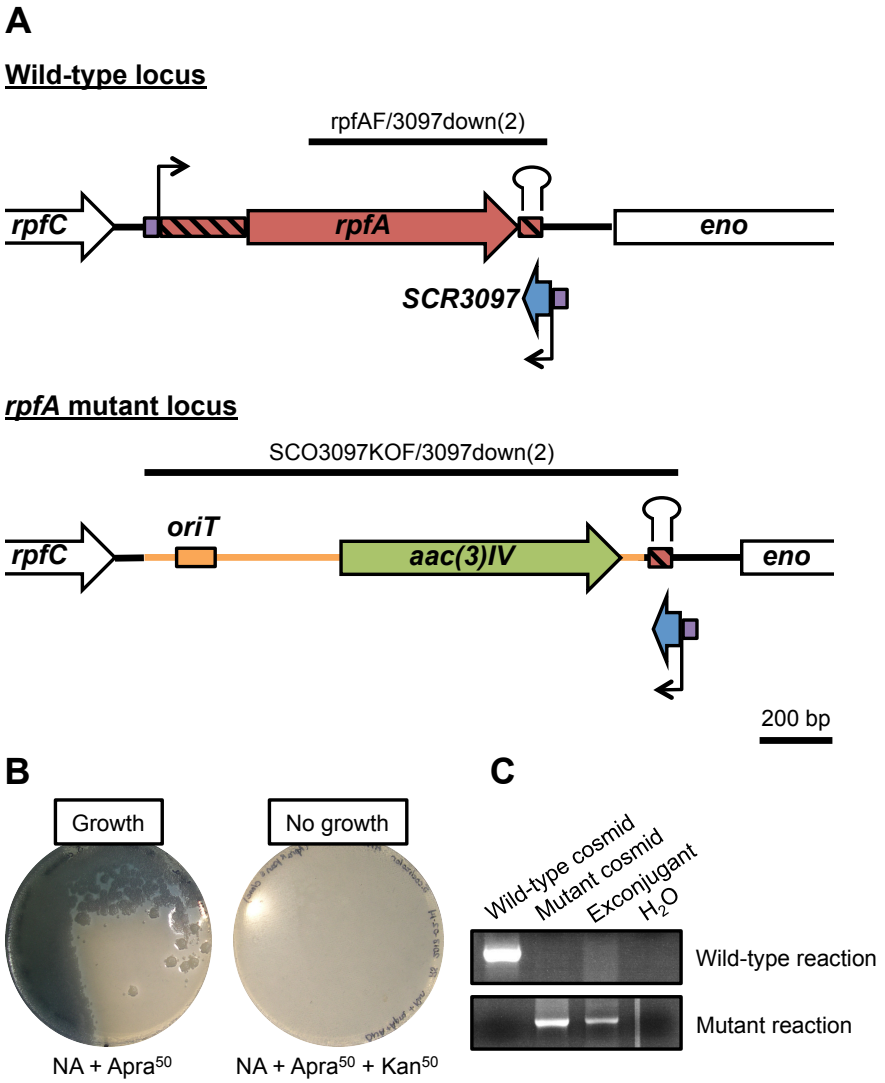

Fig. 4.8. Construction of the *rpfA* deletion mutant. (A) Schematic of the *rpfA-SCR3097* region in the wild-type and the *rpfA* deletion mutant. Hatched red blocks indicate the location of the *rpfA* 5′ and 3′ UTRs, and purple blocks specify the location of predicted promoters. Black elbow arrows denote the transcriptional start sites of *rpfA* and *SCR3097* as predicted using 5′ rapid amplification of cDNA ends (Haiser *et al.*, 2009) and RNA-seq (Moody *et al.*, 2013), respectively. Thick black lines above genes specify the location of the PCR products used to confirm the strain genotype. Primer pairs used are indicated above lines. Schematics were drawn to scale. (B) Antibiotic sensitivity phenotypes. The *S. coelicolor rpfA* deletion mutant (E118) was grown at 30°C on NA supplemented with 50 µg mL^{-1} apramycin ($Apra^{50}$) ± 50 µg mL^{-1} kanamycin (Kan^{50}). (C) The genotype of the *rpfA* mutant was confirmed by PCR-amplifying both the wild-type and mutant loci from crude cell lysates. Wild-type (StE41) and mutant (StE41a) cosmids served as controls. An equal volume of water, instead of DNA template, was added to the 'no template' negative controls (H_2O).

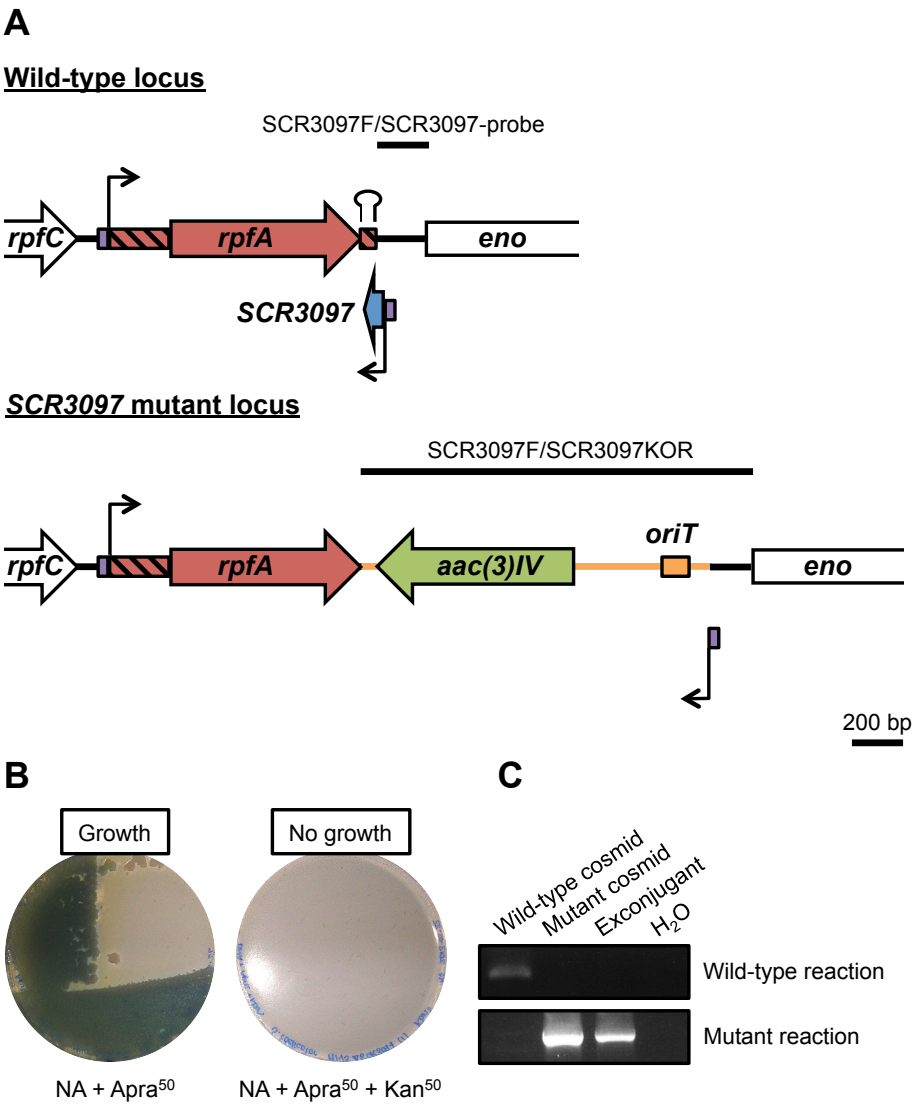

Fig. 4.9. Construction of the *SCR3097* deletion mutant. (A) Schematic of the *rpfA-SCR3097* region in the wild-type and the *SCR3097* deletion mutant. Notations are as indicated for Fig. 4.8A. (B) Antibiotic sensitivity phenotypes. The *S. coelicolor SCR3097* deletion mutant (E119) was grown at 30°C on NA supplemented with 50 µg mL^{-1} apramycin ($Apra^{50}$) ± 50 µg mL^{-1} kanamycin (Kan^{50}). (C) The genotype of the *SCR3097* mutant was confirmed by PCR-amplifying both the wild-type and mutant loci from crude cell lysates. Wild-type (StE41) and mutant (StE41b) cosmids served as controls. An equal volume of water, instead of DNA template, was added to the 'no template' negative controls (H_2O).

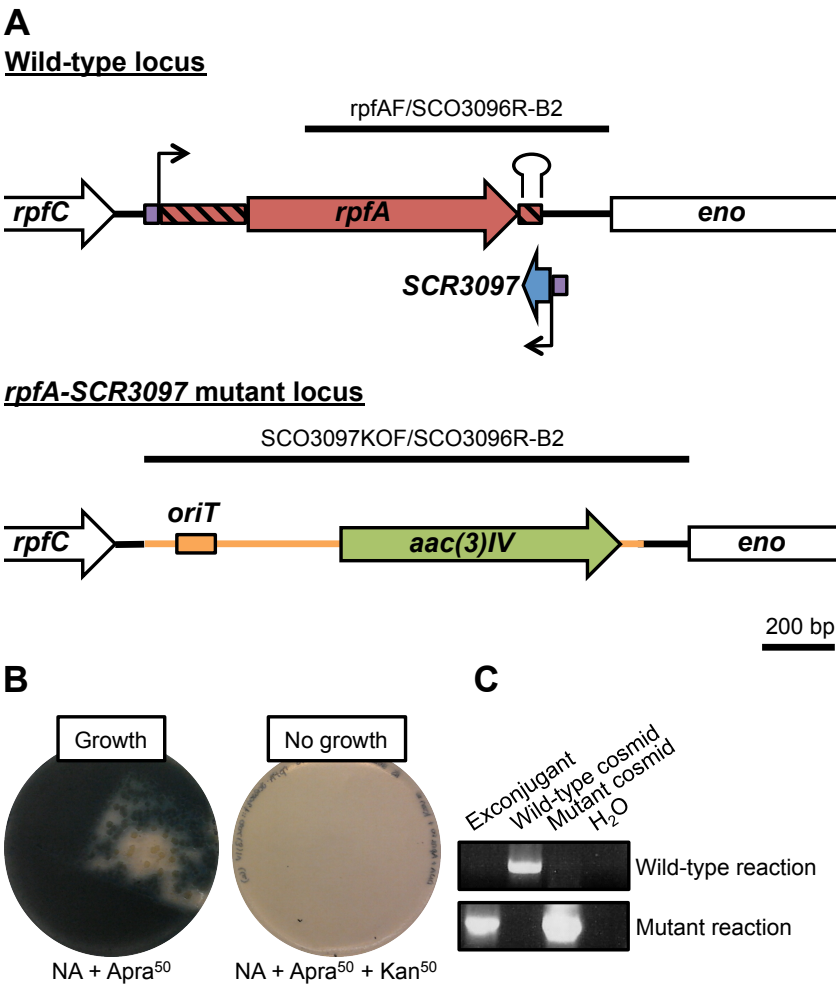

Fig. 4.10. Construction of the double mutant. (A) Schematic of the *rpfA-SCR3097* region in the wild-type and the double mutant. Notations are as indicated for Fig. 4.8A. (B) Antibiotic sensitivity phenotypes. The *S. coelicolor* double mutant (E120) was grown at 30°C on NA supplemented with 50 µg mL^{-1} apramycin ($Apra^{50}$) ± 50 µg mL^{-1} kanamycin (Kan^{50}). (C) The genotype of the double mutant was confirmed by PCR-amplifying both the wild-type and mutant loci from crude cell lysates. Wild-type (StE41) and mutant (StE41c) cosmids served as controls. An equal volume of water, instead of DNA template, was added to the 'no template' negative controls (H_2O).

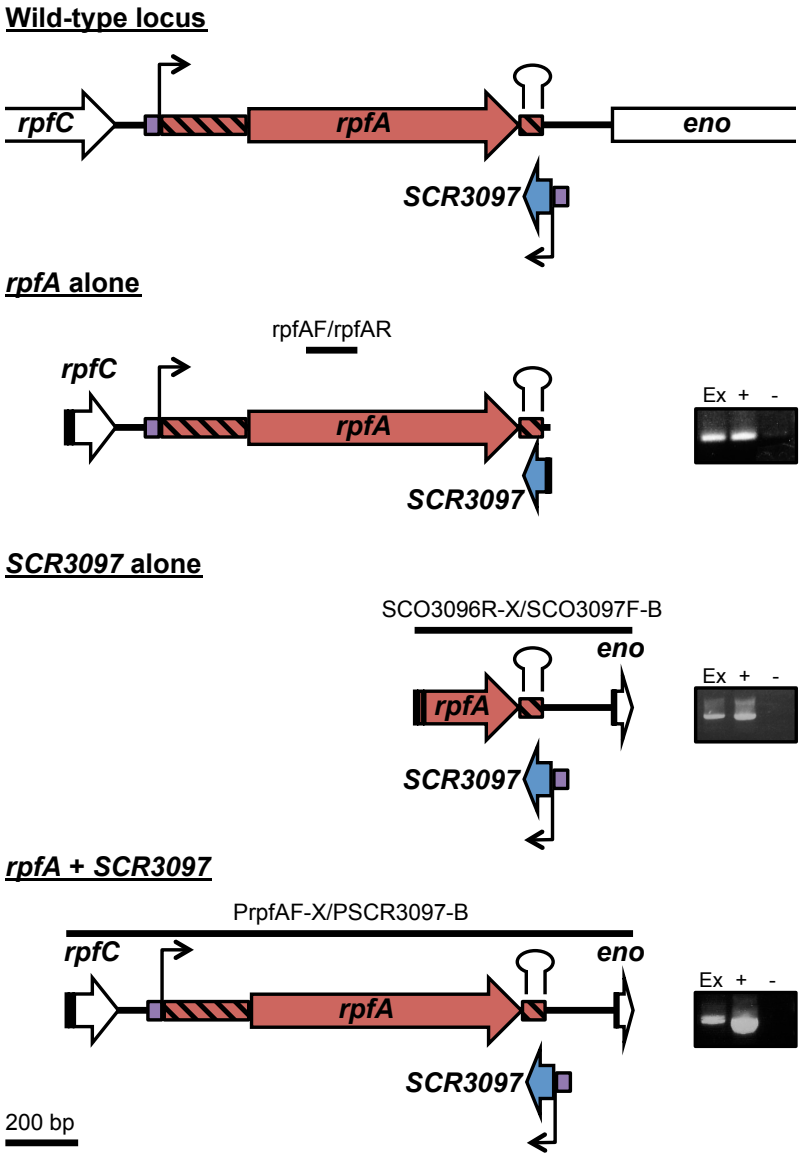

Fig. 4.11. Complementation of the double mutant. Schematic of the different complementation constructs. Notations are as indicated for Fig. 4.8A. The genotype of each complemented strain (Ex) was confirmed by PCR-amplifying the re-introduced gene from crude cell lysates. The complementation plasmid (+) and water (-) were used as positive and negative controls, respectively. *rpfA* alone, E120/pMC242; *SCR3097* alone, E120/pMC243; *rpfA* + *SCR3097*, E120/pMC244.

CHAPTER 5

GENERAL DISCUSSION

In the actinobacteria, establishing and exiting dormancy require the action of secreted muralytic enzymes belonging to the family of resuscitation-promoting factors (Rpfs) (see section 1.4). The expression and activity of these enzymes are heavily regulated owing to their potentially fatal impact. Though much of the work conducted to date on *rpf* gene regulation focused solely on transcriptional regulation by stress-responsive sigma factors (see section 1.5.1) and transcriptional regulators (see section 1.5.2), evidence collected by our group hinted at additional levels of control, notably by RNA-based regulators. In the model *Streptomyces coelicolor*, *rpfA* is flanked by non-coding regulatory RNA elements: a cyclic di-AMP-responsive riboswitch motif is embedded in the 5′ untranslated region (UTR) (Haiser *et al.*, 2009; Block *et al.*, 2010; Nelson *et al.*, 2013), and a small RNA (sRNA)-encoding gene is located immediately downstream of the *rpfA* stop codon (Moody *et al.*, 2013).

5.1 A NEW MODEL FOR *RPFA* GENE REGULATION

Using *S. coelicolor* as a model, we sought to expand our knowledge of *rpf* gene regulation, focusing in particular on non-coding RNA-mediated control. We discovered that *rpfA* is regulated at many different levels and receives regulatory inputs from different second messengers with known roles in dormancy and/or resuscitation. Based on our findings, and coupled with previous work conducted in other actinobacteria, we have elaborated a model for *rpfA* gene regulation (Fig. 5.1). During spore germination, when RpfA is required for resuscitation (Haiser *et al.*, 2009; Sexton *et al.*, 2015), the cyclic AMP (cAMP) receptor protein (Crp) directly activates *rpfA* transcription initiation (see section 2.4.2). Crp-dependent regulation of *rpfA* homologues was also noted in other actinobacteria (see section 1.5.2.2). Levels of the dormancy-promoting second messenger cyclic di-AMP are predicted to be low during this stage so as to enable efficient read-through of the cyclic di-AMP-responsive riboswitch motif embedded in the *rpfA* 5′ UTR. Alternative sigma factors likely also contribute to the regulation of *rpfA*

transcription initiation, as they do for many other *rpf* genes (see section 1.5.1), though their identity is not currently known. Future work should probe the identity of these protein regulators, which may provide valuable insight into the conditions that elicit *rpfA* expression.

Following germ tube emergence, *rpfA* promoter activity decreases (Sexton *et al.*, 2015), coinciding with decreasing cAMP levels (Süsstrunk *et al.*, 1998). During vegetative growth, cyclic di-AMP accumulates and inhibits *rpfA* transcription processivity upon binding the riboswitch motif, resulting in decreased transcript and protein abundance (see Chapters 2 and 3). Additional post-transcriptional regulation may also be provided by a small non-coding antisense RNA with the potential to base-pair with the *rpfA* 3′ UTR (see Chapter 4). Decreasing *rpfA* expression from germination to vegetative growth may reflect the dispensability of this enzyme for active growth, once resumed. Consistent with this hypothesis, deleting *rpfA* does not impact *S. coelicolor* mycelial growth (Haiser *et al.*, 2009; Sexton *et al.*, 2015).

During stationary phase, liquid-grown *S. coelicolor* expresses or activates a secreted metalloprotease to degrade extracellular RpfA proteins (see section 2.4.6). Proteolytic regulation of Rpf protein abundance has not been demonstrated previously; however, other works present evidence of Rpf protein turnover, suggesting this regulatory mechanism extends beyond the streptomycetes. Decreasing Rpf protein abundance was noted in *Micrococcus luteus* (Mukamolova *et al.*, 2002b; Telkov *et al.*, 2006) and *Mycobacterium smegmatis* (Shleeva *et al.*, 2004) cultures during the late exponential and stationary phases, and the supernatant of dormant *Rhodococcus rhodochrous* cultures accumulated a resuscitation inhibitor (Shleeva *et al.*, 2002), in line with the production of a secreted protease.

During differentiation on a solid medium, intracellular cyclic di-AMP levels decrease, thereby alleviating riboswitch-dependent inhibition and modestly increasing *rpfA* transcript abundance (see section 3.3.1) (Haiser *et al.*, 2009; Sexton *et al.*, 2015). Promoter activity is also predicted to increase at the onset of aerial growth as cAMP levels peak at this stage (Süsstrunk *et al.*, 1998). It is not clear if the metalloprotease is also secreted from plate-grown cultures during differentiation. It is, however, tempting to speculate that proteolytic regulation occurs at the onset of dormancy, and that *rpfA* transcript levels increase despite decreasing protein levels in the medium. We hypothesize that *Streptomyces* accumulates *rpfA* mRNA in spores in anticipation of subsequent germination, when RpfA proteins would need to be synthesized quickly.

5.2 RIBOSWITCH-INDEPENDENT *RPFA* REGULATION BY CYCLIC DI-AMP

The second messenger cyclic di-AMP controls cell wall homeostasis and promotes dormancy in many bacteria (Corrigan *et al.*, 2011; Oppenheimer-Shaanan *et al.*, 2011; Luo and Helmann, 2012; Mehne *et al.*, 2013), likely through its interaction with regulatory proteins (Corrigan and Gründling, 2013) and *ydaO*-like riboswitches (Nelson *et al.*, 2013), including the *rpfA* riboswitch in the actinobacteria (see Chapters 2 and 3). Indeed, cyclic di-AMP-responsive riboswitch motifs are associated with genes whose products are involved in dormancy. In *S. coelicolor*, a *ydaO*-like riboswitch motif is associated with seven cell wall remodeling genes, and at least four of these genes are involved in establishing dormancy (Haiser *et al.*, 2009; Sexton *et al.*, 2015).

ydaO-like riboswitches are also associated with potassium transport genes (Barrick *et al.*, 2004; Block *et al.*, 2010; Nelson *et al.*, 2013). In *Bacillus subtilis*, this riboswitch is thought to inhibit the expression of *ktrAB*, encoding a potassium transporter (Barrick *et al.*, 2004). In *Streptococcus pneumoniae*, cyclic di-AMP inhibits potassium uptake through its interaction with the Trk family potassium transport protein CabP, a KtrA-like protein (Bai *et al.*, 2014). Taken together, these observations suggest that cyclic di-AMP attenuates potassium uptake in diverse bacteria. Interestingly, potassium limitation triggers dormancy in the mycobacteria (Salina *et al.*, 2014), suggesting that cyclic di-AMP-dependent regulation of potassium transport may also help establish dormancy in certain organisms.

In addition to regulating *rpfA* transcript elongation through its interaction with a riboswitch, cyclic di-AMP also appears to promote transcript degradation (see section 3.3.3). These findings were somewhat unexpected for a dormancy-promoting second messenger, as bulk mRNA is generally stabilized during quiescence (Rittershaus *et al.*, 2013). Furthermore, guanosine 5′-diphosphate-3′-diphosphate (ppGpp), another second messenger involved in dormancy (Chakraburtty and Bibb, 1997; Hesketh *et al.*, 2007), increases bulk mRNA stability in the actinobacteria (Gatewood and Jones, 2010; Siculella *et al.*, 2010).

The means by which cyclic di-AMP promotes transcript degradation is unclear; however, given that degradation occurs *in vitro* solely in the presence of a crude protein extract, it is possible that the second messenger affects RNase activity through direct binding. Future work should be aimed at determining how cyclic di-AMP impacts bulk mRNA stability. This can be assessed by comparing bulk mRNA degradation rates in wild-type and cyclic di-AMP-depleted strains treated with an antibiotic inhibiting *de novo* RNA synthesis, such as actinomycin

D. Subsequent identification of effector proteins using a combination of cyclic di-AMP affinity pull-downs and liquid chromatography-coupled tandem mass spectrometry (Bai *et al.*, 2014) can provide additional insight into cyclic di-AMP-dependent regulatory mechanisms, beyond riboswitch activity modulation.

5.3 SCR3097 AND THE COORDINATION OF CELL WALL REMODELING, DORMANCY AND THE HYPOXIC RESPONSE

rpfA expression may also be regulated post-transcriptionally by an antisense RNA, Scr3097, which is predicted to base-pair with the *rpfA* 3′ UTR (see Chapter 4). Interestingly, our findings suggest that Scr3097 regulates microaerobic energy metabolism in the streptomycetes: the sRNA dampens the expression of the main respiratory nitrate reductase in mycelial cells during stationary phase (see section 4.3.4), and impacts the bacterium's ability to withstand high levels of ammonium (the product of complete nitrate reduction) and lactate (a by-product of fermentative pathways) (see section 4.3.3). We predict that the antisense RNA attenuates pathways involved in microaerobic metabolism under oxygen-replete conditions. Given its connection to *rpfA* and a ß-*N*-acetylglucosaminidase (via As2758) (see Chapter 4), Scr3097 may enable the streptomycetes to coordinate cell wall remodeling with hypoxic stress responses. In *Mycobacterium tuberculosis*, oxygen limitation triggers cell wall remodeling (Cunningham and Spreadbury, 1998) and significantly impacts the expression of four of the five *rpf* genes (Gupta *et al.*, 2010).

Given the connection between cell wall remodeling, dormancy and hypoxia, future work should focus on studying the impact of hypoxia on *Streptomyces* sporulation. This is an exciting area of research, given that *S. coelicolor* is classically thought of as an obligate microbe, and yet it undoubtedly encounters periods of hypoxic stress in its natural environment.

In moving forward with our characterization of Scr3097, we will be identifying the mRNA and protein targets of the antisense sRNA using *in vivo* pull-down assays coupled with RNA-seq and mass spectrometry, respectively. Once targets are identified, the next crucial step will involve determining how the sRNA affects their expression, and so we will monitor target gene expression in our Scr3097-positive and -negative strains using northern blotting and/or reverse transcription-coupled real-time PCR. To confirm that Scr3097-dependent regulation of mRNA targets is directly mediated through sRNA-mRNA base-pairing, we will introduce disruptive and compensatory mutations into the sRNA-

mRNA duplex and evaluate their impact on gene regulation. We also intend to probe the mode of action of the sRNA. In the case of *rpfA*, given the location of sRNA binding, we will begin by investigating Scr3097's impact on transcription termination and transcript stability using our *in vitro* assays (see Chapter 3). These assays will also prove useful to investigate sRNA-dependent regulation of other mRNA targets. Translational regulation will be assessed using primer extension inhibition (or 'toe-printing') assays.

5.4 REGULATION OF RPFA ACTIVITY

Once synthesized, Rpf enzymatic activity is regulated post-translationally by protein binding partners, as is the case with RpfB and the endopeptidase RipA in the mycobacteria (see section 1.5.5), and RpfB dimerization in *S. coelicolor* (Sexton *et al.*, 2015). We are currently exploring binding partner-mediated regulation of RpfA in *S. coelicolor*, beginning with identifying any potential binding partners using a yeast two-hybrid library screen.

5.5 IDENTIFYING THE SECRETED METALLOPROTEASE

While sigma factors and transcription regulators control transcription initiation, and riboswitches and sRNAs fine-tune gene expression post-transcriptionally, the actinobacteria must have a means of removing pre-existing Rpf proteins from their environment at the onset of dormancy. In this study, we found that the streptomycetes express or activate a secreted metalloprotease during stationary phase in response to the second messenger ppGpp (see section 2.4.6). In addition to promoting RpfA degradation, ppGpp is also thought to inhibit RpfA secretion by down-regulating the expression of the Sec protein secretion system (Hesketh *et al.*, 2007).

Expression of proteases in response to starvation and/or ppGpp is well documented in the actinobacteria. In *Streptomyces clavuligerus*, nutrient limitation stimulates the secretion of an unidentified metalloprotease (Bascarán *et al.*, 1990). Interestingly, starvation-dependent secreted metalloproteases are also implicated in dormancy. In *S. coelicolor*, the ppGpp-regulated (Hesketh *et al.*, 2007) metalloprotease SmpA, which is secreted into the growth medium during sporulation, is involved in differentiation (Kim *et al.*, 2013). Though the specific

protein targets of these enzymes are currently unknown, it is tempting to postulate that a subset impacts dormancy through its degradation of Rpf proteins.

The identity of our secreted RpfA-targeting metalloprotease is currently unknown, as is the breadth of its targets. Future work should be aimed at identifying the secreted metalloprotease by investigating the impact of deleting each annotated metalloprotease-encoding gene (of which there are eight; http://strepdb.streptomyces.org.uk/) on RpfA accumulation in culture media. In all likelihood, the metalloprotease targets other secreted proteins for degradation. Identifying these other target proteins may provide insight into proteins hindering the transition into dormancy or secreted proteins that are members of the same regulon as RpfA.

5.6 FIGURES

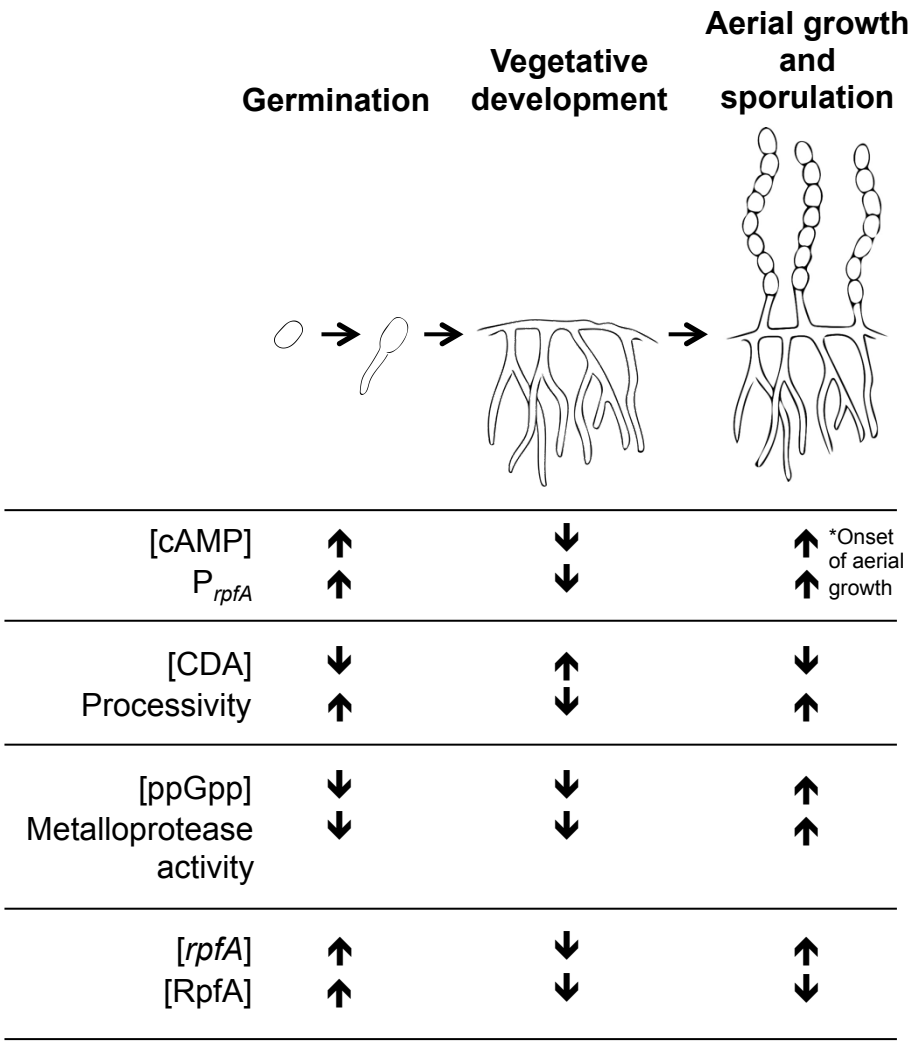

Fig. 5.1. Model of *Streptomyces* resuscitation and *rpfA* regulation. CDA, cyclic di-AMP.

REFERENCES

Abràmoff, M.D., Magalhães, P.J., and Ram, S.J. (2004) Image processing with ImageJ. *Biophotonics International* **11:** 36-42.

Akhter, Y., Tundup, S., and Hasnain, S.E. (2007) Novel biochemical properties of a CRP/FNR family transcription factor from *Mycobacterium tuberculosis*. *Int J Med Microbiol* **297:** 451-457.

Akif, M., Akhter, Y., Hasnain, S.E., and Mande, S.C. (2006) Crystallization and preliminary X-ray crystallographic studies of *Mycobacterium tuberculosis* CRP/FNR family transcription regulator. *Acta Crystallogr F Struct Biol Commun* **62:** 873-875.

Alting-Mees, M.A., and Short, J.M. (1989) pBluescript II: gene mapping vectors. *Nucleic Acids Res* **17:** 9494.

Altschul, S.F., Gish, W., Miller, W., Myers, E.W., and Lipman, D.J. (1990) Basic local alignment search tool. *J Mol Biol* **215:** 403-410.

Altuvia, S., Weinstein-Fischer, D., Zhang, A., Postow, L., and Storz, G. (1997) A small, stable RNA induced by oxidative stress: role as a pleiotropic regulator and antimutator. *Cell* **90:** 43-53.

Altuvia, S., Zhang, A., Argaman, L., Tiwari, A., and Storz, G. (1998) The *Escherichia coli* OxyS regulatory RNA represses *fhlA* translation by blocking ribosome binding. *EMBO J* **17:** 6069-6075.

Anuchin, A.M., Mulyukin, A.L., Suzina, N.E., Duda, V.I., El-Registan, G.I., and Kaprelyants, A.S. (2009) Dormant forms of *Mycobacterium smegmatis* with distinct morphology. *Microbiology* **155:** 1071-1079.

Aoki, Y., Matsumoto, D., Kawaide, H., and Natsume, M. (2011) Physiological role of germicidins in spore germination and hyphal elongation in *Streptomyces coelicolor* A3(2). *J Antibiot* **64:** 607-611.

Atrih, A., and Foster, S.J. (1999) The role of peptidoglycan structure and structural dynamics during endospore dormancy and germination. *Antonie van Leeuwenhoek* **75:** 299-307.

Aung, H.L., Berney, M., and Cook, G.M. (2014) Hypoxia-activated cytochrome *bd* expression in *Mycobacterium smegmatis* is cyclic AMP receptor protein dependent. *J Bacteriol* **196:** 3091-3097.

Bai, G., McCue, L.A., and McDonough, K.A. (2005) Characterization of *Mycobacterium tuberculosis* Rv3676 (CRP_{Mt}), a cyclic AMP receptor protein-like DNA binding protein. *J Bacteriol* **187:** 7795-7804.

Bai, Y., Yang, J., Zhou, X., Ding, X., Eisele, L.E., and Bai, G. (2012) *Mycobacterium tuberculosis* Rv3586 (DacA) is a diadenylate cyclase that converts ATP or ADP into c-di-AMP. *PLoS One* **7:** e35206.

Bai, Y., Yang, J., Zarrella, T.M., Zhang, Y., Metzger, D.W., and Bai, G. (2014) Cyclic di-AMP impairs potassium uptake mediated by a cyclic di-AMP binding protein in *Streptococcus pneumoniae*. *J Bacteriol* **196:** 614-623.

Baker, J.L., Sudarsan, N., Weinberg, Z., Roth, A., Stockbridge, R.B., and Breaker, R.R. (2012) Widespread genetic switches and toxicity resistance proteins for fluoride. *Science* **335:** 233-235.

Barrick, J.E., Corbino, K.A., Winkler, W.C., Nahvi, A., Mandal, M., Collins, J.*, et al.* (2004) New RNA motifs suggest an expanded scope for riboswitches in bacterial genetic control. *Proc Natl Acad Sci U S A* **101:** 6421-6426.

Bascarán, V., Hardisson, C., and Braña, A.F. (1990) Regulation of extracellular protease production in *Streptomyces clavuligerus*. *Appl Microbiol Biotechnol* **34:** 208-213.

Bateman, A., Holden, M.T.G., and Yeats, C. (2005) The G5 domain: a potential N-acetylglucosamine recognition domain involved in biofilm formation. *Bioinformatics* **21:** 1301-1303.

Bejerano-Sagie, M., Oppenheimer-Shaanan, Y., Berlatzky, I., Rouvinski, A., Meyerovich, M., and Ben-Yehuda, S. (2006) A checkpoint protein that scans the chromosome for damage at the start of sporulation in *Bacillus subtilis*. *Cell* **125:** 679-690.

Bentley, S.D., Chater, K.F., Cerdeño-Tárraga, A.-M., Challis, G.L., Thomson, N.R., James, K.D.*, et al.* (2002) Complete genome sequence of the model actinomycete *Streptomyces coelicolor* A3(2). *Nature* **417:** 141-147.

Bernhart, S.H., Hofacker, I.L., Will, S., Gruber, A.R., and Stadler, P.F. (2008) RNAalifold: improved consensus structure prediction for RNA alignments. *BMC Bioinformatics* **9:** 474.

Betts, J.C., Lukey, P.T., Robb, L.C., McAdam, R.A., and Duncan, K. (2002) Evaluation of a nutrient starvation model of *Mycobacterium tuberculosis* persistence by gene and protein expression profiling. *Mol Microbiol* **43:** 717-731.

Biketov, S., Potapov, V., Ganina, E., Downing, K., Kana, B.D., and Kaprelyants, A. (2007) The role of resuscitation promoting factors in pathogenesis and reactivation of *Mycobacterium tuberculosis* during intra-peritoneal infection in mice. *BMC Infect Dis* **7:** 146.

Biketov, S., Mukamolova, G.V., Potapov, V., Gilenkov, E., Vostroknutova, G., Kell, D.B.*, et al.* (2000) Culturability of *Mycobacterium tuberculosis* cells isolated from murine macrophages: a bacterial growth factor promotes recovery. *FEMS Immunol Med Microbiol* **29:** 233-240.

Bjerrum, O.J., and Schafer-Nielsen, C. (1986) Buffer systems and transfer parameters for semi-dry electroblotting with a horizontal apparatus. In *Electrophoresis '86: Proceedings of the Fifth Meeting of the International Electrophoresis Society.* Dunn, M.J. (ed). Weinheim, Germany: Wiley-VCH Verlag GmbH, pp. 315-327.

Block, K.F., Hammond, M.C., and Breaker, R.R. (2010) Evidence for widespread gene control function by the *ydaO* riboswitch candidate. *J Bacteriol* **192:** 3983-3989.

Bradley, S.G., and Ritzi, D. (1968) Composition and ultrastructure of *Streptomyces venezuelae*. *J Bacteriol* **95:** 2358-2364.

Brockmann-Gretza, O., and Kalinowski, J. (2006) Global gene expression during stringent response in *Corynebacterium glutamicum* in presence and absence of the *rel* gene encoding (p)ppGpp synthase. *BMC Genomics* **7:** 230.

Buist, G., Steen, A., Kok, J., and Kuipers, O.P. (2008) LysM, a widely distributed protein motif for binding to (peptido)glycans. *Mol Microbiol* **68:** 838-847.

Caron, M.-P., Bastet, L., Lussier, A., Simoneau-Roy, M., Massé, E., and Lafontaine, D.A. (2012) Dual-acting riboswitch control of translation initiation and mRNA decay. *Proc Natl Acad Sci U S A* **109:** E3444-E3453.

Chakraburtty, R., and Bibb, M. (1997) The ppGpp synthetase gene (*relA*) of *Streptomyces coelicolor* A3(2) plays a conditional role in antibiotic production and morphological differentiation. *J Bacteriol* **179:** 5854-5861.

Cohen-Gonsaud, M., Keep, N.H., Davies, A.P., Ward, J., Henderson, B., and Labesse, G. (2004a) Resuscitation-promoting factors possess a lysozyme-like domain. *Trends Biochem Sci* **29:** 7-10.

Cohen-Gonsaud, M., Barthe, P., Pommier, F., Harris, R., Driscoll, P.C., Keep, N.H., and Roumestand, C. (2004b) ^{1}H, ^{15}N, and ^{13}C chemical shift assignments of the resuscitation promoting factor domain of Rv1009 from *Mycobacterium tuberculosis*. *J Biomol NMR* **30:** 373-374.

Cohen-Gonsaud, M., Barthe, P., Bagnéris, C., Henderson, B., Ward, J., Roumestand, C., and Keep, N.H. (2005) The structure of a resuscitation-promoting factor domain from *Mycobacterium tuberculosis* shows homology to lysozymes. *Nat Struct Mol Biol* **12:** 270-273.

Cole, S.T., Brosch, R., Parkhill, J., Garnier, T., Churcher, C., Harris, D.*, et al.* (1998) Deciphering the biology of *Mycobacterium tuberculosis* from the complete genome sequence. *Nature* **393:** 537-544.

Collins, J.A., Irnov, I., Baker, S., and Winkler, W.C. (2007) Mechanism of mRNA destabilization by the *glmS* ribozyme. *Genes Dev* **21:** 3356-3368.

Corrigan, R.M., and Gründling, A. (2013) Cyclic di-AMP: another second messenger enters the fray. *Nat Rev Microbiol* **11:** 513-524.

Corrigan, R.M., Abbott, J.C., Burhenne, H., Kaever, V., and Gründling, A. (2011) c-di-AMP is a new second messenger in *Staphylococcus aureus* with a role in controlling cell size and envelope stress. *PLoS Pathog* **7:** e1002217.

Cramer, A., Gerstmeir, R., Schaffer, S., Bott, M., and Eikmanns, B.J. (2006) Identification of RamA, a novel LuxR-type transcriptional regulator of genes involved in acetate metabolism of *Corynebacterium glutamicum*. *J Bacteriol* **188:** 2554-2567.

Craney, A., Hohenauer, T., Xu, Y., Navani, N.K., Li, Y., and Nodwell, J. (2007) A synthetic *luxCDABE* gene cluster optimized for expression in high-GC bacteria. *Nucleic Acids Res* **35:** e46.

Cromie, M.J., Shi, Y., Latifi, T., and Groisman, E.A. (2006) An RNA sensor for intracellular Mg^{2+}. *Cell* **125:** 71-84.

Cunningham, A.F., and Spreadbury, C.L. (1998) Mycobacterial stationary phase induced by low oxygen tension: cell wall thickening and localization of the 16-kilodalton α-crystallin homolog. *J Bacteriol* **180:** 801-808.

Dahl, J.L., Kraus, C.N., Boshoff, H.I.M., Doan, B., Foley, K., Avarbock, D.*, et al.* (2003) The role of Rel_{Mtb}-mediated adaptation to stationary phase in long-term persistence of *Mycobacteriun tuberculosis* in mice. *Proc Natl Acad Sci U S A* **100:** 10026-10031.

Dainese, E., Rodrigue, S., Delogu, G., Provvedi, R., Laflamme, L., Brzezinski, R.*, et al.* (2006) Posttranslational regulation of *Mycobacterium tuberculosis* extracytoplasmic-function sigma factor σ^L and roles in virulence and in global regulation of gene expression. *Infect Immun* **74:** 2457-2461.

Dalebroux, Z.D., and Swanson, M.S. (2012) ppGpp: magic beyond RNA polymerase. *Nat Rev Microbiol* **10:** 203-212.

Dambach, M., Sandoval, M., Updegrove, T.B., Anantharaman, V., Aravind, L., Waters, L.S., and Storz, G. (2015) The ubiquitous *yybP-ykoY* riboswitch is a manganese-responsive regulatory element. *Mol Cell* **57:** 1099-1109.

Dann, C.E., Wakeman, C.A., Sieling, C.L., Baker, S.C., Irnov, I., and Winkler, W.C. (2007) Structure and mechanism of a metal-sensing regulatory RNA. *Cell* **130:** 878-892.

Darty, K., Denise, A., and Ponty, Y. (2009) VARNA: Interactive drawing and editing of the RNA secondary structure. *Bioinformatics* **25:** 1974-1975.

Datsenko, K.A., and Wanner, B.L. (2000) One-step inactivation of chromosomal genes in *Escherichia coli* K-12 using PCR products. *Proc Natl Acad Sci U S A* **97:** 6640-6645.

DebRoy, S., Gebbie, M., Ramesh, A., Goodson, J.R., Cruz, M.R., van Hoof, A.*, et al.* (2014) A riboswitch-containing sRNA controls gene expression by sequestration of a response regulator. *Science* **345:** 937-940.

DeMaio, J., Zhang, Y., Ko, C., Young, D.B., and Bishai, W.R. (1996) A stationary-phase stress-response sigma factor from *Mycobacterium tuberculosis*. *Proc Natl Acad Sci U S A* **93:** 2790-2794.

Derouaux, A., Halici, S., Nothaft, H., Neutelings, T., Moutzourelis, G., Dusart, J.*, et al.* (2004a) Deletion of a cyclic AMP receptor protein homologue diminishes germination and affects morphological development of *Streptomyces coelicolor*. *J Bacteriol* **186:** 1893-1897.

Derouaux, A., Dehareng, D., Lecocq, E., Halici, S., Nothaft, H., Giannotta, F.*, et al.* (2004b) Crp of *Streptomyces coelicolor* is the third transcription factor of the

large CRP-FNR superfamily able to bind cAMP. *Biochem Biophys Res Commun* **325:** 983-990.

Downing, K.J., Betts, J.C., Young, D.I., McAdam, R.A., Kelly, F., Young, M., and Mizrahi, V. (2004) Global expression profiling of strains harbouring null mutations reveals that the five *rpf*-like genes of *Mycobacterium tuberculosis* show functional redundancy. *Tuberculosis (Edinb)* **84:** 167-179.

Downing, K.J., Mischenko, V.V., Shleeva, M.O., Young, D.I., Young, M., Kaprelyants, A.S.*, et al.* (2005) Mutants of *Mycobacterium tuberculosis* lacking three of the five *rpf*-like genes are defective for growth *in vivo* and for resuscitation *in vitro*. *Infect Immun* **73:** 3038-3043.

Dühring, U., Axmann, I.M., Hess, W.R., and Wilde, A. (2006) An internal antisense RNA regulates expression of the photosynthesis gene *isiA*. *Proc Natl Acad Sci U S A* **103:** 7054-7058.

Duong, A., Capstick, D.S., Di Berardo, C., Findlay, K.C., Hesketh, A., Hong, H.-J., and Elliot, M.A. (2012) Aerial development in *Streptomyces coelicolor* requires sortase activity. *Mol Microbiol* **83:** 992-1005.

Dworkin, J., and Shah, I.M. (2010) Exit from dormancy in microbial organisms. *Nat Rev Microbiol* **8:** 890-896.

Eaton, D., and Ensign, J.C. (1980) *Streptomyces viridochromogenes* spore germination initiated by calcium ions. *J Bacteriol* **143:** 377-382.

Ehrlich, J., Gottlieb, D., Burkholder, P.R., Anderson, L.E., and Pridham, T.G. (1948) *Streptomyces venezuelae*, n. sp., the source of chloromycetin. *J Bacteriol* **56:** 467-477.

Elliot, M.A., and Flärdh, K. (2012) Streptomycete spores. In *Encyclopedia of Life Sciences (eLS).* Chichester, England: John Wiley & Sons, Ltd.

Epshtein, V., Mironov, A.S., and Nudler, E. (2003) The riboswitch-mediated control of sulfur metabolism in bacteria. *Proc Natl Acad Sci U S A* **100:** 5052-5056.

Feklístov, A., Sharon, B.D., Darst, S.A., and Gross, C.A. (2014) Bacterial sigma factors: a historical, structural, and genomic perspective. *Annu Rev Microbiol* **68:** 357-376.

Fernandes, N.D., Wu, Q.-L., Kong, D., Puyang, X., Garg, S., and Husson, R.N. (1999) A mycobacterial extracytoplasmic sigma factor involved in survival following heat shock and oxidative stress. *J Bacteriol* **181:** 4266-4274.

Fischer, M., Falke, D., Pawlik, T., and Sawers, R.G. (2014) Oxygen-dependent control of respiratory nitrate reduction in mycelium of *Streptomyces coelicolor* A3(2). *J Bacteriol* **196:** 4152-4162.

Fischer, M., Alderson, J., van Keulen, G., White, J., and Sawers, R.G. (2010) The obligate aerobe *Streptomyces coelicolor* A3(2) synthesizes three active respiratory nitrate reductases. *Microbiology* **156:** 3166-3179.

Flärdh, K., and Buttner, M.J. (2009) *Streptomyces* morphogenetics: dissecting differentiation in a filamentous bacterium. *Nat Rev Microbiol* **7:** 36-49.

Fontán, P.A., Voskuil, M.I., Gomez, M., Tan, D., Pardini, M., Manganelli, R.*, et al.* (2009) The *Mycobacterium tuberculosis* sigma factor σ^B is required for full response to cell envelope stress and hypoxia in vitro, but it is dispensable for in vivo growth. *J Bacteriol* **191:** 5628-5633.

Furukawa, K., Ramesh, A., Zhou, Z., Weinberg, Z., Vallery, T., Winkler, W.C., and Breaker, R.R. (2015) Bacterial riboswitches cooperatively bind Ni^{2+} or Co^{2+} ions and control expression of heavy metal transporters. *Mol Cell* **57:** 1088-1098.

Gallagher, D.T., Smith, N., Kim, S.-K., Robinson, H., and Reddy, P.T. (2009) Profound asymmetry in the structure of the cAMP-free cAMP receptor protein (CRP) from *Mycobacterium tuberculosis*. *J Biol Chem* **284:** 8228-8232.

Gao, A., and Serganov, A. (2014) Structural insights into recognition of c-di-AMP by the *ydaO* riboswitch. *Nat Chem Biol* **10:** 787-792.

Gao, C., Hindra, Mulder, D., Yin, C., and Elliot, M.A. (2012) Crp is a global regulator of antibiotic production in *Streptomyces*. *mBio* **3:** e00407-00412.

Gatewood, M.L., and Jones, G.H. (2010) (p)ppGpp inhibits polynucleotide phosphorylase from *Streptomyces* but not from *Escherichia coli* and increases the stability of bulk mRNA in *Streptomyces coelicolor*. *J Bacteriol* **192:** 4275-4280.

Geiman, D.E., Kaushal, D., Ko, C., Tyagi, S., Manabe, Y.C., Schroeder, B.G.*, et al.* (2004) Attenuation of late-stage disease in mice infected by the *Mycobacterium tuberculosis* mutant lacking the SigF alternate sigma factor and identification of SigF-dependent genes by microarray analysis. *Infect Immun* **72:** 1733-1745.

Gersch, D., Römer, W., and Krügel, H. (1979) Inverse regulation of spore germination and growth by cyclic AMP in *Streptomyces hygroscopicus*. *Experientia* **35:** 749.

Gerstmeir, R., Cramer, A., Dangel, P., Schaffer, S., and Eikmanns, B.J. (2004) RamB, a novel transcriptional regulator of genes involved in acetate metabolism of *Corynebacterium glutamicum*. *J Bacteriol* **186:** 2798-2809.

Glauert, A.M., and Hopwood, D.A. (1961) The fine structure of *Streptomyces violaceoruber* (*S. coelicolor*). III. The walls of the mycelium and spores. *J Biophys Biochem Cytol* **10:** 505-516.

Gottesman, S. (2004) The small RNA regulators of *Escherichia coli*: roles and mechanisms. *Annu Rev Microbiol* **58:** 303-328.

Green, J., Stapleton, M.R., Smith, L.J., Artymiuk, P.J., Kahramanoglou, C., Hunt, D.M., and Buxton, R.S. (2014) Cyclic-AMP and bacterial cyclic-AMP receptor proteins revisited: adaptation for different ecological niches. *Curr Opin Microbiol* **18:** 1-7.

Gregory, M.A., Till, R., and Smith, M.C.M. (2003) Integration site for *Streptomyces* phage ϕBT1 and development of site-specific integrating vectors. *J Bacteriol* **185:** 5320-5323.

Grund, A.D., and Ensign, J.C. (1978) Role of carbon dioxide in germination of spores of *Streptomyces viridochromogenes*. *Arch Microbiol* **118:** 279-288.

Grund, A.D., and Ensign, J.C. (1982) Activation of *Streptomyces viridochromogenes* spores by detergents. *Curr Microbiol* **7:** 223-227.

Grund, A.D., and Ensign, J.C. (1985) Properties of the germination inhibitor of *Streptomyces viridochromogenes* spores. *J Gen Microbiol* **131:** 833-847.

Grundy, F.J., Lehman, S.C., and Henkin, T.M. (2003) The L box regulon: lysine sensing by leader RNAs of bacterial lysine biosynthesis genes. *Proc Natl Acad Sci U S A* **100:** 12057-12062.

Gupta, R.K., Srivastava, B.S., and Srivastava, R. (2010) Comparative expression analysis of *rpf*-like genes of *Mycobacterium tuberculosis* H37Rv under different physiological stress and growth conditions. *Microbiology* **156:** 2714-2722.

Gust, B., Challis, G.L., Fowler, K., Kieser, T., and Chater, K.F. (2003) PCR-targeted *Streptomyces* gene replacement identifies a protein domain needed for

biosynthesis of the sesquiterpene soil odor geosmin. *Proc Natl Acad Sci U S A* **100:** 1541-1546.

Haiser, H.J., Yousef, M.R., and Elliot, M.A. (2009) Cell wall hydrolases affect germination, vegetative growth, and sporulation in *Streptomyces coelicolor*. *J Bacteriol* **191:** 6501-6512.

Hardisson, C., Manzanal, M.-B., Salas, J.-A., and Suárez, J.-E. (1978) Fine structure, physiology and biochemistry of arthrospore germination in *Streptomyces antibioticus*. *J Gen Microbiol* **105:** 203-214.

Hartmann, M., Barsch, A., Niehaus, K., Pühler, A., Tauch, A., and Kalinowski, J. (2004) The glycosylated cell surface protein Rpf2, containing a resuscitation-promoting factor motif, is involved in intercellular communication of *Corynebacterium glutamicum*. *Arch Microbiol* **182:** 299-312.

Hata, M., Ogura, M., and Tanaka, T. (2001) Involvement of stringent factor RelA in expression of the alkaline protease gene *aprE* in *Bacillus subtilis*. *J Bacteriol* **183:** 4648-4651.

Hesketh, A., Chen, W.J., Ryding, J., Chang, S., and Bibb, M. (2007) The global role of ppGpp synthesis in morphological differentiation and antibiotic production in *Streptomyces coelicolor* A3(2). *Genome Biol* **8:** R161.

Hesketh, A., Hill, C., Mokhtar, J., Novotna, G., Tran, N., Bibb, M., and Hong, H.-J. (2011) Genome-wide dynamics of a bacterial response to antibiotics that target the cell envelope. *BMC Genomics* **12:** 226.

Hett, E.C., Chao, M.C., and Rubin, E.J. (2010) Interaction and modulation of two antagonistic cell wall enzymes of mycobacteria. *PLoS Pathog* **6:** e1001020.

Hett, E.C., Chao, M.C., Deng, L.L., and Rubin, E.J. (2008) A mycobacterial enzyme essential for cell division synergizes with resuscitation-promoting factor. *PLoS Pathog* **4:** e1000001.

Hett, E.C., Chao, M.C., Steyn, A.J., Fortune, S.M., Deng, L.L., and Rubin, E.J. (2007) A partner for the resuscitation-promoting factors of *Mycobacterium tuberculosis*. *Mol Microbiol* **66:** 658-668.

Hey-Ferguson, A., Mitchell, M., and Elbein, A.D. (1973) Trehalose metabolism in germinating spores of *Streptomyces hygroscopicus*. *J Bacteriol* **116:** 1084-1085.

Hindra, Moody, M.J., Jones, S.E., and Elliot, M.A. (2014) Complex intra-operonic dynamics mediated by a small RNA in *Streptomyces coelicolor*. *PLoS One* **9:** e85856.

Hirsch, C.F., and Ensign, J.C. (1976a) Nutritionally defined conditions for germination of *Streptomyces viridochromogenes* spores. *J Bacteriol* **126:** 13-23.

Hirsch, C.F., and Ensign, J.C. (1976b) Heat activation of *Streptomyces viridochromogenes* spores. *J Bacteriol* **126:** 24-30.

Hirsch, C.F., and Ensign, J.C. (1978) Some properties of *Streptomyces viridochromogenes* spores. *J Bacteriol* **134:** 1056-1063.

Hollands, K., Proshkin, S., Sklyarova, S., Epshtein, V., Mironov, A., Nudler, E., and Groisman, E.A. (2012) Riboswitch control of Rho-dependent transcription termination. *Proc Natl Acad Sci U S A* **109:** 5376-5381.

Hong, H.-J., Hutchings, M.I., Hill, L.M., and Buttner, M.J. (2005) The role of the novel Fem protein VanK in vancomycin resistance in *Streptomyces coelicolor*. *J Biol Chem* **280:** 13055-13061.

Hopwood, D.A., and Wright, H.M. (1978) Bacterial protoplast fusion: Recombination in fused protoplasts of *Streptomyces coelicolor*. *Mol Gen Genet* **162:** 307-317.

Horton, R.M. (1995) PCR-mediated recombination and mutagenesis. *Mol Biotechnol* **3:** 93-99.

Hoskisson, P.A., and Hutchings, M.I. (2006) MtrAB–LpqB: a conserved three-component system in actinobacteria? *Trends Microbiol* **14:** 444-449.

Huang, J., Lih, C.-J., Pan, K.-H., and Cohen, S.N. (2001) Global analysis of growth phase responsive gene expression and regulation of antibiotic biosynthetic pathways in *Streptomyces coelicolor* using DNA microarrays. *Genes Dev* **15:** 3183-3192.

Huang, J., Shi, J., Molle, V., Sohlberg, B., Weaver, D., Bibb, M.J*., et al.* (2005) Cross-regulation among disparate antibiotic biosynthetic pathways of *Streptomyces coelicolor*. *Mol Microbiol* **58:** 1276-1287.

Jones, C.P., and Ferré-D'Amaré, A.R. (2014) Crystal structure of a c-di-AMP riboswitch reveals an internally pseudo-dimeric RNA. *EMBO J* **33:** 2692-2703.

Jungwirth, B., Emer, D., Brune, I., Hansmeier, N., Pühler, A., Eikmanns, B.J., and Tauch, A. (2008) Triple transcriptional control of the resuscitation promoting factor 2 (*rpf2*) gene of *Corynebacterium glutamicum* by the regulators of acetate metabolism RamA and RamB and the cAMP-dependent regulator GlxR. *FEMS Microbiol Lett* **281:** 190-197.

Jungwirth, B., Sala, C., Kohl, T.A., Uplekar, S., Baumbach, J., Cole, S.T.*, et al.* (2013) High-resolution detection of DNA binding sites of the global transcriptional regulator GlxR in *Corynebacterium glutamicum*. *Microbiology* **159:** 12-22.

Kahramanoglou, C., Cortes, T., Matange, N., Hunt, D.M., Visweswariah, S.S., Young, D.B., and Buxton, R.S. (2014) Genomic mapping of cAMP receptor protein (CRP^{Mt}) in *Mycobacterium tuberculosis*: relation to transcriptional start sites and the role of CRP^{Mt} as a transcription factor. *Nucleic Acids Res* **42:** 8320-8329.

Kana, B.D., and Mizrahi, V. (2010) Resuscitation-promoting factors as lytic enzymes for bacterial growth and signaling. *FEMS Immunol Med Microbiol* **58:** 39-50.

Kana, B.D., Gordhan, B.G., Downing, K.J., Sung, N., Vostroktunova, G., Machowski, E.E.*, et al.* (2008) The resuscitation-promoting factors of *Mycobacterium tuberculosis* are required for virulence and resuscitation from dormancy but are collectively dispensable for growth *in vitro*. *Mol Microbiol* **67:** 672-684.

Kaprelyants, A.S., and Kell, D.B. (1993) Dormancy in stationary-phase cultures of *Micrococcus luteus*: flow cytometric analysis of starvation and resuscitation. *Appl Environ Microbiol* **59:** 3187-3196.

Kaprelyants, A.S., Gottschal, J.C., and Kell, D.B. (1993) Dormancy in non-sporulating bacteria. *FEMS Microbiol Rev* **104:** 271-286.

Kaushal, D., Schroeder, B.G., Tyagi, S., Yoshimatsu, T., Scott, C., Ko, C.*, et al.* (2002) Reduced immunopathology and mortality despite tissue persistence in a *Mycobacterium tuberculosis* mutant lacking alternative σ factor, SigH. *Proc Natl Acad Sci U S A* **99:** 8330-8335.

Keep, N.H., Ward, J.M., Cohen-Gonsaud, M., and Henderson, B. (2006) Wake up! Peptidoglycan lysis and bacterial non-growth states. *Trends Microbiol* **14:** 271-276.

Keijser, B.J.F., Ter Beek, A., Rauwerda, H., Schuren, F., Montijn, R., van der Spek, H., and Brul, S. (2007) Analysis of temporal gene expression during *Bacillus subtilis* spore germination and outgrowth. *J Bacteriol* **189:** 3624-3634.

Kell, D.B., and Young, M. (2000) Bacterial dormancy and culturability: the role of autocrine growth factors. *Curr Opin Microbiol* **3:** 238-243.

Kieser, T., Bibb, M.J., Buttner, M.J., Chater, K.F., and Hopwood, D.A. (2000) *Practical Streptomyces genetics*. Norwich, England: The John Innes Foundation.

Kim, H.-J., Kim, T.-H., Kim, Y., and Lee, H.-S. (2004) Identification and characterization of *glxR*, a gene involved in regulation of glyoxylate bypass in *Corynebacterium glutamicum*. *J Bacteriol* **186:** 3453-3460.

Kim, H.-S., Lee, E.-J., Cho, Y.-H., and Roe, J.-H. (2013) Post-translational regulation of a developmental catalase, CatB, involves a metalloprotease, SmpA and contributes to proper differentiation and osmoprotection of *Streptomyces coelicolor*. *Res Microbiol* **164:** 327-334.

King, R.A., Banik-Maiti, S., Jin, D.J., and Weisberg, R.A. (1996) Transcripts that increase the processivity and elongation rate of RNA polymerase. *Cell* **87:** 893-903.

Kohl, T.A., Baumbach, J., Jungwirth, B., Pühler, A., and Tauch, A. (2008) The GlxR regulon of the amino acid producer *Corynebacterium glutamicum*: *in silico* and *in vitro* detection of DNA binding sites of a global transcription regulator. *J Biotechnol* **135:** 340-350.

Krawczyk, J., Kohl, T.A., Goesmann, A., Kalinowski, J., and Baumbach, J. (2009) From *Corynebacterium glutamicum* to *Mycobacterium tuberculosis*—towards transfers of gene regulatory networks and integrated data analyses with MycoRegNet. *Nucleic Acids Res* **37:** e97.

Kumar, P., Joshi, D.C., Akif, M., Akhter, Y., Hasnain, S.E., and Mande, S.C. (2010) Mapping conformational transitions in cyclic AMP receptor protein: crystal structure and normal-mode analysis of *Mycobacterium tuberculosis* apo-cAMP receptor protein. *Biophys J* **98:** 305-314.

Laemmli, U.K. (1970) Cleavage of structural proteins during the assembly of the head of bacteriophage T4. *Nature* **227:** 680-685.

Langmead, B., Trapnell, C., Pop, M., and Salzberg, S.L. (2009) Ultrafast and memory-efficient alignment of short DNA sequences to the human genome. *Genome Biol* **10:** R25.

Lavollay, M., Arthur, M., Fourgeaud, M., Dubost, L., Marie, A., Veziris, N.*, et al.* (2008) The peptidoglycan of stationary-phase *Mycobacterium tuberculosis* predominantly contains cross-links generated by L,D-transpeptidation. *J Bacteriol* **190:** 4360-4366.

Lee, E.R., Baker, J.L., Weinberg, Z., Sudarsan, N., and Breaker, R.R. (2010) An allosteric self-splicing ribozyme triggered by a bacterial second messenger. *Science* **329:** 845-848.

Lee, N., D'Souza, C.A., and Kronstad, J.W. (2003) Of smuts, blasts, mildews, and blights: cAMP signaling in phytopathogenic fungi. *Annu Rev Phytopathol* **41:** 399-427.

Legewie, S., Dienst, D., Wilde, A., Herzel, H., and Axmann, I.M. (2008) Small RNAs establish delays and temporal thresholds in gene expression. *Biophys J* **95:** 3232-3238.

Letek, M., Valbuena, N., Ramos, A., Ordóñez, E., Gil, J.A., and Mateos, L.M. (2006) Characterization and use of catabolite-repressed promoters from gluconate genes in *Corynebacterium glutamicum*. *J Bacteriol* **188:** 409-423.

Li, H., Handsaker, B., Wysoker, A., Fennell, T., Ruan, J., Homer, N.*, et al.* (2009) The Sequence Alignment/Map format and SAMtools. *Bioinformatics* **25:** 2078-2079.

Loh, E., Dussurget, O., Gripenland, J., Vaitkevicius, K., Tiensuu, T., Mandin, P.*, et al.* (2009) A *trans*-acting riboswitch controls expression of the virulence regulator PrfA in *Listeria monocytogenes*. *Cell* **139:** 770-779.

Loria, R., Kers, J., and Joshi, M. (2006) Evolution of plant pathogenicity in *Streptomyces*. *Annu Rev Phytopathol* **44:** 469-487.

Luo, Y., and Helmann, J.D. (2012) Analysis of the role of *Bacillus subtilis* σ^M in β-lactam resistance reveals an essential role for c-di-AMP in peptidoglycan homeostasis. *Mol Microbiol* **83:** 623-639.

MacNeil, D.J., Gewain, K.M., Ruby, C.L., Dezeny, G., Gibbons, P.H., and MacNeil, T. (1992) Analysis of *Streptomyces avermitilis* genes required for avermectin biosynthesis utilizing a novel integration vector. *Gene* **111:** 61-68.

Mahne, M., Tauch, A., Pühler, A., and Kalinowski, J. (2006) The *Corynebacterium glutamicum* gene *pmt* encoding a glycosyltransferase related to eukaryotic protein-O-mannosyltransferases is essential for glycosylation of the

resuscitation promoting factor (Rpf2) and other secreted proteins. *FEMS Microbiol Lett* **259:** 226-233.

Maione, V., Ruggiero, A., Russo, L., De Simone, A., Pedone, P.V., Malgieri, G.*, et al.* (2015) NMR structure and dynamics of the resuscitation promoting factor RpfC catalytic domain. *PLoS One* **10:** e0142807.

Majdalani, N., Cunning, C., Sledjeski, D., Elliott, T., and Gottesman, S. (1998) DsrA RNA regulates translation of RpoS message by an anti-antisense mechanism, independent of its action as an antisilencer of transcription. *Proc Natl Acad Sci U S A* **95:** 12462-12467.

Mandal, M., and Breaker, R.R. (2004) Adenine riboswitches and gene activation by disruption of a transcription terminator. *Nat Struct Mol Biol* **11:** 29-35.

Mandal, M., Boese, B., Barrick, J.E., Winkler, W.C., and Breaker, R.R. (2003) Riboswitches control fundamental biochemical pathways in *Bacillus subtilis* and other bacteria. *Cell* **113:** 577-586.

Mandal, M., Lee, M., Barrick, J.E., Weinberg, Z., Emilsson, G.M., Ruzzo, W.L., and Breaker, R.R. (2004) A glycine-dependent riboswitch that uses cooperative binding to control gene expression. *Science* **306:** 275-279.

Manganelli, R., Voskuil, M.I., Schoolnik, G.K., and Smith, I. (2001) The *Mycobacterium tuberculosis* ECF sigma factor σ^E: role in global gene expression and survival in macrophages. *Mol Microbiol* **41:** 423-437.

Manganelli, R., Dubnau, E., Tyagi, S., Kramer, F.R., and Smith, I. (1999) Differential expression of 10 sigma factor genes in *Mycobacterium tuberculosis*. *Mol Microbiol* **31:** 715-724.

Manganelli, R., Voskuil, M.I., Schoolnik, G.K., Dubnau, E., Gomez, M., and Smith, I. (2002) Role of the extracytoplasmic-function σ factor σ^H in *Mycobacterium tuberculosis* global gene expression. *Mol Microbiol* **45:** 365-374.

Marinelli, F. (2009) Antibiotics and *Streptomyces*: the future of antibiotic discovery. *Microbiology Today* **36:** 20-23.

Martín, M.C., Díaz, L.A., Manzanal, M.B., and Hardisson, C. (1986) Role of trehalose in the spores of *Streptomyces*. *FEMS Microbiol Lett* **35:** 49-54.

Mavrici, D., Prigozhin, D.M., and Alber, T. (2014) *Mycobacterium tuberculosis* RpfE crystal structure reveals a positively charged catalytic cleft. *Protein Sci* **23:** 481-487.

McBride, M.J., and Ensign, J.C. (1987a) Metabolism of endogenous trehalose by *Streptomyces griseus* spores and by spores or cells of other actinomycetes. *J Bacteriol* **169:** 5002-5007.

McBride, M.J., and Ensign, J.C. (1987b) Effects of intracellular trehalose content on *Streptomyces griseus* spores. *J Bacteriol* **169:** 4995-5001.

McBride, M.J., and Ensign, J.C. (1990) Regulation of trehalose metabolism by *Streptomyces griseus* spores. *J Bacteriol* **172:** 3637-3643.

McClure, R., Balasubramanian, D., Sun, Y., Bobrovskyy, M., Sumby, P., Genco, C.A.*, et al.* (2013) Computational analysis of bacterial RNA-Seq data. *Nucleic Acids Res* **41:** e140.

McDaniel, B.A.M., Grundy, F.J., Artsimovitch, I., and Henkin, T.M. (2003) Transcription termination control of the S box system: Direct measurement of *S*-adenosylmethionine by the leader RNA. *Proc Natl Acad Sci U S A* **100:** 3083-3088.

Mehne, F.M.P., Gunka, K., Eilers, H., Herzberg, C., Kaever, V., and Stülke, J. (2013) Cyclic di-AMP homeostasis in *Bacillus subtilis*: both lack and high level accumulation of the nucleotide are detrimental for cell growth. *J Biol Chem* **288:** 2004-2017.

Michele, T.M., Ko, C., and Bishai, W.R. (1999) Exposure to antibiotics induces expression of the *Mycobacterium tuberculosis sigF* gene: implications for chemotherapy against mycobacterial persistors. *Antimicrob Agents Chemother* **43:** 218-225.

Mir, M., Asong, J., Li, X., Cardot, J., Boons, G.-J., and Husson, R.N. (2011) The extracytoplasmic domain of the *Mycobacterium tuberculosis* Ser/Thr kinase PknB binds specific muropeptides and is required for PknB localization. *PLoS Pathog* **7:** e1002182.

Mironov, A.S., Gusarov, I., Rafikov, R., Lopez, L.E., Shatalin, K., Kreneva, R.A.*, et al.* (2002) Sensing small molecules by nascent RNA: a mechanism to control transcription in bacteria. *Cell* **111:** 747-756.

Mitra, A., Kesarwani, A.K., Pal, D., and Nagaraja, V. (2010) WebGeSTer DB—a transcription terminator database. *Nucleic Acids Res* **39:** D129-D135.

Moody, M.J., Young, R.A., Jones, S.E., and Elliot, M.A. (2013) Comparative analysis of non-coding RNAs in the antibiotic-producing *Streptomyces* bacteria. *BMC Genomics* **14:** 558.

Mukamolova, G.V., Yanopolskaya, N.D., Kell, D.B., and Kaprelyants, A.S. (1998a) On resuscitation from the dormant state of *Micrococcus luteus*. *Antonie van Leeuwenhoek* **73:** 237-243.

Mukamolova, G.V., Kormer, S.S., Kell, D.B., and Kaprelyants, A.S. (1999) Stimulation of the multiplication of *Micrococcus luteus* by an autocrine growth factor. *Arch Microbiol* **172:** 9-14.

Mukamolova, G.V., Kaprelyants, A.S., Young, D.I., Young, M., and Kell, D.B. (1998b) A bacterial cytokine. *Proc Natl Acad Sci U S A* **95:** 8916-8921.

Mukamolova, G.V., Yanopolskaya, N.D., Votyakova, T.V., Popov, V.I., Kaprelyants, A.S., and Kell, D.B. (1995) Biochemical changes accompanying the long-term starvation of *Micrococcus luteus* cells in spent growth medium. *Arch Microbiol* **163:** 373-379.

Mukamolova, G.V., Turapov, O.A., Young, D.I., Kaprelyants, A.S., Kell, D.B., and Young, M. (2002a) A family of autocrine growth factors in *Mycobacterium tuberculosis*. *Mol Microbiol* **46:** 623-635.

Mukamolova, G.V., Turapov, O.A., Kazarian, K., Telkov, M., Kaprelyants, A.S., Kell, D.B., and Young, M. (2002b) The *rpf* gene of *Micrococcus luteus* encodes an essential secreted growth factor. *Mol Microbiol* **46:** 611-621.

Mukamolova, G.V., Murzin, A.G., Salina, E.G., Demina, G.R., Kell, D.B., Kaprelyants, A.S., and Young, M. (2006) Muralytic activity of *Micrococcus luteus* Rpf and its relationship to physiological activity in promoting bacterial growth and resuscitation. *Mol Microbiol* **59:** 84-98.

Muttucumaru, D.G.N., Roberts, G., Hinds, J., Stabler, R.A., and Parish, T. (2004) Gene expression profile of *Mycobacterium tuberculosis* in a non-replicating state. *Tuberculosis (Edinb)* **84:** 239-246.

Nahvi, A., Sudarsan, N., Ebert, M.S., Zou, X., Brown, K.L., and Breaker, R.R. (2002) Genetic control by a metabolite binding mRNA. *Chem Biol* **9:** 1043-1049.

Nandakumar, M.P., Shen, J., Raman, B., and Marten, M.R. (2003) Solubilization of trichloroacetic acid (TCA) precipitated microbial proteins via NaOH for two-dimensional electrophoresis. *J Proteome Res* **2:** 89-93.

Nelson, J.W., Sudarsan, N., Furukawa, K., Weinberg, Z., Wang, J.X., and Breaker, R.R. (2013) Riboswitches in eubacteria sense the second messenger c-di-AMP. *Nat Chem Biol* **9:** 834-839.

Nikitushkin, V.D., Demina, G.R., Shleeva, M.O., and Kaprelyants, A.S. (2013) Peptidoglycan fragments stimulate resuscitation of "non-culturable" mycobacteria. *Antonie van Leeuwenhoek* **103:** 37-46.

Nikitushkin, V.D., Demina, G.R., Shleeva, M.O., Guryanova, S.V., Ruggiero, A., Berisio, R., and Kaprelyants, A.S. (2015) A product of RpfB and RipA joint enzymatic action promotes the resuscitation of dormant mycobacteria. *FEBS J* **282:** 2500-2511.

Nou, X., and Kadner, R.J. (2000) Adenosylcobalamin inhibits ribosome binding to *btuB* RNA. *Proc Natl Acad Sci U S A* **97:** 7190-7195.

Ochi, K., Kandala, J.C., and Freese, E. (1981) Initiation of *Bacillus subtilis* sporulation by the stringent response to partial amino acid deprivation. *J Biol Chem* **256:** 6866-6875.

Opdyke, J.A., Kang, J.-G., and Storz, G. (2004) GadY, a small-RNA regulator of acid response genes in *Escherichia coli*. *J Bacteriol* **186:** 6698-6705.

Opdyke, J.A., Fozo, E.M., Hemm, M.R., and Storz, G. (2011) RNase III participates in GadY-dependent cleavage of the *gadX-gadW* mRNA. *J Mol Biol* **406:** 29-43.

Oppenheimer-Shaanan, Y., Wexselblatt, E., Katzhendler, J., Yavin, E., and Ben-Yehuda, S. (2011) c-di-AMP reports DNA integrity during sporulation in *Bacillus subtilis*. *EMBO Rep* **12:** 594-601.

Paget, M.S.B., Kang, J.-G., Roe, J.-H., and Buttner, M.J. (1998) σ^R, an RNA polymerase sigma factor that modulates expression of the thioredoxin system in response to oxidative stress in *Streptomyces coelicolor* A3(2). *EMBO J* **17:** 5776-5782.

Paget, M.S.B., Chamberlin, L., Atrih, A., Foster, S.J., and Buttner, M.J. (1999) Evidence that the extracytoplasmic function sigma factor σ^E is required for normal cell wall structure in *Streptomyces coelicolor* A3(2). *J Bacteriol* **181:** 204-211.

Pall, G.S., and Hamilton, A.J. (2008) Improved northern blot method for enhanced detection of small RNA. *Nat Protoc* **3:** 1077-1084.

Pánek, J., Bobek, J., Mikulík, K., Basler, M., and Vohradský, J. (2008) Biocomputational prediction of small non-coding RNAs in *Streptomyces*. *BMC Genomics* **9:** 217.

Peirson, S.N., Butler, J.N., and Foster, R.G. (2003) Experimental validation of novel and conventional approaches to quantitative real-time PCR data analysis. *Nucleic Acids Res* **31:** e73.

Petersen, F., Zähner, H., Metzger, J.W., Freund, S., and Hummel, R.-P. (1993) Germicidin, an autoregulative germination inhibitor of *Streptomyces viridochromogenes* NRRL B-1551. *J Antibiot (Tokyo)* **46:** 1126-1138.

Plocinska, R., Purushotham, G., Sarva, K., Vadrevu, I.S., Pandeeti, E.V.P., Arora, N.*, et al.* (2012) Septal localization of the *Mycobacterium tuberculosis* MtrB sensor kinase promotes MtrA regulon expression. *J Biol Chem* **287:** 23887-23899.

Potrykus, K., and Cashel, M. (2008) (p)ppGpp: still magical? *Annu Rev Microbiol* **62:** 35-51.

Potúčková, L., Kelemen, G.H., Findlay, K.C., Lonetto, M.A., Buttner, M.J., and Kormanec, J. (1995) A new RNA polymerase sigma factor, σ^F, is required for the late stages of morphological differentiation in *Streptomyces* spp. *Mol Microbiol* **17:** 37-48.

Price, I.R., Gaballa, A., Ding, F., Helmann, J.D., and Ke, A. (2015) Mn^{2+}-sensing mechanisms of *yybP-ykoY* orphan riboswitches. *Mol Cell* **57:** 1110-1123.

Puspita, I.D., Uehara, M., Katayama, T., Kikuchi, Y., Kitagawa, W., Kamagata, Y.*, et al.* (2013) Resuscitation promoting factor (Rpf) from *Tomitella biformata* AHU 1821^T promotes growth and resuscitates non-dividing cells. *Microbes Environ* **28:** 58-64.

Raman, S., Hazra, R., Dascher, C.C., and Husson, R.N. (2004) Transcription regulation by the *Mycobacterium tuberculosis* alternative sigma factor SigD and its role in virulence. *J Bacteriol* **186:** 6605-6616.

Raman, S., Song, T., Puyang, X., Bardarov, S., Jacobs, W.R., and Husson, R.N. (2001) The alternative sigma factor SigH regulates major components of oxidative and heat stress responses in *Mycobacterium tuberculosis*. *J Bacteriol* **183:** 6119-6125.

Rao, F., See, R.Y., Zhang, D., Toh, D.C., Ji, Q., and Liang, Z.-X. (2010) YybT is a signaling protein that contains a cyclic dinucleotide phosphodiesterase domain and a GGDEF domain with ATPase activity. *J Biol Chem* **285:** 473-482.

Reddy, M.C.M., Palaninathan, S.K., Bruning, J.B., Thurman, C., Smith, D., and Sacchettini, J.C. (2009) Structural insights into the mechanism of the allosteric transitions of *Mycobacterium tuberculosis* cAMP receptor protein. *J Biol Chem* **284:** 36581-36591.

Redenbach, M., Kieser, H.M., Denapaite, D., Eichner, A., Cullum, J., Kinashi, H., and Hopwood, D.A. (1996) A set of ordered cosmids and a detailed genetic and physical map for the 8 Mb *Streptomyces coelicolor* A3(2) chromosome. *Mol Microbiol* **21:** 77-96.

Regulski, E.E., and Breaker, R.R. (2008) In-line probing analysis of riboswitches. In *Post-transcriptional gene regulation.* Wilusz, J. (ed). Totowa, New Jersey: Humana Press, pp. 53-67.

Ren, A., and Patel, D.J. (2014) c-di-AMP binds the *ydaO* riboswitch in two pseudo-symmetry-related pockets. *Nat Chem Biol* **10:** 780-786.

Rickman, L., Scott, C., Hunt, D.M., Hutchinson, T., Menéndez, M.C., Whalan, R.*, et al.* (2005) A member of the cAMP receptor protein family of transcription regulators in *Mycobacterium tuberculosis* is required for virulence in mice and controls transcription of the *rpfA* gene coding for a resuscitation promoting factor. *Mol Microbiol* **56:** 1274-1286.

Rittershaus, E.S.C., Baek, S.-H., and Sassetti, C.M. (2013) The normalcy of dormancy: common themes in microbial quiescence. *Cell Host Microbe* **13:** 643-651.

Robinson, J.T., Thorvaldsdóttir, H., Winckler, W., Guttman, M., Lander, E.S., Getz, G., and Mesirov, J.P. (2011) Integrative genomics viewer. *Nat Biotechnol* **29:** 24-26.

Roth, A., Winkler, W.C., Regulski, E.E., Lee, B.W.K., Lim, J., Jona, I.*, et al.* (2007) A riboswitch selective for the queuosine precursor preQ$_1$ contains an unusually small aptamer domain. *Nat Struct Mol Biol* **14:** 308-317.

Ruggiero, A., Tizzano, B., Pedone, E., Pedone, C., Wilmanns, M., and Berisio, R. (2009) Crystal structure of the resuscitation-promoting factor $_{\Delta DUF}$RpfB from *M. tuberculosis*. *J Mol Biol* **385:** 153-162.

Saier, M.H. (1996) Cyclic AMP-independent catabolite repression in bacteria. *FEMS Microbiol Lett* **138:** 97-103.

Salas, J.A., Guijarro, J.A., and Hardisson, C. (1983) High calcium content in *Streptomyces* spores and its release as an early event during spore germination. *J Bacteriol* **155:** 1316-1323.

Salina, E.G., Waddell, S.J., Hoffmann, N., Rosenkrands, I., Butcher, P.D., and Kaprelyants, A.S. (2014) Potassium availability triggers *Mycobacterium tuberculosis* transition to, and resuscitation from, non-culturable (dormant) states. *Open Biol* **4:** 140106.

Sambrook, J., and Russell, D.W. (2001) *Molecular cloning - A laboratory manual*. Cold Spring Harbor, New York: Cold Spring Harbor Laboratory Press.

Schmieder, R., and Edwards, R. (2011) Quality control and preprocessing of metagenomic datasets. *Bioinformatics* **27:** 863-864.

Schroeckh, V., and Martin, K. (2006) Resuscitation-promoting factors: distribution among actinobacteria, synthesis during life-cycle and biological activity. *Antonie van Leeuwenhoek* **89:** 359-365.

Serganov, A., and Nudler, E. (2013) A decade of riboswitches. *Cell* **152:** 17-24.

Sexton, D.L., St-Onge, R.J., Haiser, H.J., Yousef, M.R., Brady, L., Gao, C.*, et al.* (2015) Resuscitation-promoting factors are cell wall-lytic enzymes with important roles in the germination and growth of *Streptomyces coelicolor*. *J Bacteriol* **197:** 848-860.

Shah, I.M., and Dworkin, J. (2010) Induction and regulation of a secreted peptidoglycan hydrolase by a membrane Ser/Thr kinase that detects muropeptides. *Mol Microbiol* **75:** 1232-1243.

Shah, I.M., Laaberki, M.-H., Popham, D.L., and Dworkin, J. (2008) A eukaryotic-like Ser/Thr kinase signals bacteria to exit dormancy in response to peptidoglycan fragments. *Cell* **135:** 486-496.

Sharma, A.K., Chatterjee, A., Gupta, S., Banerjee, R., Mandal, S., Mukhopadhyay, J.*, et al.* (2015) MtrA, an essential response regulator of the MtrAB two-component system, regulates the transcription of resuscitation-promoting factor B of *Mycobacterium tuberculosis*. *Microbiology* **161:** 1271-1281.

Sharples, G.P., and Williams, S.T. (1976) Fine structure of spore germination in actinomycetes. *J Gen Microbiol* **96:** 323-332.

Shi, Y., Zhao, G., and Kong, W. (2014) Genetic analysis of riboswitch-mediated transcriptional regulation responding to Mn^{2+} in *Salmonella*. *J Biol Chem* **289:** 11353-11366.

Shleeva, M., Mukamolova, G.V., Young, M., Williams, H.D., and Kaprelyants, A.S. (2004) Formation of 'non-culturable' cells of *Mycobacterium smegmatis* in stationary phase in response to growth under suboptimal conditions and their Rpf-mediated resuscitation. *Microbiology* **150:** 1687-1697.

Shleeva, M., Goncharenko, A., Kudykina, Y., Young, D., Young, M., and Kaprelyants, A. (2013) Cyclic AMP-dependent resuscitation of dormant *Mycobacteria* by exogenous free fatty acids. *PLoS One* **8:** e82914.

Shleeva, M.O., Kudykina, Y.K., Vostroknutova, G.N., Suzina, N.E., Mulyukin, A.L., and Kaprelyants, A.S. (2011) Dormant ovoid cells of *Mycobacterium tuberculosis* are formed in response to gradual external acidification. *Tuberculosis (Edinb)* **91:** 146-154.

Shleeva, M.O., Bagramyan, K., Telkov, M.V., Mukamolova, G.V., Young, M., Kell, D.B., and Kaprelyants, A.S. (2002) Formation and resuscitation of 'non-culturable' cells of *Rhodococcus rhodochrous* and *Mycobacterium tuberculosis* in prolonged stationary phase. *Microbiology* **148:** 1581-1591.

Siculella, L., Damiano, F., di Summa, R., Tredici, S.M., Alduina, R., Gnoni, G.V., and Alifano, P. (2010) Guanosine 5′-diphosphate 3′-diphosphate (ppGpp) as a negative modulator of polynucleotide phosphorylase activity in a 'rare' actinomycete. *Mol Microbiol* **77:** 716-729.

Sievers, F., Wilm, A., Dineen, D., Gibson, T.J., Karplus, K., Li, W.*, et al.* (2011) Fast, scalable generation of high-quality protein multiple sequence alignments using Clustal Omega. *Mol Syst Biol* **7:** 539.

Sledjeski, D.D., Gupta, A., and Gottesman, S. (1996) The small RNA, DsrA, is essential for the low temperature expression of RpoS during exponential growth in *Escherichia coli*. *EMBO J* **15:** 3993-4000.

Spangler, C., Böhm, A., Jenal, U., Seifert, R., and Kaever, V. (2010) A liquid chromatography-coupled tandem mass spectrometry method for quantitation of cyclic di-guanosine monophosphate. *J Microbiol Methods* **81:** 226-231.

Spreadbury, C.L., Pallen, M.J., Overton, T., Behr, M.A., Mostowy, S., Spiro, S.*, et al.* (2005) Point mutations in the DNA- and cNMP-binding domains of the homologue of the cAMP receptor protein (CRP) in *Mycobacterium bovis* BCG:

implications for the inactivation of a global regulator and strain attenuation. *Microbiology* **151:** 547-556.

Squeglia, F., Romano, M., Ruggiero, A., Vitagliano, L., De Simone, A., and Berisio, R. (2013) Carbohydrate recognition by RpfB from *Mycobacterium tuberculosis* unveiled by crystallographic and molecular dynamics analyses. *Biophys J* **104:** 2530-2539.

St-Onge, R.J., Haiser, H.J., Yousef, M.R., Sherwood, E., Tschowri, N., Al-Bassam, M., and Elliot, M.A. (2015) Nucleotide second messenger-mediated regulation of a muralytic enzyme in *Streptomyces*. *Mol Microbiol* **96:** 779-795.

Stapleton, M., Haq, I., Hunt, D.M., Arnvig, K.B., Artymiuk, P.J., Buxton, R.S., and Green, J. (2010) *Mycobacterium tuberculosis* cAMP receptor protein (Rv3676) differs from the *Escherichia coli* paradigm in its cAMP binding and DNA binding properties and transcription activation properties. *J Biol Chem* **285:** 7016-7027.

Stork, M., Di Lorenzo, M., Welch, T.J., and Crosa, J.H. (2007) Transcription termination within the iron transport-biosynthesis operon of *Vibrio anguillarum* requires an antisense RNA. *J Bacteriol* **189:** 3479-3488.

Storz, G., Opdyke, J.A., and Zhang, A. (2004) Controlling mRNA stability and translation with small, noncoding RNAs. *Curr Opin Microbiol* **7:** 140-144.

Storz, G., Vogel, J., and Wassarman, K.M. (2011) Regulation by small RNAs in bacteria: expanding frontiers. *Mol Cell* **43:** 880-891.

Strauch, E., Takano, E., Baylis, H.A., and Bibb, M.J. (1991) The stringent response in *Streptomyces coelicolor* A3(2). *Mol Microbiol* **5:** 289-298.

Studier, F.W., and Moffatt, B.A. (1986) Use of bacteriophage T7 RNA polymerase to direct selective high-level expression of cloned genes. *J Mol Biol* **189:** 113-130.

Stuttard, C. (1982) Temperate phages of *Streptomyces venezuelae*: lysogeny and host specificity shown by phages SV1 and SV2. *J Gen Microbiol* **128:** 115-121.

Sudarsan, N., Wickiser, J.K., Nakamura, S., Ebert, M.S., and Breaker, R.R. (2003) An mRNA structure in bacteria that controls gene expression by binding lysine. *Genes Dev* **17:** 2688-2697.

Süsstrunk, U., Pidoux, J., Taubert, S., Ullmann, A., and Thompson, C.J. (1998) Pleiotropic effects of cAMP on germination, antibiotic biosynthesis and morphological development in *Streptomyces coelicolor*. *Mol Microbiol* **30:** 33-46.

Swiercz, J.P., Hindra, Bobek, J., Haiser, H.J., Di Berardo, C., Tjaden, B., and Elliot, M.A. (2008) Small non-coding RNAs in *Streptomyces coelicolor*. *Nucleic Acids Res* **36:** 7240-7251.

Telkov, M.V., Demina, G.R., Voloshin, S.A., Salina, E.G., Dudik, T.V., Stekhanova, T.N.*, et al.* (2006) Proteins of the Rpf (resuscitation promoting factor) family are peptidoglycan hydrolases. *Biochemistry (Mosc)* **71:** 414-422.

Townsend, P.D., Jungwirth, B., Pojer, F., Bußmann, M., Money, V.A., Cole, S.T.*, et al.* (2014) The crystal structures of apo and cAMP-bound GlxR from *Corynebacterium glutamicum* reveal structural and dynamic changes upon cAMP binding in CRP/FNR family transcription factors. *PLoS One* **9:** e113265.

Toyoda, K., Teramoto, H., Inui, M., and Yukawa, H. (2011) Genome-wide identification of *in vivo* binding sites of GlxR, a cyclic AMP receptor protein-type regulator in *Corynebacterium glutamicum*. *J Bacteriol* **193:** 4123-4133.

Tramonti, A., De Canio, M., and De Biase, D. (2008) GadX/GadW-dependent regulation of the *Escherichia coli* acid fitness island: transcriptional control at the *gadY–gadW* divergent promoters and identification of four novel 42 bp GadX/GadW-specific binding sites. *Mol Microbiol* **70:** 965-982.

Trotochaud, A.E., and Wassarman, K.M. (2004) 6S RNA function enhances long-term cell survival. *J Bacteriol* **186:** 4978-4985.

Trotochaud, A.E., and Wassarman, K.M. (2005) A highly conserved 6S RNA structure is required for regulation of transcription. *Nat Struct Mol Biol* **12:** 313-319.

Tufariello, J.M., Jacobs, W.R., and Chan, J. (2004) Individual *Mycobacterium tuberculosis* resuscitation-promoting factor homologues are dispensable for growth in vitro and in vivo. *Infect Immun* **72:** 515-526.

Tufariello, J.M., Mi, K., Xu, J., Manabe, Y.C., Kesavan, A.K., Drumm, J.*, et al.* (2006) Deletion of the *Mycobacterium tuberculosis* resuscitation-promoting factor Rv1009 gene results in delayed reactivation from chronic tuberculosis. *Infect Immun* **74:** 2985-2995.

van Keulen, G., Alderson, J., White, J., and Sawers, R.G. (2005) Nitrate respiration in the actinomycete *Streptomyces coelicolor*. *Biochem Soc Trans* **33:** 210-212.

van Keulen, G., Alderson, J., White, J., and Sawers, R.G. (2007) The obligate aerobic actinomycete *Streptomyces coelicolor* A3(2) survives extended periods of anaerobic stress. *Environ Microbiol* **9:** 3143-3149.

Vockenhuber, M.-P., Sharma, C.M., Statt, M.G., Schmidt, D., Xu, Z., Dietrich, S., *et al.* (2011) Deep sequencing-based identification of small non-coding RNAs in *Streptomyces coelicolor*. *RNA Biol* **8:** 468-477.

Vogel, J., and Papenfort, K. (2006) Small non-coding RNAs and the bacterial outer membrane. *Curr Opin Microbiol* **9:** 605-611.

Vollmer, W., Blanot, D., and de Pedro, M.A. (2008a) Peptidoglycan structure and architecture. *FEMS Microbiol Rev* **32:** 149-167.

Vollmer, W., Joris, B., Charlier, P., and Foster, S. (2008b) Bacterial peptidoglycan (murein) hydrolases. *FEMS Microbiol Rev* **32:** 259-286.

Wassarman, K.M. (2002) Small RNAs in bacteria: diverse regulators of gene expression in response to environmental changes. *Cell* **109:** 141-144.

Wassarman, K.M., and Storz, G. (2000) 6S RNA regulates *E. coli* RNA polymerase activity. *Cell* **101:** 613-623.

Wassarman, K.M., and Saecker, R.M. (2006) Synthesis-mediated release of a small RNA inhibitor of RNA polymerase. *Science* **314:** 1601-1603.

Waters, L.S., and Storz, G. (2009) Regulatory RNAs in bacteria. *Cell* **136:** 615-628.

Watson, P.Y., and Fedor, M.J. (2012) The *ydaO* motif is an ATP-sensing riboswitch in *Bacillus subtilis*. *Nat Chem Biol* **8:** 963-965.

Williams, E.P., Lee, J.-H., Bishai, W.R., Colantuoni, C., and Karakousis, P.C. (2007) *Mycobacterium tuberculosis* SigF regulates genes encoding cell wall-associated proteins and directly regulates the transcriptional regulatory gene *phoY1*. *J Bacteriol* **189:** 4234-4242.

Winkler, W., Nahvi, A., and Breaker, R.R. (2002a) Thiamine derivatives bind messenger RNAs directly to regulate bacterial gene expression. *Nature* **419:** 952-956.

Winkler, W.C., Cohen-Chalamish, S., and Breaker, R.R. (2002b) An mRNA structure that controls gene expression by binding FMN. *Proc Natl Acad Sci U S A* **99:** 15908-15913.

Winkler, W.C., Nahvi, A., Sudarsan, N., Barrick, J.E., and Breaker, R.R. (2003) An mRNA structure that controls gene expression by binding *S*-adenosylmethionine. *Nat Struct Biol* **10:** 701-707.

Winkler, W.C., Nahvi, A., Roth, A., Collins, J.A., and Breaker, R.R. (2004) Control of gene expression by a natural metabolite-responsive ribozyme. *Nature* **428:** 281-286.

Witte, G., Hartung, S., Büttner, K., and Hopfner, K.-P. (2008) Structural biochemistry of a bacterial checkpoint protein reveals diadenylate cyclase activity regulated by DNA recombination intermediates. *Mol Cell* **30:** 167-178.

Wösten, M.M.S.M. (1998) Eubacterial sigma-factors. *FEMS Microbiol Rev* **22:** 127-150.

Wright, P.R., Georg, J., Mann, M., Sorescu, D.A., Richter, A.S., Lott, S.*, et al.* (2014) CopraRNA and IntaRNA: predicting small RNA targets, networks and interaction domains. *Nucleic Acids Res* **42:** W119-W123.

Wu, Q.-L., Kong, D., Lam, K., and Husson, R.N. (1997) A mycobacterial extracytoplasmic function sigma factor involved in survival following stress. *J Bacteriol* **179:** 2922-2929.

Xu, X.-L., Lee, R.T.H., Fang, H.-M., Wang, Y.-M., Li, R., Zou, H.*, et al.* (2008) Bacterial peptidoglycan triggers *Candida albicans* hyphal growth by directly activating the adenylyl cyclase Cyr1p. *Cell Host Microbe* **4:** 28-39.

Zhu, W., Plikaytis, B.B., and Shinnick, T.M. (2003) Resuscitation factors from mycobacteria: homologs of *Micrococcus luteus* proteins. *Tuberculosis (Edinb)* **83:** 261-269.

Zuker, M. (2003) Mfold web server for nucleic acid folding and hybridization prediction. *Nucleic Acids Res* **31:** 3406-3415.